Sorbonne Université

Ecole doctorale Cerveau, Cognition, Comportement (ED3C)

Laboratoire Neuroscience Paris Seine / Equipe Réseau de Neurones et Rythmes Physiopathologiques

Functional identification of GluN3A subunit-containing NMDA receptors in the adult brain

Par Sarah ABI GERGES

Thèse de doctorat de Biologie, Spécialité Neurosciences

Dirigée par Nathalie LERESCHE et Co-Dirigée par Marco DIANA

Présentée et soutenue le 25 septembre 2020

Devant un jury composé de :

Dr. AVIGNONE Elena	Rapporteur
Dr. CANEPARI Marco	Rapporteur
Dr. BACCI Alberto	Examinateur
Dr. LERESCHE Nathalie	Directrice de thèse
Dr. DIANA Marco	Invité

Dedication

To you, closest to my heart, I love you more than words can say

To my late father, whose words still resonate in my head,

To my wonderful mother, of whose authentic grey hairs, not a few were caused by myself,

To my brother and my best friend, whose constant support I could never repay,

I dedicate my work to you. I hope this makes you proud

ACKNOWLEDGEMENTS:

Foremost, I would like to express my sincere gratitude to Dr. Hervé Chneiweiss, for welcoming me to Neuroscience Paris Seine department, allowing me to carry out this thesis.

I would also like to thank the members of the jury for kindly reviewing my work: Marco Canepari and Elena Avignone as rapporteurs, as well as Nathalie Leresche and Alberto Bacci.

I am extremely grateful to all our collaborators, especially Dr. Matyas Ferenc who thoroughly taught me how to do extremely precise injections.

My sincere thanks also goes to Nathalie Leresche and Regis Lambert, for welcoming me to their team.

My warmest gratitude goes to my supervisor, Marco Diana, who is truly one of the brightest people I've had the chance to encounter. You make science look like art. Your passion is overwhelming, and I have learned a great deal from you, in life as well as science. Thank you for your guidance, support and immense knowledge. I will always remember your (loud) music and your (very very dark) sense of humor that I quite enjoyed (the following Arabic paragraph is addressed to you as well)

"الإبداع هو عندما يصبح الذّكاء نوع من المتعة"

فأنتَ من أكثر النّاس ذكاءً وفطنةً.. ومن نظرتِكَ تبرق لمعة الإبداع.. وقد تعلّمتُ منكَ الكثير. فأنتَ كنتَ مدرستي في هذه الحياة، ولذلك سيبقى لديكَ معزّة خاصّة مهما طالت الأيّام، وبالرّغم من كلّ ما مررنا به

My gratitude also goes to all RNRP members: Thomas, thank you for our talks. Sophie, thank you for the laughs in the office, for the GOOD food, and most importantly, for the Lebanese personality buried inside you that made the office feel a bit more like home. Kasia, your presence brought life to the office. Thank you for taking care of me and for listening to my endless nagging. Thank you for just being you. Eric, thank you for your kindness at a time when I really needed it. Thank you for your patience, for everything you've taught me.

A special thanks for all the NPS members, especially Andry. Thanks for the books (and for adopting an introvert).

To the people I have met in England during the summer school, thank you for your friendship and our scientific talks.

To my friends, Roy H. (study-buddy, ex-lab parter, Sorbonne partner, AMAZING friend), JB (AKA Jano, sorry I had to), Perla, Charbel (special thanks for the food), Nour (thanks for your clothes), Martucci, Roy , elias, Polo (no you're not the first you selfish freak), Gaby, Céline, Skayem, Anna, and my students, thank you for helping me survive all the stress of the thesis and for not letting me give up.

To my family, blood and chosen: my brother Samer; my cousins, Patty, Kiki; my adopted cousins, Charly and Marouan, thank you for the laughs when I needed it the most, for your dark sense of humor, your sarcasm and mostly, your support.

Last but not least, I would like to thank my aunt, Lauraine, who took great care of me and without whom I would not be here;

Mom, you were my strength during this period; being away from you and Sam was never easy, I hope that every birthday I missed, every holiday, every family gathering, every joyous occasion, was worth it at the end. You both are my life and my happiness, and I thank you and the whole universe for your existence. I wouldn't be the woman I am today if it weren't for you.

Dad, you always believed in me. This is for you, from the bottom of my heart..

- يخلّيلنا ياك يا بيّي
- باقيين.. نشوفك دكتورة يا بيّي
قلتلّي باقي.. وما بقيت..
انشالله وين ما كنت، تكون عم تشوف
لو ما منّك ما وصلت لهون، إنتَ لّي كنت تمدح بطموحاتي، إنتَ يلّي ما كان عندك أدنى شكّ إنّي رح أوصل..
بحبّك واشتقتلّك يا بيّي، وبتمنّى تكون فخور بشغلي..

TABLE OF CONTENT

TABLE OF ILLUSTRATIONS

List Of Tables

LIST OF ABBREVIATIONS

4AP	4-Aminopyridine,
AAV	Adeno-Associated Virus
ABD	Agonist binding domain
ACSF	Artificial cerebrospinal fluid
AD	Alzheimer's disease
AgRP	Agouti-related protein
AMPA	α-amino-3-hydroxy-5-methyl-4-isoxazolepropionic acid
AMPAR	AMPA receptor
ARAS	Ascending reticular activating system
ATD	Amino-terminal domain
BNST	Bed nucleus of the stria terminalis
CALB2	Calbindin 2
CeL	central lateral nucleus of the amygdala
CGP78608	1S)-1-[[7-Bromo-1,2,3,4-tetrahydro-2,3-dioxo-5-quinoxalinyl) methyl]amino]ethyl]phosphonic acid hydrochloride
CGRP	calcitonine G related peptide
ChR2	Channerlrhodopsin 2
CIQ	(3-Chlorophenyl)[3,4-dihydro-6,7-dimethoxy-1-[(4-methoxyphenoxy)methyl]-2(1H)-isoquinolinyl]-methanone
CL	Central lateral thalamic nucleus
CM	Central medial thalamic nucleus
CMV	Cytomegalovirus
CNQX	6-cyano-7-nitroquinoxaline-2,3-dione
CNS	Central nervous system
CR	Calretinin
CS	Conditioned stimulus
CTA	Conditioned taste aversion
CTD	Carboxyl-terminal domain
D-APV	D-2-amino-5-phosphonovaleric acid
DBS	Deep brain stimulation
DCKA	5,7-Dichlorokynurenic acid
DREADD	Designer receptor exclusively activated by designer drugs
Ef1a	Human elongation factor-1 alpha
EM	Electronic microscopy
EPSC	Excitatory postsynaptic currents
eYFP	Enhanced yellow fluorescent protein
Fr	Fasciculus retroflexus

GABA	Gamma aminobutyric acid
GABAR	Gaba receptor
GluN1/GluN2/GluN3Rs	GluN1/GluN2/GluN3 receptors
GluN1/GluN3Rs	GluN1/GluN3 receptors
IL	Intralaminar nuclei of the thalamus
ILc	Infralimbic cortex
IPN	Interpeduncular nucleus
IV curve	Current-voltage characteristic curve
KI	Knock in
KO	Knock out
leEPSCs	Light-evoked excitatory postsynaptic currents
LHb	Epithalamic lateral habenula
LTD	Long term depression
LTP	Long term potentiation
MC4R	Melanocortin 4 receptor
MDL	Midline thalamic nuclei
MHb	Epithalamic medial habenula
mRNA	Messenger RNA
MS	Medial septal nucleus
MSH	Melanocyte stimulating hormone
NAC	Nucleus accumbens
NBQX	2,3-dihydroxy-6-nitro-7-sulfamoyl-benzoquinoxaline2,3-dione
NMDA	N-Methyl-D-aspartate
NMDARS	NMDA receptors
NSTS	Non-specific thalamic system
OXT	Oxytocin
OXTR	Oxytocin receptor
PAG	Periaqueductal gray nucleus
PB	Parabrachial nucleus
PBS	Phosphate buffer saline
PC	Paracentral thalamic nucleus
PDYN	Prodynorphin
PF	Parafascicular thalamic nucleus
PFA	Paraformaldehyde
PFC	Prefrontal cortex
PnC	Caudalis sub-divisions of the rostral pons
PnO	Oralis sub-divisions of the rostral pons
PS	Posterior septal nucleus

PSD	Postsynaptic density
PVT	Paraventricular thalamic nucleus
RF	Reticular formation
RNA	Ribonucleic acid
Scp	Superior cerebellar peduncle
SCN	Suprachiasmatic nucleus
ShRNA	Short hairpin RNA
SR95531	6-Imino-3-(4-methoxyphenyl)-1(6H)-pyridazinebutanoic acid hydrobromide
STS	Specific thalamic system
TEA	Tetraethylammonium
TMD	Transmembrane domain
TTX	Tetrodotoxin
US	Unconditioned stimulus
VGluT2	Vesicular glutamate transporter 2
VTA	Ventral tegmental area
WT	Wild type
YFP	Yellow fluorescent protein
ZI	Zona incerta

INTRODUCTION

Chapter I:

Conventional NMDA Receptors

CHAPTER I: CONVENTIONAL NMDA RECEPTORS

In the mammalian brain, excitatory synaptic transmission is mediated primarily by the amino acid glutamate through two distinct groups of specific receptors: metabotropic and ionotropic. Among other effects, activation of metabotropic receptors indirectly affects ion channel function via regulation of second messenger levels (by intracellular signaling through G proteins), whereas ionotropic receptors contain cation-permeable pores. Ionotropic glutamate receptors are further divided with respect to their pharmacological properties into the following sub-groups: GluA (AMPA, 2-amino-3-3-hydroxy-5-methyl-isoxazol-4-yl propanoic acid), GluK (kainate), GluD (δ) and GluN receptors (NMDA, N-Methyl-D-aspartic acid).

In particular, NMDA receptors (NMDARs) have long fascinated neuroscientists for their distinct biophysical properties and their critical roles in neuronal communication and synaptic plasticity. NMDARs possess several unique characteristics that differentiate them from other glutamate receptors, such as a block by extracellular magnesium (Mg^{2}) at hyperpolarized membrane potentials, high calcium (Ca^{2+}) permeability and the obligation of binding of both an agonist and a coagonist, glutamate and glycine respectively, for channel activation[1]. NMDARs have therefore received much attention over the last few decades, and the vast literature existing on them has incredibly advanced our understanding of their function and structure.

1. NMDARs: function

NMDARs exert important functions in neurophysiology. They are implicated in long-lasting alterations of synaptic efficacy and remodelling, such as the induction of long-term potentiation and depression (LTP and LTD, respectively)[2], which are synaptic plasticity phenomena implicated in memory and learning. Notably, the NMDAR-dependent LTP and LTD forms present at the synapses between Schaffer collaterals and the CA1 region in the hippocampus are the best described forms of synaptic plasticity in the central nervous system[2]. Moreover, and importantly, NMDAR-dysregulation is involved in numerous psychiatric disorders such as Alzheimer's disease (AD) and schizophrenia. In AD, the accumulation of the aggregating protein amyloid-β causes NMDAR internalization, thereby reducing glutamatergic transmission and inhibiting synaptic plasticity[3,4]. Furthermore, numerous studies show the implication of NMDAR hypofunction in the behavioral manifestations of schizophrenia (increased locomotor activity, social withdrawal…)[5,6]. NMDAR-dependent synaptic and circuital alterations are

also implicated in the emergence of drug addiction and of the compulsive drug-seeking and drug craving behaviors associated with addictive substance abuses[7]. In all these phenomena, NMDAR trafficking mechanisms appear fundamental for the development of abnormal behaviors. Therefore, discovering drugs that regulate this aspect of NMDAR physiology could represent an important step towards a therapeutic solution for all these NMDAR-related phenomena.

2. NMDARs: structure and gating

The NMDARs family is composed by three distinct subunits: GluN1, 2 and 3, which are encoded by 7 genes: GluN1; GluN2 A, B, C and D; GluN3 A and B[8,9]. Conventional NMDARs are heterotetrameric assemblies with a stoichiometry of two obligatory glycine-binding GluN1 subunits combined to two glutamate-binding GluN2 ones[10–12].

A significant level of homology and an analogous architecture is detected among all NMDAR subunits. Four distinct domains constitute the core of NMDARs subunits: a large extracellular amino-terminal domain (ATD), an agonist binding domain (ABD), a pore-forming transmembrane domain (TMD), and an intracellular carboxyl-terminal domain (CTD; Fig. 1). The TMD is composed by three transmembrane helices (M1, M3, and M4) and a reentrant loop (M2; reviewed in[1]). M2 borders the intracellular portion of the ion channel pore, whereas components of M3 shape the extracellular region. Residues in the pore region of all NMDAR subtypes, known to impact ion permeation, are highly conserved. At the top of the reentrant loop, M2, resides a crucial determinant of ion permeation, controlling magnesium block (much stronger in GluN2-containing NMDARs) as well as divalent ion permeability[13]. The ATDs play critical roles in regulating NMDARs function and assembly[14–17]. Moreover, the ATDs constitute binding sites for allosteric modulators, such as extracellular Zn^{2+} and ifenprodil[18–21]. The S1 and S2 segments of the polypeptide chain compose the ABD. ABDs form two lobes, D1 (upper) and D2 (lower). The agonist-binding site resides in the gap between the two lobes (Fig. 1).

3. Activation of NMDARs

In the CNS, the release of glutamate activates ionotropic glutamatergic receptors generating excitatory postsynaptic currents (EPSCs) and thus depolarizing the postsynaptic neurons. Two temporally different components, corresponding to the activation of AMPARs and NMDARs, characterize glutamatergic EPSCs. AMPAR activation results in a synaptic current with fast rise time and decay, as opposed to NMDAR activation that elicits a more slowly activated current with a decay that persists for tens to hundreds of milliseconds[22–25].

NMDARs exhibit remarkable properties that distinguish them from other types of ligand-gated ionotropic receptors[26]. At rest, the electrical driving force pushes the magnesium into the channel pore and blocks the NMDAR. Upon AMPAR activation, depolarization of the membrane potential leads to the expulsion of magnesium from the pore, releasing the block and allowing current to flow through the NMDARs. Thus, NMDARs make excellent coincidence detectors that are dependent simultaneously on the frequency of presynaptic glutamate release and on postsynaptic depolarization levels, providing slow postsynaptic current that permits Ca^{2+} entry into the dendritic spine[27–29]. Numerous changes occur in the postsynaptic neuron following an increase in intracellular Ca^{2+} leading ultimately to the implementation of short and long term plasticity[1,30–35].

Conventional NMDARs are uncommon among ionotropic receptors, as they require the binding of a co-agonist (glycine or D-serine) in addition to the agonist glutamate for receptor activation[36–40]. Ambient glycine/D-serine levels present in the extracellular environment may be sufficient to occupy the co-agonist binding sites in basal conditions[41], even if probably not to saturation[42–44]. Therefore, it is likely that both the synaptic release of glutamate and the modulation of the extracellular levels of glycine/D-serine[45–47] control synaptic NMDAR activation. Concerning the nature of the co-agonist in native systems, recently some data suggested that D-serine may be the main co-agonist at synaptic NMDARs, whereas glycine could preferentially control extrasynaptic NMDAR activation[48]. Evidently, more research is still required to unravel this important aspect of NMDAR physiology in the brain.

Studies conducted on the ABD of diheteromeric GluN1/GluN2 receptors have led to a structural model explaining their mechanisms of action[49–54]. The simultaneous binding of glycine or D-serine to the GluN1 ABD and of glutamate to the GluN2 ABD would indeed result in a quick structural rearrangement. Namely, the angle reduction between the two lobes, D1 and D2, of each ABD would lead to their clamshell-like closure, and to their connection via hydrogen bonds, which would stabilize the ABD structure[55,56]. The binding of the agonist and the clamshell-like closure of the ABD thus provide the necessary energy for the NMDAR to undergo a series of conformational changes that eventually lead to the opening of the channel pore. Hence, the clamshell-like closure of the ABD that results from agonist binding is the key that ultimately sets off ion channel gating.

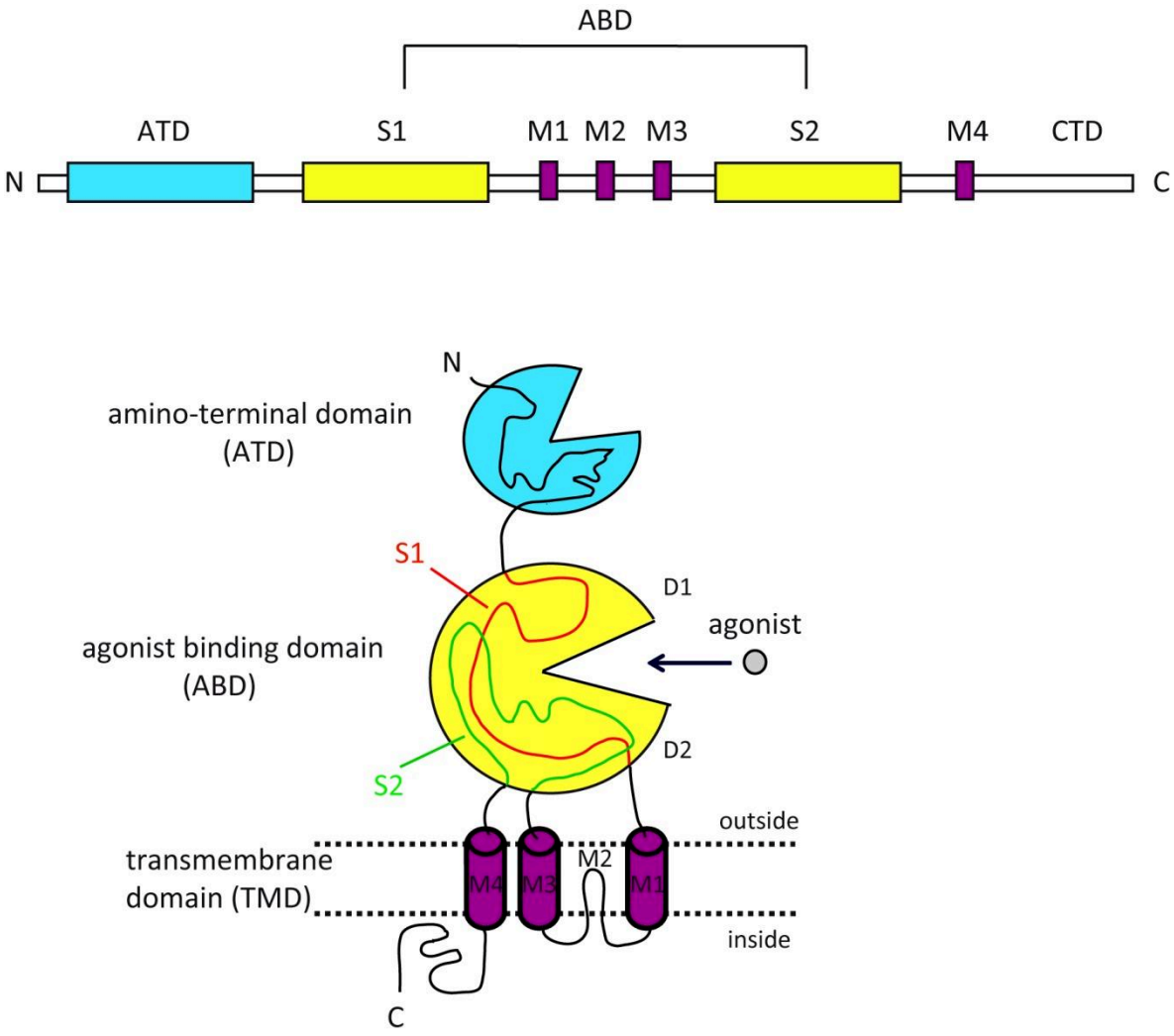

Figure 1| Domain organization and ligand-binding sites in NMDARs.

Schema illustrating the NMDAR-subunit domains: the extracellular ATD, the ABD, the TMD (formed by three transmembrane helices M1, M2, and M4 and a membrane reentrant loop, M2), and the intracellular C- terminal domain, or CTD. The ABD is formed by two polypeptide segments (S1 and S2) that fold into a bilobed structure with an upper lobe (D1) and lower lobe (D2). The agonist-binding site is located in the cleft between the two lobes.

4. NMDAR pharmacology

NMDAR activity can be either upregulated or downregulated. Positive modulators do not bind to the agonist binding site. They work by enhancing the maximal response or agonist affinity. Endogenous polyamines for instance can potentiate NMDAR activity in GluN2B-containing receptors by increasing their sensitivity for ligands[57,58]. Other compounds, also known to positively modulate NMDAR activity, include numerous neurosteroids and the recently discovered compound CIQ[59–62].

Negative modulators can be divided according to their site of action: competitive antagonists which act at the level of the agonist binding site (ABS), channel blockers which act within the ion channel pore and non-competitive antagonists which act on specific modulation sites. Competitive antagonists compete with the agonist for the ABS without activating the receptor. One of the best-known and highly selective competitive antagonists for the glutamate site of NMDARs is D-2-amino-5-phosphonovalerate or D-APV[63]. Other competitive antagonists, such as 5,7-Dichlorokynurenic acid or DCKA, act at the glycine site of NMDARs. The binding of a competitive antagonist on the ABS prevents the closure of the bilobed domain, stabilizing an open cleft conformation of the receptor that blocks channel gating. Other drugs, such as ketamine, dizocilpine maleate or MK-801 and memantine, are widely-used powerful pore blockers[64–67]. Pore blockers require prior activation of the receptor so that their effect exhibits delayed onset and depends on channel opening probability. Most pore blockers are not selective for one subunit, probably because the ion channel region is highly conserved between receptor subunits[68] (but see[69]).

5. The glycine-binding GluN1 subunit

Ubiquitously expressed in the CNS, the GluN1 subunit binds glycine (or D-serine) and is obligatorily present in all functional NMDARs. Post-transcriptional RNA processing generates eight separate splice variants of the GluN1 subunit[70–73]. GluN1 isoforms display developmental and regional heterogeneity[74–76] and confer peculiar functions and pharmacology to the receptor. For example, the GluN1-1b variant generates EPSCs of shorter duration because of its role in accelerating NMDAR deactivation upon agonist removal[77–80].

Moreover, a disulfide bond, formed by two cysteine residues on GluN1 (C744 and C798) endows conventional GluN1/GluN2 NMDARs with a sensitivity to the redox potential[81,82], NMDAR-mediated responses being enhanced in reducing conditions[83–86]. Redox modulation is viewed as a crucial mechanism to regulate NMDAR signaling[87–89] during normal and pathological conditions.

6. The glutamate-binding GluN2 subunit

The four glutamate-binding GluN2A-D subunits determine and control NMDAR properties[9,75,90–93]. A variation in subunit expression can greatly influence the NMDAR component of synaptic responses. For example, the presence of the GluN2A or GluN2B subunit in diheteromeric GluN1/GluN2 NMDARs generates receptors with high conductance, high permeability to Ca^{2+}, and sensitivity to block by extracellular Mg^{2+}. In contrast, GluN2C- or GluN2D-containing diheteromeric receptors have lower conductance, lower sensitivity to Mg^{2+} and Ca^{2+} permeability[90,93–97]. Moreover, some endogenous modulators can regulate NMDAR activity via the GluN2 subunit. Notable among these are extracellular Zn^{2+} and protons[58,98,99]. Additionally, the GluN2 subunit can impact cell-surface expression and degradation and recycling of NMDARs because of the highly variable amino acid sequence of the CTD, an interaction site for numerous kinases, phosphatases and proteins implicated in surface trafficking and anchoring at synaptic sites[1,100–102].

7. The glycine-binding GluN3 subunit

The two GluN3 subunits, GluN3A and GluN3B, were cloned last in the NMDAR subunit family. Unlike the fairly well-characterized conventional NMDARs, much less is known about GluN3-containing receptors. It was only in recent years that NMDAR including these unconventional subunits have begun to be thoroughly investigated.

Just like GluN1, GluN3 subunits bind glycine, and with much higher affinity[103]. The presence of GluN3A/B changes drastically the properties of receptors with respect to conventional GluN1/GluN2 heteromers. GluN3-containing NMDARs come in two distinct flavors, namely in triheteromeric GluN1/GluN2/GluN3 complexes and in diheteromeric GluN1/GluN3 receptors, these latter being activated purely by glycine and being insensitive to glutamate.

Many questions on the biophysics and the physiology of both receptor types are still open. My thesis work has attempted to clarify some of these properties by looking at their function in native neuronal systems. GluN3 subunits, and more specifically GluN3A, were thus the main research topic of my thesis.

I will provide a comprehensive review of what we know on their properties at present in the following chapter.

CHAPTER II:

GLUN3-CONTAINING NMDARS

CHAPTER II: GLUN3-CONTAINING NMDARs

1. Brain expression of the GluN3 subunits

Some differences have so far emerged between the properties of diheteromeric and triheteromeric NMDARs including either the GluN3A, or the GluN3B subunit (but see[104]). However, the most relevant properties identified for GluN1/GluN3B receptors, in which a substantial part of the characterization of GluN3-containing diheteromers has been done[105,106], can be extended also to GluN3A-containing receptors. Therefore, the two GluN3 subunits may participate to receptors complexes that, for the moment, may be hard to distinguish functionally. A straightforward distinction between GluN3A and GluN3B was nonetheless established shortly following the cloning of the subunits, and it concerned their expression patterns in the brain (Fig. 2-3).

1.1. Brain expression of GluN3B

The GluN3A subunit has always been assumed to have a widespread distribution, although strictly limited to early developmental stages[107,108]. In contrast, the expression of GluN3B grows steadily during development, and reaches a stable peak at adulthood (Fig. 3) although it is limited to specific caudal brain areas like the brainstem and the spinal cord[109,110]. Its expression is, in contrast, very weak in rostral areas[111]. This point is also confirmed by the Allen Atlas at the following address: *http://mouse.brain-map.org/experiment/ivt?id=536,77869800&popup=true*.

The GluN3B subunit is thus most likely **not** expressed in the adult anterior brain areas that I examined during my thesis, namely the midline and intralaminar thalamus and the epithalamic medial habenula. We will also see that our physiological data support this conclusion. Indeed, similarly to GluN3A, GluN3B subunits generate glycine-activated diheteromeric receptors with GluN1 in heterologous systems. GluN1/GluN3B receptor currents elicited by glycine would thus be expected in GluN3AKO animals if GluN3B subunits were expressed. This was never the case in all the neurons recorded in the course of my PhD, strongly supporting the lack of expression of GluN3B in the anterior brain.

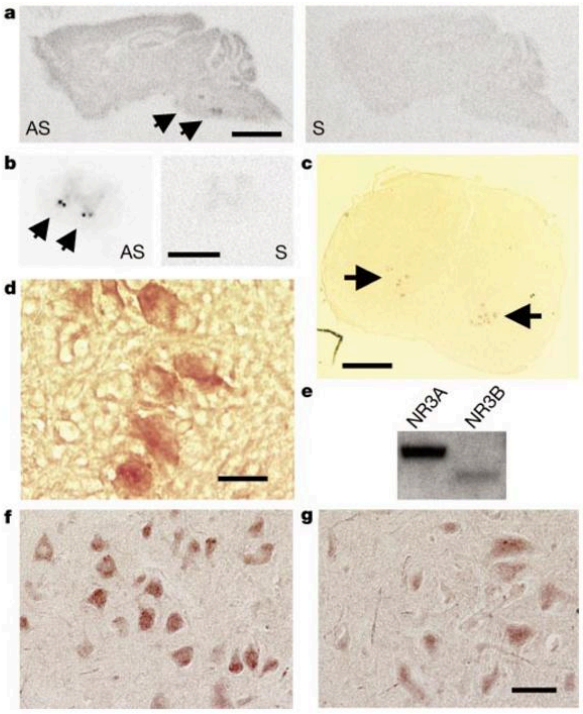

Figure 2| GluN3A and GluN3B expression pattern by immunohistochemistry and *in situ* hybridization.

a- *In situ* hybridization of the adult rat brain with antisense (AS) and sense (S) GluN3B probes labeled with ^{33}P. **b,c,d-** *In situ* hybridization of the adult spinal cord labeled with ^{33}P (b) or digoxigenin (c,d). **e-** Western blot of GluN3A or GluN3B subunit transfected HEK cell lysates probed with an anti GluN3A/B antibody. **f,g-** Antibody staining against GluN3A/B subunits in the facial nucleus (f) and spinal cord ventral horn (g) in an adult GluN3AKO mouse. Scale bars: 6mm, 3mm and 1mm for a, b and c respectively; and 50µm for d, f and g[112].

1.2. Brain expression of GluN3A

The expression pattern of the GluN3A subunit is completely different from GluN3B. Until now, it has been common assumption that GluN3A expression changes dramatically over development, being very low at embryonic stages and adulthood, and showing a peak in the anterior brain in the first 2 postnatal weeks[108,113,114].

This largely accepted dogma was mainly based on studies where the protein and/or mRNA expression levels of GluN3A were either quantified on whole-brain extracts[114–117], or examined in detail in few brain areas of particular interest and of easy experimental access like the cortex and the hippocampus[118–120]. Still, early reports hinted at a more subtle scenario, acknowledging the presence of GluN3A also in the adult brain albeit in very specific and, we believe, at the time not particularly enticing structures like the habenular complex and the thalamus[115,116].

As I will discuss thoroughly in later sections, my thesis activity developed from the reexamination of the expression pattern of GluN3A in the adult brain (Fig. 4) using an antibody developed by M. Watanabe (Hokkaido University, Japan). We could indeed confirm that the expression of the GluN3A subunit is not limited to early development and, that, in specific adult areas, it is expressed at high levels and produces functional receptors with precise physiological function.

Finally, a few words about the ultra structural localization of GluN3A in neurons. Similarly to any cellular element, the identification of possible physiological functions may indeed be helped by a preferential positioning in specific subcellular compartments. Unfortunately though, very little information is at present available on this point, with just 3 studies showing EM data on the subcellular localization of GluN3A subunits in neurons[115,121,122]. These studies show that, in general, GluN3A subunits are found in dendrites and, at lower levels, in somata. In dendrites, the distribution was found to be more abundant at perisynaptic and extrasynaptic sites than at the postsynaptic density. In contrast to a study performed in rats[115], Larsen et al., 2011[119] detected the subunit also on presynaptic specializations in the primary visual cortex of juvenile animals using the same antibody that I have exploited in my experiments. No confirmation of a presynaptic distribution has been confirmed in adult tissues so far.

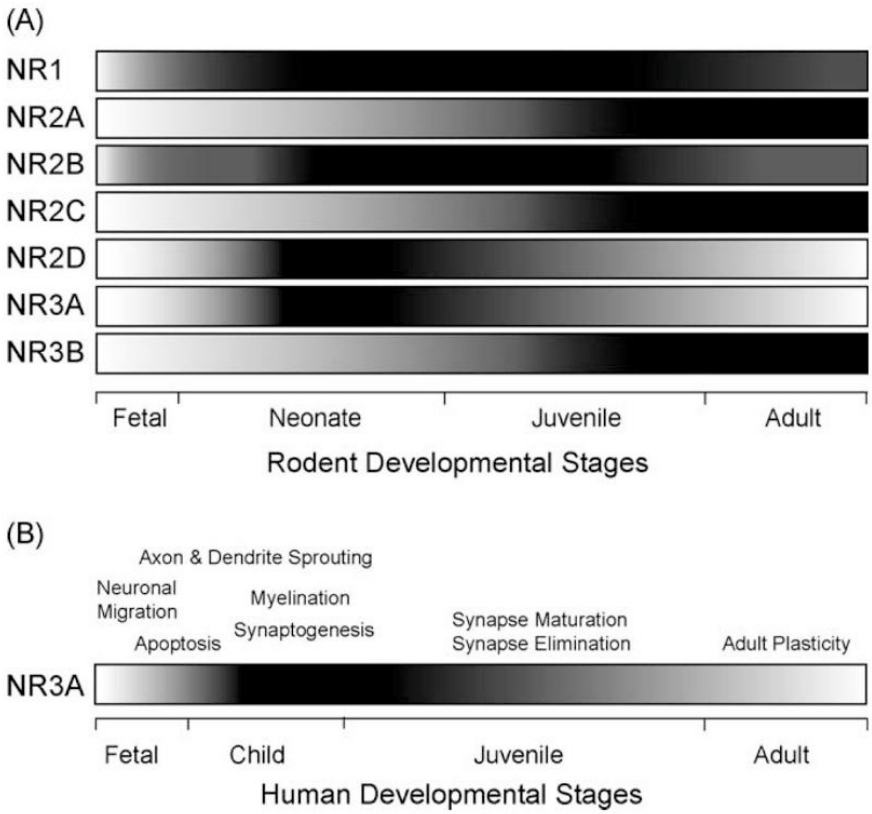

Figure 3|Schematic representation of NMDAR subunit expression during development.

A- Schematic representation of NMDA receptor subunit expression in the developing brain in rodents. In this figure the former nomenclature for NMDA receptors is used with NR3 indicating to GluN3. The grey scale gradient illustrates the differences in expression in respect to the maximum during development, with darker regions indicating stronger expression. GluN3A (as well as GluN2D) expression appears to peak between P7 and P14 and then decreases to much lower levels in adulthood. **B-** Schematic representation of GluN3A expression in the developing brain in humans. GluN3A appears to be expressed during early developmental stages, characterized by axon and dendrite sprouting, apoptosis, myelination, synaptogenesis and synapse maturation and elimination[366].

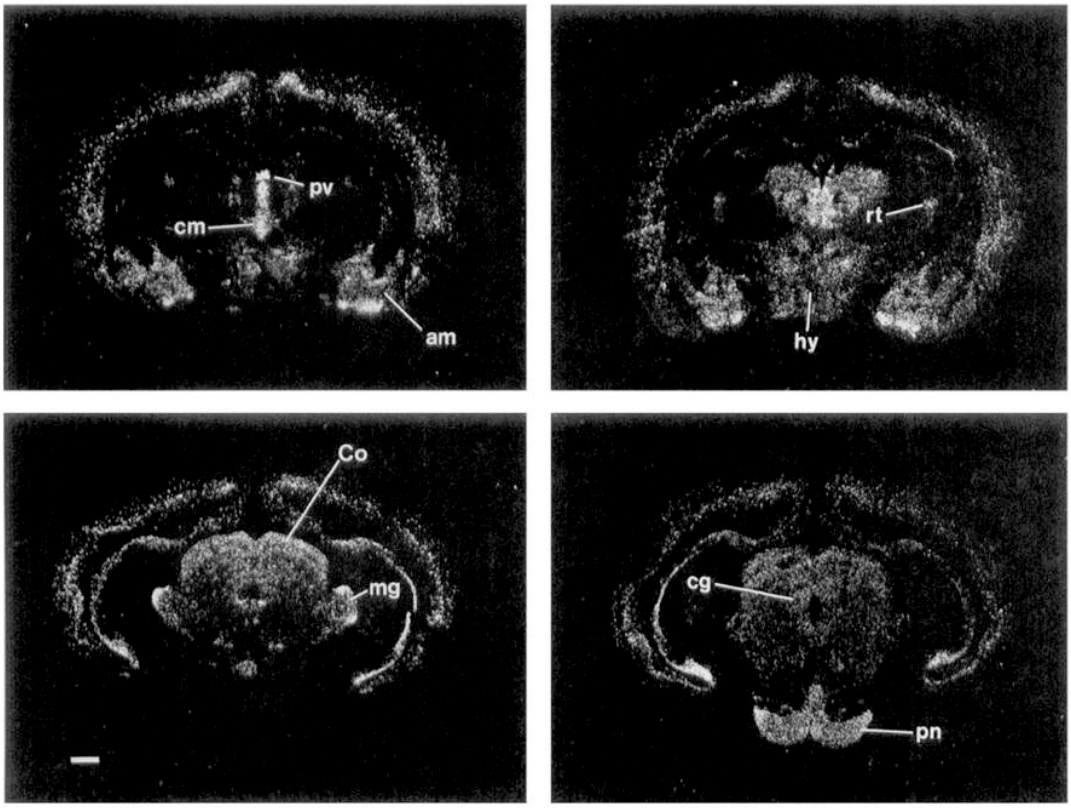

Figure 4| GluN3A subunit expression in the adult rat brain: neglected early data.

Schematic representation of hybridized coronal sections with antisense RNA probe labeled with ^{33}P. Abbreviations: am, amygdale; cm, centromedial thalamic nucleus; pv, paraventricular thalamic nucleus; rt, reticular thalamus; hy, hypothalamus; Co, superior colliculus; mg, medial geniculate nucleus; pm, pontine nucleus; scale bar: 1mm[116].

2. Properties of GluN3A subunit-containing NMDA receptors

As mentioned, GluN3 subunits participate to the formation of both diheteromeric, glycine-activated GluN1/GluN3 receptors, and of triheteromeric GluN1/GluN2/GluN3 complexes. In the former case, we are confronted with novel receptors with properties so far not encountered in neural tissues. In the latter conformation, the receptors bear some resemblance to conventional diheteromeric GluN1/GluN2 NMDARs, although several important differences suggest possibly distinct physiological functions. In the next sections, I will examine these points in more detail, shedding particular attention to the major difficulties associated with examining the properties of both recombinant and native GluN3-containing receptors.

2.1. Diheteromeric GluN1/GluN3 receptors

Since their identification in recombinant systems[112], GluN1/GluN3 receptors have represented a conundrum for researchers, to the point that many specialists have been considering them as artefactual products of recombinant systems, with no physiological interest. On one side, on a conceptual point of view, the existence of excitatory glycinergic receptors was counter-intuitive to classical dogmatic assumptions. On the other hand, their unique biophysical properties contributed decisively to the difficulties encountered in identifying their expression and physiological functions.

2.1.1. Activation of GluN1/GluN3 receptors

Activated purely by glycine, diheteromeric GluN1/GluN3 receptors possess glycine-binding sites on both GluN1 and GluN3 subunits. These sites have very different affinities for the agonist, in the nanomolar range for GluN3 and several hundred times lower, in the high micromolar range, for GluN1[123]. Although originally measured for isolated domains expressed in recombinant systems, we now know that, at least qualitatively, this difference may be maintained in native receptors[124,125]. Strikingly, binding of glycine to either GluN1 or GluN3 subunits entrains opposite functional effects.

The occupation of the high affinity site of GluN3 is indeed sufficient for channel opening, whereas binding to the lower affinity site of GluN1 leads to rapid inactivation and current suppression[105,106,124]. These properties explain the complex temporal activation dynamics of GluN1/GluN3 receptors in expression systems during application of exogenous glycine. At lower concentrations, glycine binds only GluN3 subunits, producing sub-maximal currents with minimal inactivation. As glycine concentrations increase, agonist binding to the GluN1 subunit leads to rapid channel closure with

remaining steady-state currents of much smaller amplitude with respect to the early transient peak. Interestingly, at the end of glycine applications a rebound peak can be detected, probably due to glycine unbinding from GluN1 and, thus, to transient receptor reactivation (Fig. 5). This dynamic can be observed in oocytes or other cellular recombinant systems, where glycine concentrations are controlled precisely via pressure-controlled systems, and where receptor expression levels can be high. A different scenario is instead encountered in native cells, which present an unknown pool of receptors and whose embedding in neural tissue strongly limits precise evaluations of the glycine concentrations applied. In our experience in the medial habenula (MHb) and the thalamus, graded glycine applications did not allow to reproduce faithfully the activation dynamics of the receptors described previously. Moreover, the extent of the potentiating effect of the GluN1 antagonist, CGP78608, on the responses to glycine (see results) also suggested that, overall, the inactivation effects due to glycine binding to GluN1 dominate in control conditions. Most likely, native GluN1/GluN3AR low expression levels conjoint with unfavorable electrical properties, like those encountered for example in cortical, hippocampal and/or relay thalamic cells are a plausible explanation for failed detection in the past.

Another interesting property of diheteromeric receptor currents concerns their dependence on membrane potential. Indeed, the I-V curves of GluN1/GluN3A currents are outwardly rectifying[104,125] (Fig. 6). This behavior seems to be dependent on the glycine-binding domain of GluN1, and on extracellular Ca^{2+} ions[104]. Importantly, this is the unique property so far identified that may distinguish receptors including either GluN3A, or GluN3B subunits, as the voltage dependence of GluN1/GluN3B receptors is linear[104].

Finally, in this section we want to briefly discuss the possibility that glycine may not be the only agent capable of activating GluN1/GluN3Rs in physiological conditions.

On this subject, it is of particular interest to mention the case of D-serine. D-serine is as efficient a co-agonist of the GluN1 binding site in conventional GluN1/GluN2 NMDARs as glycine, and it is naturally present in neural tissues, where it is traditionally associated with glial cell metabolism[126]. Whether, and in which conditions, the physiologically active GluN1 co-agonist is either D-serine and/or glycine, is still debated for GluN1/GluN2 NMDARs[34,48,127]. The literature existing before the onset of my doctoral activity seemed to justify the assumption that this long-standing debate does not concern diheteromeric GluN1/GluN3 receptors. Several studies indeed suggested that D-serine acts as a partial agonist of the receptors, being instead a powerful antagonist of glycine action on the binding site of the GluN3 subunit[105,112]. Our results on native receptors confirm these results.

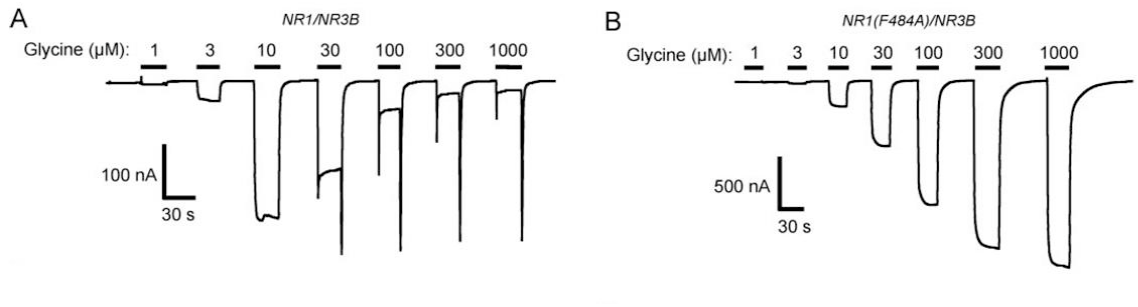

Figure 5| Preventing glycine binding to GluN1 subunits considerably potentiates glycine-induced GluN1/GluN3B currents.

A- Dose response of glycine-induced GluN1/GluN3B receptor-mediated currents. Upon agonist washout, large tail currents are observed representing re-sensitization. **B-** Dose response of glycine-evoked currents for receptors with a GluN1(F484A)/GluN3B point mutation in the S1S2 domain of GluN1, which reduces glycine binding to the subunit[105].

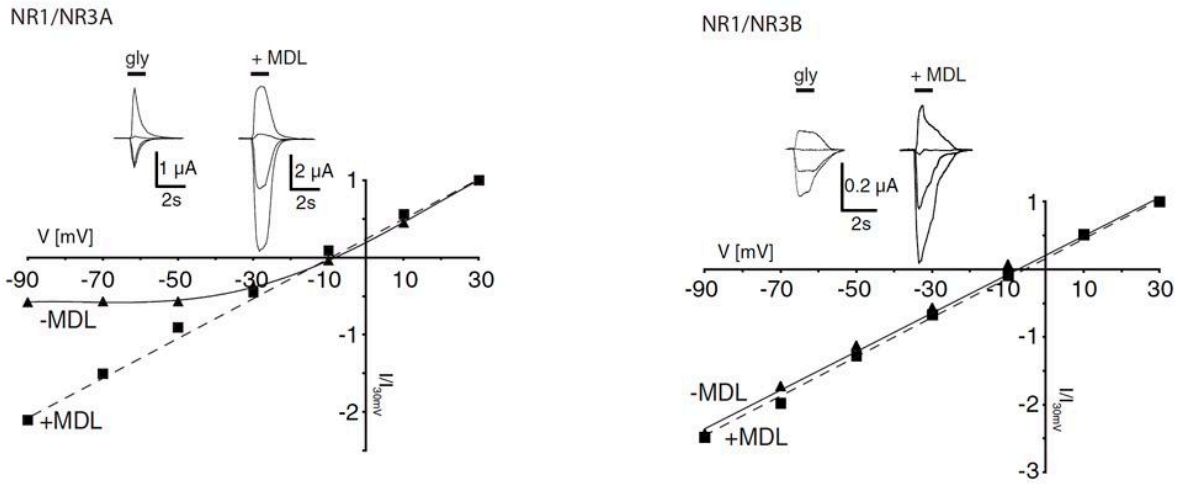

Figure 6| I-V curves of glycine-activated GluN1/GluN3 receptor currents.

Normalized I-V plots for currents mediated by GluN1/GluN3A (left) and GluN1/GluN3B (right) receptors. Currents are evoked by pressure ejection of glycine (gly, triangles) and in the presence of MDL-29951 (squares), an antagonist of the glycine binding site of GluN1 subunits[104].

At this stage, therefore, glycine remains the likeliest candidate for the role of physiological agonist of GluN1/GluN3 receptors.

2.1.2. Modulation and pharmacology of diheteromeric GluN1/GluN3 receptors

GluN1/GluN3Rs possess a rich spectrum of modulation mechanisms that may be important in physiological conditions.

The bell shape of GluN1/GluN3R dependence on glycine concentrations[112], in particular, is of great interest in this sense. Preventing glycine from binding to GluN1 indeed leads to receptors capable of producing non-inactivating currents with amplitude several folds bigger than in control conditions. This has been consistently observed in recombinant systems either expressing point-mutated GluN1 subunits, or using pharmacological agents that antagonize GluN1 with higher affinity than GluN3 subunits[105,106,124,128]. Any physiological mechanism capable of reducing glycine binding to GluN1 could thus represent a powerful amplification agent for GluN1/GluN3 receptor-generated currents. Unfortunately, at present, no such native mechanism is known.

The architecture of the receptors offers other modulation possibilities. It is indeed known that conventional GluN1/GluN2 NMDARs display a redox sensitivity mediated by two critical GluN1 cysteine residues forming a disulfide bond, which increases the magnitude of NMDAR-evoked responses when chemically reduced. Similarly to the conventional receptors, it turns out that also the agonist sensitivity and gating kinetics of GluN1/GluN3A receptors are profoundly affected by manipulating the endogenous disulfide bond of GluN3A[124]. In particular, a powerful amplification of the transient current amplitude is induced by reducing agents, together with a striking increase in the tail current following the end of glycine applications. Importantly, breaking the disulfide bonds on the receptor also leads to tonic receptor activation. These potentiating properties seem to rely almost entirely on the disulfide bond present on GluN3A subunits, and not on the one of GluN1, which is instead decisive for the modulation GluN1/GluN2 complexes[124].

Explained by a large increase of the affinity for glycine of the receptors, this fact may be relevant for controlling basal excitability levels in neurons.

GluN1/GluN3ARs are also very sensitive to pH, extracellular acidification strongly potentiating glycine-gated currents from recombinant GluN1/GluN3A receptors, with half-maximal effect in the physiologic pH range. This effect is largely due to faster recovery from slower desensitization, and is mediated by residues facing the diheteromer interface of the ligand-binding domain[129]. Relatively small changes in

extracellular pH could thus lead to modifications of neuronal excitability via potentiation of GluN1/GluN3A receptor-mediated currents. It is important to underline that, similarly to the outward rectification of I-V curves, this property is peculiar only of GluN1/GluN3A complexes, and not of GluN1/GluN3B ones[129].

Finally, GluN1/GluN3Rs are modulated also by Zinc (Zn^{2+}). Abundant in the body, the vast majority of Zn^{2+} ions are trapped within proteins as structural or catalytic cofactors. Nevertheless, a pool of loosely bound (or chelatable) Zn^{2+} ions show a restricted distribution in telencephalic regions, where it is stored in a subset of glutamatergic synaptic vesicles by a dedicated vesicular transporter. Its role as synaptic modulator has been under scrutiny for several years, because Zn^{2+} is known to allosterically inhibit conventional GluNR1/GluNR2 NMDARs in the submicromolar to micromolar concentration range[99,130]. In the case of GluN1/GluN3Rs, it was reported that Zn^{2+} acts both as a potent positive modulator of the receptors, and as a full agonist of GluN1/GluN3A receptors. The half maximal concentration for direct activation is about hundred-fold higher than for the modulatory effect[131]. Interestingly, the positive modulatory properties may be, at least in part, provided by the relief of the outward rectification properties of GluN1/GluN3AR currents[104]. I have found no data showing whether the Zn^{2+}-mediated modulation also concerns GluN1/GluN3B currents. This latter property, nonetheless, may indicate that they are not, because of the linear dependence of GluN1/GluN3BR currents on the membrane potential.

In conclusion, this richness of potential modulatory mechanisms demonstrates that the properties of GluN1/GluN3Rs are very sensitive to their microenvironment, which thus appears to be a key determinant factor for their level of activation. This reinforces the hope that, in near future, physiological mechanisms may be discovered, leading to amplification of GluN1/GluN3R-mediated currents and to easier identification of new functions in native tissues.

2.1.3. Physiological function of glycine excitatory receptors

Before the onset of my thesis activity nothing was known with precision about the possible expression of GluN1/GluN3Rs in native tissues so that many researchers in the domain were supporting the hypothesis that these receptors were artefacts of recombinant expression systems. This hypothesis was strengthened by the rather poorly convincing quality of the little available information. Only two studies indeed showed the existence of functional native GluN1/GluN3 complexes in cortical cultured neurons[112], and in olygodendrocytes[132]. In the former case, the authors reported excitation of cortical neurons during exogenous glycine puff applications, and attributed this effect to excitatory glycine receptors without bringing more supplementary evidence in support of this conclusion. Rather unsurprisingly, the same excitatory effects of glycine puffs on neurons were reported later by another research group in cortical neurons of GluN1KO mice[133], thus shedding serious doubts on the interpretation of the original data. On this point, it must be said that it is in general rather tricky to elucidate with precision the physiological effects on neurons of massive applications of anionic channel agonists because of multiple interplaying mechanisms mediating the sign of the responses in neurons (see for ex:[134]).

Concerning the expression in olygodendrocytes[132], using imaging techniques the authors showed increases in intracellular Ca^{2+} elicited by D-serine and absent in GluN3AKO mice and following application of the GluN3 antagonist CNQX. Although interesting, these data were not further expanded by the authors and thus represented nothing more significant than a hint in favor of the expression of GluN1/GluN3ARs.

The question concerning the physiological role of GluN1/GluN3 receptors was still completely open before my PhD.

2.2. Triheteromeric GluN1/GluN2/GluN3 receptors

Much more is known on the physiology (but much less on the biophysical properties) of triheteromeric GluN1/GluN2/GluN3Rs in comparison to diheteromeric GluN1/GluN3Rs. This is mainly due to identifiable physiological properties that make their presence detectable also in native neurons. Their detection is also made possible by their almost ubiquitous presence in the anterior brain at juvenile developmental stages. On one side, this fact permitted a rather comprehensive characterization, albeit developmentally limited, of their role in regions of great interest like the hippocampus, and in cortical neurons. On the other hand, however, a similar argument as for the excitatory glycine receptors is valid for triheteromeric complexes, in the sense that no data are at present

available on their functional expression in the adult brain. Even in this case, the accepted dogma concerning the lack of expression of GluN3A subunits in adult tissues has hampered initiatives aiming at analyzing their presence and function at adulthood. Thus, to our knowledge, no data have so far been published identifying GluN1/GluN2/GluN3 receptors following the first 2/3 weeks of life.

Overall, the generally accepted view is that triheteromeric GluN1/GluN2/GluN3Rs serve as brakes of synaptic activity, exerting a dominant-negative effect upon NMDAR function that regulates the stability and the maturation of synaptic structural elements (like spines) and of functional connections, and the establishment of synaptic plasticity[108,135]. I will describe some of these data in detail in a later section.

2.2.1. Biophysical and pharmacological properties of GluN1/GluN2/GluN3Rs

Co-assembly with GluN1 subunit is a necessary pre-requisite for GluN3 subunits to be released from the endoplasmic reticulum, and reach the cellular membrane in both diheteromeric and triheteromeric receptor form[136]. In the case of triheteromeric complexes, GluN3A/B and GluN1 have been shown to bind distinct GluN2 subunits, GluN2A and GluN2B in neurons[114,137], and GluN2C in olygodendrocytes[138]. It is important to specify that it is generally assumed that two GluN1 subunits assemble with one GluN3 subunit and one GluN2 subunit, although this stoichiometry was never demonstrated explicitly[139].

In recent years an important investigative effort has been devoted to understanding the trafficking mechanisms of GluN1/GluN2/GluN3Rs, with particular attention on the molecular machinery responsible for insertion into and removal from cell membranes, respectively[107]. This is potentially relevant information, because of the possible role of GluN3A-containing triheteromers in regulating forms of synaptic plasticity that are themselves expressed via regulation of receptor expression at membranes[119,140]. Similar molecular mechanisms may contribute to the role of GluN3 subunits in synaptic pruning and maturation during development[107]. In this section, however, I will not go into the detail of what is known on the signaling pathways regulating GluN3 subunit trafficking, as they do not concern the development of my experimental activity.

On a biophysical level, unfortunately, the analysis of the basic properties of GluN1/GluN2/GluN3Rs is strongly limited by the present impossibility of avoiding co-expression of conventional GluN1/GluN2Rs in recombinant systems. Indeed, transfection with plasmids encoding for GluN1, GluN2 and GluN3 subunits inevitably entrains the formation of both GluN1/GluN2 and GluN1/GluN2/GluN3 complexes (without counting also GluN1/GluN3 receptors). The ensuing current properties could

be separated and analyzed in detail only if specific pharmacological tools were available, which is unfortunately not the case at present (but see below in this chapter).

This lack of available specific tools notwithstanding, the incorporation of GluN3A/B subunits nonetheless provides NMDARs with unique and atypical properties that have been identified because of their absence in GluN3-deficient cells. These properties are similar for GluN3A- and GluN3B-containing receptors[107]. Firstly, responding to both NMDA and glutamate makes triheteromeric NMDA receptors at full right. However, there are important differences in the basic permeation properties compared with classical NMDARs. GluN3-containing NMDARs have indeed smaller single-channel conductance, much lower Ca^{2+}permeability and open probability, but longer mean open times[117,118,133,136,137]. Importantly, GluN1/GluN2/GluN3Rs are also relatively insensitive to Mg^{2+} block at hyperpolarized potentials[117,118,120,138] (Fig. 7), with subtle differences between GluN3A- and GluN3B-containing receptors[141]. This latter property is the key for detecting the presence of GluN3-containing NMDARs in whole-cell voltage-clamp experiments, the differences of the I-V curves between control and GluN3-deficient receptor currents being in our experience solid and detectable.

The present paucity of information on the basic properties of the receptors has affected also the identification and the development of pharmacological tools. It is nonetheless known that, similarly to conventional NMDA receptors, GluN1/GluN2/GluN3Rs are antagonized by APV[117], thus demonstrating that glutamate binding to GluN2 subunits remains a necessary step for activation. Furthermore, I could verify during my thesis activity that drugs antagonizing the glycine-binding sites of GluN1 and GluN3 completely block synaptic NMDAR-mediated currents, at concentrations that preferentially affect the GluN1 site (for example CGP78608, see results section). Therefore, also glycine retains its necessary function as co-agonist. A very interesting point for future research will be to elucidate the possible modulation exerted on receptor function by specifically interfering with glycine binding to GluN3 subunits. A very recent study reported the negative allosteric modulation of GluN1/GluN3 receptors by a novel compound, EU1180-438, acting specifically on GluN3 and not on GluN1 subunits[142]. This drug has not been tested so far in native systems where triheteromeric GluN1/GluN2/GluN3Rs are functional, namely for example in the associative thalamus. Our lab is nonetheless in close contact with Stephen Traynelis of Emory University, the corresponding author of this paper, and we will soon receive small quantities of the drug that we will be able to test. We will thus soon be able to verify what blocking GluN3A entrains on the function of this largely unexplored receptor type. The biophysical mechanisms determining GluN1/GluN2/GluN3R function, however, will be fully answered in the future only when

novel strategies to obtain isolated expression of these receptors in recombinant systems will be developed.

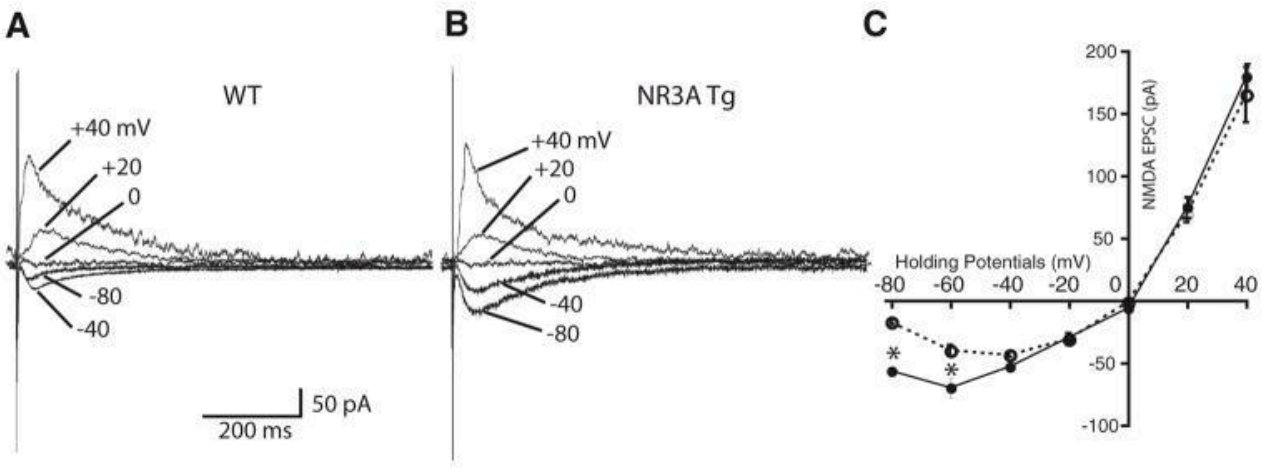

Figure 7| Transgenic over-expression of GluN3A subunits (NR3A Tg) decreases NMDAR EPSC rectification in CA1 layer hippocampal neurons.

Synaptic activated NMDAR currents were recorded in hippocampal slices prepared from NR3ATg and WT littermate mice (NR3 is the old nomenclature for GluN3 subunits). In NR3A Tg mice, GluN3A subunit expression is prolonged beyond the physiological developmental window using genetic strategies. The normalized I-V plots of the NMDAR-mediated component of the synaptic responses (**C**) show more rectification in WT (**A**) than in GluN3A Tg **(B)** neurons at hyperpolarized potentials. This illustrates the reduced block by extracellular Mg^{2+} of triheteromeric GluN1/GluN2/GluN3A receptors with respect to conventional GluN1/GluN2 receptors[367].

2.2.2. Physiological function of GluN1/GluN2/GluN3 receptors

GluN1/GluN2/GluN3 receptors and synaptic maturation

The investigations on the physiological function of GluN1/GluN2/GluN3 NMDA receptors have been greatly influenced by the conventional notion that GluN3A subunits are expressed in the brain only at early developmental stages. Before the onset of my thesis, a large part of the available evidence thus concerned mechanisms in place in the brain in the first 2 post-natal weeks, namely events related to synapse pruning and maturation and to the emergence of plasticity phenomena.

Early in development, neuronal networks are indeed characterized by an excess of weak synapses. In time, these connections undergo an intense process of remodeling, leading to the strengthening and the stabilization of only a subset of them that form long-lasting connections. This circuital refinement remains at adulthood, but is most prominent at spine-forming glutamatergic connections during critical periods of postnatal development[143].

A current view is that the subunit composition of NMDARs expressed by developing synapses influences whether specific synapses will be kept or eliminated by tuning their plasticity and signaling properties. Most studies to date have focused on the developmental switch from the expression of NMDARs containing GluN2B to classical NMDARs containing GluN2A, which correlates with the emergence of large, stable synapses and decreased pruning[144].

In this context, using genetic techniques in order to either prevent or prolong the subunit's expression, several reports have nonetheless highlighted a role for GluN3A subunits. GluN3A deletion in KO mice was shown to lead to a several fold increase in dendritic spines in cortical pyramidal neurons[137], to enhance synaptic NMDAR currents, and accelerate the developmental onset of LTP[120].

Opposite effects were obtained in transgenic models where expression was prolonged well over the physiological developmental window, with reductions of NMDAR synaptic currents and LTP, and decrease of spine density in hippocampal CA1 and striatal medium-spiny neurons[120,145].

The emerging pattern is thus consistent with a view of GluN3A subunits acting as molecular brakes for synapse maturation. GluN3A-dependent mechanisms could maintain the synapses in anatomical and functional immature states, non-apt for the development of stabilizing structural plasticity events[135]. Only following their removal

(or because of their removal via other non-identified molecular triggers), GluN3A−lacking NMDARs would permit long-term plasticity mechanisms and drive maturational changes in the general architecture of postsynaptic zones, eventually entraining synapse consolidation (Fig. 8).

The precise mechanisms, by which this braking function of GluN3A subunits on synapse stabilization is obtained, are not clear. These could include both the control of receptor/structural protein trafficking between the cytoplasm and cellular membranes with consequent changes in the organization of postsynaptic specializations, and synaptic activity-related physiological events like LTP, whose emergence is supposed to lead to stabilization of functional connections over development[120,146]. As synaptic physiologists, it is for us very fascinating to hypothesize that the reduced block of GluN3A-containing NMDARs by extracellular Mg^{2+} could be relevant because of increased activation levels of these receptors with respect to conventional GluN1/GluN2Rs.

One study has also identified a role for functional presynaptic triheteromeric GluN1/GluN2/GluN3Rs at juvenile visual cortex synapses, regulating LTD phenomena and synapse development[119]. It is nonetheless unclear whether these findings can be extended also to presynaptic specializations of other brain areas. Finally, GluN1/GluN2/GluN3Rs have been identified in olygodendrocites, where they are expressed in processes and myelin sheaths, an ideal location for sensing glutamate released from nearby cells and/or from the unsheathed axons[132,147,148].

GluN1/GluN2/GluN3 receptors in pathological conditions

Finally, I would like to briefly mention here the emerging role of Glun3 subunits in several CNS pathologies.

A growing amount of evidence has been recently accumulating associating GluN3 subunits and brain-related pathological conditions (Table 1).

Current hypotheses explain these links with the aforementioned functions of GluN3A subunits in controlling synaptic maturation and synaptic plasticity. Namely, a wrong control of the developmental window of GluN3A subunit expression could entrain abnormal changes of the architectural organization of important brain areas, in both functional and morphological terms, thus compromising both motor and cognitive

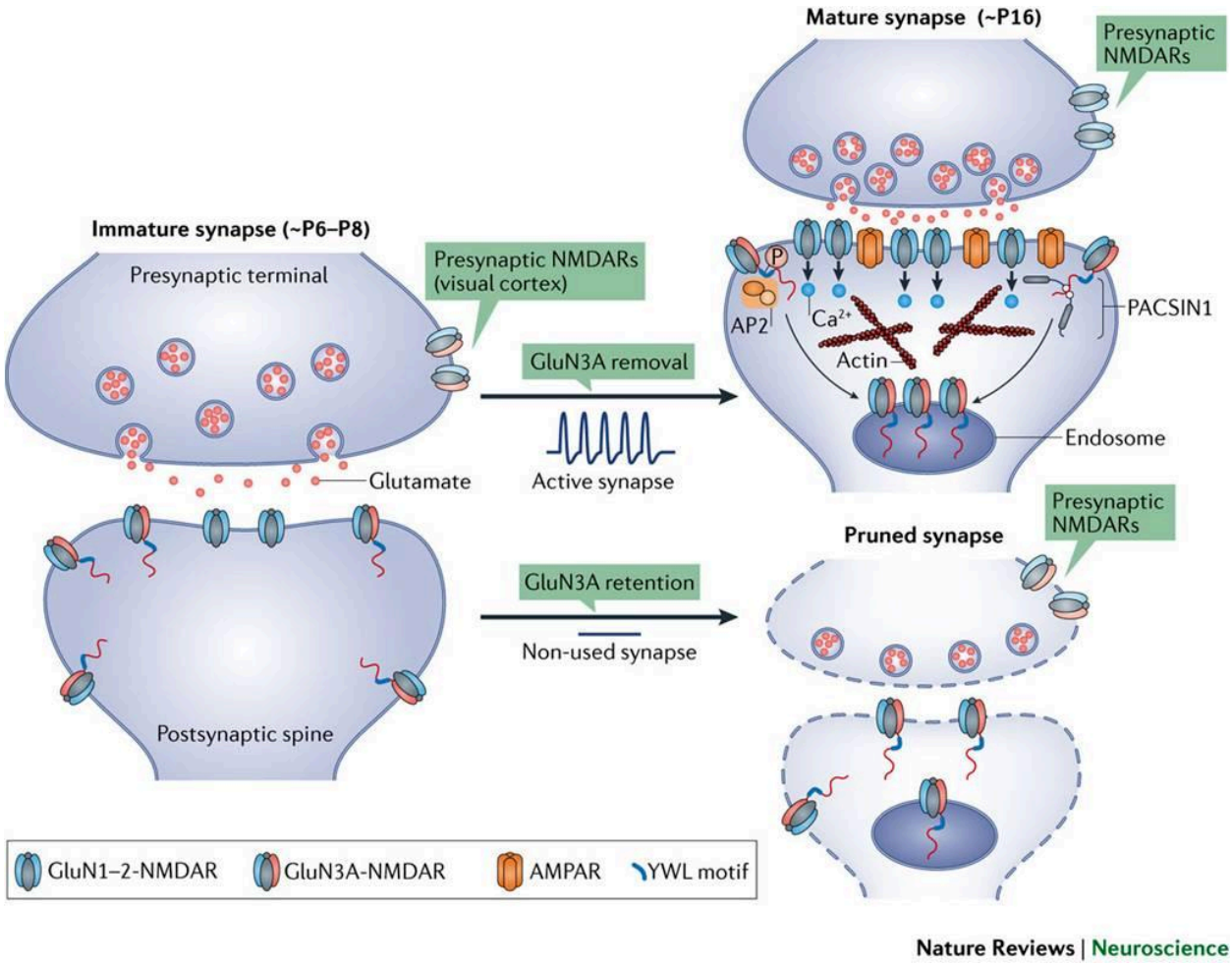

Figure 8| GluN3A-containing NMDARs: activity-dependent regulation and synapse outcome.

Schema (based on data from[120–122,137149]) showing a prototype for the possible role of activity-dependent retention or removal of GluN3A-containing NMDARs in establishing the balance between pruning and synapse maturation. During early postnatal life (~ P6-P8; left), diheteromeric GluN1/GluN2 NMDARs are clustered at the postsynaptic density (PSD) of developing immature glutamatergic synapses, whereas GluN3A-containing NMDARs exhibit extra- and peri-synaptic localization. At mature synapses (top right), endocytic removal of GluN3A-containing NMDARs is probably mediated by the molecular pathways illustrated. GluN3A-containing NMDARs are selectively removed, allowing their substitution with Ca^{2+}-permeable diheteromeric GluN1/GluN2 NMDARs. These receptors may stimulate long-term plasticity, drive the insertion of AMPA receptors into the PSD, and mediate actin rearrangements implicated in synapse stabilization. Reduced neuronal activity at certain synapses leads to the preservation of GluN3A-containing NMDARs, limiting postsynaptic stabilization and potentiation, and eventually leading to their elimination (bottom right)[135].

behavioral read-outs[120,145].

Importantly, several lines of evidence indicate modifications of both GluN3A and Glu3B function in schizophrenia in humans[150,151], a rather common (around 10% of US citizens of European origin) mutation of the latter subunit having been shown to predispose individuals to schizotypal personality traits[152].

Mutations of the GluN3A subunit are also associated with alcoholism and addiction to nicotine[135]. In contrast, cocaine leads to rapid and reversible changes in the composition of NMDARs in the ventral tegmental area (a key area for the development of addiction to this substance), with newly inserted GluN1/GluN2/GluN3ARs driving the appearance at postsynaptic sites of Glu2A-lacking Ca^{2+}-permeable AMPARs, a plastic event that probably predisposes to relapse[140].

Finally, elevated levels of GluN3A have been found in patients with Huntington disease. The possibly important role of the subunit in this severe pathology has been confirmed in mice where genetically induced reduction of GluN3A expression levels in striatal areas improved motor and cognitive symptoms and delayed neurodegeneration[145].

These reports suggest that GluN3A subunits could represent an important target for pharmacological treatment of several pathological conditions. This therapeutical potential is even more important now that we know, following my doctoral activity, that GluN3A expression is not only limited to early development, but also extends to full adulthood in areas like the habenular complex and the associative thalamus, which are heavily involved in the control of the affective responses to external stimuli and in the control of the general levels of activation of distributed cortical areas, respectively.

Overall, it can be concluded that GluN3 subunits, and GluN3A in particular, are emerging as potential key players for the regulation of brain (patho)physiological function.

Mutation	Location	Possible alleles (from dbSNP)	Phenotype	Disease association
Val132Leu	N-terminal	G/A	Possibly damaging	Nicotine dependence
Asp133Asn	N-terminal	G/A	Unknown	Schizophrenia
Val362Met	N-terminal	C/T	Increased P300 amplitude	Prefrontal cortex activation
Val362Met	N-terminal	C/T	Better associative and/or recognition memory	Episodic memory
Val389Leu	N-terminal	A/C	Possibly damaging	Nicotine dependence
Arg480Gly	N-terminal	C/G	Unknown	Schizophrenia
Arg480His	N-terminal	G/A	Possibly damaging	Nicotine dependence
Asn549Ser	N-terminal	A/C	Possibly damaging	Nicotine dependence
Asp835Asn	N-terminal	G/A	Susceptibility for Alzheimer disease pathogenesis	Alzheimer disease
Arg1024*	C-terminal	C/T	Possibly damaging	Schizophrenia
Arg1041Gln	C-terminal	G/A	Increased risk of cerebral palsy	Cerebral palsy
Arg1041Gln	C-terminal	G/A	Susceptibility for Alzheimer disease pathogenesis	Alzheimer disease
Arg1041Gln	C-terminal	G/A	Risk of post-operative delirium	Post-operative delirium
Gln1091His	C-terminal	G/C	Possibly damaging	Schizophrenia

Table 1| GluN3A mutations associations with human disease.

Table showing the association of different GluN3A subunit mutations with various diseases, including nicotine dependence, schizophrenia, Alzheimer's disease, episodic memory trouble, post-operative delirium and cerebral palsy. Abbreviations: dbSNP, single-nucleotide polymorphism database.*, Stop codon[135].

Chapter III:

The Central Thalamus And The Epithalamic Medial Habenula

CHAPTER III: CENTRAL THALAMUS AND MHB

The thalamus is a subcortical nuclear complex located in the diencephalon. Situated in an intermediate position between the brainstem and the cortex, the thalamus acts as a relay for most sensory inputs targeting different cortical areas. Thalamic outputs also project to other structures, such as the basal ganglia and the hippocampus, implicating the thalamus in different cognitive functions, among which attentional processes, memory and language[153,154]. The thalamus is an obligatory relay for all internal and external sensory modalities (from emotion and visceral function regulation to movement) except olfaction[155]. Classically, the thalamus has been described as consisting of two systems: a "specific" thalamic system (STS) that relays modality-specific information to the cortex (for example the medial geniculate nucleus, part of the auditory thalamus, representing a thalamic relay between the inferior colliculus and the auditory cortex; the ventral posterior nucleus receiving somatosensory and nociceptive inputs and projecting to the somatosensory cortex[156]), and a “non-specific” thalamic system (NSTS) comprising "non-relay" regions of the thalamus with no precise sensory modality associated with them. Nuclei from the NSTS are characterized by widespread projections to the cortex and are thus known to exert global "modulatory" effects on the targeted cortical areas[153]. The NSTS includes the anterodorsal, anteroventral and anteromedial nucleus forming the anterior thalamic nuclei; the lateral dorsal and lateral posterior nucleus forming the lateral nuclei; the central lateral (CL), paracentral (PC), central medial (CM) and parafascicular (PF) nucleus forming the intralaminar nuclei (IL) and the paratenial, paraventricular, rhomboid and reuniens forming the midline nuclei (MDL). During my thesis, we were particularly interested in the NSTS, notably the IL nuclei and the paraventricular nucleus of the thalamus (PVT). IL and MDL nuclei are often associated in what is generally defined as the “central thalamus”

1. The intralaminar nuclei

In rodents, the IL nuclei comprise two groups: a rostral group, constituted by the CM, PC and the CL; and a caudal group constituted by the PF (Fig. 9), reviewed in[157].

1.1. Afferent inputs

On a first superficial analysis, all the IL nuclei would appear to share many of their connectional characteristics. Subcortical structures seem to provide the main inputs to the IL, namely the supramammillary nuclei[158], the reticular formation[159], the pedunculopontine[160] and the laterodorsal tegmental nucleus[160], the superior colliculus[161], the deep cerebellar nuclei[162], the periaqueductal grey[163] (PAG) and the raphe[158]. In addition, the PF receives inputs from the parabrachial nucleus[164] (PB). The rostral group of the IL nuclei seem to receive denser brainstem inputs compared to the caudal group[159,160,163]. The IL also receive extensive inputs from distributed cortical areas[165].

1.2. Efferent outputs

A peculiar feature of the IL is represented by their output to distributed cortical areas. Traditionally, it has long been believed that this apparently non-specific projection pattern was at the base of the role of the IL in setting general cortical activation levels. In reality, this view has recently been challenged by findings suggesting much more specific, and thus less distributed projections for each individual IL subnucleus[157]. In general terms, nonetheless, cortical areas receiving IL inputs comprise the prefrontal cortex in its several subdivisions, the anterior cingulate cortex and the lateral entorhinal cortex. Fibers can also be found in the primary motor, primary somatosensory and gustatory visceral cortices[166].

The IL also project to several subcortical structures, such as the nucleus accumbens (NAc) and the amygdala[166]. Importantly, the IL send dense and powerful projections to the striatum, projections that for their efficacy in driving neuronal activity and in their density are comparable to cortical ones. Unlike the other IL nuclei, the PF contacts the reticular thalamic nucleus and does not project to the amygdala[166].

2. The paraventricular nucleus

The PVT is part of the midline thalamus. Located just ventrally with respect to the 3rd ventricle, it extends over a long stretch of the rostro-caudal axis of the diencephalon (Fig. 9). This fact notwithstanding, it is still not clear whether the PVT is divided in functionally distinct subnuclei, although some morpho-functional heterogeneities have been described between the anterior and the posterior PVT[167,168]. Few molecular markers have been identified distinguishing between neuronal subtypes. Similarly to all thalamic nuclei in rodents, the PVT is almost devoid of local interneurons[169,170], and is composed of VGluT2-expressing glutamatergic relay cells (VGluT2: vesicular glutamate

transporter 2). PVT cells can also express calbindin, calbindin 2 (or calb2, or calretinin) and somatostatin. In contrast, they do not express parvalbumin[171–174]. Populations expressing diverse types of dopamine receptors have been identified[167,168]. A PVT subneuronal type also expresses the receptors for oxytocin (our observation, unpublished data). Very few physiological correlates have been reported in correspondence with this potential cellular heterogeneity[167,168].

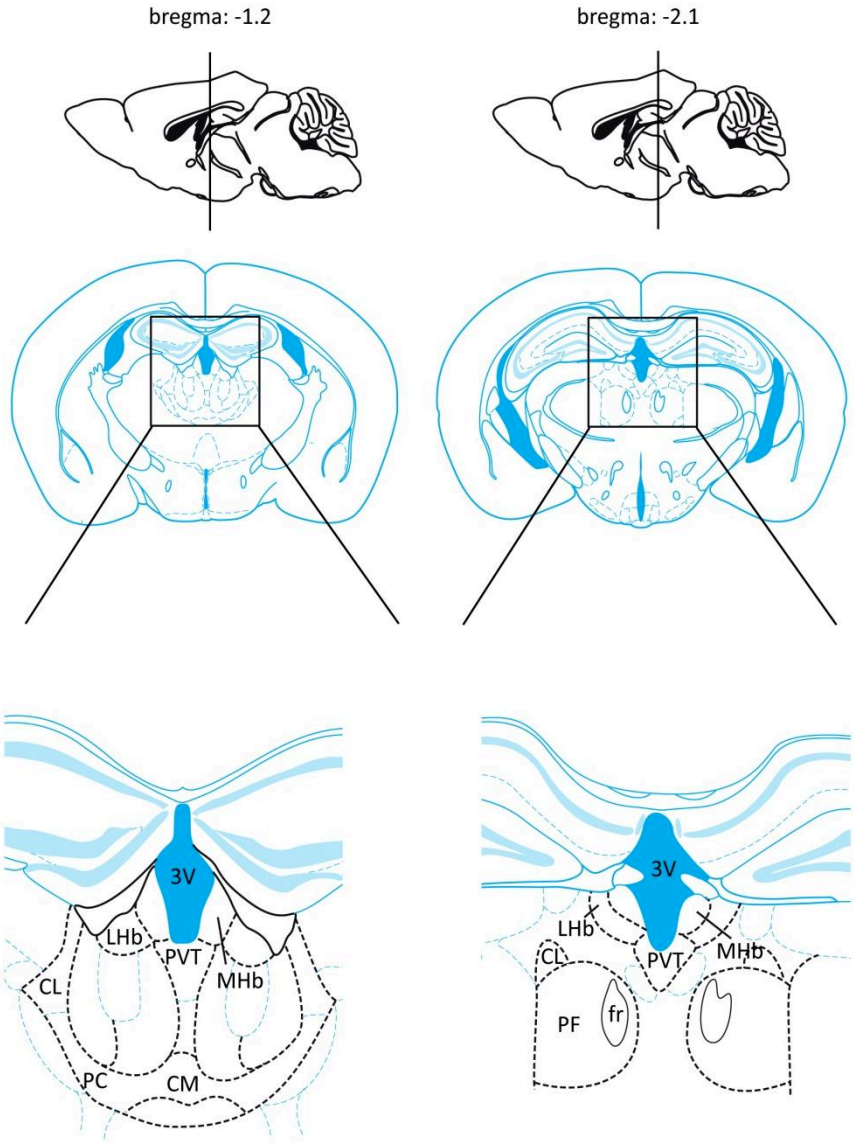

Figure 9| Coronal section of a mouse brain showing the intralaminar nuclei and the paraventricular nucleus of the thalamus.

Schematic representation of a coronal section of a mouse brain at -1.2mm (left) and -2.1mm (right) from bregma on the antero-posterior axis. The anterior section shows the CL, PC and CM of the intralaminar nuclei of the thalamus, the PVT of the thalamus, and the epithalamic medial and later habenula (Mhb and LHb). The posterior section shows the intralaminar PF, the PVT, as well as the MHb and LHb. Abbreviations: CL, central lateral nucleus; PC: paracentral nucleus; CM: central medial nucleus; PVT: paraventricular nucleus of the thalamus; LHb: lateral habenula; MHb: medial habenula; PF: parafascicular nucleus; fr: fasciculus retroflexus.

2.1. Afferent inputs to the PVT

The PVT of the thalamus receives afferences from both the cerebral cortex and the rostral brainstem. The injection of retrograde tracers in the PVT revealed inputs originating from the brainstem structures implicated in stress and the regulation of arousal such as the dorsal and median raphe, the locus coeruleus, the pedunculopontine tegmentum[175,176]. Other brainstem structures involved in nociception, visceral information and anxiety, among which we can note the nucleus of the solitary tract, the periaqueductal gray (PAG) and the parabrachial nucleus (PB),also convey signals to the PVT[177].Moreover, important structures within the limbic system contact the PVT. These includesubcortical regions such as the ventral subiculum and the amygdala, as well as cortical regions involving the infralimbic, prelimbic, entorhinal and agranular insular cortices[176,178]. In addition, the PVT isknown to receive massive inputs from the hypothalamus[179].Devoid of GABAergic interneurons, the PVT relies on inhibitory inputs from the hypothalamus, zona incerta, reticular thalamus and potentially the amygdala for inhibitory regulation[180,181](Fig.10).

2.2. Efferent outputs of the PVT

The PVTsends prominent projections to the nucleus accumbens, a structure highly implicated in addiction[182]. The massive outputs to the accumbensconfers tothe PVT a crucial role in the regulation of the behavioral read-outs generated by the modifications of neural circuits peculiar ofaddictive states[183,184].

ThePVT also innervates the bed nucleus of the stria terminalis (BNST) and the basal and central amygdala, regions highly involved in anxiety and fear behaviours. Therefore, the PVT has also been placed at the center of neural circuits underlyingfear[185,186].

As previously said, morphological differences appearbetween anterior and posterior PVT areas, namely in the distributionsof output projections. The anterior part of the PVT showsa relatively widespread efferent pattern, including outputs to thehypothalamus, the septum, the BNST, the infralimbic cortex, the hippocampus, the olfactory tubercle andendopiriform nucleus. On the contrary, projections from the posterior part are more restricted, including the BNST, the olfactory tubercle and the anterior olfactory nucleus[187–190] (Fig.10).

It is worth stating that a single PVT neuron can innervate several cortical and subcortical structures[191,192], thus coordinating the activity of multiple brain areas.

Overall, the PVT appears to be a central hub for the distribution of information from the periphery to more anterior areas, greatly apt at triggering rapid behavioral responses to a large variety of modifications of the physiological homeostasis.

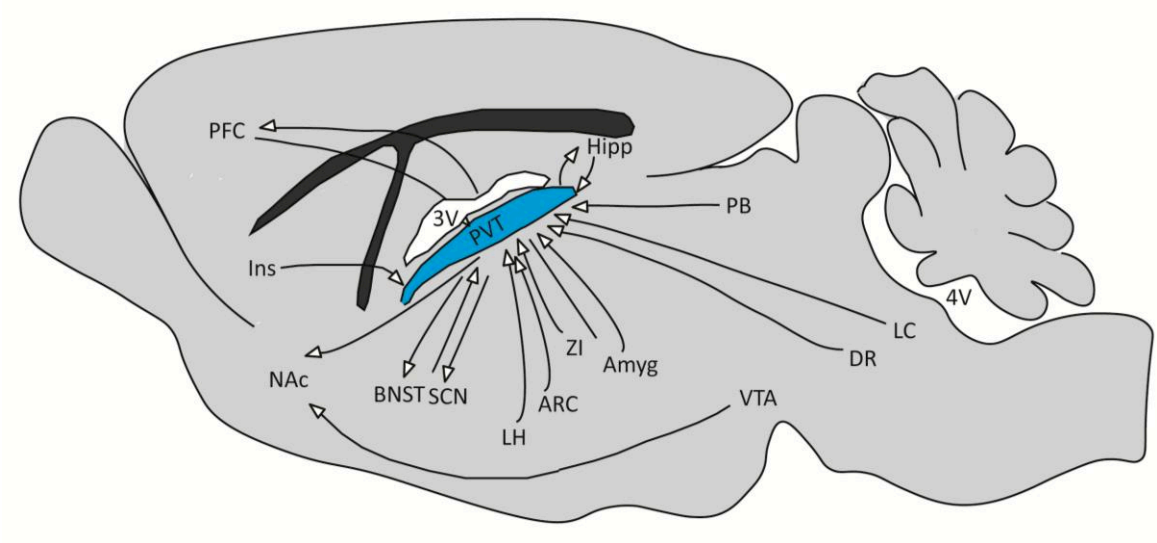

Figure 10| Sagittal section of a mouse brain showing the inputs and the outputs of the paraventricular nucleus of the thalamus.

Schematic representation of a sagittal section of a mouse brain showing the inputs (PFC, Ins, SCN, LH, ARC, ZI, amyg, DR, LC, PB, hipp) and outputs (PFC, Nac, BNST, SCN, hipp) of the paraventricular nucleus of the thalamus. Abbreviations: PFC: prefrontal cortex; Ins: insular cortex; Nac: nucleus accumbens; BNST: bed nucleus of the stria terminalis; SCN: suprachiasmatic nucleus; LH: lateral hypothalamus; ARC: arcuate nucleus; ZI: zona incerta; amyg: amygdala; VTA: ventral tegmental area; DR: dorsal raphe; LC: locus coeruleus; PB: parabrachial nucleus; hipp: hippocampus; 3V: third ventricle; 4V: fourth ventricle; PVT: paraventricular nucleus of the thalamus.

3. Functional specializations of the central thalamus

3.1. Role in arousal and awareness

3.1.1. Role of the IL in wakefulness

At the outset of modern neuroscience research in the 20th century, Giuseppe Moruzzi and Horace Magoun showed that the reticular formation (RF) of the brainstem plays a critical role in wakefulness[193]. Indeed, a lesion of the reticular formation triggered a comatose state in the cat, whereas its stimulation produced a state of arousal. This brain region was therefore called the ascending reticular activating system (ARAS).

Given their strong brainstem inputs, the IL (and the MDL) are believed to be a part of the ARAS. For instance, IL neurons have been shown to receive monosynaptic afferences from the RF and to form in turn monosynaptic connections with several cortical areas[194]. Moreover, many functional imaging studies showed that IL activation correlates with wakefulness levels[195,196]. In line with this, studies revealed the involvement of the IL in auditory vigilance[197] and visual awareness[198]. In persistent vegetative states, the functional connectivity between the IL/MDL nuclei and the cortex is often greatly reduced[199]. Additionally, sudden onset of coma can occur after small bilateral lesions affecting the IL[200].

Highlighting their function in controlling consciousness, directly stimulating the IL using deep brain stimulation (DBS) was proposed as an experimental therapeutic strategy capable of inducing long term changes in the cortex. A recent study conducted on a 38-year-old patient in minimally conscious state for 6 years demonstrated that DBS of the midline thalamus can partial reinstate arousal and improve behavioral responsiveness[201]. However, it is to be noted that the patient remained incapable of regaining the capacity to reliably communicate despite neuroimaging data displaying well-preserved large-scale cerebral language networks. In rodents, microinfusion of an antibody specific for a potassium channel type present in midline thalamic neurons was sufficient to reinstate vigilance[202]. Similar results were recently obtained in primates following stimulation of the CL[203].

Our laboratory has recently shown that optogenetic activation of a powerful inhibitory projection to the IL originating from the pons in freely moving mice led to an immediate and reversible behavioral arrest, as well as to a rapidly reversible interruption of awake cortical activity with the induction of sleep-like large amplitude slow waves[204]. These latter experiments importantly demonstrated that the basal activity of the IL is necessary for vigilance.

The role of the IL in controlling vigilance is supported also by a recent report showing a key role for the CM nucleus in the transitions between non-REM sleep and wake[205,206].

It is important to mention that neither the IL nor the MDL would necessarily "produce" or "generate" awareness directly, but rather that they could promote the "entry into a functional mode involved in the control of states of consciousness and perceptual awareness"[207].

This action is probably due to the long-known capability of the central thalamus to drive global cortical rhythmic activity, as it was shown in the middle of the 20th century by Jasper and colleagues, who were the first researchers to demonstrate that low and high stimulation frequencies of the IL led to either the synchronization or desynchronization of large cortical areas, respectively[208]. This capacity of the IL of controlling global cortical activity was recently confirmed with more modern investigative approaches by a study that highlighted, in particular, the role of the CL nucleus in this task[209].

3.1.2. Role of the PVT in wakefulness

Evidence suggests that the PVT is linked to the circadian pacemaker system. The dominant circadian pacemaker in the anterior hypothalamus of the mammalian brain (the suprachiasmatic nucleus, SCN) projects directly to the PVT[210–212]. It also projects to the dorsomedial nucleus and subparaventricular zone of the hypothalamus that in turn send efferences to the PVT[213–215]. Reciprocally, the PVT projects to the SCN[189,190,216]. Moreover, the cells in the PVT express prokineticin 2, a protein that plays a role in the regulation of biological rhythms[217].

Another interesting feature of the PVT related to the control of vigilant states, is provided by the expression of melatonin receptors[218]. Melatonin is a hormone secreted by the pineal gland. Its release peaks at night, providing the SCN with information on the duration of darkness[219–221]. Furthermore, it has been shown that glutamatergic neurons of the PVT are highly active during vigil states[222]. Suppressing PVT neural activity induces a decrease in the time spent in vigilance, whereas activating PVT neurons causes transitions from sleep to wakefulness and accelerates the emergence from general anesthesia. In addition, PVT-NAc and lateral hypothalamus-PVT pathways seem to mediate at least part of these effects[222]. Overall, the PVT thus appears to be a key element in the control of wakefulness and of its bidirectional transitions with sleep states.

3.2. Role of the PVT in addiction

Interestingly, in addition to its role in arousal[157,223], the PVT has been identified as a key hub of neural circuits underlying drug addiction[224–227]. From an anatomical point of view, the PVT interacts with brain regions implicated in motivation and reward[224], as exemplified by the prominent PVT inputs to the NAc[183,184].

Three stages characterize the development of addiction-associated behaviors in animal models: acquisition, withdrawal/extinction, and reinstatement[228,229]. The acquisition stage represents the phase where drug use escalates[230] (via direct intervention of the experimenters or through self-administration). During the withdrawal/extinction phase, the animal is denied access to the drug, resulting in negative withdrawal symptoms[231]. The reinstatement stage follows drug seeking behavior termination (after forced or spontaneous extinction). In this stage, animals are re-exposed to the drug-related cues or environmental context, often leading to relapse[232]. The PVT contributes to all the different stages of drug addiction.

Several reports show PVT activation following exposure to an array of addictive substances, such as morphine[233,234], amphetamine[235], cocaine[236], nicotine[237] and ethanol[238]. Interestingly, ethanol drinking led to an increased activation of the anterior but not of the posterior PVT[239]. Moreover, it was demonstrated that the lateral hypothalamus-PVT pathway is activated upon ethanol drinking and nicotine administration[227,240], whereas acute exposure to morphine or amphetamine activated PVT-NAc connections[184,191]. These data suggest that drugs of abuse can distinctly affect subregions and pathways involving the PVT. Moreover, recent findings indicate that NAc-projecting PVT neurons are implicated in morphine withdrawal[184]. Furthermore, an increase in PVT neuronal activation is observed upon re-exposure to drug-linked stimuli and environment contexts[241–243].

Additional studies further highlight the importance of PVT activity in drug addiction regulation. Indeed, overall suppression of PVT activity led to a significant reduction of drug seeking behavior[241,244], and suppressing the PVT-NAc pathway reduced cocaine self-administration[245] and symptoms of morphine withdrawal[184].

The role of PVT inputs to other brain areas implicated in addiction such as the BNST and the amygdala are yet to be elucidated.

Taken together, these findings convincingly support the notion that the PVT holds a central place within the neural circuits that control drug addiction, at all levels of its development during drug abuse.

3.3. PVT and feeding

The PVT is implicated in even more physiological events. For example, it also contributes to food intake control and appetitive motivation. Research indeed shows activation of PVT neurons after food intake[246]. Lesions of the PVT led to significant increase of food consumption and body weight[247], and inhibition of PVT neurons induced an increase in chow intake[181,248]. In contrast, PVT activation reduced food intake[181].

Optogenetically activating GABAergic inputs from the Zona Incerta (ZI) to the PVT promoted a robust increase in food intake[181], similarly to the GABAergic afferences from the lateral hypothalamus that provoked hyperphagia[181].

The activation of hypothalamic agouti-related protein (AgRP) projecting to the PVT also induced an increase of food consumption[249]. Further highlighting the implication of the PVT in feeding, a recent study has identified a sub-population of "glucose-sensing" neurons within the PVT that project to the NAc[250]. Specifically activating this population of neurons led to an increase in the motivation to acquire sucrose, whereas silencing this population of neurons prevented glucose sensing[250].

In addition, cues associated with delivery of food strongly trigger the activation of PVT neurons. Rats under food restriction presented enhanced PVT cell activation before food delivery[251], and optogenetic inhibition of NAc-projecting neurons in the anterior PVT enhanced cue-induced sucrose inquiry, only when the reward was withheld.

The PVT thus serves a crucial role in regulating food intake and food-seeking behavior. Although recent investigations are starting to reveal the complexity of the PVT and the mechanisms responsible for its contribution to feeding behavior, much more is yet to be learned to fully understand PVT functions in food intake control.

3.4. Role of the PVT in affective behavior

The PVT also acts as a stress sensor in the mammalian brain, as it is activated by both psychological and physical negatively-valued stimuli[252,253]. This important property of this nucleus is probably mediated by its powerful connections with several brain areas involved in regulating negative emotional states and in signaling potentially noxious sensory events, like the amygdala, the PB and the PAG.

3.5. The PVT and fear memory retrieval

The PVT plays a crucial role in fear memory retrieval. It has been shown that lesions in the posterior PVT attenuated fear expression[254]. Furthermore, PVT projections to the

amygdala are necessary for both fear memory consolidation and fear memory retrieval[178,186]. The PVT is particularly critical for fear memory retrieval at the 24h time point following conditioning.

3.6. The PVT-amygdala circuit

PVT inputs the amygdala play several physiological functions. The majority of PVT inputs to the amygdala target the central lateral nucleus of the amygdala (CeL)[189,190]. In the rat, lesions in the PVT generated a significant increase in cFos expression in CeL neurons in response to stress[252]. Similarly, an increase in cFos expression in the CeL was also observed during a fear retrieval task as the PVT was inactivated[255]. Interestingly, CeL inhibiton also seems to play a crucial role in fear memory retrieval[256,257]. It is thus hypothesized that the PVT could promote CeL inhibition by activating GABAergic somatostatin-expressing cells in the CeL[186,258], and thus controlling fear memory retrieval.

3.7. Role in aversion and negatively-valued emotional states

Consistent with this general context, it has been shown that functional impairment of the PVT results in a heightened vulnerability to stress, anxiety and depressive-like phenotypes comprising lack of motivation, anhedonia and despair[185,259]. An exposure to different stressors such as foot shock, restraint, and ether led to an increase of PVT neuronal activity[253,260–262] indicating that the PVT is implicated in responses to stressful situations regardless of the nature of the stimulus. Furthermore, the PVT seems to be engaged in conditions of chronic stress (but not acute stress[263]) and is necessary for the facilitation and habituation of the hypothalamic-pituitary-adrenal axis[264–266]. Pharmacologically activating the PVT generated fear-like behavior[267]. As stated earlier, the PVT is also implicated in addiction-related behavior, notably in negative states triggered by drug withdrawal[226]. Other data showed that blocking orexin receptors in the PVT reduced the expression of negative emotional states following morphine withdrawal[268].

Together, these findings portray a potential role for the PVT in stress, fear expression and aversive states. Moreover, together with the suggested role of the PVT in modulating sleep and wake states, they also suggest that this important MDL nucleus may represent an efficient physiological alarm system responsible for triggering behavioral responses to potentially dangerous external stimulations, and for regulating vigilance levels accordingly.

The multiplicity of functions mediated by both the IL and the MDL (namely the PVT in our case) highlight the importance of investigating the synaptic mechanisms determining information transfer through them. This was a major goal of my doctoral research activity.

4. The Medial Habenula

The Medial Habenula (MHb) forms the epithalamus, together with its lateral habenular counterpart (LHb), and the pineal gland. A small but easily identifiable structure, bilaterally juxtaposed to the 3rd ventricle, the MHb relays afferent information from medial and posterior septal regions[269–271] (MS and PS, Fig. 11) to caudal neuromodulatory nuclei. Its control on brain neuromodulation is exerted via the interpeduncular nucleus (IPN), which constitutes the almost exclusive postsynaptic target of the fasciculus retroflexus (fr), the fiber bundle formed by habenular axons that is a morphological hallmark of the rodent brain (Fig. 11). Importantly, the prevalently GABAergic projections from the IPN have long been known to impinge onto a variety of mid- and hind-brain structures deeply implicated in the regulation of affective states, and in the neurophysiology of addiction[272–274]. Further acknowledging its physiological relevance, this morphological organization is present and maintained in virtually all vertebrates.

These facts notwithstanding, the functions of the MHb have long been neglected, especially when compared to the well-determined role of the LHb in reward processing and goal-directed behaviors. Only in recent years an increasing number of studies have firmly established the involvement of the MHb-IPN axis in a large spectrum of behavioral responses, namely to pain, stress, anxiety, and fearful stimuli[270,271,275–277]. The synaptic physiology of the MHb has also emerged as a domain of investigation of unequalled interest, following the recent identification of unique molecular mechanisms contributing to information transfer[125,277].

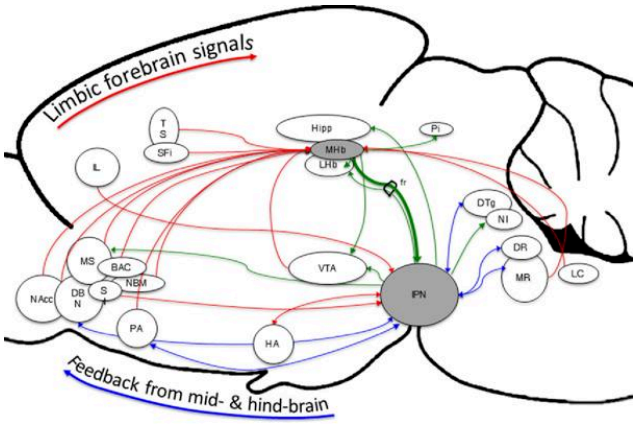

Figure 11| Afferent and efferent connections to the MHb-IPN pathway.

Red lines indicate afferent projections to the MHb or IPN, and green lines identify efferent pathways (from McLaughlin et al., 2017[272]).

On a cellular level, the MHb is composed exclusively of excitatory neurons, and hosts no local interneurons [278]. MHb cells are either only glutamatergic (in its dorsal subdivisions, dMHb), or mixed glutamatergic/cholinergic (in the ventral part), and project to the IPN without forming local functional connections. Although apparently homogeneous, medial habenular neurons likely form a highly heterogeneous population, as suggested by recent data associating the specific expression of molecular markers[279,280] with distinct physiological properties[280]. Furthermore, the projections to the IPN have long been known to follow a precise topological organization[281], thus suggesting that separate cell subpopulations in the MHb may mediate distinct behavioral read-outs via dedicated neural circuits. A more detailed analysis of these subtypes in the context of well-defined behavioral tests appears thus necessary in order to elucidate the spectrum of physiological functions of the MHb.

A striking contrast exists between the extent of available knowledge on the morphological organization of the MHb, and the dearth of information on its synaptic properties and functions. Very little is indeed known regarding the synaptic physiology and the mechanisms controlling neuronal excitability in the MHb. It has long been known from morphological studies that the MHb receives GABAergic and glutamatergic afferents from MS and PS areas, respectively[282]. Functionally, recent reports have shown that GABAa receptor-mediated currents increase, rather than decrease, MHb neuronal excitability [283]. The physiological implications of this intriguing property remain elusive. Earlier reports also suggested the existence of mixed purinergic/glutamatergic postsynaptic currents in MHb neurons produced by PS afferences. The validity of these data was later disputed. Only recently our team clarified these contradictory data[278]. Using both classical and optogenetic investigation methods, the nature of the PS inputs to the MHb was shown to be purely glutamatergic, and not mixed. A comprehensive description of the unusual dynamic properties of PS synapses onto MHb cells during physiologically relevant stimulation patterns was also provided, and allowed the authors to assess some behavioral implications of the activity of these excitatory afferences.

The atypical properties of both glutamatergic and GABAergic inputs to the MHb conjoint with the specific properties of MHb cellular organization (i.e. the complete absence of both local inhibitory neurons, and of local functional connections) raise important questions about the modalities of information transfer through the medial habenular relay.

Overall the many facets of MHb physiology that remain undisclosed, stress the urgency for a more comprehensive identification of how molecular, synaptic and cellular properties are integrated and translated into the circuital activity determining the possible (dis)functions of this important information route.

Chapter IV:

The Parabrachial Nucleus

CHAPTER IV: THE PARABRACHIAL NUCLEUS

The parabrachial nucleus (PB) is located in the dorsolateral part of the rostral brainstem, where it surrounds the superior cerebellar peduncle (scp). The scp divides the lateral from the medial subdivision of the PB[284], which, in turn, are themselves further separated into multiple sub-regions[285].

The PB is known to receive inputs from the nucleus tractus solitaries, the dorsal laminae of the spinal cord and from various forebrain regions[286–293]. Its main projections include forebrain regions such as the thalamus (the PVT, among others), the amygdala, the cortex, the BNST and the hypothalamus[177,294–296]. Thus, the PB may act as a relay transmitting sensory information from caudal to forebrain structures, and receiving afferent feedback from some of the same regions it targets.

Interestingly, the PVT, our main nucleus of interest, receives strong glutamatergic inputs from the PB. Consistent with this, the PB has been shown to be implicated in similar roles as the PVT, namely pain, responses to heat and cold, taste and aversion[287,297–300]. The majority of cells in the PB are glutamatergic and express the vesicular glutamate transporter VGluT2. However, the PB is remarkably heterogeneous as to neuropeptides, transcription factors and receptors expression (Table 2). Intriguingly, sub-cellular groups show diverse and only partially superimposing localization within the PB and projection targets. As an example, not all PB sub-populations project to the PVT. Consistently with this picture, distinct behavioral outcomes are associated with separate sub-groups. Barik et al (2018) provided a rather detailed description of the targets contacted by several PB cell types, in particular highlighting that PB neurons expressing prodynorphin (Pdyn) and melanocortin 4 receptor (MC4R) project to the PVT[301] (Table 3). During my thesis work, neurons expressing Pdyn and MC4Rs thus became key centers of attention of my investigation, although I extended my analysis to several other sub-populations including cells expressing calcitonin G related peptide (CGRP), oxytocin receptor (OxtR) and calbindin 2 (calb2, or calretinin), which are other markers defining PB neurons.

Transcription factors
Foxp2
Lmx1b
Satb2
Neuropeptides
Calcitonin gene-related protein
Cholecystokinin
Corticotropin releasing hormone
Neurotensin
Prodynorphin
Pituitary adenylate cyclase-activating peptide (PACAP)
Tachykinin 1 (substance P)
Proenkephalin
Receptors
Bombesin subtype 3 receptor
Corticotropin releasing protein receptor 1
Leptin receptor
Mu opioid receptor
Melanocortin 4 receptor
Neuropeptide Y receptor 1
Oxytocin receptor
G-protein couple receptor 88
Tachykinin 1 receptor
Other
Cerebellin 4
Calbindin 2

Table 2| Genetic markers identified in cell subtypes of the PB nucleus.

PB cell type	PVT
PB^{Vglut2}	✓
PB^{Tac1}	-
PB^{CGRP}	-
PB^{Nts1}	-
PB^{Pdyn}	✓
PB^{Chat}	-
PBTh	-
PB^{MC4R}	✓
PB^{Grp}	-

Table 3| Neuronal PB sub-groups projecting to the PVT.

Abbreviations: PB, parabrachial nucleus; PVT, paraventricular nucleus of the thalamus; VGluT2, vesicular glutamate transporter; Tac1, tachykinin Precursor 1; CGRP, calcitonin related polypeptide alpha; Nts1, neurotensin receptor 1; Pdyn, prodynorphin; Chat, choline acetyltransferase; Th, tyrosine hydroxylase; MC4R, melanocortin 4 receptor; Grp, gastrin-releasing peptide.

1. CGRP-expressing neurons in the PB

CGRP stands for calcitonin gene-related peptide. CGRP is a potent peptide vasodilator and has been shown to play a role in the transmission of nociceptive information[302,303]. In the PB, CGRP-expressing neurons reside within the external later region (Fig. 12). They mainly project to the amygdala (primarily to the "nociceptive" region of the central lateral amygdala), the BNST, the thalamus, the hypothalamus and the cortex[304].

1.1. Role of CGRP-expressing neurons in satiety and anorexia

CGRP-expressing neurons in the PB are implicated in feeding control. For instance, photoactivation of CGRP neurons in the PB was shown to reversibly inhibit feeding in hungry mice[304]. Moreover, CGRP neurons are activated after a large meal and their inactivation led to continuous food consumption[305]. This indicates that the activation of CGRP-expressing PB neurons could play a role in facilitating meal termination. Interestingly, when mice were presented with highly palatable food for the first time, CGRP PB neurons were activated and the mice took a longer time to consume it[305]. The rise of activity of CGRP neurons in the PB correlates with neophobia, a stereotypical negative reaction to novelty whose function is protecting animals from consuming potentially toxic food. Furthermore, CGRP neurons were activated following gastric bypass surgery[306], suggesting a potential role in the weight and appetite loss that result from this surgery[307,308].

CGRP-expressing PB neurons seem to be implicated also in the onset of conditioned-taste aversion (CTA). CTA is a behavioral paradigm that consists in pairing the consumption of a novel food with an injection of sickness inducing substances, typically lithium chloride (LiCl)[309,310]. LiCl injections cause rodents to feel sick and nauseous, leading them to avoid the consumption of a novel food after pairing. Interestingly, CTA can be generated by pairing novel food presentation with photoactivation of CGRP-positive PB neurons, thus demonstrating that CGRP-expressing PB neurons activation can lead to the creation of aversive associations related to feeding[311].

Finally, CGRP neurons appear to be involved in cancer-induced anorexia. A variety of cancers are known to cause cachexia, a syndrome often associated with anorexia, malaise, lethargy and muscle wasting[312]. Some cancer treatments that cause nausea activate CGRP-expressing PB cells[313]. Moreover, the anorexia and lethargy promoted by cancer progression can be relieved by inactivation of CGRP PB neurons[313]. These

observations indicate that illness-induced anorexia could be mediated by CGRP-expressing neurons in the PB.

1.2. CGRP-expressing neurons, fear and pain responses

Pain is an extremely efficient teacher. Animals rapidly learn to associate a conditioned stimulus (CS) that consists of an environmental cue to a painful unconditioned stimulus (US). Following learning, CS presentation alone elicits aversive behavioral responses (flight or freeze, for the example), which spontaneously and gradually disappear in time (normally within days in mice) if the association between US and CS is not reinstated. This phenomenon is known as fear conditioning[314].

CGRP-expressing neurons in the PB play an important role also in responses to pain. Indeed, the external lateral PB (where CGRP-expressing cells reside) is activated in response to both visceral (rectal balloon) and somatic pain (pinches and heat)[293]. A pathway originating from the dorsal laminae of the spinal cord, passing by the PB and targeting the amygdala was uncovered[293].

Moreover, CGRP-expressing PB neurons were activated in response to foot shocks[315] and fear memory was successfully established when optogenetic activation of CGRP-expressing PB neurons was associated with a novel environment[315]. In line with this, the induction of fear memory induced by foot shocks was significantly attenuated after the inactivation of CGRP-expressing PB neurons with tetanus toxin[315]. Furthermore, after pairing a CS with an US (a tone with a foot shock), CGRP PB neurons were activated upon presenting the tone alone[316]. CGRP PB neurons are also responsive to thermal and irritating harmful stimulations. Exposure of mice tails to a temperature that exceeds 44°C, and administration of chloroquine, an itch-inducing compound, indeed activated nearly all CGRP-expressing PB neurons[316,317]. In case of chloroquine, its noxious scratching effects are greatly reduced if CGRP neurons were inhibited[316,318].

Overall, these studies reveal the importance of CGRP-expressing PB neurons in fear learning and in the establishment of fear memory, and in the physiological responses to pain.

1.3. Role of CGRP-expressing neurons in sensory modalities

In addition to their role in satiety, anorexia and pain, evidence has been presented that CGRP-expressing PB neurons are also implicated in sleep apnea[319]. It has been shown that asphyxia, which is a dangerous symptom of sleep apnea, activated CGRP-expressing

PB neurons. In fact, CGRP cells within the PB transmit life-threatening hypercapnic conditions to the extended amygdala to promote arousal[320].

Moreover, other sensory modalities, such as loud noise, moving objects, fox odor, bitter taste, vestibular disturbance activate the lateral PB subdivision hosting CGRP cells[321–323]. Thus, CGRP-expressing PB neurons seem to receive inputs from several primary sensory systems, and to transmit alarm signals to posterior brain areas.

2. OxtR-expressing neurons in the PB

The lateral region of the PB nucleus also contains neurons that express the receptors for oxytocin (OxtR)[324] (Fig. 13). Oxytocin (Oxt) is a neuropeptide that exerts a wide spectrum of peripheral and central effects. The actions of Oxt range from establishment of bonding and complex social behaviors in relation to care for offspring and reproduction to the modulation of neuroendocrine reflexes[325]. OxtRs are expressed in several brain areas and are responsible for "mediating the central effects of oxytocin"[325]. Chemogenetic activation of OxtR-positive PB neurons caused drinking inhibition in thirsty mice without any effect on food intake; however, following dehydration, the activation of OxtR-positive PB neurons prevented excessive NaCl consumption[325]. In contrast, the inactivation of OxtR-expressing PB neurons led to an increase in drinking. Furthermore, OxtR-expressing PB neurons receive direct inputs from Oxt neurons located in the paraventricular nucleus of the hypothalamus and the nucleus of the solitary tract, and project to multiple brain regions implicated in water intake[325]. Thus, OxtR-expressing PB neurons seem to play a key role in fluid intake regulation by decreasing water/saline intake and preventing hypernatremia and hypervolemia.

3. Pdyn-expressing neurons in the PB

The PB is also involved in thermoregulation. There are indications that physiological and behavioral responses to non-noxious heat (but not cold) are relayed by neurons expressing Pdyn in the PB[326] (Fig. 14). Pdyn is an opioid polypeptide hormone. It is a precursor of endorphins involved in pain, learning and memory[327]. Pdyn-expressing PB neurons mainly project to the preoptic area[326,328], although outputs to the thalamic PVT have recently been hinted at[301]. They are thought to be crucial mediators of thermoregulation, although recent reports identified a role for them both in regulating satiety by relaying mechanic gastric information on ingestion[329] and in transmitting pain information[330].

4. MC4R and Calb2 PB neurons

MC4R is a receptor for melanocortin. It has been shown to be involved in feeding and sexual behavior, the regulation of metabolism, and male erectile function[331–333]. Calb2 (also known as calretinin) is a calcium-binding protein involved in calcium signaling[334]. Calretinin plays a crucial role as a modulator of neuronal excitability and is involved in the induction of LTP[335]. Not much is known about the role of neurons expressing MC4R and Calb2 within the PB (Fig. 15-16). Some neurons in the lateral PB have been shown to relay taste sensations to the thalamus[323]. Others have been implicated in reward and aversion regarding food intake[336,337]. Other unidentified subpopulations of cells within the PB are involved in cardiac function modulation[338] and behavioral and physiological responses to cold[328]. The molecular identity of these neurons has not been uncovered until present.

We can nonetheless speculate that MC4R and/or Calb2 neurons could be involved in one or more of these functions. Similarly to all other identified cell types in the PB, both Calb2- and MC4R-positive cells are located in specific areas of the PB. For example, MC4R and CGRP cells are mainly concentrated in the medio-dorsal and ventro-lateral areas of the lateral PB, respectively, with basically no superposition. Pdyn cells instead lie in between, with a minority of neurons “invading” areas mainly characterized by other molecular markers like CGRP (see for ex[324]). The emerging pattern suggests that these morphological segregations in the PB also correspond to distinct input/output patterns and, thus, to clearly separate physiological functions.

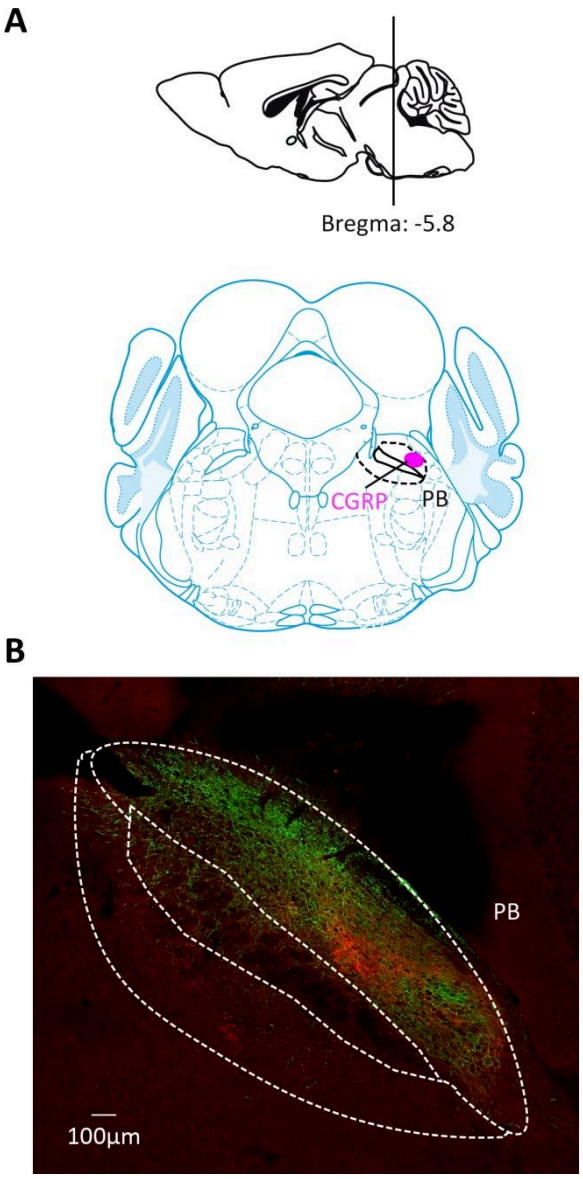

Figure 12| Coronal section of the parabrachial nucleus of the brainstem: localization of OxtR- and CGRP-expressing neurons.

A- Schematic representation of a coronal section of the mouse brain showing the position of CGRP-positive neurons in the ventro-lateral region of the PB. **B-** Confocal image of the PB (delineated by the white dotted line) of an adult WT mouse. The green fluorescence stems from neurons infected with a mix of an AAV expressing the recombinase Cre under the control of the Oxytocin receptor promoter (AAV2/OxtR.Cre) and an AAV expressing YFP in a Cre-dependent way (AAV2/DIO.Chr2-YFP). CGRP-positive cells (red) were revealed by immunocytochemistry using a specific antibody.

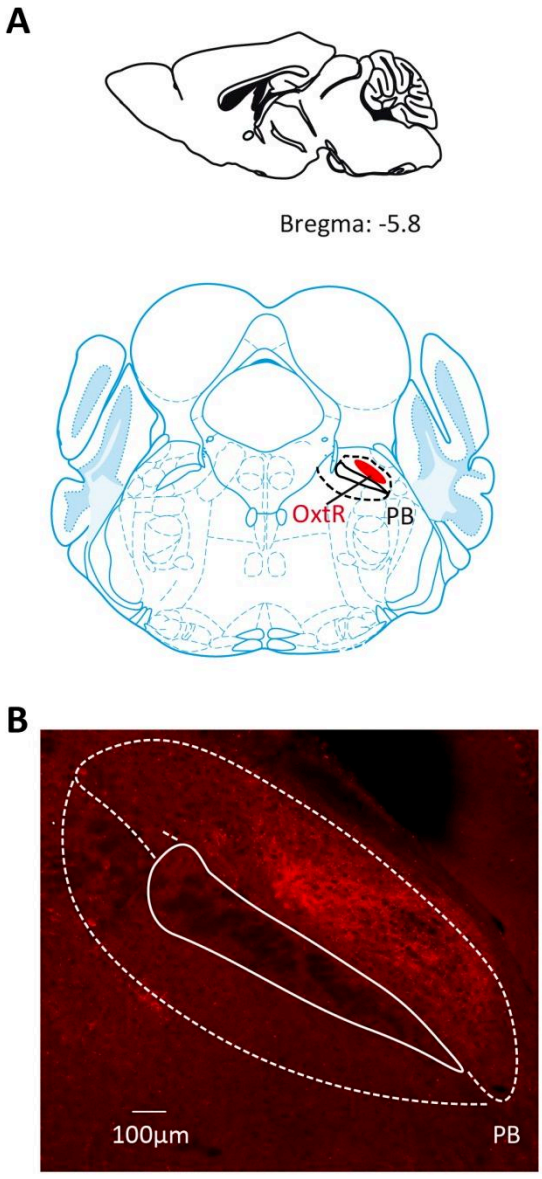

Figure 13| Immunohistochemical detection of OxtR-positive PB neurons.

A- Schematic representation of a coronal section of a mouse brain showing the location of OxtR-positive neurons in the lateral region of the parabrachial nucleus. **B-** OxytR neurons were revealed here by immunocytochemistry.

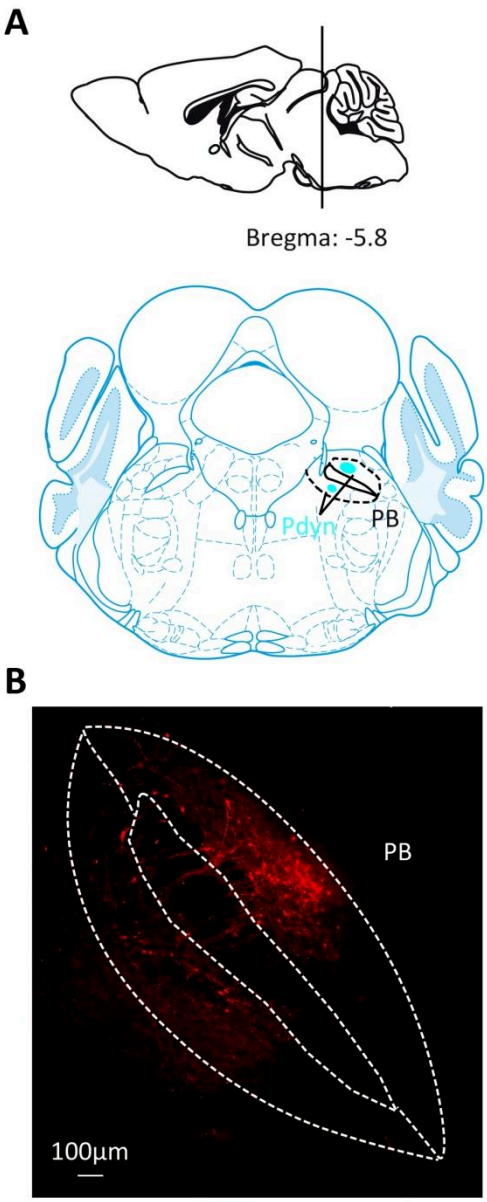

Figure 14|Distribution of Pdyn-positive PB neurons.

A- Schematic representation of a coronal section of a mouse brain showing the position of Pdyn-positive neurons in the dorso-lateral PB. **B-** Injection into the PB of an adult Pdyn-Cre mouseof a virus expressing the red fluorescent protein mCherry in a Cre-recombinase dependent manner revealed the distribution of Pdyn-positive neurons.

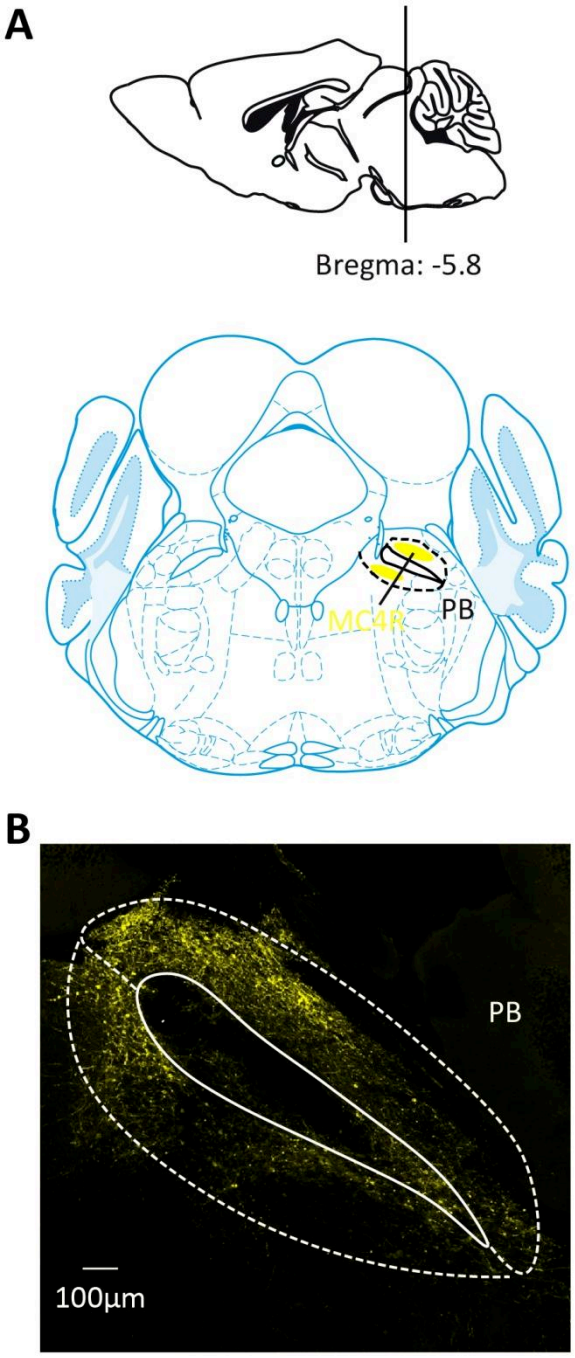

Figure 15| Distribution of MC4R-positive cells in the PB.

A- Schematic representation of a coronal section of a mouse brain showing the location of MC4R-positive neurons in the medio-dorsal PB. **B-** Injection into the PB of an adult MC4R-Cre mouse of a virus expressing the fluorescent protein YFP in a Cre-recombinase dependent manner revealed the distribution of MC4R-positive neurons. Note the very peculiar distribution of the cells in the very medio-dorsal part of the PB.

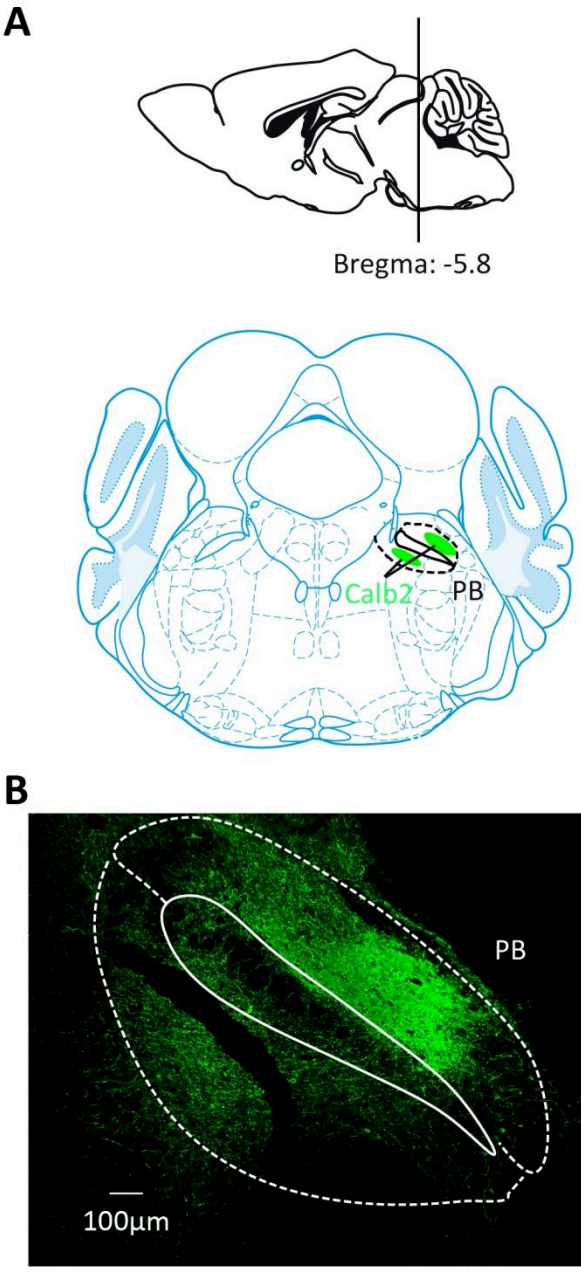

Figure 16| Distribution of Calb2-positive cells in the PB.

A- Schematic representation of a coronal section of a mouse brain showing the location of Calb2-positive neurons in the parabrachial nucleus. **B-** Injection into the PB of an adult Calb2-Cre mouse of a virus expressing the fluorescent protein YFP in a Cre-recombinase dependent manner revealed the distribution of Calb2-positive neurons.

Problem Definition And Research Objective

PROBLEM DEFINITION AND RESEARCH OBJECTIVE

Diheteromeric GluN1/ GluN3A receptors

As mentioned previously, unconventional diheteromeric GluN1/GluN3 NMDARs have sparked controversy. They are activated by the inhibitory neurotransmitter glycine alone, thus forming a novel type of excitatory glycine receptors. These receptors have so far been observed in recombinant systems, their presence in native tissues remaining a debatable subject. GluN1/GluN3A NMDARs elicit small and unstable glycine-induced currents, complicating their detection in native tissues. Moreover, GluN1/GluN3ARs pharmacology is at present insufficiently developed: selective antagonists with good potency are missing. My first goal during the thesis was thus to identify a compound that could efficiently potentiate GluN1/GluN3A receptor current by selectively blocking GluN1 glycine-binding sites without affecting GluN3, in order to permit a comprehensive biophysical characterization of the receptors in recombinant systems (this part performed by external collaborators). Using this information, I would set out to identify the presence of functional diheteromeric GluN1/GluN3ARs in the adult brain, in specific regions identified by my immunohistochemical morphological analysis.

Triheteromeric GluN1/GluN2/GluN3A receptors

As stated in the previous chapters, the physiology of GluN3A-containing NMDARs has been only partially characterized in the past, mainly because of their window of expression restricted at early postnatal stages. My main objective was, first, to investigate if the abundant presence of GluN3A subunits in the adult PVT (as demonstrated by my immohistochemical experiments) led to the formation of functional triheteromeric GluN1/GluN2/GluN3A NMDARs. Secondly, our aim was to identify a glutamatergic pathway that could activate these receptors synaptically. Several plausible brain areas presynaptic to the PVT would be tested. As we will show in a later section, we specifically examined the glutamatergic inputs arising from the rostral brainstem PB.

Overall, my thesis work aimed at re-defining our knowledge on GluN3A-containing NMDARs, and at laying the bases for future investigations examining their role also in the adult brain.

METHODS

METHODS

1. Animals

For all experiments, we used male and female mice, entrained to a 12-h light/dark cycle. All animals used for this study were housed in groups of up to 5 per cage with *ad libitum* access to food and water. Breeding conditions and experimental procedures were approved by the Federation for Laboratory Animal Science Association (FELASA), in agreement with ethics committee for health and life sciences and the French ministry of higher education, science, research and innovation.

To target subpopulations of cells within the PB that may project to the PVT, we tested 5 Cre-expressing mouse lines (calcitonin G related peptide- or CGRP-Cre, oxytocin receptor- or OxtR-Cre, calbindin 2- or Calb2-cre, prodynorphin- or Pdyn-cre and melanocortin 4 receptor- or MC4R-cre). KO mice for the GluN3A subunit or GluN3AKO, were instead used for control experiments when the presence of functional GluN3A-containing triheteromeric NMDARs had to be determined. The selective expression of ChannelRhodopsin (ChR2) into specific subpopulations of PB neurons was obtained by performing stereotaxic injections of viral vectors coding for double floxed sequences of ChR2 (DIO.ChR2) into the PB. Alternatively, we injected viral vectors coding for Cre recombinase either under the control of specific promoters (see table 5), or under the control of non-specific ones in combination with viral vectors coding for DIO.ChR2 in the PB of C57BL/6J wild type (WT) mice. Here follows a more detailed description of the mouse lines:

Calb2-Cre: in B6(Cg)-Calb2$^{tm1(cre)Zjh}$/J mice, Cre recombinase expression is controlled by the endogenous promoter/enhancer elements of the Calb2 locus (note that calbindin 2 is also called calretinin or CR; the Jackson Laboratory, reference 010774).

MC4R-Cre: in the MC4R$^{tm3.1(cre)Lowl}$/J knock-in mice, the original gene is followed by a viral 2A oligopeptide (T2A) fused to a Cre recombinase gene replacing the stop codon for MC4R gene. (The Jackson Laboratory, reference 030759).

Pdyn-Cre: Pdyn$^{tm1.1(cre)MjkrLowl}$/J knock-in mice have an internal ribosomal entry sequence (IRES) fused to the sequences of Cre recombinase, and inserted downstream of the endogenous Pdyn gene. (The Jackson Laboratory, reference 027958).

GluN3AKO: KO mice for the gene coding for the NMDAR GluN3A subunit. This line was a kind gift from Pierre Paoletti of the IBENS Institute in Paris, and were originally

developed by Nobuki Nakanishi and Stuart Lipton of the Scripps and the Scintillon Institute in San Diego, USA[137].

Genotyping for all these lines was done either in our laboratory, or at the Centre de Recherche des Cordeliers, Centre de Génotypage et de Biochimie, of Sorbonne University in Paris.

2. Stereotactic injections

All injections were performed on adult (>3 months old) mice. Mice were anesthetized with either isoflurane (set at 1.5%. The depth of anesthesia was constantly followed by monitoring the breathing rate during surgery) or with an intraperitoneal injection of a mix of ketamine-xylazine (100mg/and 10mg/kg; see table 4) and placed in a stereotactic apparatus (Kopf Instruments). Eye drops, made of vitamin B12, were applied regularly to prevent dryness. A subcutaneous injection of 1mL of sterile saline solution (NaCl, 0.9%) was performed to avoid dehydration. The scalp was shaved with an electric razor and the surgical area was cleaned with ethanol and sanitized with iodine solution (Vetedin). Lidocaine, a local anesthetic, was administered subcutaneously five minutes prior to making a less than 1cm-long incision on the scalp.

A craniotomy was performed above the region of interest using a dental bur. Bleeding was controlled with the application of sterile saline solution and/or the use of a hemostatic sponge. Injections were performed using pipettes pulled from graduated capillaries (Drummond) on a vertical puller (Narishige PE2), at a rate of 20-100nL/min. The virus was pressure-injected via an injection wheel (Narishige, model MO-10, SN 11005) allowing delivery of very small volumes (minimal total volume injected: 20nL).

Bilateral injections were performed either in the PB, using the following coordinates: Bregma ML, ±1.4mm; AP, −5.2mm; DV, -3.4mm, or in the MHb, using the following coordinates: Bregma ML, ± 0.25mm; AP, −1.34mm; DV, -2.75mm. Injections in the PVT were performed at the following coordinates: Bregma ML, 0mm; AP, −1.5mm; DV, −3.5mm. Finally, bilateral injections in the infralimbic cortex were at: Bregma ML, ±0.3mm; AP, +1.8mm; DV, −3.25 and 3.0mm.

Following craniotomy, the injection pipette was slowly lowered to the target coordinates and left in place for 5 min before starting expelling the virus. The pipette was slowly raised between 5 and 10 minutes after delivery of the desired viral volume, in order to reduce viral backflow along the injection track of the glass pipette. Saline was regularly applied to the skull to prevent drying. At the end of the surgery, the skin was sutured using a Vicryl 4-0 (Ethicon) thread. Mice were finally placed in a cage on a

heating mat and put back in their original housing following recovery from anesthesia. After surgery, animals were monitored and weighed daily until normal weight and behavior were restored. Mice showing obvious signs of suffering or a weight loss greater than 20% were euthanized with cervical dislocation following anesthesia with isoflurane.

Anesthetic	Brand	Dilution	Administration route	Dosage
Isofluorane	Iso-Vet	2%	Inhaled	300 µL
Pentobarbital	Euthasol Vet	362.9 mg/mL	Intraperitoneal	500 mg/kg
Ketamine	Imalgene 1000	10 mg/mL	Intraperitoneal	100 mg/kg
Xylazine	Rompun 2%	1 mg/mL	Intraperitoneal	10 mg/kg
Lidocain	Lurocaine	20 mg/mL	subcutaneous	Non pertinent

Table 4| List of the anesthetics used.

2.1. Viruses

Throughout my thesis work, I worked uniquely with adeno-associated viruses (AAVs), because of their broad tropism and their ability to sustain long-term transgene expression without damaging cells.

To specifically target PB afferent inputs to the PVT, we injected the following AAVs: AAV1/Ef1a-DIO.hChR2(H134R)-eYFP (Vector Core, Pennsylvania University, Penn Univ.), AAV2/Ef1α-DIO.hChR2(H134R)-eYFP (Ef1α: Eukaryotic translation elongation factor 1 alpha; UNC Vector core, North Carolina University, UNC) and AAV9/CMV-Cre (Penn Univ.; CMV: cytomegalovirus) in distinct combinations. Namely, when we targeted the PB in mouse lines not expressing Cre recombinase (ex.: C57BL/6 mice from Janvier laboratories or the GluN3AKO animals), we co-injected a mix of AAV9/CMV-Cre plus either AAV1/Ef1a-DIO.hChR2(H134R)-eYFP, or AAV2/Ef1α-DIO.hChR2(H134R)-eYFP. In contrast, when the PB of Pdyn-Cre and MC4R-Cre mice was targeted, we typically injected the AAV1/Ef1a-DIO.hChR2(H134R)-eYFP alone. The AAV serotype 2 was typically used to spatially restrict infection areas because, in our hands, AAV2 viruses showed much more restricted spatial diffusion in neural tissues than, for example, serotypes 1, 5, 8 and 9. Injections of calb2-Cre mice were done in collaboration with Dr.

Ferenc Matyas's team at the Research Centre for Natural Sciences, Institute of Cognitive Neurosciences and Psychology in Budapest, Hungary, who host the colony. An AAV5-EF1α-DIO.hChR2(H134R)-eYFP (UNC vector core) was used in this case.

To exclusively target CGRP-expressing neurons in the PB, we injected WT mice with a mix of either AAV1/Ef1a-DIO.hChR2(H134R)-eYFP or AAV2/Ef1a-DIO.hChr2(H134R)-eYFP plus an AAV2/CGRP-Cre expressing Cre recombinase under the control of the CGRP promoter (custom production by the Laboratory of genetic Therapy, INSERM U1089, Nantes, France). A similar strategy was exploited for infecting OxtR-expressing PB neurons. In WT mice we injected either AAV1/Ef1a-DIO.hChR2(H134R)-eYFP or AAV2/Ef1a-DIO.hChr25(H134R)-eYFP and an AAV2/OxtR-Cre expressing Cre recombinase under the OxtR promoter (custom production by the Laboratory of Genetic Therapy, INSERM U1089, Nantes, France).

Finally, to specifically silence GluN3A gene expression, AAV5 viruses expressing either a GluN3A-targeting short hairpin RNA (AAV5/shRNA.GluN3A-GFP) or a scrambled RNA sequence (AAV5/scr.GluN3A-GFP[140]) were injected bilaterally in the MHb of adult C57B6 mice. The AAV5/shRNA.GluN3A-GFP was also injected in the PVT of adult C57B6 mice for verifying triheteromeric GluN1/GluN2/GluN3AR functional expression. Both viruses were produced expressly for our team by the Laboratory of genetic Therapy in Nantes.

Injection sites were verified *post-hoc* for all animals, and were retained when most fluorescence was restricted to the targeted nucleus (as shown in Fig. 17-A for the PB). Mice showing significant viral spillover into adjacent nuclei (i.e. ventro-lateral PAG, dorsal raphe, peduncolopontine nucleus for the PB) were rejected (as shown in Fig. 17-B). See Table 6 for details about virus origin and titer.

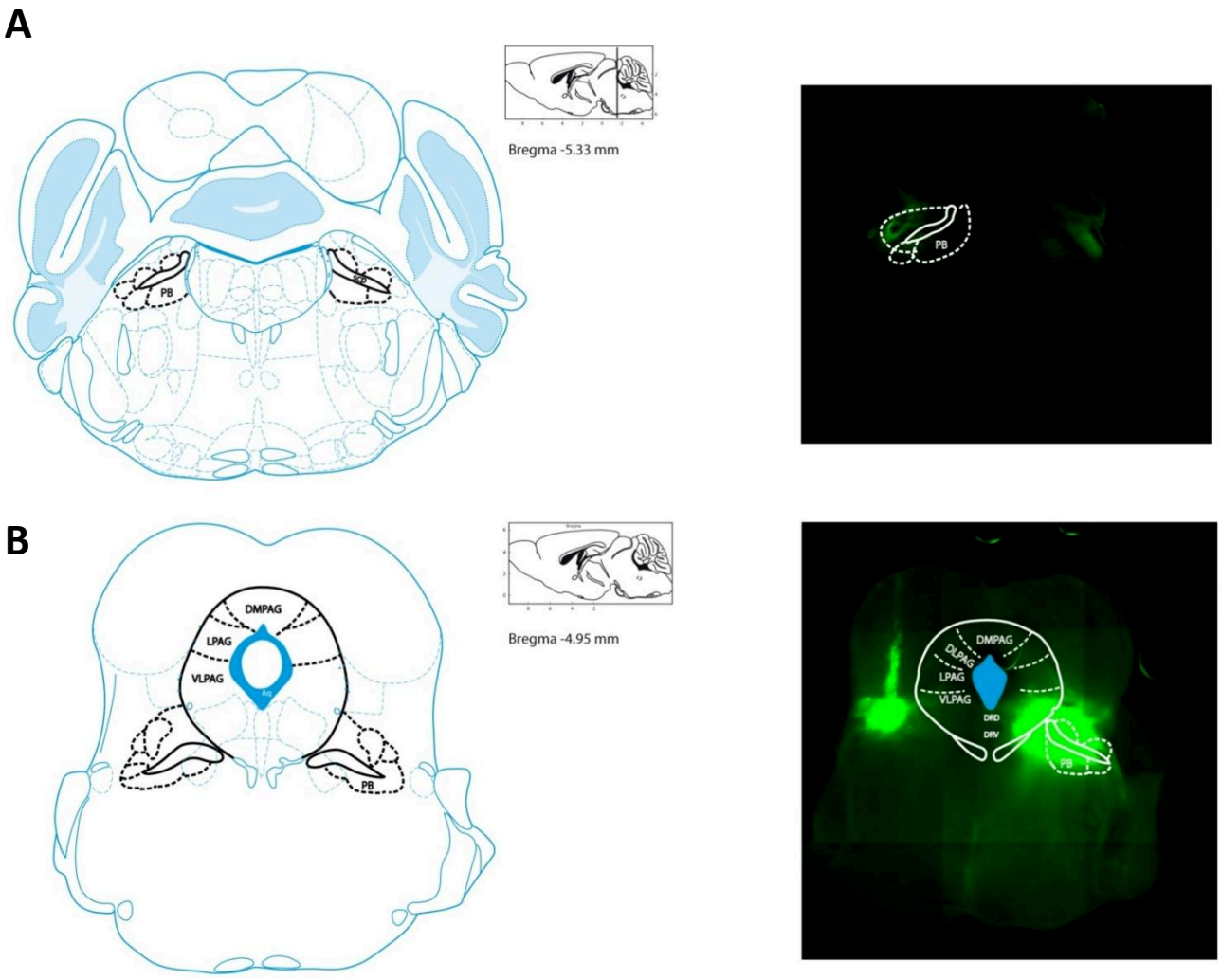

Figure 17| Evaluation of viral injection sites.

A- An example of a successful injection site in the PB of a WT mouse (a mix of AAV2/Ef1a-DIO.hChr2(H134R)-eYFP and AAV9/CMV-Cre was injected). **B-** Example of an injection site that was rejected due to viral spreading into the periaqueductal gray (PAG), a nucleus that also projects to the PVT (a mix of AAV1/Ef1a-DIO.hChR2(H134R)-eYFP and AAV9/CMV-Cre was injected).

Mouse species	Injected virus(es)	volume(nL)	Injection site
C57/B6	AAV2/Ef1α-DIO.hChr2(H134R)-mCherry **and** AAV9/CMV-Cre	30-50	PB
C57/B6	AAV1/Ef1α-DIO.hChR2(H134R)-eYFP **and** AAV9/CMV-Cre	30-50	PB
C57/B6	AAV2/Ef1α-DIO.hChr2(H134R)-eYFP **and** AAV9/CMV-Cre	30-50	PB
C57/B6	AAV2/Ef1α-DIO.hChr2(H134R)-eYFP **and** AAV2/CGRP-Cre	30-50	PB
C57/B6	AAV2/Ef1α-DIO.hChr2(H134R)-eYFP **and** AAV2/OxtR-Cre	30-50	PB
Calb2-Cre	AAV5-EF1α-DIO.hChR2(H134R)-eYFP	100	PB
Pdyn-Cre	AAV1/Ef1α-DIO.hChR2(H134R)-eYFP	100	PB
Mc4R-Cre	AAV1/Ef1α-DIO.hChR2(H134R)-eYFP	100	PB
C57/B6	AAV5/shRNA.GluN3A-GFP **or** AAV5/scrRNA.GluN3A-GFP	200	PVT/MHb

Table 5| Mouse lines and virus combinations used for viral injections.

Virus	Provider	Titer (vm/mL)
AAV2/Ef1a-DIO.hChr2(H134R)-mCherry	UNC	$5.1x10^{12}$
AAV1/Ef1a-DIO.hChR2(H134R)-eYFP	Penn U.	$7x10^{12}$
AAV2/Ef1a-DIO.hChR2(H134R)-eYFP	UNC	$4.4x10^{12}$
AAV5/EF1a-DIO.hChR2(H134R)-eYFP	Penn U.	$3.2x10^{12}$
AAV9/CMV-Cre	Penn U.	$3.9x10^{13}$
AAV2/CGRP-Cre	INSERM U1089	$1x10^{13}$
AAV2/OxtR-Cre	INSERM U1089	$1.8x10^{13}$
AAV5/shRNA.GluN3A-GFP	INSERM U1089	$1x10^{13}$
AAV5/scrRNA.GluN3A-GFP	INSERM U1089	$8x10^{12}$

Table 6| List of the origin and titer of the viruses used for stereotactic injections.

3. Slice preparation

Ex-vivo electrophysiological experiments were all performed on coronal slices from injected animals at least 3 weeks after infection. Mice were anesthetized with isofluorane before decapitation. After isolation, the portion of the brain of interest was placed at 2–5 °C for a few minutes in oxygenated bicarbonate-buffered saline (BBS) containing (in mM): 115 NaCl, 2.5 KCl, 1.6 $CaCl_2$, 1.5 $MgCl_2$, 1.25 NaH_2PO_4, 26 $NaHCO_3$, 30 glucose and 0.0005 minocycline (pH 7.4 after equilibration with 95% O_2 and 5% CO_2).

Slices (300µm) were then cut using a vibratome (Campden Instruments 7000 SMZ2). The slicing procedure was performed in an ice-cold solution containing (in mM): 130 potassium gluconate, 15 KCl, 2 EGTA, 20 Hepes, 25 glucose, 1 $CaCl_2$ and 6 MgCl2, pH 7.4 (after equilibration with NaOH 1M). Slices were then transferred for a few minutes to a recovery solution containing (in mM): 225 D-mannitol, 2.5 KCl, 1.25 NaH_2PO_4, 25 $NaHCO_3$, 25 glucose, 1 $CaCl_2$ and 6 $MgCl_2$, and finally stored for the rest of the experimental day at 32-35°C in oxygenated BBS. For all recordings, slices were continuously superfused at a rate of 1.5-2mL/min with oxygenated BBS at 32–34 °C.

4. Electrophysiology

All *ex-vivo* electrophysiological recordings were performed at least 40 minutes after cutting. Cells were identified and patched in the transmitted deep red light with which slices were visualized using a CoolSnap HQ CCD camera (Photometrics) run by Metamorph software (Universal Imaging) and mounted on a microscope (Olympus). Recording pipettes were pulled using a horizontal micropipette puller (Sutter Instrument Co.) from borosilicate glass capillaries (Hilgenberg) and had a resistance of 2–4 MΩ.

Series resistance was compensated (60-70%) during all the experiments (except for the experiments made in the MHb where compensation induced unstable recordings). All electrophysiological recordings were performed with a double EPC-10 amplifier (HekaElektronik) run by Patchmaster software (Heka). Data were recorded with a sampling frequency of 40kHz, filtered at 3kHz, and analyzed using Igor (Wavemetrics, Lake Oswego, OR) with routines developed in-house. Statistical comparisons were performed using non-parametric tests, namely the Mann-Whitney or Wilcoxon signed rank tests. Statistical significance was set at 0.05. Results are given as mean ± SEM.

4.1. ***Ex vivo* optogenetic stimulation:**

Light-evoked excitatory postsynaptic currents (leEPSCs) were recorded in voltage-clamped neurons of the PVT using an intracellular solution containing the following (in

mM): 135 CsMeSO3, 4.6 MgCl2, 10 HEPES, 0.5 EGTA, 10 K_2-creatinine phosphate, 4 Na_2-ATP, 0.4 Na_2-GTP; pH 7.35 with 1M CsOH, ~305mOsm. The junction potential of this solution (estimated at around -7mV) was not corrected during analysis. The PVT was clearly recognizable by the distribution of eYFP–positive fibers just ventrally with respect to the third ventricle following virus injections in the PB (Fig. 18). Brief (1–2ms long) flashes of blue light were used to evoke synaptic responses using a 470-nm wavelength LED (Thorlabs) coupled to the slice chamber via the epifluorescence pathway of the microscope, and triggered via the amplifier.

The AMPAR- and NMDAR-mediated responses of the excitatory PB-to-PVT synapses were studied by alternating optogenetic stimulations at + 50mV and -60mV.

For each cell, the amplitude of the two components was measured from averaged traces resulting from several individual stimulations (≥10). All optogenetic experiments were performed after application of SR95531 (also known as gabazine), a competitive inhibitor of GABAa receptors (2µM); strychnine, a glycine receptor blocker (2µM); 4-AP (50µM) and or TEA (500nM), non-specific voltage-sensitive potassium channel blockers that lead to a presynaptic increase of release probability, and thus of synaptic current amplitudes. NMDAR-mediated responses were isolated following the additional application of NBQX, an AMPA-kainate receptor blocker (10µM) in the bath solution.

4.2. Pressure ejection of NMDA:

Ex-vivo whole-cell voltage-clamp recordings were performed from cells of the PVT of adult GluN3AKO and control mice originating from the same litters, with the following intracellular solution (in mM): 120 $CsMeSO_3$, 4.6 $MgCl_2$, 10 HEPES, 15 BAPTA, 10 K_2-creatinine phosphate, 4 Na_2-ATP, 0.4 Na_2-GTP; pH 7.35 with 1M CsOH; ~305mOsm. The high calcium buffering capacity of this solution was found to ameliorate recording stability. Puffing pipettes filled with BBS supplemented with NMDA (5mM), NBQX (10µM), SR95531 (10µM) and strychnine (50µM) were placed above the slice surface, close to the recording pipettes. NMDA puffs were applied with a Picospritzer II (General Valve Corporation) for 300 to 500ms, at pressures comprised between 12 and 20 psi. These parameters were adjusted for every slice depending on the resistance of the puff pipette and on its position with respect to the tissue. Pressure, application time and position of the pipette were typically adjusted to have amplitude responses comprised between 30 and 50pA at -60mV. The puffs were performed in the constant presence in the bath of TTX, an inhibitor of voltage-dependent sodium channels (500nM); NBQX (10µM); SR95531 (2µM) and strychnine (2µM) in the bath solution.

4.3. Pressure ejection of Glycine:

Whole-cell voltage-clamp recordings of hippocampal CA1 pyramidal cells were performed on coronal slices from the brains of juvenile (8-12 days old) of WT and GluN3AKO mice from the same litters. Similar recordings were performed in the MHb of coronal slices obtained from adult WT and GluN3AKO animals. The following intracellular solution was used (in mM): 120 $CsMeSO_3$, 4.6 $MgCl_2$, 10 HEPES, 10 K_2-creatine phosphate, 15 BAPTA, 4 Na_2-ATP, 0.4 Na_2-GTP, 1QX-314, pH 7.35 with CsOH (~300mOsm). Puffing pipettes contained BBS supplemented with glycine (10mM), NBQX (10µM), SR95531 (10µM), strychnine (50µM), and DL-APV (100µM). Brief (0.5–1s) puffs were then delivered every 60–120s via the Picospritzer II. The puffs were performed in the presence of TTX, NBQX, DL-APV (100µM) and SR95531 and strychnine in the bath solution. CGP78608 (1µM), a GluN1 subunit blocker, was added to the bath solution to reveal the presence of diheteromeric GluN1/GluN3ARs.

5. Pharmacology

1S)-1-[[7-Bromo-1,2,3,4-tetrahydro-2,3-dioxo-5-quinoxalinyl)methyl]amino]ethyl] phosphonic acid hydrochloride or CGP-78608, a GluN1 NMDAR subunit blocker; D-2-amino-5-phosphonovaleric acid or D-APV, a competitive antagonist of the glutamate binding site of the NMDAR GluN2 subunits; 5,7-Dichlorokynurenic acid or DCKA, NMDAR antagonist acting at the glycine binding sites of both GluN1 and GluN3 NMDAR subunits; 2,3-dihydroxy-6-nitro-7-sulfamoyl-benzoquinoxaline2,3-dione or NBQX, an AMPA-kainate receptor blocker; 6-Imino-3-(4-methoxyphenyl)-1(6H)-pyridazinebutanoic acid hydrobromide or SR95531, or gabazine, competitive inhibitor of GABAaRs; strychnine, a glycine receptor blocker; 4-aminopyridine or 4-AP and Tetraethylammonium or TEA, non-specific voltage-sensitive potassium channel blockers; Tetrodotoxin or TTX, inhibitor of voltage-dependent sodium channels, glycine and N-Methyl-D-aspartate, or NMDA (Table 7).

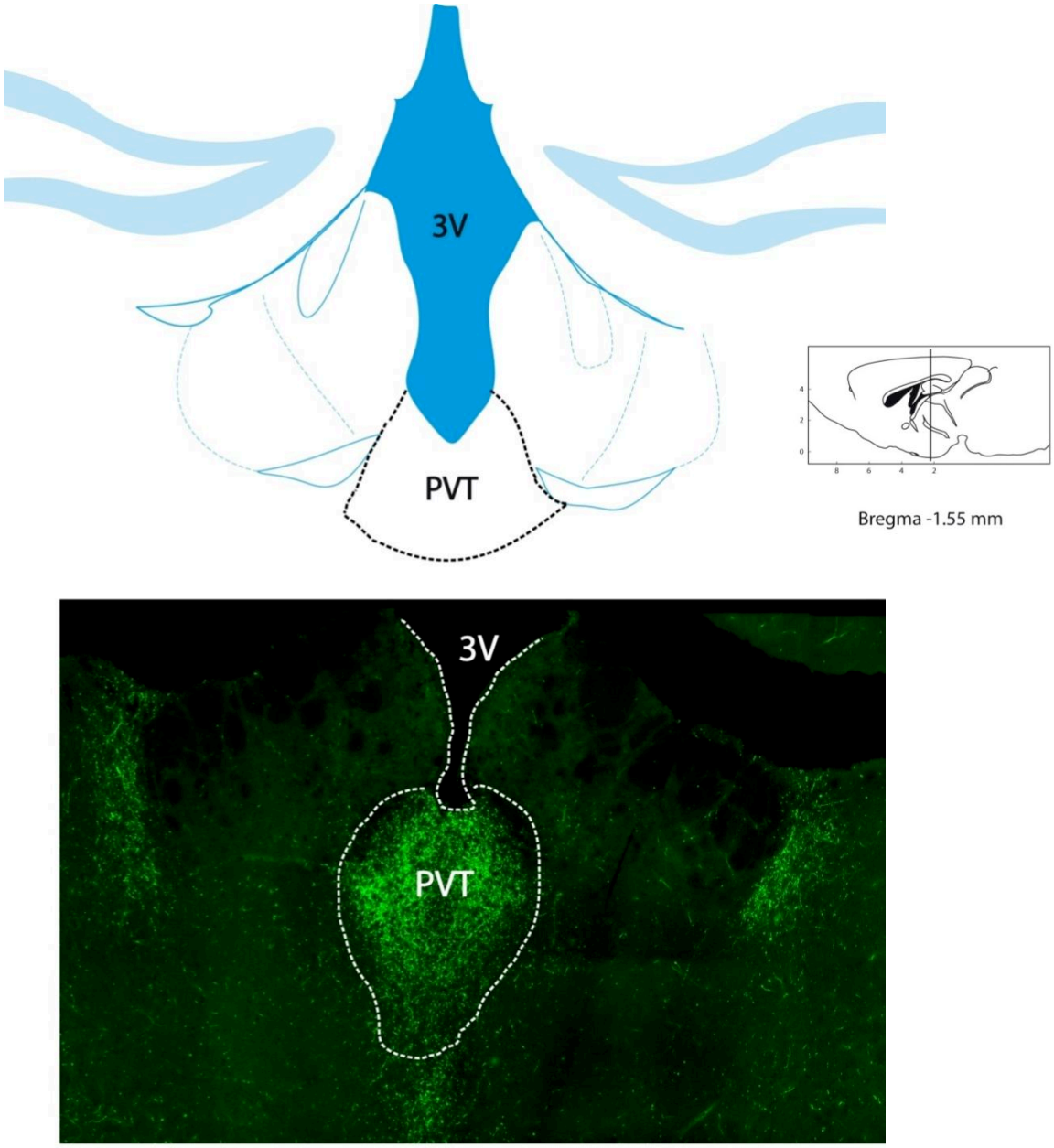

Figure 18 | eYFP-positive fibers identifying the PVT in a WT mouse following co-injection of AAV1/Ef1a-DIO.hChr2(H134R)-eYFP and AAV9/CMV-Cre in the PB.

Drug	Solvent and Stock concentration	Concentration used
CGP78608	2.2 eq NaOH solution, 25 mM	1 µM
D-APV	Water, 50 mM	100 µM
DCKA	1 eq NaOH solution, 50mM	500 µM
Glycine	Water, 1 M	10 mM
NBQX	Water, 10 mM	10 µM
NMDA	Water, 100mM	5mM
SR95531	Water, 10 mM	2 µM
Strychnine	Water, 10mM	2µM
Strychnine (Glycine puffs)	Water, 10mM	50µM
TEA	Water, 500mM	500nM
TTX	Acetic acid (2%) water solution, 500µM	500nM
4-AP	Water, 10mM	50µM

Table 7| List of the drugs used for electrophysiological experiments, their solvent, their stock concentration and final concentration in the bath solution.

6. Immunohistochemistry

Mice were anesthetized with 2% isoflurane, injected intraperitoneally with a lethal dose of pentobarbital and then perfused with oxygenated cold BBS. The brains were rapidly extracted and placed in a 4% paraformaldehyde (PFA) solution in phosphate buffer saline (PBS) at 4°C overnight. Subsequently, 100µm-thick slices were cut using a vibratome (Leica VT1000S) in PBS.

Immunohistochemistry staining was performed at room temperature. The slices were rinsed 3 times in PBS solution at pH 7.5, and then incubated for 60 minutes in a PBS solution containing 0.2% triton100X for cell membranes permeabilization, and 3% bovine serum albumin for blocking non-specific binding sites (PBSTB). The slices were then incubated overnight in PBSTB solution containing the primary antibodies (Table 8), rinsed 3 times with PBS, incubated with PBSTB solution containing the secondary antibodies (table 9) for 2 hours and then rinsed again for 2 hours in PBS before being mounted on slides with Prolong Gold antifade reagent (ThermoFisher).

We often performed an antigen retrieval protocol before the conventional immunohistochemistry protocol described above. Sections were rinsed 3 times in PBS solution at pH 7.5 then transferred to a sodium citrate solution (10mM in distilled water, pH 8.5) preheated to 90°C in a water bath. Sections were kept at 90°C for 30 min, then rinsed 3 times in PBS. The conventional immunohistochemistry protocol then followed.

7. Image acquisition

Images were acquired using an upright confocal miscoscopy (Leica TCS SP5) with 20X and 40X objectives and then processed with Fiji/ImageJ software.

Antigen	Species	Dilution	Provider	Reference
GFP	chicken	1/500	Life Technologies	A10262
GFP	rabbit	1/500	Chromotek	PABG1
RFP	rat	1/500	Chromotek	5f8-100
CGRP	mouse	1/500	Abcam	AB81887
OxyR	rabbit	1/250	Thermo Fischer	PA5-32961

Table 8| List of the primary antibodies used.

Antibody	Species	Dilution	Provider	Reference
Anti-chicken488	Goat	1/500	Life Technologies	A11039
Anti-rabbit488	Donkey	1/500	Invitrogen	31568
Anti-rat555	Goat	1/500	Invitrogen	A21434
Anti-mouse488	Goat	1/500	Life Technologies	A11001
Anti-mouse555	Goat	1/500	Life Technologies	A21422
Anti-rabbit555	Goat	1/500	Invitrogen	A211430

Table 9| List of secondary antibodies used.

Product	Provider	Reference
NaCL	Sigma Aldrich	A10262
KCl	Sigma Aldrich	PABG1
NaH2PO4	Sigma Aldrich	5f8-100
NaHCO3	Sigma Aldrich	AB81887
K-gluconate	Sigma Aldrich	32961
D-(+)-glucose	Sigma Aldrich	49159
EGTA	Sigma Aldrich	E3889
HEPES	Sigma Aldrich	H3375
CaCl2	Sigma Aldrich	21114
MgCl2	Sigma Aldrich	63020
PBS	Sigma Aldrich	D1408
PFA liquide 16%	Delta Microscopies	15710
PFA powder	Sigma Aldrich	158127
Triton100X	Sigma Aldrich	T8787
Bovine serum	Sigma Aldrich	A7906
Prolong Gold Antifadereagent	Life technologies	P36930
Mineral oil	Sigma Aldrich	M5904
CGP78608	Tocris	1493
DCKA	Tocris	3698
TTX	Latoxan	L8503
NBQX	Abcam	ab120046
D-APV	HelloBio	HB0225
NMDA	Tocris	0114
Glycine	Sigma Aldrich	410225
Strychnine	Sigma Aldrich	S0532

$CsMeSO_3$	Sigma Aldrich	C1426
K_2-creatine phosphate	Calbiochem	237911
BAPTA	Sigma Aldrich	A4926
Na_2-ATP	Sigma Aldrich	A7699
Na_2-GTP	Sigma Aldrich	G8817
QX-314	HelloBio	HB1030
4-AP	Sigma Aldrich	275875
TEA	Sigma Aldrich	T2265
Sodium citrate	Sigma Aldrich	S4641
Minocycline	Tocris	3268
SR95531	HelloBio	HB0901

Table 10| List of all the chemical compounds used and their reference.

RESULTS

RESULTS

Diheteromeric GluN1/GluN3Rs possess unique activation properties. Unlike conventional GluN1/GluN2Rs, they do not require glutamate for their activation and are activated by glycine alone[112]. As we mentioned in the Introduction, the GluN1 and GluN3A glycine-binding sites mediate the opposing actions of glycine on activation. Glycine binding to GluN3 leads to channel opening, whereas binding to the lower affinity GluN1 site induces rapid receptor inactivation and channel closure[123,339]. Glycine applications thus typically elicit rapid GluN1/GluN3ARs inward currents (as glycine binds to the GluN3A subunit) followed by fast desensitization (as glycine binds to the GluN1) and a small steady state plateau[339]**.** Mutating the glycine binding site on GluN1 prevents the inactivation of the receptor and results in currents of much larger amplitude[105].

Before the onset of my thesis, GluN1/GluN3Rs had been identified only in heterologous recombinant systems, and their existence in native tissues was vividly debated[105,112,131] (but see[132]). Any pharmacological agent antagonizing glycine binding to GluN1 without acting on GluN3 subunits could facilitate their possible detection in *ex-vivo* neurons by amplifying receptor currents. Although no perfectly specific pharmacology exists at present, early studies reported the existence of compounds that, at least in expression systems and isolated ABDs, show much higher affinity for GluN1 subunits than for GluN3[123]. Theoretically, these differences should assure the desired effect. However, how and whether these properties are maintained in native receptors was not investigated and remained unclear before my PhD. During my doctoral activity, we thus explored a few of these drugs trying to identify one (or more) that could mimic the effects observed when mutating the agonist binding site on GluN1 in recombinant receptors. Our attention finally focused on an NMDAR GluN1 competitive antagonist[340], CGP78608, which displays a thousand-fold higher affinity for GluN1 than for GluN3 subunits in ABDs[123].

Our first tests with this drug in slices produced astounding preliminary results that prompted us to implicate Paoletti's team at the IBENS Institute at the Ecole Normale Supérieure in Paris for a more thorough characterization in recombinant systems of the biophysical mechanisms implicated. Our collaborators thus expressed GluN1/GluN3ARs in HEK293 cells and performed whole cell patch clamp recordings coupled to a fast perfusion system for glycine pressure applications. The use of CGP78608 resulted in unprecedented massive potentiation of the amplitudes of glycine-induced currents also in their hands. Paoletti and colleagues were thus able to perform a comprehensive

biophysical characterization of these receptors in the potentiated conformation[124]. Our contribution to this study was then to provide a long-awaited first identification of these receptors in native neurons. We chose the juvenile hippocampus for a proof-of-principle demonstration that GluN1/GluN3ARs are indeed functional in the brain[124].

1. CGP78608 reveals functional glycine-activated diheteromeric GluN1/GluN3A NMDARs in the juvenile brain

Functional diheteromeric GluN1/GluN3A NMDARs had not been identified in native neurons before the onset of my thesis. The very rapid desensitization peculiar of these receptors in control conditions, imply that responses to glycine puff applications onto voltage-clamped cells in slices could easily be interpretable as mechanical artefacts. In this context, finding a pharmacological tool amplifying the responses to glycine and facilitating their detection would thus represent a fundamental step.

We tested a few candidate drugs[123], concentrating in particular on 2 of them, L689560 and CGP78608, which showed the most promising effects in preliminary tests. L689560 appeared to be of impossible use in slices, its high lipophilicity compromising a fine control of the final concentrations reached during recordings in slices. In tests performed in MHb cells, CGP78608 immediately appeared as the best choice, for the reproducibility of its effects and the astounding potentiation produced.

In the context of our aforementioned collaboration with Pierre Paoletti, given the striking effect of CGP78608 on GluN1/GluN3ARs in recombinant systems, we predicted that CGP78608 could be a powerful instrument to help reveal endogenous currents mediated by GluN1/GluN3ARs in native neurons. It is known that the GluN3A subunit is expressed at high levels almost ubiquitously during the first two weeks of postnatal life[115]. Therefore, as a proof-of-principle, we investigated the presence of functional GluN1/GluN3ARs in the hippocampal CA1 region of juvenile mouse slices (P8-P12). We explored the effect of bath application of CGP78608 (1 µM) on currents activated by glycine (10 mM) in voltage-clamped CA1 pyramidal cells (Fig. 19). To avoid potential activation of other receptors, these experiments were conducted in the presence of a mix of neurotransmitter receptor inhibitors including the AMPAR antagonist NBQX, the antagonist of GluN1/GluN2 NMDARs D-APV, the inhibitor of voltage-dependent sodium channels TTX, the GABAaR antagonist SR95531 (also called gabazine) and the glycine receptor inhibitor strychnine (see methods). Upon pressure ejection of glycine, a small inward current was observed in control conditions in neurons from both WT and GluN3AKO mice, with amplitudes of 9.3±1.4 pA (n=10) and 6.0±0.8 pA (n=11), respectively (Fig. 19). The currents observed were not significantly different (p=0.3;

Mann–Whitney test). We hypothesized that these currents might be due, at least partially, to mechanical artefacts caused by the ejection pressure, given the proximity between the puffing pipette and the recording electrode. However, the effect of bath application of CGP780608 was drastically different in WT and in GluN3AKO animals. A massive potentiation of the glycine-induced inward currents was observed in WT upon application of CGP78608, to 190.1±58.3 pA (n=10; range: 16.8–640.6 pA; p=0.007 with respect to control conditions; Wilcoxon signed-rank test). In contrast, this potentiation was absent in GluN3AKO mice, where current amplitudes amounted to 5.0±0.6 pA (n=17; p=0.9 with respect to control, pre-drug puffs; p<0.001 with respect to currents obtained in the presence of CGP78608 in WT mice; Mann–Whitney; Fig. 19). Bath application of the dual GluN1 and GluN3 glycine-binding site antagonist DCKA (500 µM), nearly entirely blocked the currents obtained in CGP78608 (10.2±2.7 pA, n=9; p=0.001; Mann–Whitney). Altogether, these results proved, for the first time, that diheteromeric GluN1/GluN3ARs are expressed and functional in native tissues, more specifically in the juvenile hippocampus. This result would not have been possible without the use of CGP78608, which confirmed its potential as a powerful tool for unmasking the presence of GluN1/GluN3ARs in native neurons.

These results were published in a study appeared in Nature Communication[124], of which I was first co-author.

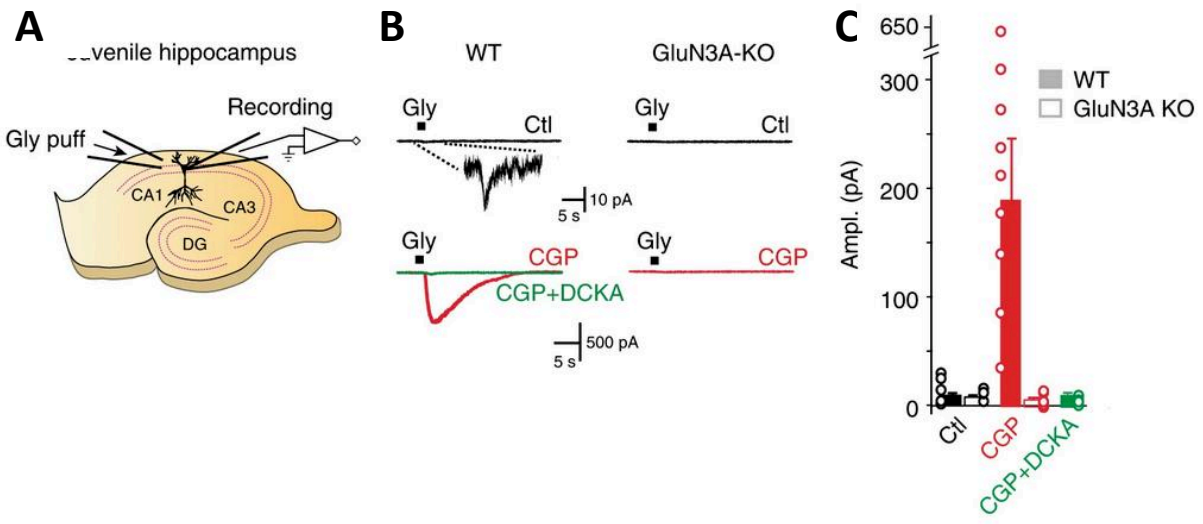

Figure 19| GluN1/GluN3ARs are expressed and functional in juvenile hippocampal slices.

A- The schematic representation of the experimental protocol is depicted in the panel. Glycine (10 mM) was puffed onto voltage-clamped CA1 cells in acute hippocampal slices from juvenile (P8-12) mice. **B-** In control conditions, glycine puffs triggered very small inward currents in both wild-type (WT) and GluN3AKO mice (upper black traces on both left and right). A typical response obtained in WT mice is shown at larger magnification and time scale in the top left inset. Bath application of CGP78608 (CGP) led to massive potentiation of the glycine-elicited currents in WT mice, but had no effect in GluN3AKO animals (bottom red traces). In WT mice, addition of DCKA (500 µM), a GluN1 and GluN3A glycine-binding site antagonist, inhibited the currents obtained in the presence of CGP78608 (bottom left green trace), thus further confirming that GluN1/GluN3ARs mediated the responses. **C-** Quantification of the experimental results obtained in panel **B**. WT mice, full bars; GluN3AKO mice, empty bars. Data are illustrated as mean ± SEM.

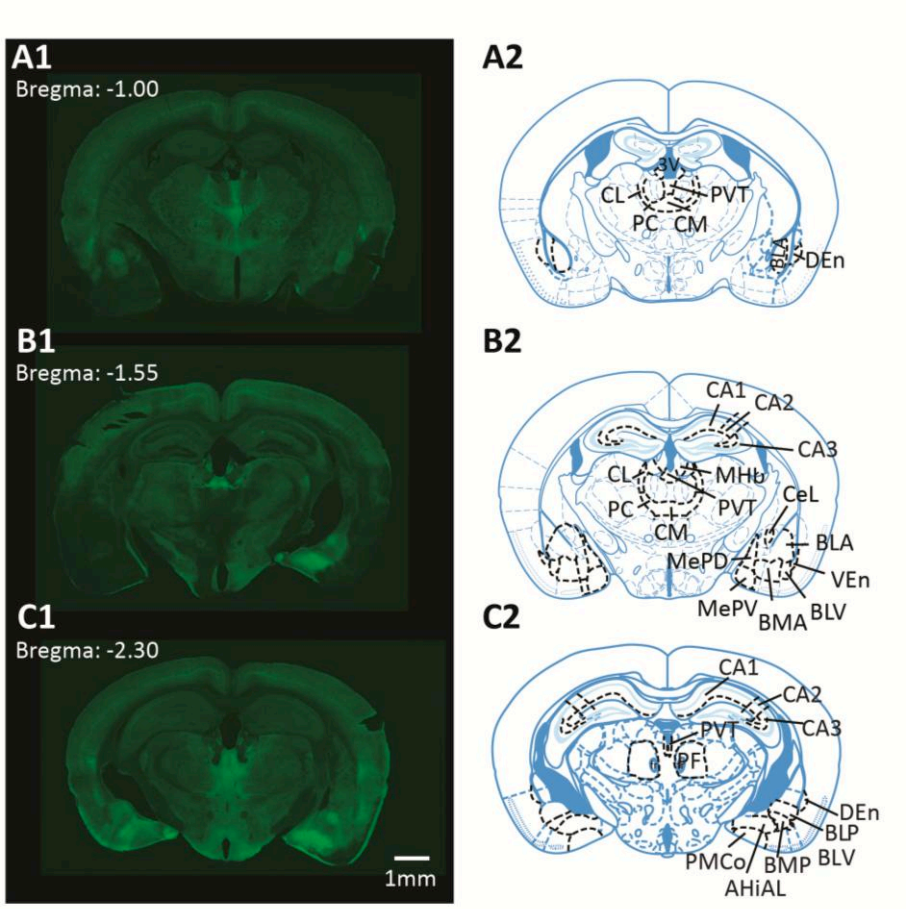

Figure 20| Distribution of GluN3A subunit immunostaining in the adult mouse brain.

Coronal brain section showing immunostaining with an antibody targeting GluN3A at -1.00mm **(A1)**, -1.55mm **(B1)** and -2.30mm **(C1)** from bregma along the rostro-caudal axis. Abbreviations: CM, centromedial thalamic nucleus; PVT, paraventricular thalamic nucleus; CL, centrolateral thalamic nucleus; PC, paracentral thalamic nucleus; BLA, anterior basolateral amygdaloid nucleus; DEN, dorsal endopiriform nucleus; CA1, CA2, CA3, fields CA1, CA2 and CA3 of the hippocampus; MHb, medial habenular nucleus; Cel, lateral central amygdaloid nucleus; Ven, ventral endopiriform nucleus; BLV, ventral basolateral amygdaloid nucleus; BMA, anterior basomedial amygdaloid nucleus; MePV, posteroventral medial amygdaloid nucleus; MePD, posterodorsal medial amygdaloid nucleus; PMCo, posteromidial cortical amygdaloid nucleus; AHiAL, anterolateral amygdalohippocampal area; BMP, posterior basomedial amygdaloid nucleus; BLP, posterior basolateral amygdaloid nucleus; PF, parafascicular thalamuc nucleus.

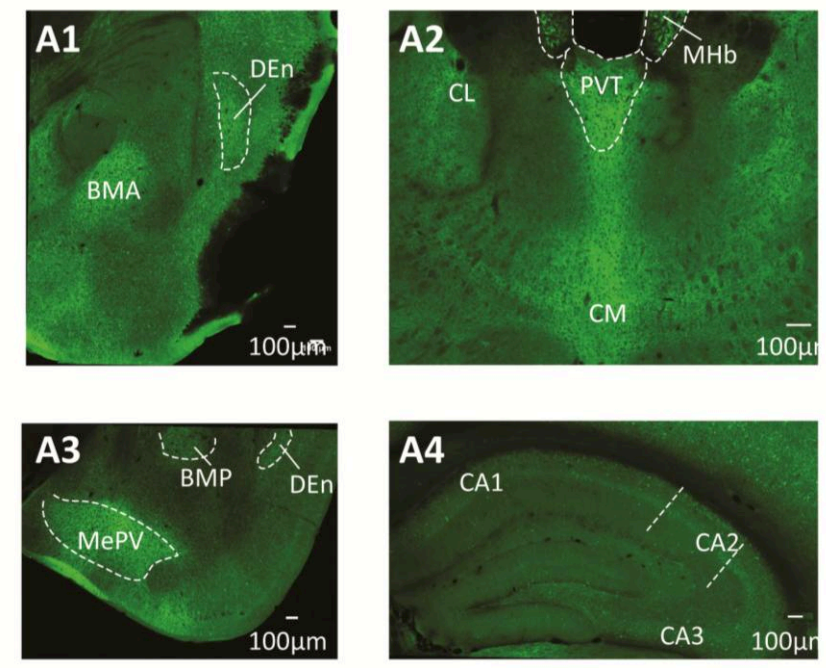

Figure 21| Distribution of GluN3A subunit immunostaining in the adult brain, larger magnification images.

Coronal brain section showing immunohistochemical staining for the GluN3A subunit. In these excerpts from brain coronal sections of an adult mouse, staining is observed in the amygdala, hippocampus, intralaminar (IL) nuclei, PVT and MHb. Weak staining is observed in the hippocampus. Abbreviations: BMA, anterior basomedial amygdaloid nucleus; DEn, dorsal endopiriform nucleus; CL, central lateral IL thalamic nucleus; CM, central medial IL thalamic nucleus; PVT, paraventricular thalamic nucleus; MHb, medial habenula; MePV, posteroventral medial amygdaloid nucleus; BMP, posterior basomedial amygdaloid nucleus; CA1, CA2, CA3, are the well-known hippocampal subdivisions.

2. GluN3A subunit mapping in the adult mouse brain reveals strong expression in specific nuclei

Until present, it has conventionally been assumed that GluN3A subunit is almost ubiquitous in the brain in the first weeks of postnatal life, but that its expression diminishes to almost undetectable levels at adulthood[108]. We re-examined this point immunohistologically using a previously characterized specific antibody targeting the GluN3A subunit[119] (Fig. 20-21). Our staining revealed several specific brain areas, where GluN3A expression remained high also at adult ages. We indeed found strong immunohistochemical expression in the associative thalamus, namely in all the thalamic intralaminar nuclei (central lateral or CL, central medial or CM, paracentral or PC, parafascicular or PF) and in the midline paraventricular nucleus, or PVT. Intense GluN3A staining was also found in the epithalamic MHb and, to much lesser extent, in the LHB (Fig. 20-21). Finally, expression was detected in sparse cortical neurons and hippocampal interneurons. As opposed to the forebrain, GluN3A was instead completely absent in the rostral brainstem.

Motivated by these morphological findings, and by our discovery of the effects of CGP78608 on receptor activation, we set out investigating the possible functionality of diheteromeric GluN1/GluN3ARs in the adult brain.

3. Diheteromeric GluN1/GluN3Ars are functional in the mouse adult MHb

We first decided to concentrate on the MHb, an epithalamic structure long known for its role in aversion[125,325]**.** To examine whether GluN3A and GluN1 subunits assemble into functional glycine-activated NMDARs, we puffed glycine (10mM) onto whole-cell voltage-clamped MHb cells (Fig. 22-23) in the presence of a cocktail of neurotransmitter inhibitors, including D-APV and strychnine (see methods). A unique case in our experience on diheteromeric GluN1/GluN3ARs in the brain, glycine puffs induced comfortably detectable, rapidly rising and inactivating inward currents, which were significantly bigger than in GluN3AKO mice[125] (Fig. 22) with total transmitted charges amounting to 17.1±2.1 pC (n=24) and 0.27±0.2 pC (n=10; $p < 0.001$; Mann-Whitney) in control and mutant animals, respectively.

As expected, bath application of CGP78608 induced huge current potentiation in WT (5429.8±1236.0 %, n=15, p=0.0006 vs pre-drug conditions, Mann–Whitney test) but not in GluN3AKO animals (12.5±1.7 %, n=7, p=0.0002 vs CGP applications in WT mice, Mann–Whitney; Fig. 23). Further experiments showed that glycine-elicited GluN1/GluN3AR currents increased MHb neuron firing rates recorded in the cell-

attached configuration, and that they showed similar pharmacology as recombinant receptors[125]. This pharmacology was preserved when currents potentiated by CGP78608 were tested. Namely, the GluN1 and GluN3 glycine binding site antagonists CNQX (100µM) and DCKA (500µM) reduced current amplitudes to 12.5±1.7 % (n=10; p=0.005; Wilcoxon-signed rank) and 10.1±2.4 % (n=9; p=0.0006; Wilcoxon; Fig. 24) of the control conditions in the presence of CGP78608. The effect of D-serine on GluN1/GluN3AR currents was also interesting. On one side, we indeed found that D-serine was a partial receptor agonist, triggering smaller maximal currents than glycine in MHb neurons[125]. In contrast, D-serine was a very efficient antagonist of glycine-evoked responses, both in control conditions[125] and during CGP78608 applications, reducing current amplitude to 6.6±3.5 % with respect to pre-application periods in the latter case (n=7; p=0.002; Wilcoxon; Fig. 24).

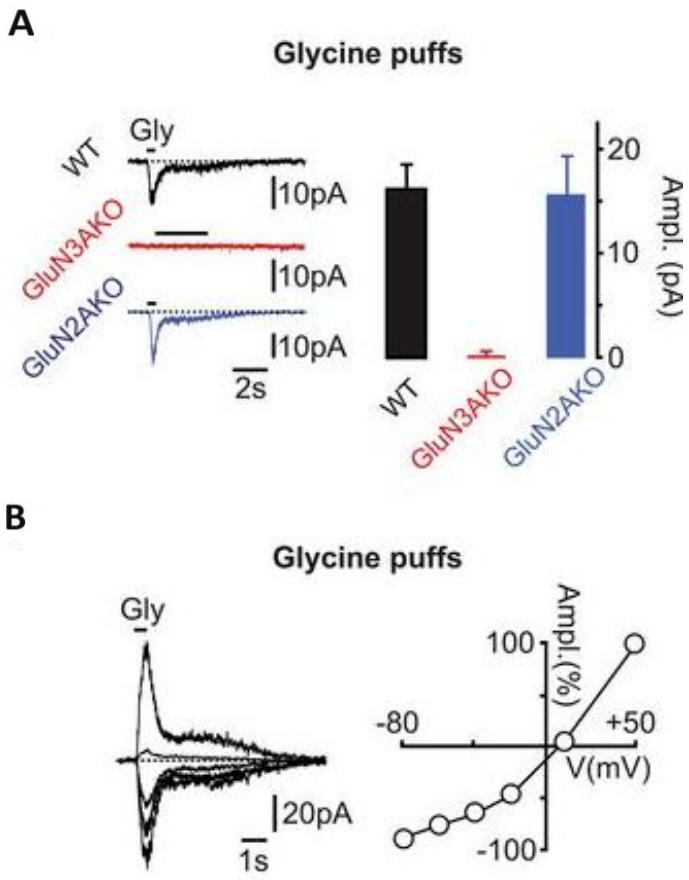

Figure 22| Glycine-induced GluN1/GluN3AR currents are detected in the adult MHb of control and GluN2K0, but not in GluN3AKO mice.

A,B- Glycine (10mM) was puffed onto clamped MHb cells in acute MHb-containing slices from adult control, GluN2KO and GluN3KO mice, in the presence of D-APV and strychnine. **A**- Glycine evoked rapidly rising and inactivating currents in control and GluN2AKO cells but had no effect in GluN3AKO animals**.** In GluN2AKO mice conventional NMDARs are almost undetectable (see[125]). **B-** Similar to recombinant systems, the glycine-induced currents displayed minor outward rectification. Data are illustrated as averages ± SEM.

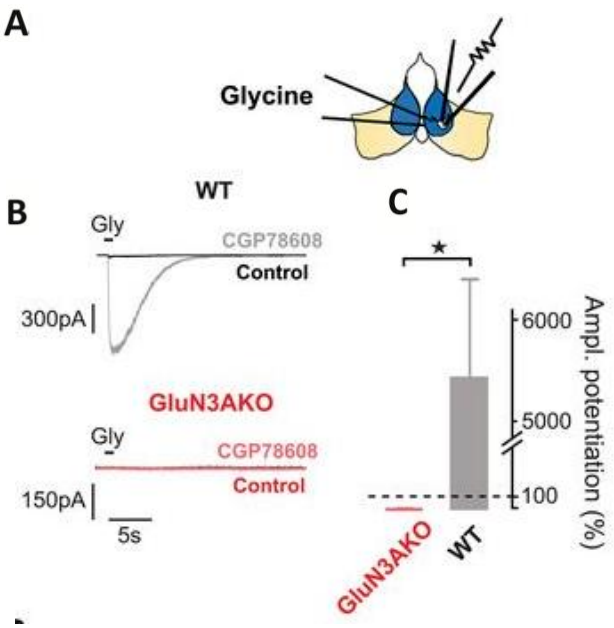

Figure 23| GluN1/GluN3ARs are expressed and functional in adult MHb slices.

A- Schematic representation of the experimental protocol. Glycine was puffed onto voltage-clamped MHb cells in acute slices from adult WT mice. **B-** In control conditions, glycine puffs triggered very small but detectable inward currents. Bath application of CGP78608 (CGP) led to massive potentiation of glycine-elicited currents in WT mice (top black traces) but had no effect in GluN3AKO animals (bottom red traces). **C-** Quantification of the experimental results obtained in panel B. WT, grey; GluN3AKO, red. Data are illustrated as mean ± SEM

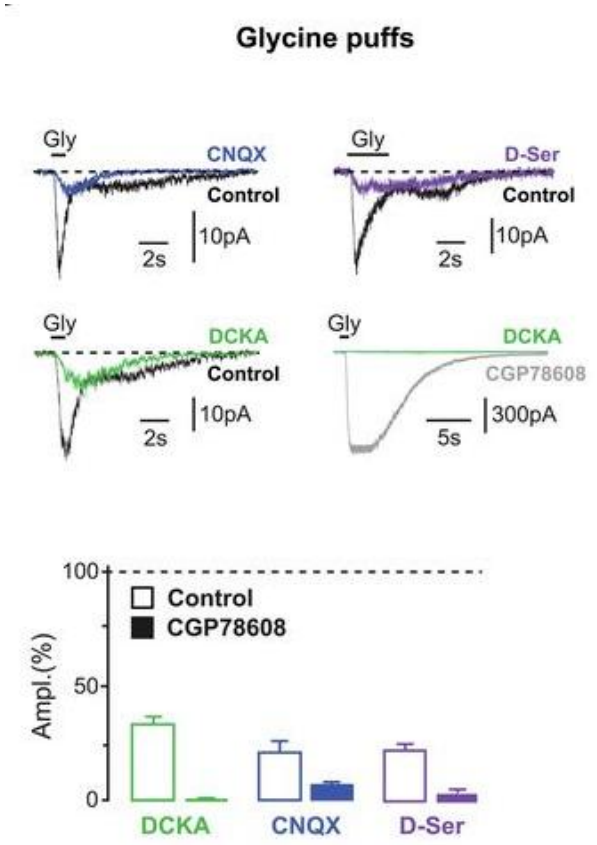

Figure 24| GluN1/GluN3ARs currents in the MHb show analogous pharmacology as recombinant receptors .

Bath applications of the GluN1 and GluN3 glycine binding site antagonists CNQX (100 µM, blue) and 5,7-DCKA (500µM, green) antagonized glycine-evoked responses, reducing current amplitudes in control conditions and in the presence of CGP78608. Similarly, the partial receptor agonist D-serine (purple), interestingly acted, in control conditions and in the presence of CGP78608, as a very efficient inhibitor of glycine-elicited responses. Data are illustrated as mean ± SEM.

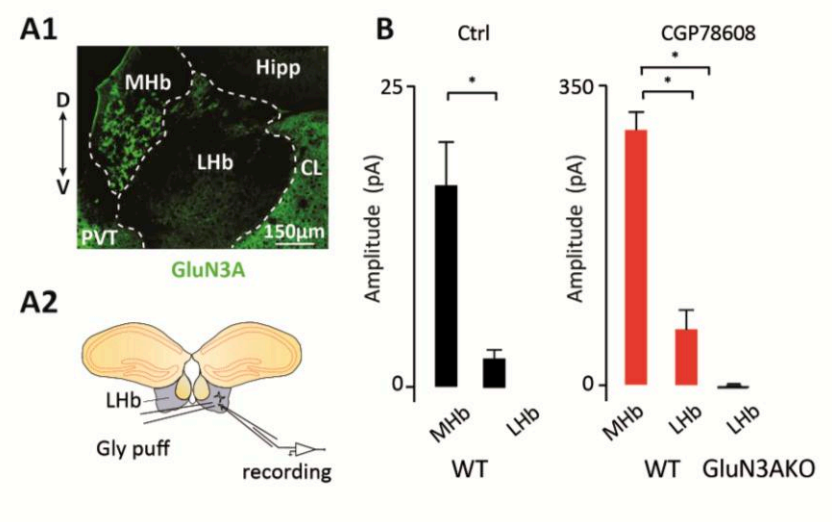

Figure 25| GluN1/GluN3ARs are weakly expressed in adult LHb slices, but still elicit detectable currents following CGP78608 application.

A- Schematic representation of the experimental protocol. **(A1)** Coronal brain section showing immunostaining for the GluN3A subunit. Weaker (but not absent) GluN3A expression is detected in the LHb compared to the MHb and the thalamic intralaminar CL. **(A2)** Glycine was puffed onto voltage-clamped LHb cells in slices from adult mice. **B-** Diheteromeric GluN1/GluN3ARs are expressed at very weak levels compared to the MHb. Glycine puffs elicited much smaller currents in the LHb with respect to the MHb both in control (left) and following CGP78608 bath applications (right). Currents recorded in the LHb were nonetheless elicited by activation of GluN1/GluN3ARs because they were absent in GluN3AKO mice.

4. Low expression levels of functional diheteromeric GluN1/GluN3ARs in the adult LHB

Our immunohistochemical study revealed sparse punctual GluN3A staining in the LHb, much weaker than in the MHb and in the midline and intralaminar thalamus (Fig. 25-A1). In the course of the study that we recently published in Science[125], this fact led us to test whether GluN3AR-containing NMDARs were functional in the LHb, and could thus mediate the behavioral effects we observed when interfering with GluN3A expression levels in the MHb using shRNA-based approaches[125]. Furthermore, examining the effects of CGP78608 on glycine puffs in a brain region with extremely low immunohistological GluN3A expression could represent an interesting test for the capacity of this drug to reveal GluN1/GluN3AR currents. Using NMDA puffs in acute slices we first demonstrated that triheteromeric GluN1/GluN2/GluN3A were not functional in LHb cells (see Suppl. Fig. 9 in[125]). We then examined the effects of pressure ejections of glycine (10mM; Fig. 25). In LHb cells glycine puffs elicited hardly detectable inward currents in control (2.9±0.7 pA, n=9), which were significantly smaller than the ones recorded in the MHb (17.3±3.6 pA, n=9, p=0.001, Mann-Whitney test; Fig. 25)

Bath application of CGP78608 resulted in significant potentiation (Fig. 25) of the currents, which was nonetheless still significantly smaller in the LHb (71.9±21.9 pA, n=11) than in the MHb (304.9±20.2 pA, n=11, p=0.001, Mann-Whitney). In the context of our Science publication, these data indicated that GluN3A expression in the LHb most probably did not affect the outcome of our behavioral tests. Furthermore, these experiments also highlighted the efficacy of CGP78608 in leading to detection of functional GluN1/GluN3ARs even when GluN3A subunits are expressed at very weak levels.

5. Diheteromeric GluN1/GluN3ARs are functional in the mouse adult midline thalamus

We then proceeded to investigate the presence of functional GluN1/GluN3ARs in the associative thalamus, concentrating on the intralaminar CL nucleus, and on the midline PVT nucleus. The same experiment as in Fig. 23 was conducted in both nuclei. As previously, all experiments were performed in the presence of a combination of neurotransmitter inhibitors, including strychnine and D-APV (see methods).

5.1. CL:

In the CL, we recorded the currents elicited upon pressure ejection of glycine (10mM) at -60mV, and then measured the total charge transmitted by channel opening. In control

conditions, the total charge recorded was 0.006±0.003 nC (n=11), and was dramatically potentiated by bath application of CGP78608 (to 2.40±0.88 nC, n=11, p=0.003, Wilcoxon signed-rank test). Currents were almost completely abolished by bath application of DCKA (9.40±7.28 pC, n=7; Fig. 26).

5.2. PVT:

In the PVT, glycine puffs induced hardly detectable inward currents in control conditions. The total charge recorded (0.004±0.001 nC, n=9) was again hugely potentiated by bath application of CGP78608 (to 2.37± 9.42 nC, n=9, p=0.004, Wilcoxon signed-rank test). Even in this case, the currents were almost completely eliminated by DCKA (5.58±3.64 pC, n=7, p=0.0001, Mann-Whitney).

Overall, these data demonstrate that GluN1/GluN3ARs are expressed and functional in several brain areas at adult developmental stages, thus establishing a new functional principle for glycine as a neurotransmitter in the CNS.

These results were made possible by our discovery of the potentiating effects on receptor current amplitudes of CGP78608, a compound that thus could represent a fundamental tool for the detection of these receptors in native tissues. Our recent paper[125] also demonstrated that Conditioned Place Aversion, a paradigmatic behavioral paradigm for the association of internal affective states to negatively-values external cues is strictly dependent on the full function of GluN1/GluN3ARs in the MHb. In a later section I will discuss more thoroughly the possible meaning of our results, and the new perspectives that these open.

I will now describe my experimental work concerning the other flavor of GluN3A subunit-containing NMDARs, the triheteromeric GluN1/GluN2/GluN3A receptor complexes.

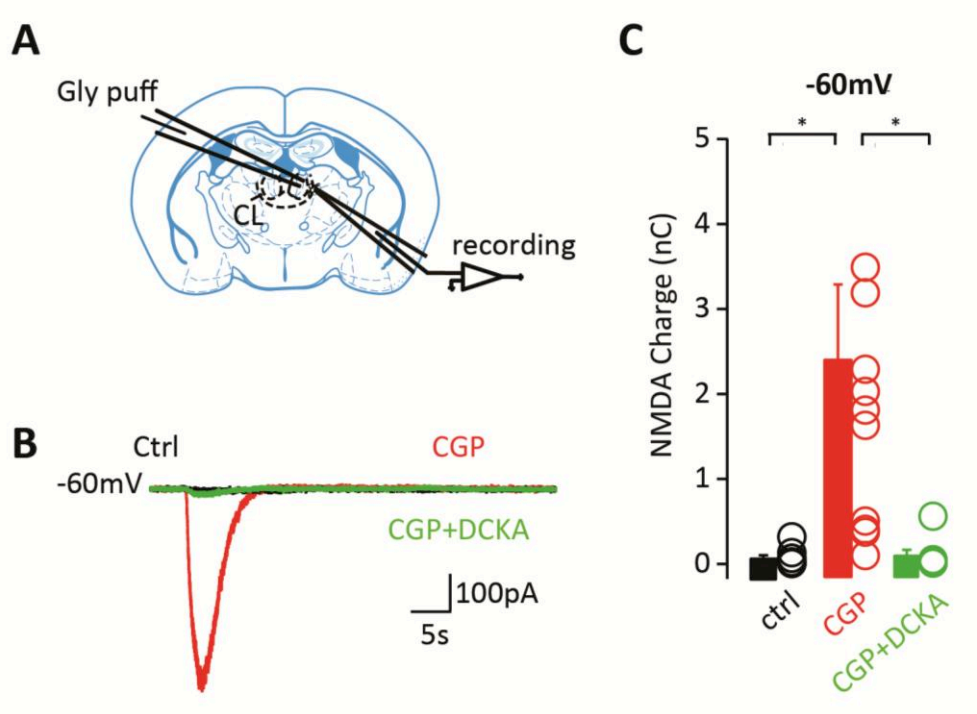

Figure 26| GluN1/GluN3ARs are expressed and functional in the CL of adult mice.

A- Glycine was puffed onto voltage-clamped neurons in the CL of adult mice. **B-** In control conditions, glycine puffs triggered small inward currents in WT mice (black trace). Bath application of CGP78608 (CGP) led to massive potentiation of glycine-elicited currents in WT (red trace). The addition of DCKA (500 µM), a GluN1 and GluN3A glycine-binding site competitive antagonist, eliminated the currents obtained in the presence of CGP (green trace) **C-** Quantification of the results obtained. The value of the total charge resulting from GluN1/GluN3AR activation at -60mV is shown for all cells tested in control conditions (black bar and points, the latter representing individual cells), after bath application of CGP78608 (red) and after application of DCKA (green). Data are illustrated as mean ± SEM.

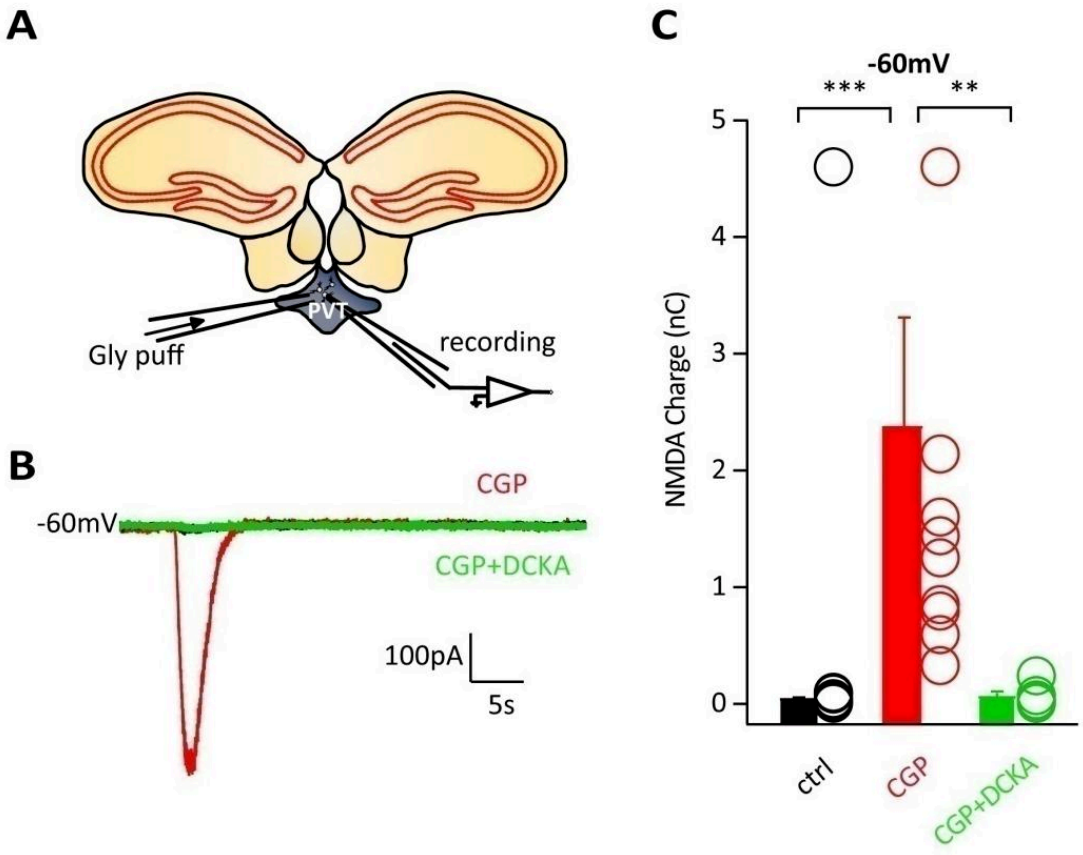

Figure 27| GluN1/GluN3ARs are expressed and functional in the PVT of adult mice.

A- Schematic representation of glycine in the adult PVT. **B-** In control conditions, glycine puffs triggered very small inward currents (black trace). Bath application of CGP78608 (CGP) led to massive potentiation (red trace). The addition of DCKA (500 µM) almost completely inhibited the responses (green trace). **C-** The value of the total transmitted charge at -60mV for all cells tested in WT mice in control conditions (black bar and points), after bath application of CGP (red) and after application of DCKA (green). Data are illustrated as mean± SEM.

6. Triheteromeric NMDA receptors are functional in the PVT of adult mice

We examined whether the GluN3A subunit could associate with GluN1 and GluN2 to form functional triheteromeric GluN1/GluN2/GluN3ARs in the adult brain. As previously mentioned, these receptors have been consistently detected in both cortical and hippocampal areas at juvenile developmental stages, and a rather rich literature exists concerning their possible role in the maturation of synaptic connections and circuits[122]. Detection using electrophysiological techniques is possible because these receptors exhibit weaker block by extracellular Mg^{2+} at hyperpolarized potentials, when compared to conventional GluN1/GluN2 NMDARs[112,116,117,136,137]. We used this unique characteristic of triheteromeric GluN1/GluN2/GluN3ARs to detect their presence in the PVT. We explored the effect of applying brief (300-500ms) pressure ejection of NMDA (5mM) onto voltage-clamped PVT neurons (Fig. 28). These experiments were performed in the presence of a cocktail of neurotransmitter receptor inhibitors including the AMPAR antagonist NBQX, the glycine receptor antagonist strychnine, the GABAaR antagonist SR95531 and the sodium channel blocker TTX (see methods), added both to the puff pipette, and to the bath solution. We recorded the currents elicited at 3 distinct holding potentials, -60mV, -40mV and +50mV in both WT and GluN3AKO mice. The NMDAR current rectification was quantified by calculating the ratio between the transmitted charges at -60mV and at +50mV, and between the values at -40mV and +50mV. Results obtained in WT and GluN3AKO mice were then compared to detect possible significant differences.

As shown in Fig. 28, the extracellular Mg^{2+}-mediated block at hyperpolarized potentials was significantly reduced in WT in comparison to GluN3AKO mice. The charges measured in WT mice at -40mV and at -60mV amounted to 29.33±3.46 % (n=8) and 16.36±2.52 % (n=8) of those obtained at +50mV, respectively. In GluN3AKO animal, these values were significantly smaller at both potentials, amounting to 13.85±2.08% (n=10; p=0.003; Mann-Whitney) and 8.48±1.91 % (n=8; p=0.02) at -40 and -60 mV, respectively, indicating greater rectification for NMDARs in the PVT when GluN3A subunits are not expressed.

This difference in rectification between WT and GluN3AKO neurons strongly indicates the presence of functional triheteromeric GluN1/GluN2/GluN3ARs in the PVT of adult mice.

We pursued a second approach to confirm these results. Indeed, the use of KO mice always entrains the risk that the detected effects could be due to developmental compensation mechanisms. This argument is particularly important in the case of

GluN3A subunits, because of their control of synaptic organization at early postnatal stages. We thus envisaged a strategy allowing us to reduce GluN3A expression specifically in the PVT, and at precise developmental moments, namely, in our case, at adulthood.

We therefore repeated the NMDA puffs experiments in WT mice injected in the PVT with an AAV expressing a short hairpin RNA targeting the GluN3A subunit, and GFP (AAV5-shRNA.GluN3A-GFP). This method provides temporal and spatial control over GluN3A subunit knock-down. The virus expressed sequences designed by Isabel Perez-Otano of the Institute of Neuroscience in Alicante, and was a gift from Camilla Bellone of the University of Geneva, who used it for a previous study focusing on the contribution of GluN3A subunits to synaptic plasticity forms induced by cocaine in the ventral tegmental area[140]. We verified that the virus efficiently reduced the levels of GluN3A messenger RNA in our regions of interest, namely in the MHb[125]. As shown in Fig. 28, injected mice displayed reduced extracellular Mg^{2+}-mediated inhibition at hyperpolarized potentials compared to WT, with the total charge recorded at -40mV amounting to 17.36±3.25 % of the one recorded at +50mV, a significantly greater value than that quantified in non-injected WT mice.

These results confirmed that the GluN3A subunit is not only present, but also forms functional triheteromeric NMDARs on the cellular membranes of PVT neurons in adult mice.

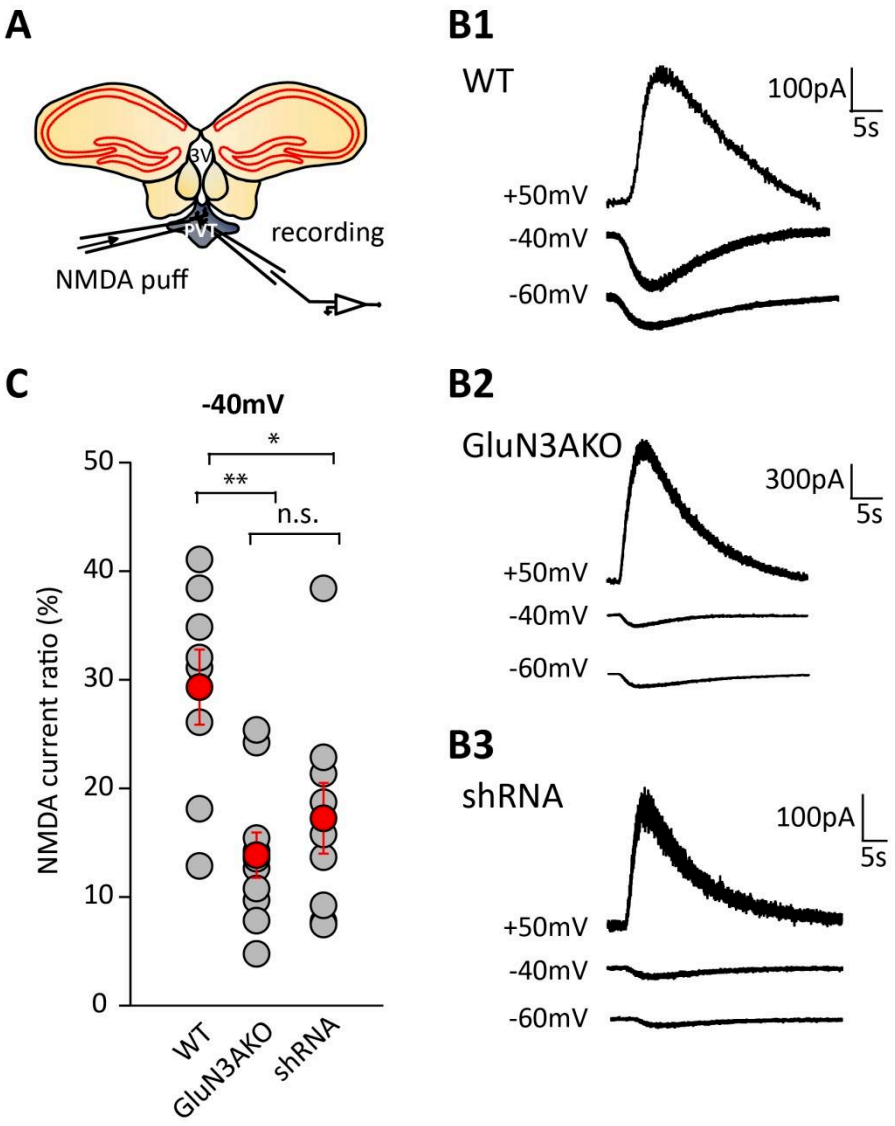

Figure 28| NMDAR current rectifications in WT, GluN3AKO and shRNA. GluN3A-expressing mice reveal the presence of functional triheteromeric NMDARs in the midline PVT.

A- Experimental configuration. PVT neurons were voltage-clamped and the currents elicited by pressure ejection of NMDA (5 mM) were recorded in the whole-cell configuration. **B-** Representative currents recorded at a holding potential of +50mV, -40mV and -60mV (as indicated), in response to brief NMDA puffs onto a neuron from a WT **(B1)** and a GluN3AKO mouse **(B2)** and from an animal in which GluN3A subunit expression was reduced by viral delivery of a specific shRNA **(B3)**. **C-** The ratio between the total charges due to NMDA channel opening at -40mV and +50mV for all cells tested in WT (left circles), GluN3AKO (middle), and shRNA-expressing mice (right) are shown in the graph. Data are illustrated as mean± SEM.

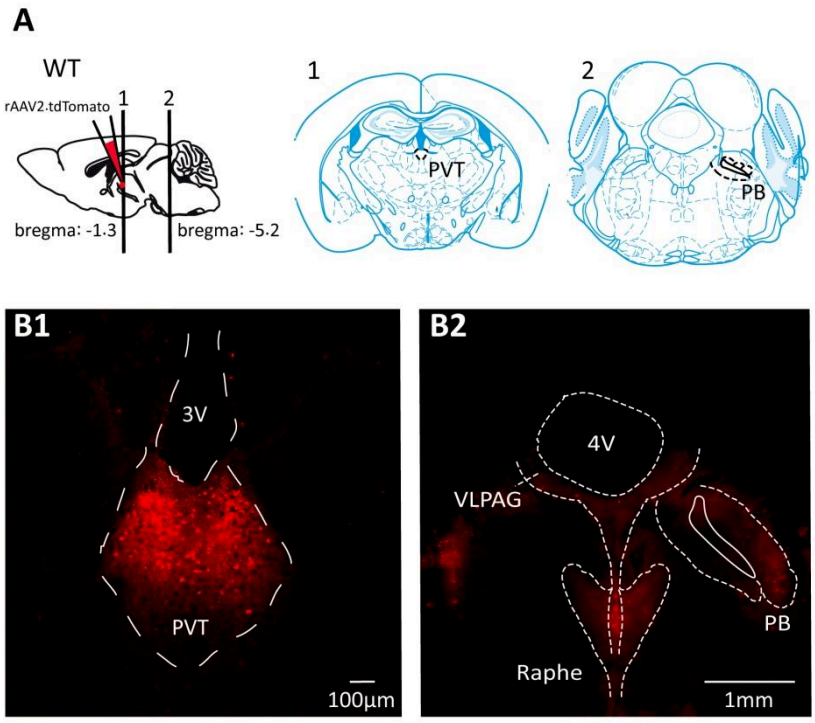

Figure 29| Retrograde labeling of PVT-projecting cells in the PB.

A- Graphics representing the injection of a retrograde virus, rAAV.tdTomato, in the PVT (left). The coronal slices on the right were adapted from the Paxinos mouse atlas, and illustrate the position in the brain of the PVT (1) and of the presynaptic nucleus of interest for us, the PB (2) **B-** Exemplary images from the brain of an adult WT mouse injected with rAAV.dtTomato, showing the injection site in the PVT of an adult WT mouse (B1) and the corresponding tdTomato-positive areas hosting retrogradely labeled cell bodies in the PB (B2). Retrograde labeling was also observed in the raphe and the ventro-lateral periaqueductal gray (VLPAG).

However, puff applications of NMDA activate both synaptic and extra-synaptic receptors. We wondered whether triheteromeric GluN1/GluN2/GluN3ARs could also be activated synaptically by extrinsic glutamatergic inputs. We thus searched for possible physiological sources of glutamate leading to GluN1/GluN2/GluN3AR activation. We exploited viral retrograde tracing strategies to localize inputs to the PVT (Fig. 29). We injected a red fluorescent tdTomato-expressing AAV virus with capsids optimized for retrograde transport[341] into the PVT of C57B6 mice (Fig. 29). Consistently with the existing literature[177,204,265], retrogradely labeled cell bodies were identified mainly in rostral brainstem nuclei known to project to the midline thalamus, namely in the periaqueductal grey (PAG), the parabrachial nucleus (PB), the pedunculopontine nucleus, the pons and the raphe. Labeled neurons were also found in the insular cortex and the hypothalamus. We examined the synaptic inputs originating from several potential presynaptic nuclei (the PAG, the PB, the pons and the insular cortex) to the PVT and studied the nature of their efferences to the PVT. To do so, we chose an optogenetic approach. We injected the targeted nuclei of either WT or GluN3AKO mice with a mix of an AAV expressing Cre recombinase in a non-specific way and an AAV expressing double floxed sequences of the optogenetic activator Channerlrhodopsin 2 (ChR2) and the yellow fluorescent reporter protein (YFP; Fig. 30). This viral combination turned out to infect quite efficiently the neuronal population of all targeted nuclei and allowed us to examine in detail the properties of the existing synaptic connections using optogenetic stimulations.

We prepared PVT-containing acute slices minimum 3-4 weeks following viral delivery. At this post-injection stage fibers expressing YFP could typically be observed in the PVT if the presynaptic nucleus had been correctly targeted.

Our results are described in the following sections.

7. GluN1/GluN2/GluN3A NMDARs in PVT neurons are activated by PB inputs

We first examined the PVT inputs originating from the PB (Fig. 30), infected as we described previously. In voltage-clamped PVT neurons, broad field illumination with brief (1-2 ms) flashes of blue light reliably induced light-evoked excitatory postsynaptic currents (leEPSCs) that were blocked by the co-application of the AMPAR antagonist NBQX and the NMDAR antagonist DL-APV (Fig. 31). PB inputs to the PVT were thus glutamatergic. Currents recorded at -60mV had an average amplitude of 179.0±57.9 pA (n=8) and were almost completely blocked by bath application of NBQX alone (10µM), to 7.3±2.1 pA (n=8, $p<0.001$, Wilcoxon test). Bath application of DL-APV (100µM) hardly

reduced further the remaining currents (Fig. 31-C). The currents recorded at +50mV had in contrast an average maximal amplitude of 123.0±43.6 pA, they showed much slower decay rates than the responses at the hyperpolarized holding potential, and were only partially reduced by bath application of NBQX, to 91.9±35.2 pA (n=8, p=0.23). The application of DL-APV greatly blocked the remaining component to 30.3±9.68 pA (n=8, p=0.04; Fig. 31-D), demonstrating the glutamatergic nature of the optically activated synapses. We believe that the significant leEPSC amplitude remaining after NBQX and DL-APV application was still mediated by NMDARs, because in these experiments we unfortunately used DL-APV and not D-APV, DL-APV being a mixture of the active enantiomer D-APV with the inactive one L-APV, present in unknown percentages. Furthermore, and importantly, applications of strychnine and SR95531, blockers of glycinergic and GABAa receptors, respectively, never had any significant effect on the currents (data not shown), thus excluding the presence of a conventional inhibitory projection from the PB.

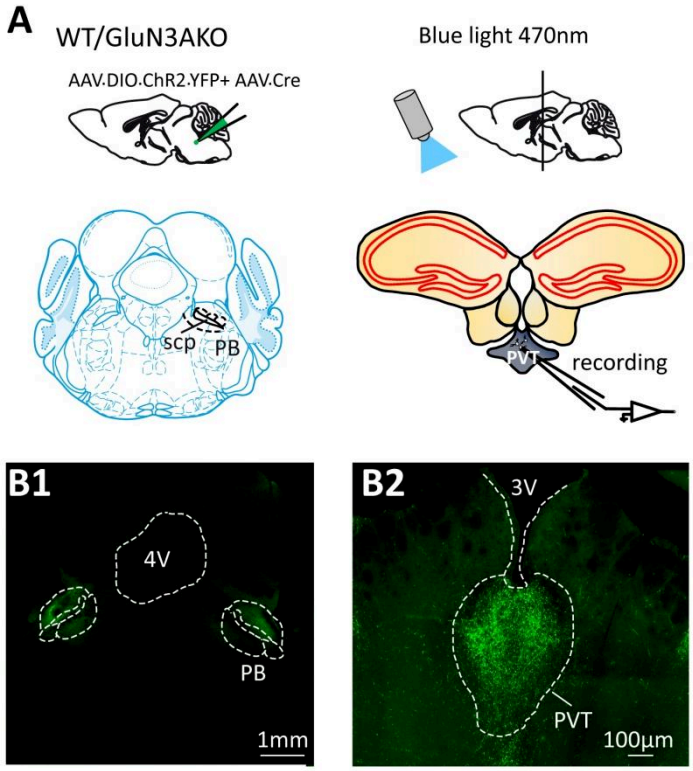

Figure 30| Expression of ChR2 in PB afferents to the PVT.

A- Schematic representation depicting the co-injection of AAV2/Ef1a-DIO.hChr2-YFP and AAV9/CMV.Cre in the PB (top left). The light blue illustrative coronal slice was adapted from the Paxinos atlas. The stimulation of PB afferents during voltage clamp recordings in the PVT is graphically depicted in the top right panel. **B-** Example of YFP fluorescence at the injection site in the PB of an adult WT mouse (B1) and corresponding YFP-containing fibers in the PVT (B2). 3V and 4V stand for third and fourth ventricle, respectively.

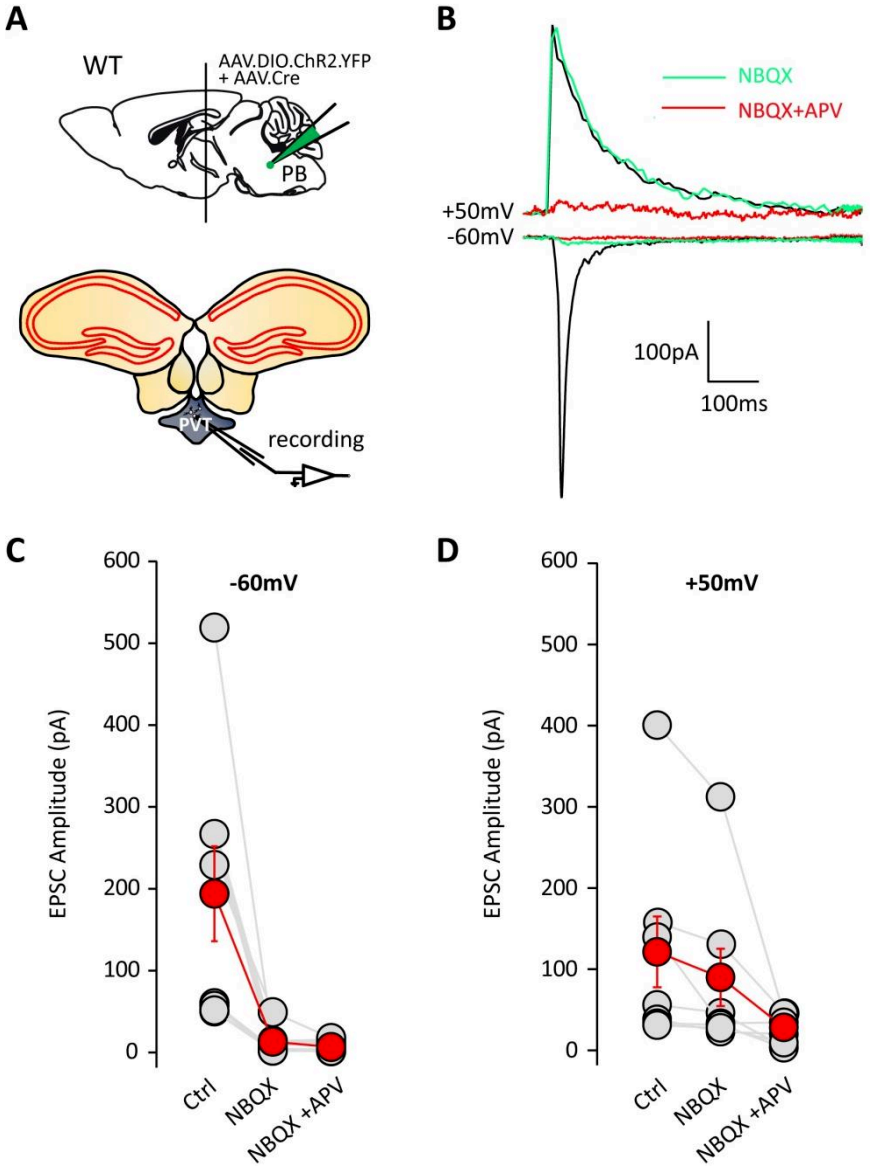

Figure 31| The PB projection to the PVT is glutamatergic.

A- Schematic experimental configuration. **B-** Averaged sample traces of leEPSCs recorded at +50mV and -60mV in the PVT in control conditions (black), after the application of NBQX (green) and co-application of NBQX and DL-APV (red). **C-** Summary of the results obtained in all the tested cells. Grey circles represent individual recordings, red ones the average values. The fast inward currents recorded at -60mV were almost completely blocked by NBQX. **D-** The outward currents recorded at +50mV showed much slower decay rates and were only slightly reduced by NBQX. Application of DL-APV strongly inhibited the remaining component. Data are illustrated as mean ± SEM.

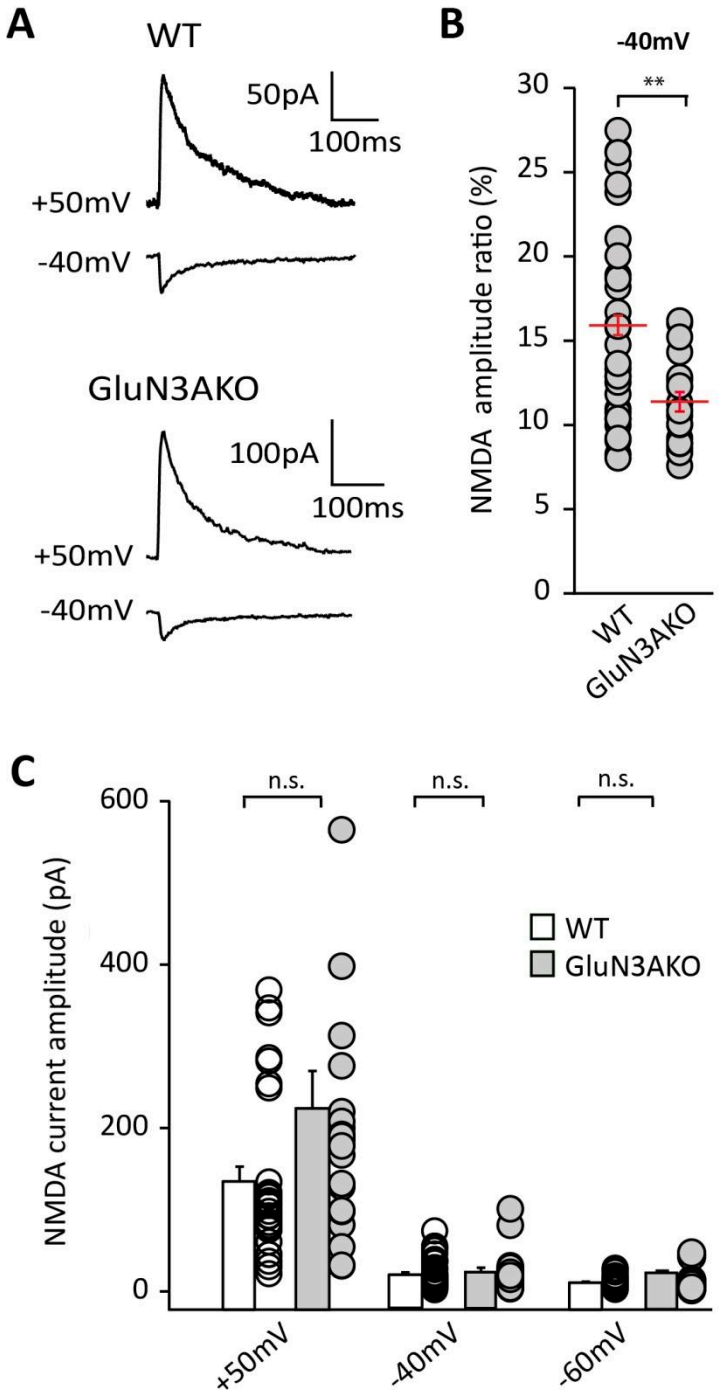

Figure 32| Glutamatergic PB afferents activate triheteromeric GluN1/GluN2/GluN3ARs in the PVT.

A- Averaged sample traces of leEPSCs at +50mV and -40mV in WT and GluN3AKO mice. **B-** The graphs represent the NMDAR current amplitude ratio calculated from leEPSCs recorded at -40mV and +50mV in WT and GluN3AKO mice. NMDA rectification is significantly smaller in WT mice than in GluN3AKO mice. **C-** The amplitudes of the NMDAR-mediated responses recorded at +50mV, -40mV and -60mV are shown for WT and GluN3AKO animals, as indicated. No significant difference was observed between WT and GluN3AKO at all holding potentials. Data are illustrated as mean ± SEM**.**

After verifying the glutamatergic nature of the PB-PVT synapse, we examined whether these inputs activated triheteromeric GluN1/GluN2/GluN3ARs. We pharmacologically isolated the NMDAR-mediated component by adding SR95531, strychnine, and NBQX to the bath solution, and recorded series of optogenetically-stimulated responses at distinct holding potentials, namely at −60mV, -40 mV and at +50mV (Fig. 32).

At hyperpolarized potentials GluN1/GluN2/GluN3ARs are inhibited by extracellular Mg^{2+} less potently than conventional GluN1/GluN2 NMDARs[107]**.** To determine whether triheteromeric GluN1/GluN2/GluN3ARs were activated, we estimated the NMDAR current rectification by quantifying the ratio between the leEPSC amplitudes obtained at the hyperpolarized potentials and those obtained at +50mV in both WT and GluN3AKO mice. Our results show that NMDAR-mediated leEPSCs rectified significantly less in WT than in GluN3AKO mice. The current amplitude ratio at -40mV was significantly greater in WT (15.9±1.1 %, n=31) than in GluN3AKO mice (10.7±0.7 %, n=21; $p < 0.001$; Mann-Whitney test). We found a similar result for current rectification at -60mV, with a statistically significant difference between WT (10.1±1.0 %, n=31) and GluN3AKO animals (5.4±0.4 %, n=21, $p<0.001$, Mann-Whitney; Fig. 32-B).

It is worth noting that a large variability was also observed in the cells recorded from WT mice.

Triheteromeric GluN1/GluN2/GluN3ARs show smaller single channel conductance than conventional GluN1/GluN2Rs[107,118]. However, we found no significant differences between NMDAR current amplitudes between WT (134.8±18.1 pA at +50mV, n=30; 20.4±3.0 pA at -40mV, n=30; 10.9±1.1 at -60mV, n=31) and GluN3AKO mice (195.0±67.9 pA at +50mV, n=22, p=0.3, Mann-Whitney; 22.4±5.5 pA at -40mV, n=21, p=0.8, Mann-Whitney; 10.4±2.5 pA at -60mV, n=22, p=0.2, Mann-Whitney) at all tested holding potentials (Fig. 32-C), although a clear trend was present at +50mV, where leEPSCs tended to be greater in neurons from GluN3AKO animals.

Together, these results strongly indicate that triheteromeric GluN3A-containing NMDARs are activated in the PVT at the glutamatergic inputs originating from the PB.

As we were examining in detail the glutamatergic pathway from the PB to the PVT, we were intrigued by one long-known characteristic of the PB: although eminently glutamatergic, the neuronal population of this nucleus is highly heterogeneous, with several distinct molecular markers expressed in specific PB sub-divisions that are often associated with diverse behavioral read-outs[315,329,330,342–344]. This fact, conjoint with the high variability of the rectification indexes observed in WT mice, led us to hypothesize

that triheteromeric GluN1/GluN2/GluN3ARs could be specifically activated by a precise cell sub-type within the PB.

To test this hypothesis, we targeted specific PB neuronal sub-populations, known (or supposed) to project to the PVT, and explored whether one (or more) of them activated triheteromeric NMDARs in the PVT. We targeted 5 different subgroups, namely cells expressing calcitonin G-related peptide (CGRP), oxytocin receptor (OxtR), prodynorphin (Pdyn), melanocortin 4 receptor (MC4R) and calbindin 2 (Calb2, also known as calretinin, or CR). Our choice to specifically work on these sub-populations was mostly based on the literature. We selected cellular groups implicated in behaviors similar to the PVT[304,305,315,326,336,337,343], and we followed hints found in a recent publication where the projection patterns in the anterior brain of several PB cell sub-groups were examined (see the supplementary data in[301]). Here follow our results.

8. OxtR-expressing PB inputs do not activate triheteromeric NMDARs in the PVT

Within the PB, cells expressing OxtRs are implicated in regulating fluid intake. Chemogenetic activation of these neurons via DREAAD receptors inhibits drinking in water-restricted mice. In opposition, their inactivation promotes fluid consumption[343].

To specifically target OxtR-expressing neurons in the PB, we co-injected into the PB of adult WT mice a serotype 2 AAV virus expressing double-floxed sequences for ChR2 and YFP and a virus expressing Cre recombinase under the OxtR promoter (AAV2/OxtR-Cre; Fig. 33). This latter virus was a custom preparation performed for us by the Laboratoire de Thérapie Génique, INSERM unit U1089 in Nantes. Three to four weeks following injections, fluorescent fibers could be observed in the PVT, indicating that the viral mix successfully infected PVT-projecting PB neurons (Fig. 33-A3).

In whole-cell patch clamp recordings, the NMDAR component of the leEPSCs was pharmacologically isolated as described previously (Fig. 33-B). We calculated the rectification of the NMDAR-mediated currents at -40mV and -60mV (Fig. 33-C). No difference in the ratio calculated between the amplitude values at -40mV and+50mV was found between the injected mice (12.2±0.6 %, n=19, p=0.05, Mann-Whitney) and GluN3AKO animals. In contrast, the NMDA current amplitude ratio at -60mV and +50mV was significantly different (AAV2/OxtR-Cre-injected mice: 6.7±0.3 %, n=16). The results obtained were thus ambiguous, making it difficult to draw a clear-cut conclusion. We nonetheless speculated as to whether the uncertainty of the data could be the result of lack of specificity of the AAV2/OxtR-Cre virus. Immunohistological verification of the

specificity of the newly produced Cre-expressing AAV2 indeed cast serious doubts on this point.

9. The AAV2/OxtR-Cre virus is not specific

We examined the specificity of the AAV2/OxtR-Cre virus by comparing the distribution of YFP-positive fibers following viral injections and immunohistological staining using a commercially available antibody against the oxytocin receptor (Thermo Fischer, PA5-32961, see methods; Fig. 34). These morphological experiments indicated the presence of colocalized signal from YFP and OxtR. However, a population of OxtR-negative ChR2-YFP-positive cells was also clearly observed (Fig. 34 C-D). These results indicate that AAV2/OxtR-Cre expression may not be specific for OxtR-expressing PB neurons. The lack of specificity of the virus could thus explain the ambiguous results illustrated in Fig. 34. Additional experiments should be conducted using a more reliable approach, for example a transgenic mouse line. The OxtR-Cre line was recently purchased from the Jackson Labsby our laboratory, and the first tests are now being performed in order to clarify the open questions illustrated here.

10. CGRP-expressing PB inputs do not activate triheteromeric NMDARs in the PVT

A vast literature exists on the physiology of CGRP-expressing neurons in the PB. These neurons have been shown to play a role in food intake regulation and satiation by preventing overeating, in pain, fear behavior, aversion and itching[284,293,305,311,315,318]. CGRP-positive cells are concentrated quite exclusively in the more ventro-lateral part of the PB, in contrast to OxtR-positive ones, which preferentially sit medio-laterally. Only 6% of the OxytR cells have been shown to express also CGRP in specific Cre recombinase mouse lines[343].

We followed a similar strategy as for the OxtR-positive cells in order to specifically target CGRP neurons in the PB. We co-injected the PB of B6/C57 mice with a virus expressing double-floxed ChR2-YFP together with a custom-made AAV2 expressing Cre recombinase under the control of the CGRP promoter. YFP-ChR2-containing fibers could be observed in the PVT weeks after the injections, demonstrating the infection efficacy of the viral mix used (Fig. 35-A3).

The NMDAR component of the optogenetically stimulated synaptic responses was pharmacologically isolated, and its rectification at -60mV and -40mV was calculated as before (Fig. 35-C). We found that leEPSC rectification was not different from the one

calculated in GluN3AKO mice, amplitude ratios amounting to 11.8±0.9 % (n=16, p=0.4, Mann-Whitney) at -40mV and to 6.3±0.4 % (n=16, p=0.03) at -60mV. These results suggest that GluN3A subunits were not incorporated in the NMDARs present at these synapses.

Given our previous concerns regarding the specificity of the AAV2/OxtR-Cre virus, we investigated the expression pattern of the AAV2/CGRP-Cre vector. We analysed the level of colocalization of the YFP signal and of the immunohistochemical staining for CGRP in the PB of injected mice. Similarly as for the AAV2/OxtR-Cre virus, we found not only YFP- and CGRP-positive cells and neurites, but also YFP-positive but CGRP-negative structures, thus once again suggesting lack of viral (Fig. 36).

From these experiments, we can thus conclude that CGRP-positive cells (and the other cell subtypes infected by the AAV2/CGRP-Cre virus) did not activate triheteromeric GluN3A-containing receptors in the PVT. Unfortunately, these experiments cannot tell us whether CGRP cells in the PB do project to the PVT at all. The little information available on the subject, in reality, seems to suggest that they do not (see supplementary data in[301]).

With all the uncertainties of the case, therefore, overall, this series of experiments was very useful because it allowed us to exclude CGRP cells as plausible candidates for GluN1/GluN2/GluN3A receptor activation in the PVT.

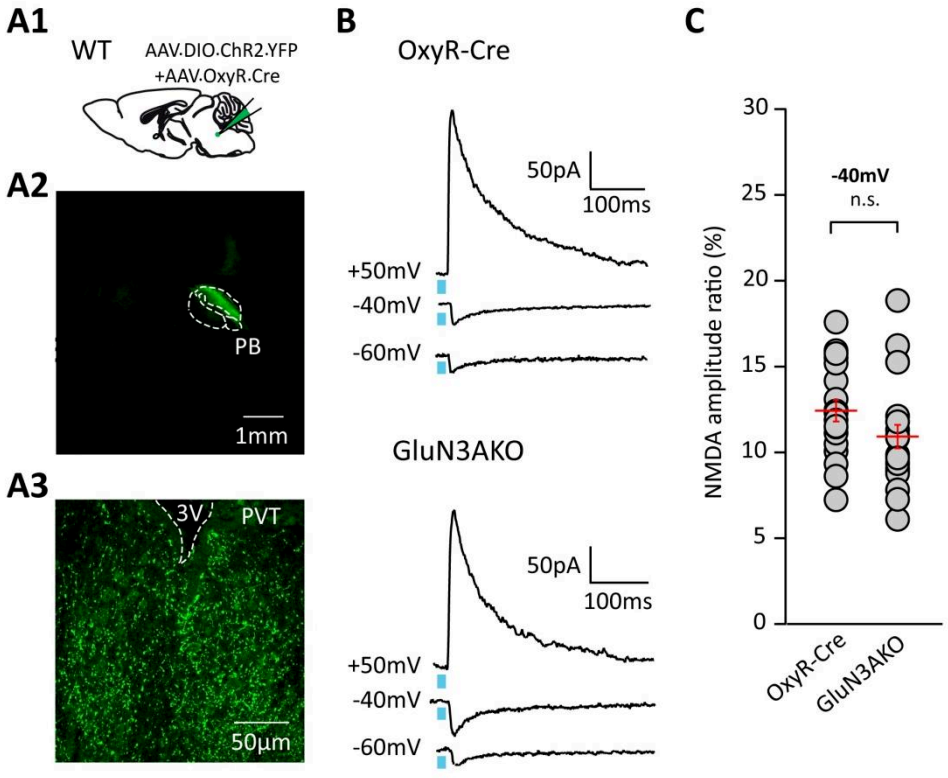

Figure 33| Synaptic triheteromeric GluN1/GluN2/GluN3ARs in the PVT are not activated by projections from OxtR-expressing cells in the PB.

A- Schematic representation of the experimental protocol **(A1)**. An example of a monolateral co-injection of AAV2/Ef1a-DIO.hChr2(H134R)-YFP and AAV2/OxyR.Cre into the PB of an adult B6/C57 mouse is illustrated in **(A2)** with the corresponding ChR2.YFP-containing fibers in the PVT **(A3)**. **B-** Averaged sample traces of leEPSCs at +50mV, -40mV and -60mV in a cell from an injected mouse (top), are compared with currents recorded in a GluN3AKO mice (bottom) **C-** The NMDAR current amplitude ratio at -40mV and +50mV calculated from all the recorded cells in viral injected (left) and GluN3AKO animals (right) are depicted. No significant difference in NMDA rectification was found. Results are shown as mean ± SEM**.**

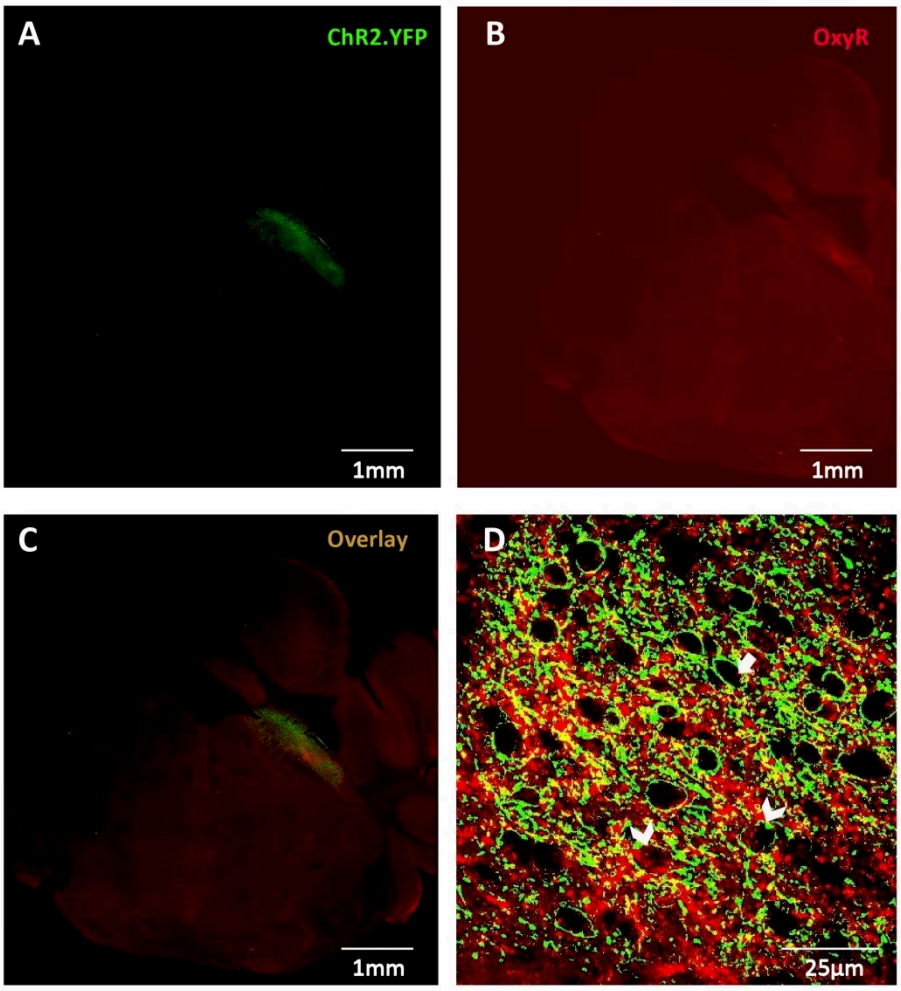

Figure 34|Lack of specificity of the AAV2/OxtR-Cre virus in the PB.

A- Fluorescence in the PB produced by co-injections of AAV1/DIO.ChR2-YFP and of AAV2/OxyR.Cre. **B-** Immunostained OxtR-positive structures in the PB. **C-** Overlay of ChR2-YFP and OxtR immunostaining in the PB. **D-** At larger magnification, white arrowheads indicate colocalization in the PB of ChR2-eYFP and OxtR, white arrows indicate OxyR-negative but ChR2.YFP-positive labeled cells.

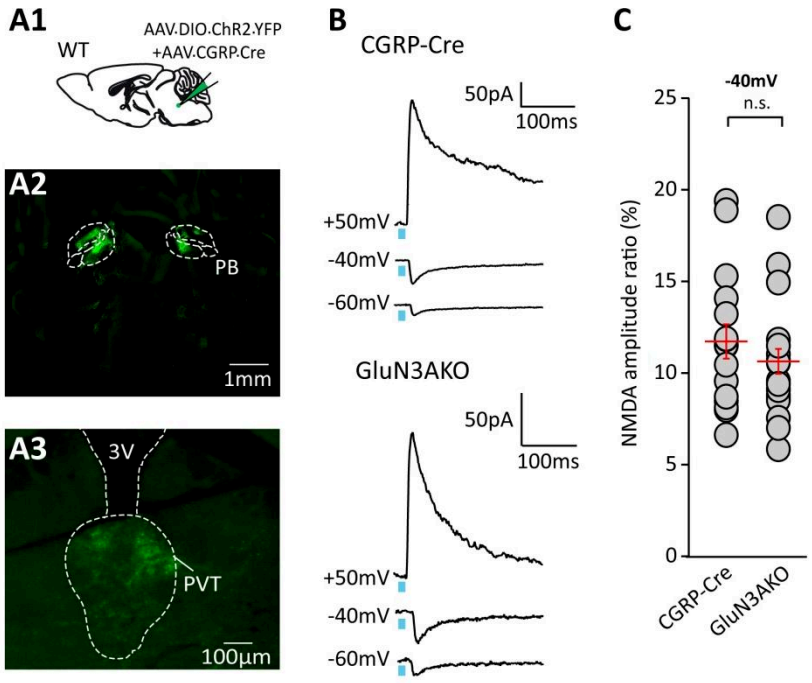

Figure 35| No activation of PVT GluN1/GluN2/GluN3ARs by CGRP-positive cells in the PB

A- Schematic representation of this series of viral injections **(A1)**, with an example of the fluorescence obtained in the PB **(A2)** and in the PVT **(A3)**. **B-** Averaged sample traces of leEPSCs. **C-** NMDAR current amplitude ratios in control (left) and GluN3AKO mice (right). No significant differences were found. Results are shown as mean ± SEM**.**

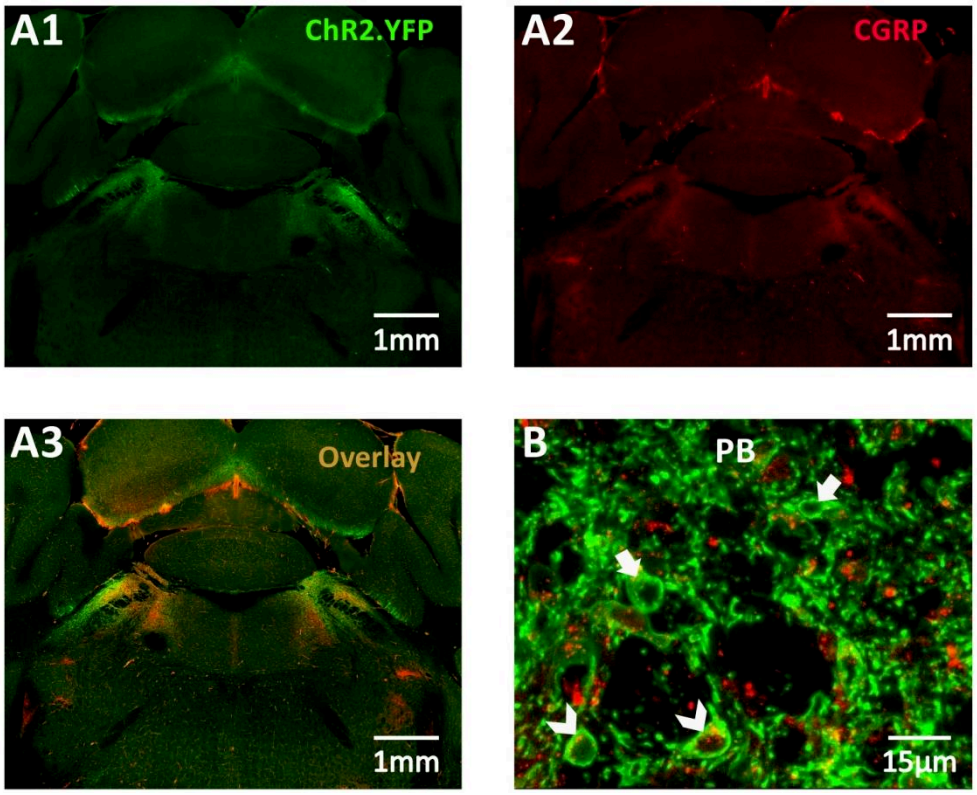

Figure 36| Lack of specificity of the AAV2/CGRP-Cre virus in the PB.

A- Fluorescence in the PB produced by co-injections of AAV1/DIO.ChR2-YFP and of AAV2/CGRP-Cre. **A2-** Immunostained CGRP-positive structures in the PB. **C-** Overlay of ChR2-YFP and CGRP immunostaining in the PB. **B-** At larger magnification, white arrowheads indicate colocalization in the PB of ChR2-YFP and CGRP, white arrows indicate CGRP-negative but YFP-positive labeled cells.

11. Pdyn-expressing PB inputs to the PVT do not activate triheteromeric NMDARs

The few studies conducted in the PB on prodynorphin-, or Pdyn-expressing neurons showed their implication in thermoregulation and their contribution to autonomic reflexes triggered by changes in skin temperature. Only in the recent months, further physiological roles for this cellular type have been found, namely in the control of responses to pain[330], and in the transmission to anterior brain areas of mechanosensory information on gastric dilatation, with consequences on the control of feeding behaviors[329].

Given the specificity problems encountered previously with viral approaches aiming at expressing the Cre recombinase in specific cell subtypes, we pursued a different strategy for targeting Pdyn-expressing neurons. We thus exploited a transgenic mouse line that expresses Cre recombinase under the Pdyn promoter (purchased from the Jackson laboratories). The specificity of this transgenic line was validated previously[345]. We injected into the PB of Pdyn-Cre adult mice a virus expressing double-floxed sequences of ChR2 and YFP. Interestingly, we found that Pdyn-Cre positive cells were housed in medio-lateral areas of the PB that superimposed with those hosting OxtR cells. YFP fluorescence was detected in the PVT of the injected mice weeks following viral delivery, confirming that Pdyn-positive cells project to the midline thalamus. We could thus record pharmacologically isolated NMDAR-mediated leEPSCs, as we described before (Fig. 37). We found that the difference in NMDAR rectification between Pdyn-Cre and GluN3AKO mice was not significant at both holding potentials tested, the current amplitude ratio amounting to 10.5±1.4 % (n=10, p=0.27; Mann-Whitney) and to 5.4±0.6 %, (n=10, p=0.4, Mann-Whitney) at -40mV and -60mV, respectively. These results indicate that triheteromeric GluN3A-containing NMDARs are not activated in the PVT at the projections from Pdyn-expressing neurons of the PB.

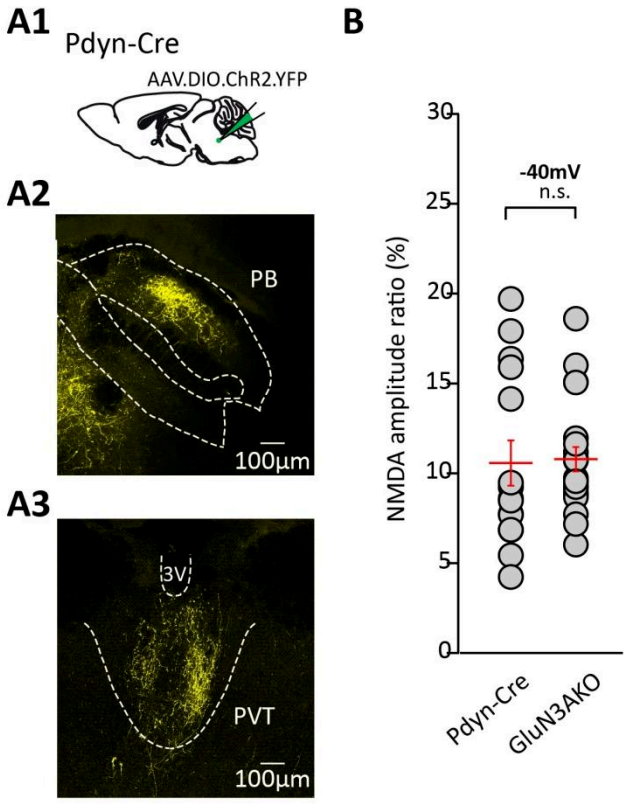

Figure 37| The PB neuronal sub-group expressing prodynorphin projects to the PVT but does not activate GluN1/GluN2/GluN3ARs.

A- Schema depicting the experimental configuration **(A1)**, with an example of an injection of AAV1/Ef1a-DIO.ChR2-YFP into the PB of an adult Pdyn-Cre mouse **(A2)** and the corresponding fluorescence in the PVT **(A3)**. **B-** No significant difference in NMDAR current rectification was found between Pdyn-Cre and GluN3AKO mice. Results are depicted as mean ± SEM**.**

12. Synaptic GluN1/GluN2/GluN3A NMDARs in the PVT are activated by inputs from MC4R-expressing parabrachial neurons.

Neurons expressing the melanocortin receptor 4 (MC4R) have been shown to promote satiety and induce weight loss, as well as to play a role in aversion and sickness behaviors[346,347]. These functions are performed principally by MC4R-expressing cells in the paraventricular nucleus of the hypothalamus, which are known to be critical also for energy balance. These hypothalamic cells project to the medio-lateral PB (in areas not hosting CGRP-positive neurons), where bidirectional control of their excitability critically controls food intake[348]. For our experiments, similarly to the tests in Pdyn-Cre mice, we exploited a transgenic mouse line that expresses Cre recombinase under the MC4R promoter. The reliability of this line, developed by Brad Lowell at Harvard University, has been demonstrated previously[348].

We thus injected a virus expressing double-floxed ChR2-YFP into the PB of adult MC4R-Cre mice (Fig. 38A), and quantified NMDAR current rectification as usual.

The results obtained were surprising and extremely interesting. First of all, we found fluorescent fibers in the PVT, confirming the existence of the projection[349]. We then found that triheteromeric GluN1/GluN2/GluN3ARs were indeed activated by the inputs originating from PB MC4R-expressing cells. Current amplitude ratios were significantly greater in MC4R-Cre cells with respect to GluN3A-deficient neurons at both -40mV and -60mV, amounting to 16.5±2.4 % (n=12, p=0.02, Mann-Whitney) and 7.5±0.9 %(n=12, p=0.009, Mann-Whitney; Fig. 38-B), respectively.

Experiments are now under way to further verify these results, by repeating the same experiments in MC4R-Cre mice injected in the PB with the double floxed ChR2-expressing AAV, and in the PVT with the shRNA-expressing virus targeting the GluN3A subunit.

Overall, these results are strongly in favor of a specific expression of triheteromeric GluN3A-containing NMDARs in the PVT at the synapses arising from PB MC4R-expressing cells. Possible physiological implications of this finding will be discussed in a later section of my thesis.

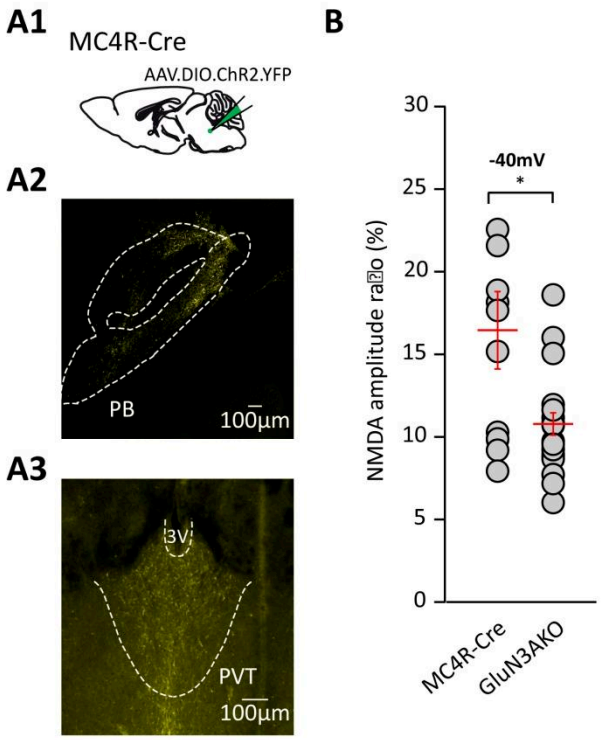

Figure 38| Synaptic afferences from melanocortin receptor 4-expressing parabrachial neurons do activate triheteromeric GluN1/GluN2/GluN3ARs in the PVT.

A- Schematic representation of the experiment **(A1)**, with an example of an injection of the AAV1/Ef1a-DIO.ChR2-YFP virus into the PB of an adult MC4R-Cre mouse **(A2)** and the corresponding fluorescence in the PVT (A3). **B-** The NMDAR current rectification is significantly smaller in MC4R-Cre mice than GluN3AKO animals. Data are illustrated as mean± SEM.

13. Triheteromeric GluN1/GluN2/GluN3AR are functional at connections between Calb2-expressing PB neurons and PVT relay cells

Extensive research has been conducted on CGRP- and OxtR-positive cells in the PB and their functions are now relatively well known. Recent studies involving Pdyn and MC4R cells have also been published, and their roles are becoming clearer. However, no PB-related physiological function has been so far associated with the last sub-cellular type we decided to look into during my thesis. Our collaborators at the Institute of Cognitive Neuroscience and Psychology (Research Center for Natural Sciences, Hungarian Academy of Sciences, Budapest, Hungary), who were investigating Calbindin 2-expressing cells (also known as Cabl2, or calretinin as the protein is most commonly designated) in the forebrain[174], noticed that an abundant population of cells in the PB expressed Calb2. We thus decided to explore their possible projections to the PVT in collaboration with our Hungarian colleagues, who host a Calb2-Cre mouse line in their facilities. I performed the injections in Budapest in collaboration with Dr. Ferenc Matyas, whereas morphological analysis and electrophysiological recordings were pursued in our laboratory in Paris following transfer of the injected animals.

The first question needing an answer was whether Calb2-expressing PB cells did project to the PVT. We thus targeted Calb2-expressing neurons in the PB by injecting Calb2-Cre mice with the usual AAV1/EF1α-DIO.ChR2-YFP viral vector. Weeks later, YFP fluorescence could be consistently observed in the midline thalamus, indicating that Calb2-positive cells in the PB sent axonal efferences to the PVT.

We then inspected the rectification properties of the NMDAR-mediated component of the leEPSCs. Similarly to the situation encountered for the projections from MC4R-expressing cells, we found a significant difference in current rectification between MC4R-Cre and GluN3AKO mice.

NMDAR leEPSC amplitude ratios were significantly greater in cells from the Cre-expressing mouse line, amounting to 16.0±1.0 % (n=23; $p<0.001$, Mann-Whitney) and 9.7±0.9 % (n=24, $p<0.001$, Mann-Whitney) at -40mV and -60mV, respectively (Fig. 39-C).

Triheteromeric GluN3A-containing NMDARs are thus activated in the PVT at the synapses formed by the Calb2-expressing cells in the PB.

We also explored the possible differences in the NMDAR current amplitudes between Calb2-Cre and GluN3AKO cells at depolarized and hyperpolarized potentials (Fig. 39-D). No significant difference was detected between Calb2-Cre (105.8±13.6 pA at +50mV, n=24; 17.1±2.6 pA at -40mV, n=23; 8.8±1.1 at -60mV, n=23) and GluN3AKO mice

(195.0±44.6 pA at +50mV, n=22, p=0.05; 22.4±5.5 pA at -40mV, n=21, p=1.0; 10.4±2.5 pA at -60mV, n=21, p=0.4, Mann-Whitney). Consistently with the reduced single channel conductance of GluN3A-containing triheteromeric NMDARs, it is to be noted that the current amplitudes recorded at +50mV in GluN3AKO mice again showed a trend towards greater values (Fig. 39-E), without however reaching statistical significance.

We also compared leEPSC decay kinetics between cells recorded in Calb2-Cre and GluN3AKO mice. Conventional NMDAR current kinetics depends upon GluN2 subunit composition. We thus hypothesized that inclusion of the GluN3A subunit could also entrain detectable differences in this parameter. In general, transient jumps of a neuron's holding potential to depolarized values (such as +50mV) trigger activation of several distinct voltage-dependent conductances that render the kinetic analysis of synaptic responses difficult and unreliable. Amplitude quantifications are instead less critical because they can be performed over shorter excerpts of a recorded trace. This was true also in the case of our voltage-clamp recordings of PVT cells. For decay time analysis, we were thus obliged to discard most of the neurons that were instead pooled into the averaged amplitude results. Only a qualitative examination of the decay kinetics of the leEPCSs was thus possible. It would appear that leEPSCs showed a slower decay in GluN3AKO mice with respect to Calb2-Cre animals (Fig. 39-F). Unfortunately, at this point this information must be still regarded more as an impression than as a statistical trend. To become so, we will obviously need to considerably expand the number of analyzable recordings in the future, something that was not possible in the course of my thesis.

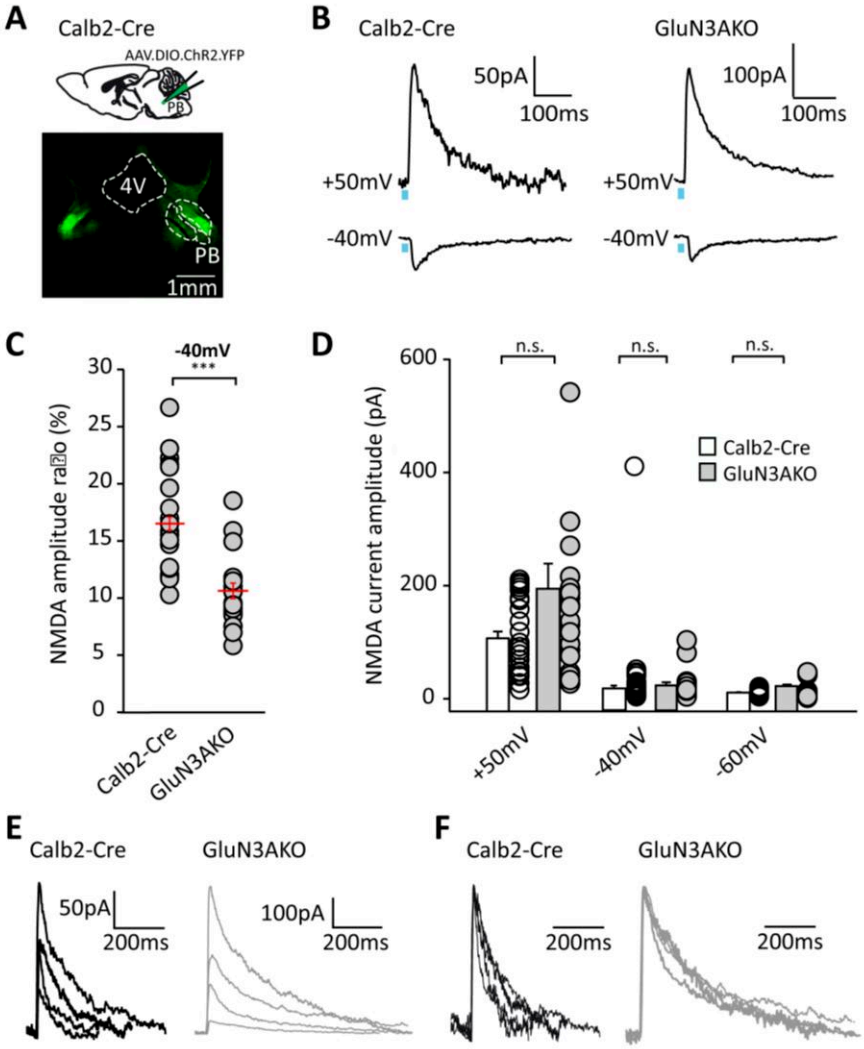

Figure 39| PVT afferences from Calb2-expressing cells in the PB activate synaptic GluN1/GluN2/GluN3ARs.

A- Schematic representation of the experimental protocol and exemplary image from the injection site of an adult Calb2-Cre mouse (bottom). **B-** Averaged sample traces of leEPSCs at +50mV and -40mV from a Calb2-Cre and a GluN3AKOmouse. **C-** The NMDAR current amplitude ratios from all recorded cells. NMDA rectification is significantly greater in GluN3AKO compared to Calb2-Cre. **D-** leEPSC amplitudes in Calb2-Cre and GluN3AKO animals. Qualitative examples of variability in amplitudes (**E**) and decay kinetics (**F**) in Calb2-Cre and GluN3AKO mice of synaptic responses recorded at +50mV. Data are illustrated as mean± SEM.

14. Infralimbic cortical inputs do not activate GluN3A-containing triheteromeric NMDARs in the PVT

At the beginning of this result section I mentioned that injections in the PVT of an AAV vector optimized for retrograde transport identified inputs to the PVT from several rostral and caudal brain nuclei, consistently with what was reported in the literature. At the onset of my thesis my intention was to examine the projections to the PVT from as many of these putative presynaptic nuclei as possible, in order to detect which of them would give rise to leEPSCs mediated by GluN3A-containing triheteromeric NMDARs. My early identification of the PB as a source of GluN3A-mediated responses radically modified my work plan. The potential physiological interest of the PB and of its projections to the PVT, conjoint with the urgency of dissecting as carefully as possible the cellular heterogeneity hidden behind the results observed, motivated me to dedicate the largest portion of my research activity to this structure. However, my interest in examining projections to the PVT other than those originating from the PB still remains intact. For example, it would be fascinating if MC4R-Cre and Calb2-Cre cells in the PB were the only neuronal sub-types presynaptic to the PVT that activate the triheteromeric NMDARs in the midline thalamus. Such a finding, unlikely as it may appear at this stage, would indeed be of tremendous significance for a very specific (and important) role played by GluN3A subunits in CNS physiology.

All these considerations notwithstanding, during my thesis I had the opportunity to examine in detail another projection to the PVT, namely the one originating from the infralimbic cortex (ILc). Our retrograde staining indeed displayed the existence of a powerful (in terms of number of stained cells) projection to the PVT originating from this area of the prefrontal cortex.

We thus co-injected the ILc of WT and GluN3AKO mice with a mix of an AAV expressing double floxed ChR2-YFP together with an AAV expressing the recombinase Cre in a non-specific manner. A rich plexus of fluorescent fibers could be observed in the PVT of acute slices weeks after viral injections, indicating that ILc neurons did indeed contact the PVT. As expected from cortical projections, the optogenetically evoked leEPSCs in the PVT were purely glutamatergic. We could then estimate the rectification of the NMDAR component following a protocol similar to the one described for PB inputs. The only difference was represented by the fact that we quantified the ratios between NMDAR leEPSC amplitudes recorded at -60mV and +50mV, and between the amplitudes recorded at -80mV and +50mV. We could not exploit the recordings performed at a holding potential of -40mV because leEPSCs could not be clamped. This was probably because cortical projections impinge onto more distal dendritic compartments of

thalamic relay cells than PB inputs, thus compromising voltage clamping at depolarized potentials, where thalamic cells are extremely excitable.

Overall, we found no significant difference between NMDAR current rectifications in PVT neurons of WT and GluN3AKO mice, the ratios between leEPSC amplitudes recorded at -80mV and +50mV and at -60mV and +50mV amounting to 4.9±0.3, 8.3±0.6 % (n=10) and 8.3±0.6 % (n=10), respectively, in WT mice and to 3.7±0.6 % (n=8; p=0.1 ; Mann-Whitney) and 5.7 ± 0.6% (n =12; p=0.7; Mann-Whitney) in GluN3AKO animals (data not shown graphically).

We can thus conclude that triheteromeric GluN3A subunit-containing NMDARs are not functional at ILc synapses to the PVT.

Overall, my thesis activity led the bases for a comprehensive re-analysis and re-evaluation of the role of the unconventional NMDAR GluN3A in brain physiology by demonstrating the functional expression of GluN3A-containing NMDARs in native neurons of the adult brain.

On one side, diheteromeric GluN1/GluN3A complexes are completely novel ionic receptor types that expand the palette of functions in the CNS of the typically inhibitory neurotransmitter glycine. On the other hand, the discovery of functional GluN1/GluN2/GluN3ARs at adult synapses to the PVT originating from a specific cell sub-type of a specific rostral brainstem nuclei, open the way for further investigations. These will have to aim at understanding the physiological implications deriving from the presence of such an exotic subunit at key locations for information transfer between the periphery and the central subdivisions of the nervous system.

I will discuss all these points in more detail in a later section of my manuscript.

Discussion

DISCUSSION

During my thesis, I examined in detail the expression of the unconventional NMDAR subunit GluN3A in native neurons of the adult central nervous system, both on a morphological and on a functional point of view.

My experimental work led to a radical shift in our perception of how this subunit is expressed in the brain and opens new hypotheses on how it can contribute to the activity of neural circuits.

In view of my results, the conventionally assumed notion that this subunit is uniquely expressed at early developmental stages and, thus, that its physiological functions are mainly limited to control of synaptic maturation processes[107], must be revisited and expanded. From now on, GluN3A subunit-containing NMDARs will have to be considered as integral components of the molecular machinery that mediates information transfer in the brain, and understanding how the specificity of their properties affects neurons will be an important task for obtaining comprehensive clarification of circuital functions.

In the next sections, I will discuss the meaning of my data and the perspectives that they open for future investigations.

1. Glycine excitatory receptors are functional and physiologically relevant

My first significant result is the discovery that GluN3A-containing, glycine-activated excitatory receptors are functional in the brain.

The mutually exclusively excitatory or inhibitory activity of an ion channel ligand on postsynaptic neurons is a basic notion in neuroscience. Rare exceptions are given by developmentally or regionally regulated changes in the ionic gradients determining the reversal potential of specific receptor type families, which nonetheless show invariable permeability properties (see for example the long-known excitatory actions of GABAaRs at very early developmental stages[350], and in the adult MHb[283]). Ours is a completely different and original case. We are indeed dealing here with a channel showing the typical cationic permeability of excitatory receptors, but whose agonist is a neurotransmitter, glycine, that in the large majority of the cases controls the opening of anion-permeable channels originating from a different set of genes.

At least to my knowledge, the activation by glycine of ionic receptors possessing diverse permeability specificities is a unique event, one that clearly sets this neurotransmitter apart and that potentially multiplies the spectrum of its physiological implications.

In this context, my task was to identify novel pharmacological tools to facilitate the detection of GluN1/GluN3ARs in native cells. As explained previously, this was necessary because of the peculiar properties of these receptors, namely the dual actions of glycine on channel activation deriving from the occupation levels of the higher affinity glycine-binding site of GluN3A and of the lower affinity one on GluN1. The powerful inhibitory actions of the glycine-binding site of GluN1 subunits on channel opening has probably been the main reason why, so far, GluN1/GluN2/GluN3ARs have never been detected, neither in juvenile nor in adult native cells. Upon glycine application in *ex-vivo* preparations, either by pressure ejection or in bath solutions, the fast inactivation produced by GluN1 binding produces currents that can be hardly distinguished from basal noise and/or mechanical artefacts. Our experiments in the juvenile hippocampal CA1 strongly support this view. It is extremely likely that the same thing, happening in neurons of the cortex or in other brain areas of major interest for neuroscientific research, may have critically hindered the identification of the currents in the past.

The case of the MHb is, nonetheless, an important exception. In the MHb, cells are small and electrically tight (for comparison, shape and dimensions may be comparable to those of cerebellar granule cells), two elements that considerably improve the quality of voltage-clamp recordings. Moreover, the expression of diheteromeric GluN1/GluN3ARs is particularly high, so that glycine puff-induced currents powerfully increase MHb neuronal firing recorded in the cell-attached configuration, and can be clearly distinguished from basal noise in the whole-cell mode[125]. This was a decisive factor that allowed us to detect the currents and to pursue their investigation.

Identifying the potentiating actions of CGP78608 was another important step. CGP78608 effects are unprecedented for ionic receptors[124]. My work demonstrated that CGP78608 is a powerful tool for the detection of GluN1/GluN3ARs also in brain nuclei where conventional morphological methods would suggest low or no GluN3A subunit expression, like in the LHb.

However, the development of a specific and clearly separate pharmacology for both GluN1 and GluN3 subunits remains fundamental. The lack of specificity between NMDAR subunit families of the available compounds severely limits their possible utility. As an example, the *in-vivo* use of CGP78608 to identify the role of GluN1/GluN3ARs in intact circuits is strongly discouraged. Its actions on GluN1 subunits imply that it is also an efficient antagonist of conventional GluN1/GluN2Rs, an event that I could verify

repeatedly during my experimental activity. Moreover, CGP78608 unexpectedly appears to be a powerful blocker also of AMPARs, probably because of its synthesis as a derivative of CNQX, the classical AMPAR antagonist that also binds to NMDAR glycine binding sites at higher concentrations[103]. In my experience, CGP78608 effects are rapidly reversible in slices, which is very interesting under an electrophysiologist's point of view. CGP78608 indeed blocks both ionic components mediating glutamatergic synaptic responses, and its reversibility permits the use of an individual slice for several consecutive recordings, something not possible with the irreversible actions of NBQX and CNQX. This positive side notwithstanding, however, the antagonizing actions on AMPARs and on GluN1/GluN2 NMDARs clearly represent an insurmountable obstacle for the use of CGP78608 for *in-vivo* electrophysiological and behavioural tests in the context of GluN3-related studies.

2. Physiological role and activation of GluN1/GluN3A receptors.

In our most recent publication[125], we described not only the expression of GluN1/GluN3A receptors in the MHb but we also illustrated a possible physiological role for them. We indeed demonstrated that their full function in the MHb is necessary for the expression of conditioned place aversion (CTA). CTA is a classical paradigm testing an animal's capacity of associating aversive external events (like a pharmacologically induced malaise) with environmental cues (here, an easily recognizable compartment of a conditioning box). We showed that a reduction of GluN3A subunit expression levels in the MHb via the viral shRNA-based approach described also in this thesis prevented the development of such associations. Importantly, we also ascertained that the effect was due to the diheteromeric receptors because we were able to demonstrate that the triheteromeric GluN1/GluN2/GluN3ARs were not functional in the MHb (see Fig. 1 of[125]). Place aversion is a typical behavioural read-out associated with the MHb[351], a structure that is traditionally associated with affective responses elicited by negatively-valued external events[269]. So, this role of the GluN3A subunit is perfectly in line with the known physiology of the MHb.

Our study also approached another aspect of GluN3A-containing diheteromeric receptors, concerning the possible sources of the glycine capable of activating the currents. This point is extremely intriguing under several points of view. In the MHb, the complete lack of a glycinergic axonal plexus, either of intrinsic origin from local interneurons or from extrinsic afferences[125], led us to identify glial cells as plausible candidates for triggering a chain of events resulting in receptor activation. We indeed showed that glial activation via chemogenetic DREADD receptor-based technology triggered increases of MHb cell firing that were mediated by GluN1/GluN3ARs[125]. Our

data did not directly demonstrate the release of glycine by glial cells, but they provided convincing evidence that a glia-dependent pathway other than conventional synaptic release was likely leading to receptor activation. Glial vesicular release of neurotransmitters is itself a long-debated, and to my knowledge not a completely solved point[352]. Otherwise, glia-mediated mechanisms affecting neuronal function are typically slower than conventional synaptic communication, and a slow release of glycine (for example via inversion of specific transporters[353]) could affect neuronal excitation on time scales much longer than those associated with conventional synapses. However, some considerations would point against this hypothesis. First, slow extracellular increases of glycine levels would build up on non-null basal ACSF concentrations of the neurotransmitter, that have been evaluated at a few tens of micromolar[354]. Although GluN1 and GluN3 native subunit affinities for glycine are not known, in most brain nuclei, comprising the MHb[278], conventional GluN1/GluN2 NMDARs are activated by synaptic liberation of glutamate without need for concomitant phasic releases of the co-agonist, either glycine or D-serine. This would suggest that GluN1 glycine binding sites are largely occupied and, thus, that GluN1/GluN3ARs are inactivated in basal conditions. It is thus not straightforward to imagine how the channel inactivation mechanisms mediated by GluN1 subunits could be prevented from maintaining the receptors in a non-conducive state during slow augmentations of extracellular glycine levels. Several questions on how these receptors can perform their function in native tissues thus arise spontaneously. We envisage a few possible solutions to these apparent contradictions. First, GluN1/GluN3ARs could be preferentially addressed to very specific compartments of a cell's outer membranes, where surrounding structures may be able to bidirectionally modulate extracellular glycine concentrations in an extremely fine manner. In the MHb, we could evaluate on a very qualitative EM level that the receptors are preferentially located extrasynaptically and juxtaposed to glial sheaths[125]. Secondly, some of the possible physiological mechanisms capable of potentiating GluN1/GluN3AR currents in recombinant systems (namely reducing microenvironment, acidic pH, Zn^{2+} ions), could be in place in native tissues, thus rendering the receptors less sensitive to the inhibition deriving from glycine occupation of the GluN1 subunits. In this context, the use of CGP78608 permits an evaluation of the maximal potentiation attainable, which in the MHb is more than 50-fold with respect to control receptors (Fig. 2A of[125]). The dramatic extent of the potentiation suggests that only a minor activation of such mechanisms in physiological conditions could radically modify neuronal excitability following changes in extracellular glycine, with plausible behavioural consequences.

Finally, using CGP78608 I demonstrated that GluN1/GluN3ARs are functional in both the intralaminar CL nucleus and the midline PVT. Our team recently showed the existence of

a very powerful glycinergic projection to both IL and MDL nuclei from the oralis and caudalis sub-divisions of the rostral pons[204] (PnO and PnC). In these thalamic nuclei, therefore, a more conventional activation via synaptic release of glycine could be contemplated. The use of CGP78608 during recordings of the responses to optogenetic stimulation of the pontine glycinergic inputs[204], could help detect possible GluN1/GluN3AR-mediated currents. We recently performed some preliminary experiments to examine this hypothesis. Unfortunately, CGP78608 had no effects in the few cells that we examined.

Although our team will have to perform more tests in order to draw a final conclusion, these negative preliminary results increase the mystery related to the physiological mechanisms leading to GluN1/GluN3AR activation, and greatly stress the urgency for further investigation on the subject.

3. Triheteromeric GluN1/GluN2/GluN3A receptors in the adult brain: technical trivia.

My results show that, similarly to the diheteromeric receptors, triheteromeric GluN1/GluN2/GluN3A NMDARs are also functional in the adult brain and suggest that their expression may be tightly and specifically controlled. I will discuss these points later but, first, I would like to spend a few words on methodological issues.

Before the onset of my thesis, GluN1/GluN2/GluN3ARs were detected in juvenile cortical and hippocampal neurons, both in control conditions and in transgenic mouse models where GluN3A expression was prolonged after the closure of the physiological developmental window peculiar to this subunit[118,120]. In these studies, the differences in NMDAR current rectification properties with respect to conventional GluN1/GluN2Rs were calculated by comparing response amplitudes at hyperpolarized potentials, normalized by those obtained at a depolarized potential (typically either +40mV or +50mV), between GluN3A-expressing and deficient cells. These early studies demonstrated the solidity of this experimental strategy for detecting the receptors. This approach turned out to be very useful also for my recordings and provided highly significant results both for synaptic and NMDA puff-elicited currents.

During my voltage-clamp experiments, I paid particular attention to avoid pernicious artefacts. Clamping problems at hyperpolarized potentials were indeed not unusual during my recordings, and almost live adjustments had to be made in the course of experiments. For example, performing puffs of high concentrations of NMDA onto voltage-clamped neurons is an experimental configuration showing a largely underestimated level of difficulty. NMDA puffs indeed produce very large currents in

thalamic cells, even at hyperpolarized potentials where block by extracellular Mg^{2+} is a limiting factor for the responses. The position of the puff pipettes with respect to the recorded cells, and the ejection pressure levels must thus be set in such a way to produce currents not showing regenerative components due to voltage escapes. This can be a tricky task to fulfil, one that must be performed for each individual recording, but that I pursued with intense dedication. In contrast, in most cases the quality of light evoked EPSC recordings was good. We encountered relevant issues only when synaptic responses originating from infralimbic cortical inputs were examined in the PVT. In this case, in fact, leEPSCs recorded at -40mV almost invariably gave rise to unclamped responses. Immediately realizing this caveat, we extended our analysis to leEPCSs recorded at -80mV, and discarded the responses obtained at -40mV. This adjustment allowed us to compare two series of values obtained in WT and GluN3AKO mice (at -60mv and -80mV), thus increasing the solidity of our conclusions. These clamping problems, hardly ever present when recording leEPSCs originating from the PB, were most likely due to the long-known fact that, in contrast to subcortical inputs, cortical synapses onto thalamic relay cells impinge on distal dendritic compartments (see for example "The Thalamus" by Edward G. Jones, Cambridge University Press), where space clamp is probably quite poor.

3.1. Expression specificity of GluN1/GluN2/GluN3ARs

My results suggest that the expression of GluN1/GluN2/GluN3ARs could be tightly controlled. We examined the functional presence of GluN3A-containing NMDARs in several brain areas, namely the IL and MDL nuclei of the thalamus, the epithalamic MHB and LHb, the juvenile hippocampus and the amygdala, this last region in very preliminary tests not shown in this thesis. In all these structures we could invariably detect glycine-elicited responses. In contrast, our team recently demonstrated that MHb and LHb cells did not express triheteromeric complexes, neither at synaptic nor at extrasynaptic sites[125].

Moreover, our glycine- and NMDA-puff experiments demonstrated that virtually all PVT cells possessed both CGP78608-sensitive GluN1/GluN3AR and GluN1/GluN2/GluN3AR currents, illustrating that GluN3A subunits are ubiquitous in the nucleus independently from neuronal sub-types and nuclear subdivisions. Among several PVT-projecting PB cell subtypes, however, only calb2- and MC4R-positive neurons synaptically activated the triheteromeric receptors, an indication of a very specific control of the insertion of GluN1/GluN2/GluN3ARs at postsynaptic specializations. This hypothesis is further strengthened by the absence of GluN3A subunits at infralimbic cortical afferences, which exert powerful excitatory action on the whole population of PVT cells[168].

We still do not know with certainty whether calb2- and MC4R-positive PB cells contact specific PVT neuronal sub-types and, thus, whether synaptic GluN3A-containing triheteromeric NMDARs are postsynaptic cell-specific or synapse/projection specific. We know from preliminary experiments performed using an AAV expressing ChR2 in cells **NOT** expressing the recombinase Cre ("Cre-OFF" ChR2) that leEPCSs originating from MC4R-Cre negative cells do not activate GluN1/GluN2/GluN3ARs (we will discuss this point in the context of PB physiology later). Soon, our team will co-inject the PB of MC4R-cre mice with a mix of the Cre-OFF ChR2-expressing AAV and of an AAV expressing red-light drivable variations of channelrhodopsin, like ReaChR[355] and ChrimsonR[356] in a Cre-dependent manner. Independent light-driven stimulation of different optogenetic actuators expressed in distinct presynaptic cell types promises to provide important information on the type of specificity of GluN1/GluN2/GluN3AR expression in the PVT.

3.2. Cellular function(s) of GluN1/GluN2/GluN3ARs

Other important questions concern the possible reasons why GluN1/GluN2/GluN3AR expression would be so carefully regulated. In other words, what do these receptors provide to synaptic responses that cannot be delivered by conventional GluN1/GluN2Rs? Unfortunately during my thesis I did not have time to perform current clamp recordings of PVT cells. It would nonetheless be very interesting to record firing activity of current-clamped PVT cells in MC4R-Cre mice during either red-light optogenetic stimulation of Cre-ON ReaChR/CrimsonR or blue-light stimulation of Cre-OFF ChR2 using the viral approaches described above. This experimental configuration could permit a direct dissection of the effect of triheteromeric receptor activation on postsynaptic excitability levels. Some hypotheses can nonetheless be envisaged, based on the known properties of the receptors. Namely, extracellular Mg^{2+} blocks GluN1/GluN2/GluN3ARs at hyperpolarized potentials less efficiently than conventional GluN1/GluN2Rs. Thalamic relay cells are spontaneously hyperpolarized in basal conditions. Synaptic activation of GluN1/GluN2/GluN3ARs could thus have more robust and rapid depolarizing effects on a cell than conventional NMDARs, thus leading to faster activation of downstream circuital targets and, possibly, to faster behavioural outcomes. This is a particularly enticing hypothesis in the context of PB physiology. This nucleus has indeed been proposed to represent a powerful alarm system for the brain, capable of activating widespread cortical areas in response to potentially threatening modifications of the external environment or of internal homeostatic states (reviewed in[284]). GluN1/GluN2/GluN3ARs could thus be functional to this role.

Another interesting property of the receptors is their smaller single-channel conductance and their reduced permeability to Ca^{2+} with respect to conventional NMDARs[107]. This feature could be relevant for possible activity-dependent plasticity forms of either neuronal intrinsic excitability, or incoming synaptic efficacy. GluN1/GluN2/GluN3A NMDARs have already been shown to be key actors in mediating the synaptic plasticity phenomena induced in the ventral tegmental area (VTA) by exposure to cocaine[140]. Afferences to thalamic neurons are not known to show activity-dependent plasticity (but see a form of long-term depression of the GABAergic inputs from the nucleus reticularis to the sensory thalamus[357]). However, GluN3A subunits are at the centre of a complex network of molecular mechanisms controlling receptor insertion to and endocytosis from cell membranes (reviewed extensively in[107]). Similarly to the VTA, activation of GluN3A-containing receptors by specific activation patterns of PB glutamatergic inputs could thus lead to re-adjustments of the population of receptors present at postsynaptic specializations, and thus to modifications of neuronal integrative properties.

Clearly, future work will have to shed light on these still largely unknown aspects of the physiology of GluN3A-expressing NMDARs.

3.3. GluN1/GluN2/GluN3ARs and parabrachial physiology

At its onset, my thesis project aimed at performing a comprehensive analysis of the projections from cortical and rostral brainstem areas to the PVT[358], with the goal of identifying inputs activating postsynaptic GluN1/GluN2/GluN3ARs. This explorative part rapidly came to an end because, very early, I identified the PB efferences as plausible candidates for this role.

The PB is a mainly glutamatergic nucleus. However, it has long been known to host a highly heterogeneous population of cells as for molecular marker expression (see table 1 of [284]), consistently with the large palette of behaviours it controls [359].

We thus started out exploring this heterogeneity.

To my knowledge, at present only one study explored distinct PB cell sub-types in terms of their possible projections to the PVT, and this key piece of information is hidden in a supplementary table of not immediate access[349]. We noticed these data well after we started the production of the AAV2/CGRP-Cre and AAV2/OxtR-Cre viruses, whose use I described in the results section. We initially concentrated on CGRP and OxtR cells because, at the time, they represented the best characterized cell types in the PB, and

because they had been shown to control well-identified behavioural read-outs[311,313,324,344,360].

I learned many things from these experiments. First, we immediately realized that our approach was not totally correct. Our immunohistological analysis, performed in parallel with the electrophysiological experiments, suggested that both viruses were leading to expression of the Cre recombinase not only in the targeted cell types, but also non-specifically in other neuronal sub-groups. We now know that, in general, this is not an unusual event when specific promoter sequences are chosen to drive optogenetic actuators in viral vectors, and that a more viable approach is always the use of genetically modified, possibly knock-in mouse lines. Luckily, though, the results obtained with these early viral strategies could be retained because ChR2 expression in CGRP- and OxtR-positive cells was verified, and because the outcome of the experiments was homogeneously negative.

The data illustrated by Barik and colleagues[301], strongly motivated us to purchase 2 KI mouse lines (Pdyn-Cre and MC4R-Cre) that would presumably permit the analysis of other PVT-projecting cell types. An ongoing collaboration[125] also gave us the opportunity of testing calb2-positive neurons, whose projections to the PVT had been noticed by our Hungarian colleagues[174]. We thus managed to create a rather large portfolio of transgenic tools for the examination of PB neuronal types presynaptic to the PVT, in the hope that they could give us as wide a perspective as possible on the specificities of PB inputs to the PVT. We had no illusions of examining ALL PB cellular sub-populations projecting to the PVT. We believe this to be an almost impossible task, even more so now following the explosion in the number of molecular markers (with accompanying transgenic mice and associated behaviors) identified in the last 2-3 years[329,330,349,361,362]. We are still nonetheless confident that our choice led to important information. We indeed chose cell types with clearly separate localization in the PB, covering the whole extent of its lateral part from medio-dorsal sites (where MC4R-Cre cells reside) to the most ventro-lateral ones (property mainly of CGRP-positive neurons), passing through more intermediate locations where calb2, OxtR- and Pdyn-positive cells are nested. Very little superposition exists between the areas hosting MC4R, Pdyn and OxytR cells. Similarly, CGRP and OxtR co-expression is minimal[324]. We had serious doubts only on the utility of examining calb2-expressing cells, because we immediately realized that they were spread on a very wide portion of the lateral PB, extending over territories specific not only of MC4R-, but also of Pdyn- and OxtR-positive cells. This is why we believe that the most important and promising results that we obtained are represented by the activation of GluN1/GluN2/GluN3ARs by Mc4R-expressing cells. This conviction is supported by the fact that, as we mentioned before, ongoing experiments are showing

that PB cells in MC4R-Cre mice infected with an AAV expressing ChR2 in a Cre-OFF dependent way produce leEPSCs in the PVT with properties strongly resembling those of leEPSCs generated by Pdyn and OxtR cells, among which the non-activation of postsynaptic GluN3A subunit-containing NMDARs is the most notable. We thus believe that the likeliest explanation for this finding is that calb2 is expressed in a very wide population of PB cells, which also include MC4R-positive neurons.

In the near future, therefore, our team will most likely concentrate on the MC4R-expressing population of PB neurons in order to identify possible physiological correlates associated with GluN3A subunit function in the PVT.

The central melanocortin system has been extensively studied[363,364]. Most of its actions in the CNS are mediated by the G protein-coupled MC4Rs, whose expression has been principally associated with the hypothalamic (NOT the thalamic) periventricular nucleus (PVN). To my knowledge, MC4Rs constitute the only receptor type in the brain for which endogenously released ligands exist having either agonist (α- and β-melanocyte-stimulating hormone, or α- and β-MSH), or antagonist (Agouti-related peptide, or AgRP) actions. In the PVN these ligands are released by inputs from separate cell types located in the hypothalamic arcuate nucleus. Ligand-mediated inhibition of MC4Rs has a relevant physiological importance because these receptors have a high basal level of activation even without the binding of their agonists[364]. Overwhelming evidence supports a role for MC4Rs in the control of feeding, with even small modifications in the level of expression and in the function of the receptors leading to dramatic changes in food consumption, body weight and, in general, in physiological energy homeostasis[363]. Unfortunately, though, all known physiological functions associated with the central MC4R system are at present explained by their expression in the PVN, and a role in food-associated behaviors for PB MC4Rs has been directly excluded[365]. Moreover, in the PB feeding-related behaviors appear to be mediated by CGRP- and Pdyn- positive neurons[284,329]. The role of MC4Rs in the PB, and of the cells where they are expressed, thus remains totally mysterious at present. In principle, no physiological function for MC4R-positive PB cells can be excluded *a priori*. The whole plethora of PB-associated behaviors will have to be considered when, in the future, my team will approach the subject. Similarly, new strategies will have to be developed for interfering with GluN1/GluN2A/GluN3AR function specifically at the projections from PB MC4R cells to the PVT, in order to assess their possible physiological implications.

4. Conclusion

In conclusion, I believe that my experimental activity led to significant advances in our understanding of the organization of GluN3A-containing NMDARs in the CNS.

I can affirm with satisfaction that my thesis work has laid important bases for the future development of new research lines, which will hopefully shed light on the physiological role of what I consider one of the most intriguing receptor subunit of the (now we know: adult) brain.

BIBLIOGRAPHY

BIBLIOGRAPHY

1. Traynelis, S. F. *et al.* Glutamate Receptor Ion Channels: Structure, Regulation, and Function. *Pharmacol. Rev.* (2010). doi:10.1124/pr.109.002451

2. Collingridge, G. L., Isaac, J. T. R. & Yu, T. W. Receptor trafficking and synaptic plasticity. *Nature Reviews Neuroscience* (2004). doi:10.1038/nrn1556

3. Mattson, M. P. Pathways towards and away from Alzheimer's disease. *Nature* (2004). doi:10.1038/nature02621

4. Snyder, E. M. *et al.* Regulation of NMDA receptor trafficking by amyloid-β. *Nat. Neurosci.* (2005). doi:10.1038/nn1503

5. Mohn, A. R., Gainetdinov, R. R., Caron, M. G. & Koller, B. H. Mice with reduced NMDA receptor expression display behaviors related to schizophrenia. *Cell* (1999). doi:10.1016/S0092-8674(00)81972-8

6. Sawa, A. & Snyder, S. H. Schizophrenia: Diverse approaches to a complex disease. *Science* (2002). doi:10.1126/science.1070532

7. Borgland, S. L., Taha, S. A., Sarti, F., Fields, H. L. & Bonci, A. Orexin a in the VTA is critical for the induction of synaptic plasticity and behavioral sensitization to cocaine. *Neuron* (2006). doi:10.1016/j.neuron.2006.01.016

8. Moriyoshi, K. *et al.* Molecular cloning and characterization of the rat NMDA receptor. *Nature* (1991). doi:10.1038/354031a0

9. Ishii, T. *et al.* Molecular characterization of the family of the N-methyl-D-aspartate receptor subunits. *J. Biol. Chem.* (1993).

10. Ulbrich, M. H. & Isacoff, E. Y. Subunit counting in membrane-bound proteins. *Nat. Methods* (2007). doi:10.1038/nmeth1024

11. Karakas, E. & Furukawa, H. Crystal structure of a heterotetrameric NMDA receptor ion channel. *Science (80-.).* (2014). doi:10.1126/science.1251915

12. Lee, C. H. *et al.* NMDA receptor structures reveal subunit arrangement and pore architecture. *Nature* (2014). doi:10.1038/nature13548

13. Wollmuth, L. P. Ion permeation in ionotropic glutamate receptors: still dynamic after all these years. *Current Opinion in Physiology* (2018).

doi:10.1016/j.cophys.2017.12.003

14. Atlason, P. T., Garside, M. L., Meddows, E., Whiting, P. & McIlhinney, R. A. J. N-methyl-D-aspartate (NMDA) receptor subunit NR1 forms the substrate for oligomeric assembly of the NMDA receptor. *J. Biol. Chem.* (2007). doi:10.1074/jbc.M702778200

15. Gielen, M., Retchless, B. S., Mony, L., Johnson, J. W. & Paoletti, P. Mechanism of differential control of NMDA receptor activity by NR2 subunits. *Nature* (2009). doi:10.1038/nature07993

16. Yuan, H., Hansen, K. B., Vance, K. M., Ogden, K. K. & Traynelis, S. F. Control of NMDA receptor function by the NR2 subunit amino-terminal domain. *J. Neurosci.* (2009). doi:10.1523/JNEUROSCI.1365-09.2009

17. Farina, A. N. *et al.* Separation of domain contacts is required for heterotetrameric assembly of functional NMDA receptors. *J. Neurosci.* (2011). doi:10.1523/JNEUROSCI.6041-10.2011

18. Karakas, E., Simorowski, N. & Furukawa, H. Structure of the zinc-bound amino-terminal domain of the NMDA receptor NR2B subunit. *EMBO J.* (2009). doi:10.1038/emboj.2009.338

19. Karakas, E., Simorowski, N. & Furukawa, H. Subunit arrangement and phenylethanolamine binding in GluN1/GluN2B NMDA receptors. *Nature* (2011). doi:10.1038/nature10180

20. Romero-Hernandez, A., Simorowski, N., Karakas, E. & Furukawa, H. Molecular Basis for Subtype Specificity and High-Affinity Zinc Inhibition in the GluN1-GluN2A NMDA Receptor Amino-Terminal Domain. *Neuron* (2016). doi:10.1016/j.neuron.2016.11.006

21. Tajima, N. *et al.* Activation of NMDA receptors and the mechanism of inhibition by ifenprodil. *Nature* (2016). doi:10.1038/nature17679

22. Hestrin, S., Sah, P. & Nicoll, R. A. Mechanisms generating the time course of dual component excitatory synaptic currents recorded in hippocampal slices. *Neuron* (1990). doi:10.1016/0896-6273(90)90162-9

23. Sah, P., Hestrin, S. & Nicoll, R. A. Properties of excitatory postsynaptic currents recorded in vitro from rat hippocampal interneurones. *J. Physiol.* (1990). doi:10.1113/jphysiol.1990.sp018310

24. Trussell, L. O., Zhang, S. & Ramant, I. M. Desensitization of AMPA receptors upon

multiquantal neurotransmitter release. *Neuron* (1993). doi:10.1016/0896-6273(93)90066-Z

25. Geiger, J. R. P., Lübke, J., Roth, A., Frotscher, M. & Jonas, P. Submillisecond AMPA receptor-mediated signaling at a principal neuron- interneuron synapse. *Neuron* (1997). doi:10.1016/S0896-6273(00)80339-6

26. Paoletti, P., Bellone, C. & Zhou, Q. NMDA receptor subunit diversity: Impact on receptor properties, synaptic plasticity and disease. *Nature Reviews Neuroscience* (2013). doi:10.1038/nrn3504

27. Bourne, H. R. & Nicoll, R. Molecular machines integrate coincident synaptic signals. *Cell* (1993). doi:10.1016/S0092-8674(05)80029-7

28. SEEBURG, P. H. *et al.* The NMDA Receptor Channel: Molecular Design of a Coincidence Detector. in *Proceedings of the 1993 Laurentian Hormone Conference* (1995). doi:10.1016/b978-0-12-571150-0.50006-8

29. Nevian, T. & Sakmann, B. Single Spine Ca2+ Signals Evoked by Coincident EPSPs and Backpropagating Action Potentials in Spiny Stellate Cells of Layer 4 in the Juvenile Rat Somatosensory Barrel Cortex. *J. Neurosci.* (2004). doi:10.1523/JNEUROSCI.3332-03.2004

30. Lau, C. G. & Zukin, R. S. NMDA receptor trafficking in synaptic plasticity and neuropsychiatric disorders. *Nature Reviews Neuroscience* (2007). doi:10.1038/nrn2153

31. Holtmaat, A. & Svoboda, K. Experience-dependent structural synaptic plasticity in the mammalian brain. *Nature Reviews Neuroscience* (2009). doi:10.1038/nrn2699

32. Higley, M. J. & Sabatini, B. L. Calcium signaling in dendritic spines. *Cold Spring Harb. Perspect. Biol.* (2012). doi:10.1101/cshperspect.a005686

33. Zorumski, C. F. & Izumi, Y. NMDA receptors and metaplasticity: Mechanisms and possible roles in neuropsychiatric disorders. *Neuroscience and Biobehavioral Reviews* (2012). doi:10.1016/j.neubiorev.2011.12.011

34. Paoletti, P., Bellone, C. & Zhou, Q. NMDA receptor subunit diversity: impact on receptor properties, synaptic plasticity and disease. *Nat Rev Neurosci* **14**, 383–400 (2013).

35. Volianskis, A. *et al.* Long-term potentiation and the role of N-methyl-D-aspartate receptors. *Brain Res.* (2015). doi:10.1016/j.brainres.2015.01.016

36. Johnson, J. W. & Ascher, P. Glycine potentiates the NMDA response in cultured

mouse brain neurons. *Nature* (1987). doi:10.1038/325529a0

37. Kleckner, N. W. & Dingledine, R. Requirement for glycine in activation of NMDA receptors expressed in xenopus oocytes. *Science (80-.).* (1988). doi:10.1126/science.2841759

38. Benveniste, M. & Mayer, M. L. Kinetic analysis of antagonist action at N-methyl-D-aspartic acid receptors. Two binding sites each for glutamate and glycine. *Biophys. J.* (1991). doi:10.1016/S0006-3495(91)82272-X

39. Clements, J. D. & Westbrook, G. L. Activation kinetics reveal the number of glutamate and glycine binding sites on the N-methyl-d-aspartate receptor. *Neuron* (1991). doi:10.1016/0896-6273(91)90373-8

40. Clements, J. D. & Westbrook, G. L. Kinetics of AP5 dissociation from NMDA receptors: Evidence for two identical cooperative binding sites. *J. Neurophysiol.* (1994). doi:10.1152/jn.1994.71.6.2566

41. Li, Y., Krupa, B., Kang, J. S., Bolshakov, V. Y. & Liu, G. Glycine site of NMDA receptor serves as a spatiotemporal detector of synaptic activity patterns. *J. Neurophysiol.* (2009). doi:10.1152/jn.91342.2008

42. Berger, A. J., Dieudonné, S. & Ascher, P. Glycine uptake governs glycine site occupancy at NMDA receptors of excitatory synapses. *J. Neurophysiol.* (1998). doi:10.1152/jn.1998.80.6.3336

43. Bergeron, R., Meyer, T. M., Coyle, J. T. & Greene, R. W. Modulation of N-methyl-D-aspartate receptor function by glycine transport. *Proc. Natl. Acad. Sci. U. S. A.* (1998). doi:10.1073/pnas.95.26.15730

44. Billups, D. & Attwell, D. Active release of glycine or D-serine saturates the glycine site of NMDA receptors at the cerebellar mossy fibre to granule cell synapse. *Eur. J. Neurosci.* (2003). doi:10.1111/j.1460-9568.2003.02996.x

45. Ahmadi, S. *et al.* Facilitation of spinal NMDA receptor currents by spillover of synaptically released glycine. *Science (80-.).* (2003). doi:10.1126/science.1083970

46. Sullivan, S. J. & Miller, R. F. AMPA receptor-dependent, light-evoked D-serine release acts on retinal ganglion cell NMDA receptors. *J. Neurophysiol.* (2012). doi:10.1152/jn.00264.2012

47. Meunier, C. N. J., Chameau, P. & Fossier, P. M. Modulation of synaptic plasticity in the cortex needs to understand all the players. *Frontiers in Synaptic Neuroscience* (2017). doi:10.3389/fnsyn.2017.00002

48. Papouin, T. *et al.* Synaptic and extrasynaptic NMDA receptors are gated by different endogenous coagonists. *Cell* **150**, 633–646 (2012).

49. Furukawa, H. & Gouaux, E. Mechanisms of activation, inhibition and specificity: Crystal structures of the NMDA receptor NR1 ligand-binding core. *EMBO J.* (2003). doi:10.1093/emboj/cdg303

50. Inanobe, A., Furukawa, H. & Gouaux, E. Mechanism of partial agonist action at the NR1 subunit of NMDA receptors. *Neuron* (2005). doi:10.1016/j.neuron.2005.05.022

51. Vance, K. M., Simorowski, N., Traynelis, S. F. & Furukawa, H. Ligand-specific deactivation time course of GluN1/GluN2D NMDA receptors. *Nat. Commun.* (2011). doi:10.1038/ncomms1295

52. Hansen, K. B. *et al.* Structural determinants of agonist efficacy at the glutamate binding site of n-methyl-d-Aspartate receptorss. *Mol. Pharmacol.* (2013). doi:10.1124/mol.113.085803

53. Yao, Y., Belcher, J., Berger, A. J., Mayer, M. L. & Lau, A. Y. Conformational analysis of NMDA receptor GluN1, GluN2, and GluN3 ligand-binding domains reveals subtype-specific characteristics. *Structure* (2013). doi:10.1016/j.str.2013.07.011

54. Jespersen, A., Tajima, N., Fernandez-Cuervo, G., Garnier-Amblard, E. C. & Furukawa, H. Structural insights into competitive antagonism in NMDA receptors. *Neuron* (2014). doi:10.1016/j.neuron.2013.11.033

55. Kalbaugh, T. L., VanDongen, H. M. A. & VanDongen, A. M. J. Ligand-binding residues integrate affinity and efficacy in the NMDA receptor. *Mol. Pharmacol.* (2004). doi:10.1124/mol.66.2.209

56. Paganelli, M. A., Kussius, C. L. & Popescu, G. K. Role of cross-cleft contacts in NMDA receptor gating. *PLoS One* (2013). doi:10.1371/journal.pone.0080953

57. Williams, K., Dawson, V. L., Romano, C., Dichter, M. A. & Molinoff, P. B. Characterization of polyamines having agonist, antagonist, and inverse agonist effects at the polyamine recognition site of the NMDA receptor. *Neuron* (1990). doi:10.1016/0896-6273(90)90309-4

58. Traynelis, S. F., Hartley, M. & Heinemann, S. F. Control of proton sensitivity of the NMDA receptor by RNA splicing and polyamines. *Science (80-.).* (1995). doi:10.1126/science.7754371

59. Wu, F. S., Gibbs, T. T. & Farb, D. H. Pregnenolone sulfate: A positive allosteric

modulator at the N-methyl-D-aspartate receptor. *Mol. Pharmacol.* (1991).

60. Malayev, A., Gibbs, T. T. & Farb, D. H. Inhibition of the NMDA response by pregnenolone sulphate reveals subtype selective modulation of NMDA receptors by sulphated steroids. *Br. J. Pharmacol.* (2002). doi:10.1038/sj.bjp.0704543

61. Horak, M., Vlcek, K., Chodounska, H. & Vyklicky, L. Subtype-dependence of N-methyl-D-aspartate receptor modulation by pregnenolone sulfate. *Neuroscience* (2006). doi:10.1016/j.neuroscience.2005.08.058

62. Mullasseril, P. *et al.* A subunit-selective potentiator of NR2C- and NR2D-containing NMDA receptors. *Nat. Commun.* (2010). doi:10.1038/ncomms1085

63. Watkins, J. C. & Evans, R. H. Excitatory Amino Acid Transmitters. *Annu. Rev. Pharmacol. Toxicol.* (1981). doi:10.1146/annurev.pa.21.040181.001121

64. Wong, E. H. F. *et al.* The anticonvulsant MK-801 is a potent N-methyl-D-aspartate antagonist. *Proc. Natl. Acad. Sci. U. S. A.* (1986). doi:10.1073/pnas.83.18.7104

65. Anis, N. *et al.* Structure-activity relationships of philanthotoxin analogs and polyamines on N-methyl-D-aspartate and nicotinic acetylcholine receptors. *J. Pharmacol. Exp. Ther.* (1990).

66. Lodge, D. & Johnson, K. M. Noncompetitive excitatory amino acid receptor antagonists. *Trends Pharmacol. Sci.* (1990). doi:10.1016/0165-6147(90)90323-Z

67. Kalia, L. V., Kalia, S. K. & Salter, M. W. NMDA receptors in clinical neurology: excitatory times ahead. *The Lancet Neurology* (2008). doi:10.1016/S1474-4422(08)70165-0

68. Dravid, S. M. *et al.* Subunit-specific mechanisms and proton sensitivity of NMDA receptor channel block. *J. Physiol.* (2007). doi:10.1113/jphysiol.2006.124958

69. Legendre, P. & Westbrook, G. L. Ifenprodil blocks N-methyl-D-aspartate receptors by a two-component mechanism. *Mol. Pharmacol.* (1991).

70. Durand, G. M. *et al.* Cloning of an apparent splice variant of the rat N-methyl-D-aspartate receptor NMDAR1 with altered sensitivity to polyamines and activators of protein kinase C. *Proc. Natl. Acad. Sci. U. S. A.* (1992). doi:10.1073/pnas.89.19.9359

71. Nakanishi, N., Axel, R. & Shneider, N. A. Alternative splicing generates functionally distinct N-methyl-D-aspartate receptors. *Proc. Natl. Acad. Sci. U. S. A.* (1992). doi:10.1073/pnas.89.18.8552

72. Sugihara, H., Moriyoshi, K., Ishii, T., Masu, M. & Nakanishi, S. Structures and properties of seven isoforms of the NMDA receptor generated by alternative splicing. *Biochem. Biophys. Res. Commun.* (1992). doi:10.1016/0006-291X(92)91701-Q

73. Hollmann, M. *et al.* Zinc potentiates agonist-induced currents at certain splice variants of the NMDA receptor. *Neuron* (1993). doi:10.1016/0896-6273(93)90209-A

74. Laurie, D. J. & Seeburg, P. H. Regional and developmental heterogeneity in splicing of the rat brain NMDAR1 mRNA. *J. Neurosci.* (1994). doi:10.1523/jneurosci.14-05-03180.1994

75. Zhong, J., Carrozza, D. P., Williams, K., Pritchett, D. B. & Molinoff, P. B. Expression of mRNAs Encoding Subunits of the NMDA Receptor in Developing Rat Brain. *J. Neurochem.* (1995). doi:10.1046/j.1471-4159.1995.64020531.x

76. Paupard, M. C., Friedman, L. K. & Zukin, R. S. Developmental regulation and cell-specific expression of N-methyl-D-aspartate receptor splice variants in rat hippocampus. *Neuroscience* (1997). doi:10.1016/S0306-4522(96)00677-X

77. Rumbaugh, G., Prybylowski, K., Wang, J. F. & Vicini, S. Exon 5 and spermine regulate deactivation of NMDA receptor subtypes. *J. Neurophysiol.* (2000). doi:10.1152/jn.2000.83.3.1300

78. Vance, K. M., Hansen, K. B. & Traynelis, S. F. GluN1 splice variant control of GluN1/GluN2D NMDA receptors. *J. Physiol.* (2012). doi:10.1113/jphysiol.2012.234062

79. Swanger, S. A. *et al.* NMDA receptors containing the GluN2D subunit control neuronal function in the subthalamic nucleus. *J. Neurosci.* (2015). doi:10.1523/JNEUROSCI.1702-15.2015

80. Yi, F., Zachariassen, L. G., Dorsett, K. N. & Hansen, K. B. Properties of triheteromeric N-methyl-D-aspartate receptors containing two distinct GluN1 isoforms. *Mol. Pharmacol.* (2018). doi:10.1124/mol.117.111427

81. Sullivan, J. M. *et al.* Identification of two cysteine residues that are required for redox modulation of the NMDA subtype of glutamate receptor. *Neuron* (1994). doi:10.1016/0896-6273(94)90258-5

82. Choi, Y. B., Chen, H. S. V. & Lipton, S. A. Three pairs of cysteine residues mediate both redox and ZN2+ modulation of the NMDA receptor. *J. Neurosci.* (2001).

83. Aizenman, E., Lipton, S. A. & Loring, R. H. Selective modulation of NMDA responses by reduction and oxidation. *Neuron* (1989). doi:10.1016/0896-6273(89)90310-3

84. Tang, L. H. & Aizenman, E. The modulation of N-methyl-D-aspartate receptors by redox and alkylating reagents in rat cortical neurones in vitro. *J. Physiol.* (1993). doi:10.1113/jphysiol.1993.sp019678

85. Köhr, G., Eckardt, S., Lüddens, H., Monyer, H. & Seeburg, P. H. NMDA receptor channels: Subunit-specific potentiation by reducing agents. *Neuron* (1994). doi:10.1016/0896-6273(94)90311-5

86. Choi, Y. B. & Lipton, S. A. Redox modulation of the NMDA receptor. *Cellular and Molecular Life Sciences* (2000). doi:10.1007/PL00000638

87. Sanchez, R. M. *et al.* Novel role for the NMDA receptor redox modulatory site in the pathophysiology of seizures. *J. Neurosci.* (2000). doi:10.1523/jneurosci.20-06-02409.2000

88. Yang, Y. J. *et al.* Reversal of aging-associated hippocampal synaptic plasticity deficits by reductants via regulation of thiol redox and NMDA receptor function. *Aging Cell* (2010). doi:10.1111/j.1474-9726.2010.00595.x

89. Kumar, A. & Foster, T. C. Linking redox regulation of NMDAR synaptic function to cognitive decline during aging. *J. Neurosci.* (2013). doi:10.1523/JNEUROSCI.2176-13.2013

90. Monyer, H. *et al.* Heteromeric NMDA receptors: Molecular and functional distinction of subtypes. *Science (80-.).* (1992). doi:10.1126/science.256.5060.1217

91. Watanabe, M., Inoue, Y., Sakimura, K. & Mishina, M. Developmental changes in distribution of nmda receptor channel subunit m rim as. *Neuroreport* (1992). doi:10.1097/00001756-199212000-00027

92. Akazawa, C., Shigemoto, R., Bessho, Y., Nakanishi, S. & Mizuno, N. Differential expression of five N-methyl-D-aspartate receptor subunit mRNAs in the cerebellum of developing and adult rats. *J. Comp. Neurol.* (1994). doi:10.1002/cne.903470112

93. Monyer, H., Burnashev, N., Laurie, D. J., Sakmann, B. & Seeburg, P. H. Developmental and regional expression in the rat brain and functional properties of four NMDA receptors. *Neuron* (1994). doi:10.1016/0896-6273(94)90210-0

94. Burnashev, N., Zhou, Z., Neher, E. & Sakmann, B. Fractional calcium currents

through recombinant GluR channels of the NMDA, AMPA and kainate receptor subtypes. *J. Physiol.* (1995). doi:10.1113/jphysiol.1995.sp020738

95. Kuner, T. & Schoepfer, R. Multiple structural elements determine subunit specificity of Mg2+ block in NMDA receptor channels. *J. Neurosci.* (1996). doi:10.1523/JNEUROSCI.16-11-03549.1996

96. Qian, A., Buller, A. L. & Johnson, J. W. NR2 subunit-dependence of NMDA receptor channel block by external Mg2+. *J. Physiol.* (2005). doi:10.1113/jphysiol.2004.076737

97. Retchless, B. S., Gao, W. & Johnson, J. W. A single GluN2 subunit residue controls NMDA receptor channel properties via intersubunit interaction. *Nat. Neurosci.* (2012). doi:10.1038/nn.3025

98. Traynelis, S. F., Burgess, M. F., Zheng, F., Lyuboslavsky, P. & Powers, J. L. Control of voltage-independent Zinc inhibition of NMDA receptors by the NR1 subunit. *J. Neurosci.* (1998). doi:10.1523/jneurosci.18-16-06163.1998

99. Paoletti, P., Ascher, P. & Neyton, J. High-affinity zinc inhibition of NMDA NR1-NR2A receptors. *J Neurosci* **17**, 5711–5725 (1997).

100. Sanz-Clemente, A., Nicoll, R. A. & Roche, K. W. Diversity in NMDA receptor composition: Many regulators, many consequences. *Neuroscientist* (2013). doi:10.1177/1073858411435129

101. Aman, T. K., Maki, B. A., Ruffino, T. J., Kasperek, E. M. & Popescu, G. K. Separate intramolecular targets for protein kinase A control N-Methyl-D-aspartate receptor gating and Ca2+ permeability. *J. Biol. Chem.* (2014). doi:10.1074/jbc.M113.537282

102. Lussier, M. P., Sanz-Clemente, A. & Roche, K. W. Dynamic regulation of N-methyl-D-aspartate (NMDA) and α-amino-3-hydroxy-5-methyl-4-isoxazolepropionic acid (AMPA) receptors by posttranslational modifications. *J. Biol. Chem.* (2015). doi:10.1074/jbc.R115.652750

103. Yao, Y. & Mayer, M. L. Characterization of a soluble ligand binding domain of the NMDA receptor regulatory subunit NR3A. *J. Neurosci.* (2006). doi:10.1523/JNEUROSCI.0560-06.2006

104. Madry, C., Betz, H., Geiger, J. R. & Laube, B. Potentiation of Glycine-Gated NR1/NR3A NMDA Receptors Relieves Ca-Dependent Outward Rectification. *Front Mol Neurosci* **3**, 6 (2010).

105. Awobuluyi, M. *et al.* Subunit-specific roles of glycine-binding domains in activation

of NR1/NR3 N-methyl-D-aspartate receptors. *Mol Pharmacol* **71**, 112–122 (2007).

106. Madry, C. *et al.* Principal role of NR3 subunits in NR1/NR3 excitatory glycine receptor function. *Biochem Biophys Res Commun* **354**, 102–108 (2007).

107. Perez-Otano, I., Larsen, R. S. & Wesseling, J. F. Emerging roles of GluN3-containing NMDA receptors in the CNS. *Nat Rev Neurosci* **17**, 623–635 (2016).

108. Henson, M. A., Roberts, A. C., Perez-Otano, I. & Philpot, B. D. Influence of the NR3A subunit on NMDA receptor functions. *Prog Neurobiol* **91**, 23–37 (2010).

109. Matsuda, K., Kamiya, Y., Matsuda, S. & Yuzaki, M. Cloning and characterization of a novel NMDA receptor subunit NR3B: A dominant subunit that reduces calcium permeability. *Mol. Brain Res.* **100**, 43–52 (2002).

110. Nishi, M., Hinds, H., Lu, H.-P., Kawata, M. & Hayashi, Y. Motoneuron-Specific Expression of NR3B, a Novel NMDA-Type Glutamate Receptor Subunit That Works in a Dominant-Negative Manner. *J. Neurosci.* **21**, RC185–RC185 (2018).

111. Wee, K. S. L., Zhang, Y., Khanna, S. & Low, C. M. Immunolocalization of NMDA receptor subunit NR3B in selected structures in the rat forebrain, cerebellum, and lumbar spinal cord. *J. Comp. Neurol.* (2008). doi:10.1002/cne.21747

112. Chatterton, J. E. *et al.* Excitatory glycine receptors containing the NR3 family of NMDA receptor subunits. *Nature* **415**, 793–798 (2002).

113. Low, C. M. & Wee, K. S. L. New insights into the not-so-new NR3 subunits of N-methyl-D-aspartate receptor: Localization, structure, and function. *Mol. Pharmacol.* **78**, 1–11 (2010).

114. Al-Hallaq, R. A. *et al.* Association of NR3A with the N-methyl-D-aspartate receptor NR1 and NR2 subunits. *Mol. Pharmacol.* **62**, 1119–1127 (2002).

115. Wong, H. K. *et al.* Temporal and regional expression of NMDA receptor subunit NR3A in the mammalian brain. *J Comp Neurol* **450**, 303–317 (2002).

116. Ciabarra, A. M. *et al.* Cloning and characterization of chi-1: a developmentally regulated member of a novel class of the ionotropic glutamate receptor family. *J Neurosci* **15**, 6498–6508 (1995).

117. Sasaki, Y. F. *et al.* Characterization and comparison of the NR3A subunit of the NMDA receptor in recombinant systems and primary cortical neurons. *J. Neurophysiol.* **87**, 2052–2063 (2002).

118. Tong, G. *et al.* Modulation of NMDA receptor properties and synaptic transmission

by the NR3A subunit in mouse hippocampal and cerebrocortical neurons. *J Neurophysiol* **99**, 122–132 (2008).

119. Larsen, R. S. *et al.* NR3A-containing NMDARs promote neurotransmitter release and spike timing-dependent plasticity. *Nat Neurosci* **14**, 338–344 (2011).

120. Roberts, A. C. *et al.* Downregulation of NR3A-containing NMDARs is required for synapse maturation and memory consolidation. *Neuron* **63**, 342–356 (2009).

121. Larsen, R. S. *et al.* NR3A-containing NMDARs promote neurotransmitter release and spike timing-dependent plasticity. *Nat. Neurosci.* (2011). doi:10.1038/nn.2750

122. Pérez-Otaño, I. *et al.* Endocytosis and synaptic removal of NR3A-containing NMDA receptors by PACSIN1/syndapin1. *Nat. Neurosci.* **9**, 611–621 (2006).

123. Yao, Y. & Mayer, M. L. Characterization of a soluble ligand binding domain of the NMDA receptor regulatory subunit NR3A. *J Neurosci* **26**, 4559–4566 (2006).

124. Grand, T., Abi Gerges, S., David, M., Diana, M. A. & Paoletti, P. Unmasking GluN1/GluN3A excitatory glycine NMDA receptors. *Nat Commun* **9**, 4769 (2018).

125. Otsu, Y. *et al.* Control of aversion by glycine-gated GluN1/GluN3A NMDA receptors in the adult medial habenula. *Science (80-.).* **366**, 250–254 (2019).

126. Oliet, S. H. R. & Mothet, J. P. Regulation of N-methyl-d-aspartate receptors by astrocytic d-serine. *Neuroscience* **158**, 275–283 (2009).

127. Papouin, T., Henneberger, C., Rusakov, D. A. & Oliet, S. H. R. Astroglial versus Neuronal D-Serine: Fact Checking. *Trends Neurosci* **40**, 517–520 (2017).

128. Kvist, T., Greenwood, J. R., Hansen, K. B., Traynelis, S. F. & Brauner-Osborne, H. Structure-based discovery of antagonists for GluN3-containing N-methyl-D-aspartate receptors. *Neuropharmacology* **75**, 324–336 (2013).

129. Cummings, K. A. & Popescu, G. K. Protons Potentiate GluN1/GluN3A Currents by Attenuating Their Desensitisation. *Sci Rep* **6**, 23344 (2016).

130. Vergnano, A. M. *et al.* Zinc dynamics and action at excitatory synapses. *Neuron* **82**, 1101–1114 (2014).

131. Madry, C., Betz, H., Geiger, J. R. & Laube, B. Supralinear potentiation of NR1/NR3A excitatory glycine receptors by Zn2+ and NR1 antagonist. *Proc Natl Acad Sci U S A* **105**, 12563–12568 (2008).

132. Pina-Crespo, J. C. *et al.* Excitatory glycine responses of CNS myelin mediated by NR1/NR3 'NMDA' receptor subunits. *J Neurosci* **30**, 11501–11505 (2010).

133. Matsuda, K., Fletcher, M., Kamiya, Y. & Yuzaki, M. Specific Assembly with the NMDA Receptor 3B Subunit Controls Surface Expression and Calcium Permeability of NMDA Receptors. *J. Neurosci.* **23**, 10064–10073 (2003).

134. Chavas, J., Forero, M. E., Collin, T., Llano, I. & Marty, A. Osmotic tension as a possible link between GABAA receptor activation and intracellular calcium elevation. *Neuron* **44**, 701–713 (2004).

135. Pérez-Otaño, I., Larsen, R. S. & Wesseling, J. F. Emerging roles of GluN3-containing NMDA receptors in the CNS. *Nature Reviews Neuroscience* (2016). doi:10.1038/nrn.2016.92

136. Pérez-Otaño, I. *et al.* Assembly with the NR1 subunit is required for surface expression of NR3A-containing NMDA receptors. *J. Neurosci.* **21**, 1228–1237 (2001).

137. Das, S. *et al.* Increased NMDA current and spine density in mice lacking the NMDA receptor subunit NR3A. *Nature* (1998). doi:10.1038/30748

138. Burzomato, V., Frugier, G., Pérez-Otaño, I., Kittler, J. T. & Attwell, D. The receptor subunits generating NMDA receptor mediated currents in oligodendrocytes. *J. Physiol.* **588**, 3403–3414 (2010).

139. Pachernegg, S., Strutz-Seebohm, N. & Hollmann, M. GluN3 subunit-containing NMDA receptors: Not just one-trick ponies. *Trends Neurosci.* **35**, 240–249 (2012).

140. Yuan, T. *et al.* Expression of cocaine-evoked synaptic plasticity by GluN3A-containing NMDA receptors. *Neuron* **80**, 1025–1038 (2013).

141. McClymont, D. W., Harris, J. & Mellor, I. R. Open-channel blockade is less effective on GluN3B than GluN3A subunit-containing NMDA receptors. *Eur. J. Pharmacol.* **686**, 22–31 (2012).

142. Zhu, Z. *et al.* Negative allosteric modulation of GluN1/GluN3 NMDA receptors. *Neuropharmacology* 108117 (2020). doi:10.1016/j.neuropharm.2020.108117

143. Zuo, Y., Lin, A., Chang, P. & Gan, W. B. Development of long-term dendritic spine stability in diverse regions of cerebral cortex. *Neuron* **46**, 181–189 (2005).

144. Pérez-Otaño, I. & Ehlers, M. D. Learning from NMDA receptor trafficking: Clues to the development and maturation of glutamatergic synapses. *NeuroSignals* **13**, 175–189 (2004).

145. Marco, S. *et al.* Suppressing aberrant GluN3A expression rescues synaptic and behavioral impairments in Huntington's disease models. *Nat Med* **19**, 1030–1038

(2013).

146. Kehoe, L. A. *et al.* GluN3A promotes dendritic spine pruning and destabilization during postnatal development. *J. Neurosci.* **34**, 9213–9221 (2014).

147. Salter, M. G. & Fern, R. NMDA receptors are expressed in developing oligodendrocyte processes and mediate injury. *Nature* **438**, 1167–1171 (2005).

148. Káradóttir, R., Cavelier, P., Bergersen, L. H. & Attwell, D. NMDA receptors are expressed in oligodendrocytes and activated in ischaemia. *Nature* **438**, 1162–1166 (2005).

149. Chowdhury, D. *et al.* Tyrosine phosphorylation regulates the endocytosis and surface expression of GluN3A-containing NMDA receptors. *J. Neurosci.* (2013). doi:10.1523/JNEUROSCI.2721-12.2013

150. Mueller, H. T. & Meador-Woodruff, J. H. NR3A NMDA receptor subunit mRNA expression in schizophrenia, depression and bipolar disorder. *Schizophr. Res.* **71**, 361–370 (2004).

151. Shen, Y. C. *et al.* Exomic sequencing of the glutamate receptor, ionotropic, N-methyl-d-aspartate 3A gene (GRIN3A) reveals no association with schizophrenia. *Schizophr. Res.* **114**, 25–32 (2009).

152. Matsuno, H. *et al.* A naturally occurring null variant of the NMDA type glutamate receptor NR3B subunit is a risk factor of schizophrenia. *PLoS One* **10**, 1–19 (2015).

153. Herrero, M. T., Barcia, C. & Navarro, J. M. Functional anatomy of thalamus and basal ganglia. *Child's Nervous System* (2002). doi:10.1007/s00381-002-0604-1

154. Latchoumane, C. F. V., Ngo, H. V. V., Born, J. & Shin, H. S. Thalamic Spindles Promote Memory Formation during Sleep through Triple Phase-Locking of Cortical, Thalamic, and Hippocampal Rhythms. *Neuron* (2017). doi:10.1016/j.neuron.2017.06.025

155. Guillery, R. W. Anatomical pathways that link perception and action. in *Progress in Brain Research* (2005). doi:10.1016/S0079-6123(05)49017-2

156. Sherman, S. M. & Guillery, R. W. *Exploring the Thalamus and Its Role in Cortical Function*. *Exploring the Thalamus and Its Role in Cortical Function* (2018). doi:10.7551/mitpress/2940.001.0001

157. Groenewegen, H. J. & Berendse, H. W. The specificity of the 'nonspecific' midline and intralaminar thalamic nuclei. *Trends in Neurosciences* (1994). doi:10.1016/0166-2236(94)90074-4

158. Vertes, R. P. PHA-L analysis of projections from the supramammillary nucleus in the rat. *J. Comp. Neurol.* (1992). doi:10.1002/cne.903260408

159. Peschanski, M. & Besson, J. M. A spino-reticulo-thalamic pathway in the rat: An anatomical study with reference to pain transmission. *Neuroscience* (1984). doi:10.1016/0306-4522(84)90145-3

160. Hallanger, A. E., Levey, A. I., Lee, H. J., Rye, D. B. & Wainer, B. H. The origins of cholinergic and other subcortical afferents to the thalamus in the rat. *J. Comp. Neurol.* (1987). doi:10.1002/cne.902620109

161. Yamasaki, D. S. G., Krauthamer, G. M. & Rhoades, R. W. Superior collicular projection to intralaminar thalamus in rat. *Brain Res.* (1986). doi:10.1016/0006-8993(86)90925-X

162. Haroian, A. J., Massopust, L. C. & Young, P. A. Cerebellothalamic projections in the rat: An autoradiographic and degeneration study. *J. Comp. Neurol.* (1981). doi:10.1002/cne.901970205

163. Villanueva, L., Desbois, C., Le Bars, D. & Bernard, J. F. Organization of diencephalic projections from the medullary subnucleus reticularis dorsalis and the adjacent cuneate nucleus: A retrograde and anterograde tracer study in the rat. *J. Comp. Neurol.* (1998). doi:10.1002/(SICI)1096-9861(19980105)390:1<133::AID-CNE11>3.0.CO;2-Y

164. Vertes, R. P. Brainstem afferents to the basal forebrain in the rat. *Neuroscience* (1988). doi:10.1016/0306-4522(88)90077-2

165. Kaitz, S. S. & Robertson, R. T. Thalamic connections with limbic cortex. II. Corticothalamic projections. *J. Comp. Neurol.* (1981). doi:10.1002/cne.901950309

166. Van Der Werf, Y. D., Witter, M. P. & Groenewegen, H. J. The intralaminar and midline nuclei of the thalamus. Anatomical and functional evidence for participation in processes of arousal and awareness. *Brain Research Reviews* (2002). doi:10.1016/S0165-0173(02)00181-9

167. Beas, B. S. *et al.* The locus coeruleus drives disinhibition in the midline thalamus via a dopaminergic mechanism. *Nature Neuroscience* (2018). doi:10.1038/s41593-018-0167-4

168. Gao, C. *et al.* Two genetically, anatomically and functionally distinct cell types segregate across anteroposterior axis of paraventricular thalamus. *Nat. Neurosci.* **23**, 217–228 (2020).

169. Bentivoglio, M., Balercia, G. & Kruger, L. Chapter 4 The specificity of the nonspecific thalamus: The midline nuclei. *Prog. Brain Res.* (1991). doi:10.1016/S0079-6123(08)63047-2

170. Christie, M. J., Summers, R. J., Stephenson, J. A., Cook, C. J. & Beart, P. M. Excitatory amino acid projections to the nucleus accumbens septi in the rat: A retrograde transport study utilizing d[3H]aspartate and [3H]GABA. *Neuroscience* (1987). doi:10.1016/0306-4522(87)90345-9

171. Frassoni, C., Spreafico, R. & Bentivoglio, M. Glutamate, aspartate and co-localization with calbindin in the medial thalamus. An immunohistochemical study in the rat. *Exp. Brain Res.* (1997). doi:10.1007/PL00005689

172. Moutsimilli, L. *et al.* Antipsychotics increase vesicular glutamate transporter 2 (VGLUT2) expression in thalamolimbic pathways. *Neuropharmacology* (2008). doi:10.1016/j.neuropharm.2007.10.022

173. Uroz, V., Prensa, L. & Giménez-Amaya, J. M. Chemical Anatomy of the Human Paraventricular Thalamic Nucleus. *Synapse* (2004). doi:10.1002/syn.10298

174. Mátyás, F. *et al.* A highly collateralized thalamic cell type with arousal-predicting activity serves as a key hub for graded state transitions in the forebrain. *Nat. Neurosci.* (2018). doi:10.1038/s41593-018-0251-9

175. Cornwall, J. & Phillipson, O. T. Afferent projections to the dorsal thalamus of the rat as shown by retrograde lectin transport-I. The mediodorsal nucleus. *Neuroscience* (1988). doi:10.1016/0306-4522(88)90085-1

176. Li, S. & Kirouac, G. J. Sources of inputs to the anterior and posterior aspects of the paraventricular nucleus of the thalamus. *Brain Struct. Funct.* (2012). doi:10.1007/s00429-011-0360-7

177. Krout, K. E. & Loewy, A. D. Parabrachial nucleus projections to midline and intralaminar thalamic nuclei of the rat. *J. Comp. Neurol.* (2000). doi:10.1002/1096-9861(20001218)428:3<475::AID-CNE6>3.0.CO;2-9

178. Do-Monte, F. H., Quinõnes-Laracuente, K. & Quirk, G. J. A temporal shift in the circuits mediating retrieval of fear memory. *Nature* (2015). doi:10.1038/nature14030

179. Hsu, D. T. & Price, J. L. Paraventricular thalamic nucleus: Subcortical connections and innervation by serotonin, orexin, and corticotropin-releasing hormone in Macaque monkeys. *J. Comp. Neurol.* (2009). doi:10.1002/cne.21934

180. Peng, Z. C. & Bentivoglio, M. The thalamic paraventricular nucleus relays information from the suprachiasmatic nucleus to the amygdala: A combined anterograde and retrograde tracing study in the rat at the light and electron microscopic levels. *J. Neurocytol.* (2004). doi:10.1023/B:NEUR.0000029651.51195.f9

181. Zhang, X. & Van Den Pol, A. N. Rapid binge-like eating and body weight gain driven by zona incerta GABA neuron activation. *Science (80-.).* (2017). doi:10.1126/science.aam7100

182. Volkow, N. D. & Morales, M. The Brain on Drugs: From Reward to Addiction. *Cell* (2015). doi:10.1016/j.cell.2015.07.046

183. Su, H. -S & Bentivoglio, M. Thalamic midline cell populations projecting to the nucleus accumbens, amygdala, and hippocampus in the rat. *J. Comp. Neurol.* (1990). doi:10.1002/cne.902970410

184. Zhu, Y., Wienecke, C. F. R., Nachtrab, G. & Chen, X. A thalamic input to the nucleus accumbens mediates opiate dependence. *Nature* (2016). doi:10.1038/nature16954

185. Hsu, D. T., Kirouac, G. J., Zubieta, J. K. & Bhatnagar, S. Contributions of the paraventricular thalamic nucleus in the regulation of stress, motivation, and mood. *Frontiers in Behavioral Neuroscience* (2014). doi:10.3389/fnbeh.2014.00073

186. Penzo, M. A. *et al.* The paraventricular thalamus controls a central amygdala fear circuit. *Nature* (2015). doi:10.1038/nature13978

187. Li, S. & Kirouac, G. J. Projections from the paraventricular nucleus of the thalamus to the forebrain, with special emphasis on the extended amygdala. *J. Comp. Neurol.* (2008). doi:10.1002/cne.21502

188. Berendse, H. W. & Groenewegen, H. J. Restricted cortical termination fields of the midline and intralaminar thalamic nuclei in the rat. *Neuroscience* (1991). doi:10.1016/0306-4522(91)90151-D

189. Vertes, R. P. & Hoover, W. B. Projections of the paraventricular and paratenial nuclei of the dorsal midline thalamus in the rat. *J. Comp. Neurol.* (2008). doi:10.1002/cne.21679

190. Moga, M. M., Weis, R. P. & Moore, R. Y. Efferent projections of the paraventricular thalamic nucleus in the rat. *J. Comp. Neurol.* (1995). doi:10.1002/cne.903590204

191. Bubser, M. & Deutch, A. Y. Thalamic paraventricular nucleus neurons collateralize to innervate the prefrontal cortex and nucleus accumbens. *Brain Res.* (1998). doi:10.1016/S0006-8993(97)01373-5

192. Unzai, T., Kuramoto, E., Kaneko, T. & Fujiyama, F. Quantitative Analyses of the Projection of Individual Neurons from the Midline Thalamic Nuclei to the Striosome and Matrix Compartments of the Rat Striatum. *Cereb. Cortex* (2017). doi:10.1093/cercor/bhv295

193. Moruzzi, G. & Magoun, H. W. Brain stem reticular formation and activation of the EEG. *Electroencephalogr. Clin. Neurophysiol.* (1949). doi:10.1016/0013-4694(49)90219-9

194. Steriade, M. & Glenn, L. L. Neocortical and caudate projections of intralaminar thalamic neurons and their synaptic excitation from midbrain reticular core. *J. Neurophysiol.* (1982). doi:10.1152/jn.1982.48.2.352

195. Fiset, P. *et al.* Brain mechanisms of propofol-induced loss of consciousness in humans: A positron emission tomographic study. *J. Neurosci.* (1999). doi:10.1523/JNEUROSCI.19-13-05506.1999

196. Kinomura, S., Larsson, J., Gulyás, B. & Roland, P. E. Activation by attention of the human reticular formation and thalamic intralaminar nuclei. *Science (80-.).* (1996). doi:10.1126/science.271.5248.512

197. Paus, T. *et al.* Time-related changes in neural systems underlying attention and arousal during the performance of an auditory vigilance task. *J. Cogn. Neurosci.* (1997). doi:10.1162/jocn.1997.9.3.392

198. Purpura, K. P. & Schiff, N. D. The thalamic intralaminar nuclei: A role in visual awareness. *Neuroscientist* (1997). doi:10.1177/107385849700300110

199. Kinney, H. C. & Samuels, M. A. Neuropathology of the persistent vegetative state. A review. *J. Neuropathol. Exp. Neurol.* (1994). doi:10.1097/00005072-199411000-00002

200. Bogen, J. E. On the Neurophysiology of Consciousness: Part II. Constraining the Semantic Problem. *Consciousness and Cognition* (1995). doi:10.1006/ccog.1995.1020

201. Schiff, N. D. *et al.* Behavioural improvements with thalamic stimulation after severe traumatic brain injury. *Nature* (2007). doi:10.1038/nature06041

202. Alkire, M. T., Asher, C. D., Franciscus, A. M. & Hahn, E. L. Thalamic microinfusion of

antibody to a voltage-gated potassium channel restores consciousness during anesthesia. *Anesthesiology* (2009). doi:10.1097/ALN.0b013e31819c461c

203. Redinbaugh, M. J. *et al.* Thalamus Modulates Consciousness via Layer-Specific Control of Cortex. *Neuron* **106**, 66-75.e12 (2020).

204. Giber, K. *et al.* A subcortical inhibitory signal for behavioral arrest in the thalamus. *Nat. Neurosci.* (2015). doi:10.1038/nn.3951

205. Gent, T. C., Bandarabadi, M., Herrera, C. G. & Adamantidis, A. R. Thalamic dual control of sleep and wakefulness. *Nat. Neurosci.* **21**, 974–984 (2018).

206. Adamantidis, A. R., Gutierrez Herrera, C. & Gent, T. C. Oscillating circuitries in the sleeping brain. *Nat. Rev. Neurosci.* **20**, 746–762 (2019).

207. Fabbro, F. Consciousness at the Frontiers of Neuroscience: Advances in Neurology by H.H. Jasper, L. Descarrier, V.F. Castellucci, S. Rossignol (Eds.), vol. 77. Lippincott-Raven, 1998, £110.00. *Neuropsychologia* (2001). doi:10.1016/s0028-3932(00)00089-0

208. Hunter, J. & Jasper, H. H. Effects of thalamic stimulation in unanaesthetised animals. *Electroencephalogr. Clin. Neurophysiol.* (1949). doi:10.1016/0013-4694(49)90196-0

209. Liu, J. *et al.* Frequency-selective control of cortical and subcortical networks by central thalamus. *Elife* **4**, 1–27 (2015).

210. Chen, S. & Su, H. Sen. Afferent connections of the thalamic paraventricular and parataenial nuclei in the rat - a retrograde tracing study with iontophoretic application of Fluoro-Gold. *Brain Res.* (1990). doi:10.1016/0006-8993(90)91570-7

211. Leak, R. K. & Moore, R. Y. Topographic organization of suprachiasmatic nucleus projection neurons. *J. Comp. Neurol.* (2001). doi:10.1002/cne.1142

212. Watts, A. G. & Swanson, L. W. Efferent projections of the suprachiasmatic nucleus: II. Studies using retrograde transport of fluorescent dyes and simultaneous peptide immunohistochemistry in the rat. *J. Comp. Neurol.* (1987). doi:10.1002/cne.902580205

213. Deurveilher, S. & Semba, K. Indirect projections from the suprachiasmatic nucleus to major arousal-promoting cell groups in rat: Implications for the circadian control of behavioural state. *Neuroscience* (2005). doi:10.1016/j.neuroscience.2004.08.030

214. Saper, C. B. The central circadian timing system. *Current Opinion in Neurobiology*

(2013). doi:10.1016/j.conb.2013.04.004

215. Saper, C. B., Lu, J., Chou, T. C. & Gooley, J. The hypothalamic integrator for circadian rhythms. *Trends in Neurosciences* (2005). doi:10.1016/j.tins.2004.12.009

216. Moga, M. M. & Moore, R. Y. Organization of neural inputs to the suprachiasmatic nucleus in the rat. *J. Comp. Neurol.* (1997). doi:10.1002/(SICI)1096-9861(19971222)389:3<508::AID-CNE11>3.0.CO;2-H

217. Zhang, C., Truong, K. K. & Zhou, Q. Y. Efferent projections of prokineticin 2 expressing neurons in the mouse suprachiasmatic nucleus. *PLoS One* (2009). doi:10.1371/journal.pone.0007151

218. Von Gall, C., Noton, E., Lee, C. & Weaver, D. R. Light does not degrade the constitutively expressed BMAL1 protein in the mouse suprachiasmatic nucleus. *Eur. J. Neurosci.* (2003). doi:10.1046/j.1460-9568.2003.02735.x

219. Dibner, C., Schibler, U. & Albrecht, U. The Mammalian Circadian Timing System: Organization and Coordination of Central and Peripheral Clocks. *Annu. Rev. Physiol.* (2010). doi:10.1146/annurev-physiol-021909-135821

220. Golombek, D. A. & Rosenstein, R. E. Physiology of circadian entrainment. *Physiological Reviews* (2010). doi:10.1152/physrev.00009.2009

221. Stehle, J. H., von Gall, C. & Korf, H. W. Melatonin: A clock-output, a clock-input. *Journal of Neuroendocrinology* (2003). doi:10.1046/j.1365-2826.2003.01001.x

222. Ren, S. *et al.* The paraventricular thalamus is a critical thalamic area for wakefulness. *Science (80-.).* (2018). doi:10.1126/science.aat2512

223. Bubser, M. & Deutch, A. Y. Stress induces Fos expression in neurons of the thalamic paraventricular nucleus that innervate limbic forebrain sites. *Synapse* (1999). doi:10.1002/(SICI)1098-2396(199904)32:1<13::AID-SYN2>3.0.CO;2-R

224. Kirouac, G. J. Placing the paraventricular nucleus of the thalamus within the brain circuits that control behavior. *Neuroscience and Biobehavioral Reviews* (2015). doi:10.1016/j.neubiorev.2015.08.005

225. James, M. H. & Dayas, C. V. What about me...? The PVT: A role for the paraventricular thalamus (PVT) in drug-seeking behaviour. *Front. Behav. Neurosci.* (2013). doi:10.3389/fnbeh.2013.00018

226. Matzeu, A., Zamora-Martinez, E. R. & Martin-Fardon, R. The paraventricular nucleus of the thalamus is recruited by both natural rewards and drugs of abuse: Recent evidence of a pivotal role for orexin/hypocretin signaling in this thalamic

nucleus in drug-seeking behavior. *Frontiers in Behavioral Neuroscience* (2014). doi:10.3389/fnbeh.2014.00117

227. Martin-Fardon, R. & Boutrel, B. Orexin/hypocretin (Orx/Hcrt) transmission and drug-seeking behavior: Is the paraventricular nucleus of the thalamus (PVT) part of the drug seeking circuitry? *Frontiers in Behavioral Neuroscience* (2012). doi:10.3389/fnbeh.2012.00075

228. Gass, J. T. & Chandler, L. J. The Plasticity of Extinction: Contribution of the Prefrontal Cortex in Treating Addiction through Inhibitory Learning. *Front. Psychiatry* (2013). doi:10.3389/fpsyt.2013.00046

229. Koob, G. F. & Volkow, N. D. Neurobiology of addiction: a neurocircuitry analysis. *The Lancet Psychiatry* (2016). doi:10.1016/S2215-0366(16)00104-8

230. Panlilio, L. V. & Goldberg, S. R. Self-administration of drugs in animals and humans as a model and an investigative tool. *Addiction* (2007). doi:10.1111/j.1360-0443.2007.02011.x

231. Koob, G. F. & Le Moal, M. Drug abuse: Hedonic homeostatic dysregulation. *Science (80-.).* (1997). doi:10.1126/science.278.5335.52

232. Shaham, Y., Shalev, U., Lu, L., De Wit, H. & Stewart, J. The reinstatement model of drug relapse: History, methodology and major findings. *Psychopharmacology* (2003). doi:10.1007/s00213-002-1224-x

233. Gutstein, H. B., Thome, J. L., Fine, J. L., Watson, S. J. & Akil, H. Pattern of c-fos mRNA induction in rat brain by acute morphine. *Can. J. Physiol. Pharmacol.* (1998). doi:10.1139/cjpp-76-3-294

234. Garcia, M. M., Brown, H. E. & Harlan, R. E. Alterations in immediate-early gene proteins in the rat forebrain induced by acute morphine injection. *Brain Res.* (1995). doi:10.1016/0006-8993(95)00625-Z

235. Deutch, A. Y. Psychostimulant-lnduced fos protein expression in the thalamic paraventricular nucleus. *J. Neurosci.* (1998). doi:10.1523/jneurosci.18-24-10680.1998

236. Young, C. D. & Deutch, A. Y. The effects of thalamic paraventricular nucleus lesions on cocaine- induced locomotor activity and sensitization. *Pharmacol. Biochem. Behav.* (1998). doi:10.1016/S0091-3057(98)00051-3

237. Ren, T. & Sagar, S. M. Induction of c-fos immunostaining in the rat brain after the systemic administration of nicotine. *Brain Res. Bull.* (1992). doi:10.1016/0361-

9230(92)90127-J

238. Ryabinin, A. E. & Wang, Y. M. Repeated alcohol administration differentially affects c-Fos and FosB protein immunoreactivity in DBA/2J mice. *Alcohol. Clin. Exp. Res.* (1998). doi:10.1111/j.1530-0277.1998.tb03962.x

239. Barson, J. R., Ho, H. T. & Leibowitz, S. F. Anterior thalamic paraventricular nucleus is involved in intermittent access ethanol drinking: Role of orexin receptor 2. *Addict. Biol.* (2015). doi:10.1111/adb.12139

240. Pasumarthi, R. K. & Fadel, J. Activation of orexin/hypocretin projections to basal forebrain and paraventricular thalamus by acute nicotine. *Brain Res. Bull.* (2008). doi:10.1016/j.brainresbull.2008.09.014

241. Hamlin, A. S., Clemens, K. J., Choi, E. A. & McNally, G. P. Paraventricular thalamus mediates context-induced reinstatement (renewal) of extinguished reward seeking. *Eur. J. Neurosci.* (2009). doi:10.1111/j.1460-9568.2009.06623.x

242. Matzeu, A. & Martin-Fardon, R. Drug seeking and relapse: New evidence of a role for orexin and dynorphin co-transmission in the paraventricular nucleus of the thalamus. *Frontiers in Neurology* (2018). doi:10.3389/fneur.2018.00720

243. Matzeu, A., Cauvi, G., Kerr, T. M., Weiss, F. & Martin-Fardon, R. The paraventricular nucleus of the thalamus is differentially recruited by stimuli conditioned to the availability of cocaine versus palatable food. *Addict. Biol.* (2017). doi:10.1111/adb.12280

244. James, M. H. *et al.* Cocaine- and Amphetamine-Regulated Transcript (CART) signaling within the paraventricular thalamus modulates cocaine-seeking behaviour. *PLoS One* (2010). doi:10.1371/journal.pone.0012980

245. Neumann, P. A. *et al.* Cocaine-induced synaptic alterations in thalamus to nucleus accumbens projection. *Neuropsychopharmacology* (2016). doi:10.1038/npp.2016.52

246. Timofeeva, E., Picard, F., Duclos, M., Deshaies, Y. & Richard, D. Neuronal activation and corticotropin-releasing hormone expression in the brain of obese (fa/fa) and lean (fa/?) Zucker rats in response to refeeding. *Eur. J. Neurosci.* (2002). doi:10.1046/j.1460-9568.2002.01942.x

247. Bhatnagar, S. & Dallman, M. F. The paraventricular nucleus of the thalamus alters rhythms in core temperature and energy balance in a state-dependent manner. *Brain Res.* (1999). doi:10.1016/S0006-8993(99)02108-3

248. Stratford, T. R. & Wirtshafter, D. Injections of muscimol into the paraventricular thalamic nucleus, but not mediodorsal thalamic nuclei, induce feeding in rats. *Brain Res.* (2013). doi:10.1016/j.brainres.2012.10.043

249. Betley, J. N., Cao, Z. F. H., Ritola, K. D. & Sternson, S. M. Parallel, redundant circuit organization for homeostatic control of feeding behavior. *Cell* (2013). doi:10.1016/j.cell.2013.11.002

250. Labouèbe, G., Boutrel, B., Tarussio, D. & Thorens, B. Glucose-responsive neurons of the paraventricular thalamus control sucrose-seeking behavior. *Nat. Neurosci.* (2016). doi:10.1038/nn.4331

251. Poulin, A. M. & Timofeeva, E. The dynamics of neuronal activation during food anticipation and feeding in the brain of food-entrained rats. *Brain Res.* (2008). doi:10.1016/j.brainres.2008.06.039

252. Spencer, S. J., Fox, J. C. & Day, T. A. Thalamic paraventricular nucleus lesions facilitate central amygdala neuronal responses to acute psychological stress. *Brain Res.* (2004). doi:10.1016/j.brainres.2003.10.054

253. Chastrette, N., Pfaff, D. W. & Gibbs, R. B. Effects of daytime and nighttime stress on Fos-like immunoreactivity in the paraventricular nucleus of the hypothalamus, the habenula, and the posterior paraventricular nucleus of the thalamus. *Brain Res.* (1991). doi:10.1016/0006-8993(91)91559-J

254. Li, Y., Dong, X., Li, S. & Kirouac, G. J. Lesions of the posterior paraventricular nucleus of the thalamus attenuate fear expression. *Front. Behav. Neurosci.* (2014). doi:10.3389/fnbeh.2014.00094

255. Padilla-Coreano, N., Do-Monte, F. H. & Quirk, G. J. A time-dependent role of midline thalamic nuclei in the retrieval of fear memory. in *Neuropharmacology* (2012). doi:10.1016/j.neuropharm.2011.08.037

256. Ciocchi, S. *et al.* Encoding of conditioned fear in central amygdala inhibitory circuits. *Nature* (2010). doi:10.1038/nature09559

257. Haubensak, W. *et al.* Genetic dissection of an amygdala microcircuit that gates conditioned fear. *Nature* (2010). doi:10.1038/nature09553

258. Li, H. *et al.* Experience-dependent modification of a central amygdala fear circuit. *Nat. Neurosci.* (2013). doi:10.1038/nn.3322

259. Kasahara, T. *et al.* Depression-like episodes in mice harboring mtDNA deletions in paraventricular thalamus. *Mol. Psychiatry* (2016). doi:10.1038/mp.2015.156

260. Sharp, F. R., Sagar, S. M., Hicks, K., Lowenstein, D. & Hisanaga, K. c-fos mRNA, Fos, and Fos-related antigen induction by hypertonic saline and stress. *J. Neurosci.* (1991). doi:10.1523/jneurosci.11-08-02321.1991

261. Imaki, T., Shibasaki, T., Hotta, M. & Demura, H. Intracerebroventricular administration of corticotropin-releasing factor induces c-fos mRNA expression in brain regions related to stress responses: comparison with pattern of c-fos mRNA induction after stress. *Brain Res.* (1993). doi:10.1016/0006-8993(93)90199-W

262. Cullinan, W. E., Helmreich, D. L. & Watson, S. J. Fos expression in forebrain afferents to the hypothalamic paraventricular nucleus following swim stress. *J. Comp. Neurol.* (1996). doi:10.1002/(SICI)1096-9861(19960422)368:1<88::AID-CNE6>3.0.CO;2-G

263. Fenoglio, K. A., Chen, Y. & Baram, T. Z. Neuroplasticity of the hypothalamic-pituitary-adrenal axis early in life requires recurrent recruitment of stress-regulating brain regions. *J. Neurosci.* (2006). doi:10.1523/JNEUROSCI.4080-05.2006

264. Bhatnagar, S. & Dallman, M. Neuroanatomical basis for facilitation of hypothalamic-pituitary- adrenal responses to a novel stressor after chronic stress. *Neuroscience* (1998). doi:10.1016/S0306-4522(97)00577-0

265. Bhatnagar, S. *et al.* A cholecystokinin-mediated pathway to the paraventricular thalamus is recruited in chronically stressed rats and regulates hypothalamic-pituitary- adrenal function. *J. Neurosci.* (2000). doi:10.1523/jneurosci.20-14-05564.2000

266. Bhatnagar, S., Huber, R., Nowak, N. & Trotter, P. Lesions of the posterior paraventricular thalamus block habituation of hypothalamic-pituitary-adrenal responses to repeated restraint. *J. Neuroendocrinol.* (2002). doi:10.1046/j.0007-1331.2002.00792.x

267. Li, Y. *et al.* Orexins in the paraventricular nucleus of the thalamus mediate anxiety-like responses in rats. *Psychopharmacology (Berl).* (2010). doi:10.1007/s00213-010-1948-y

268. Li, Y. *et al.* Orexins in the midline thalamus are involved in the expression of conditioned place aversion to morphine withdrawal. *Physiol. Behav.* (2011). doi:10.1016/j.physbeh.2010.10.006

269. Hikosaka, O. The habenula: from stress evasion to value-based decision-making. *Nat Rev Neurosci* **11**, 503–513 (2010).

270. Yamaguchi, T., Danjo, T., Pastan, I., Hikida, T. & Nakanishi, S. Distinct roles of segregated transmission of the septo-habenular pathway in anxiety and fear. *Neuron* **78**, 537–544 (2013).

271. Otsu, Y. *et al.* Functional Principles of Posterior Septal Inputs to the Medial Habenula. *Cell Rep.* (2018). doi:10.1016/j.celrep.2017.12.064

272. McLaughlin, I., Dani, J. A. & De Biasi, M. The medial habenula and interpeduncular nucleus circuitry is critical in addiction, anxiety, and mood regulation. *J. Neurochem.* **142**, 130–143 (2017).

273. Metzger, M. *et al.* Habenular connections with the dopaminergic and serotonergic system and their role in stress-related psychiatric disorders. *Eur. J. Neurosci.* 1–24 (2019). doi:10.1111/ejn.14647

274. Quina, L. A., Harris, J., Zeng, H. & Turner, E. E. Specific connections of the interpeduncular subnuclei reveal distinct components of the habenulopeduncular pathway. *J. Comp. Neurol.* **525**, 2632–2656 (2017).

275. Darcq, E. *et al.* RSK2 signaling in medial habenula contributes to acute morphine analgesia. *Neuropsychopharmacology* **37**, 1288–1296 (2012).

276. Soria-Gomez, E. *et al.* Habenular CB1 Receptors Control the Expression of Aversive Memories. *Neuron* **88**, 306–313 (2015).

277. Zhou, J. *et al.* Presynaptic Excitation via GABA B Receptors in Habenula Cholinergic Neurons Regulates Fear Memory Expression. *Cell* **166**, 716–728 (2016).

278. Otsu, Y. *et al.* Functional Principles of Posterior Septal Inputs to the Medial Habenula. *Cell Rep* **22**, 693–705 (2018).

279. Aizawa, H., Kobayashi, M., Tanaka, S., Fukai, T. & Okamoto, H. Molecular characterization of the subnuclei in rat habenula. *J Comp Neurol* **520**, 4051–4066 (2012).

280. Hashikawa, Y. *et al.* Transcriptional and Spatial Resolution of Cell Types in the Mammalian Habenula. *Neuron* **106**, 743-758.e5 (2020).

281. Lima, L. B. *et al.* Afferent and efferent connections of the interpeduncular nucleus with special reference to circuits involving the habenula and raphe nuclei. *J. Comp. Neurol.* (2017). doi:10.1002/cne.24217

282. Qin, C. & Luo, M. Neurochemical phenotypes of the afferent and efferent projections of the mouse medial habenula. *Neuroscience* **161**, 827–837 (2009).

283. Koppensteiner, P., Galvin, C. & Ninan, I. Development- and experience-dependent plasticity in the dorsomedial habenula. *Mol. Cell. Neurosci.* (2016). doi:10.1016/j.mcn.2016.10.006

284. Palmiter, R. D. The Parabrachial Nucleus: CGRP Neurons Function as a General Alarm. *Trends in Neurosciences* (2018). doi:10.1016/j.tins.2018.03.007

285. Hashimoto, K., Obata, K. & Ogawa, H. Characterization of parabrachial subnuclei in mice with regard to salt tastants: Possible independence of taste relay from visceral processing. *Chem. Senses* (2009). doi:10.1093/chemse/bjn085

286. Ricardo, J. A. & Tongju Koh, E. Anatomical evidence of direct projections from the nucleus of the solitary tract to the hypothalamus, amygdala, and other forebrain structures in the rat. *Brain Res.* (1978). doi:10.1016/0006-8993(78)91125-3

287. Tokita, K., Inoue, T. & Boughter, J. D. Afferent connections of the parabrachial nucleus in C57BL/6J mice. *Neuroscience* (2009). doi:10.1016/j.neuroscience.2009.03.046

288. Norgren, R. & Leonard, C. M. Taste pathways in rat brainstem. *Science (80-.).* (1971). doi:10.1126/science.173.4002.1136

289. Norgren, R. Taste pathways to hypothalamus and amygdala. *J. Comp. Neurol.* (1976). doi:10.1002/cne.901660103

290. Herbert, H., Moga, M. M. & Saper, C. B. Connections of the parabrachial nucleus with the nucleus of the solitary tract and the medullary reticular formation in the rat. *J. Comp. Neurol.* (1990). doi:10.1002/cne.902930404

291. Wiberg, M. & Blomqvist, A. The spinomesencephalic tract in the cat: Its cells of origin and termination pattern as demonstrated by the intraaxonal transport method. *Brain Res.* (1984). doi:10.1016/0006-8993(84)90645-0

292. Cechetto, D. F., Standaert, D. G. & Saper, C. B. Spinal and trigeminal dorsal horn projections to the parabrachial nucleus in the rat. *J. Comp. Neurol.* (1985). doi:10.1002/cne.902400205

293. Gauriau, C. & Bernard, J. F. Pain pathways and parabrachial circuits in the rat. *Exp. Physiol.* (2002). doi:10.1113/eph8702357

294. Saper, C. B. & Loewy, A. D. Efferent connections of the parabrachial nucleus in the rat. *Brain Res.* (1980). doi:10.1016/0006-8993(80)91117-8

295. Bernard, J. -F, Alden, M. & Besson, J. -M. The organization of the efferent projections from the pontine parabrachial area to the amygdaloid complex: A

phaseolus vulgaris leucoagglutinin (PHA-L) study in the rat. *J. Comp. Neurol.* (1993). doi:10.1002/cne.903290205

296. Fulwiler, C. E. & Saper, C. B. Subnuclear organization of the efferent connections of the parabrachial nucleus in the rat. *Brain Research Reviews* (1984). doi:10.1016/0165-0173(84)90012-2

297. Gauriau, C. & Bernard, J. Nociceptors as Homeostatic Afferents : Central Processing Pain pathways and parabrachial circuits in the rat. *Exp. Physiol.* (2001).

298. Menendez, L., Bester, H., Besson, J. M. & Bernard, J. F. Parabrachial area: Electrophysiological evidence for an involvement in cold nociception. *J. Neurophysiol.* (1996). doi:10.1152/jn.1996.75.5.2099

299. Geran, L. C. & Travers, S. P. Bitter-responsive gustatory neurons in the rat parabrachial nucleus. *J. Neurophysiol.* (2009). doi:10.1152/jn.91168.2008

300. Bernard, J. F., Huang, G. F. & Besson, J. M. The parabrachial area: Electrophysiological evidence for an involvement in visceral nociceptive processes. *J. Neurophysiol.* (1994). doi:10.1152/jn.1994.71.5.1646

301. Barik, A., Thompson, J. H., Seltzer, M., Ghitani, N. & Chesler, A. T. A Brainstem-Spinal Circuit Controlling Nocifensive Behavior. *Neuron* **100**, 1491-1503 e3 (2018).

302. Brain, S. D., Williams, T. J., Tippins, J. R., Morris, H. R. & MacIntyre, I. Calcitonin gene-related peptide is a potent vasodilator. *Nature* (1985). doi:10.1038/313054a0

303. McCulloch, J., Uddman, R., Kingman, T. A. & Edvinsson, L. Calcitonin gene-related peptide: Functional role in cerebrovascular regulation. *Proc. Natl. Acad. Sci. U. S. A.* (1986). doi:10.1073/pnas.83.15.5731

304. Carter, M. E., Soden, M. E., Zweifel, L. S. & Palmiter, R. D. Genetic identification of a neural circuit that suppresses appetite. *Nature* (2013). doi:10.1038/nature12596

305. Campos, C. A., Bowen, A. J., Schwartz, M. W. & Palmiter, R. D. Parabrachial CGRP Neurons Control Meal Termination. *Cell Metab.* (2016). doi:10.1016/j.cmet.2016.04.006

306. Mumphrey, M. B. *et al.* Eating in mice with gastric bypass surgery causes exaggerated activation of brainstem anorexia circuit. *Int. J. Obes.* (2016). doi:10.1038/ijo.2016.38

307. Schauer, P. R. *et al.* Bariatric surgery versus intensive medical therapy for diabetes - 3-Year outcomes. *N. Engl. J. Med.* (2014). doi:10.1056/NEJMoa1401329

308. Evers, S. S., Sandoval, D. A. & Seeley, R. J. The Physiology and Molecular Underpinnings of the Effects of Bariatric Surgery on Obesity and Diabetes. *Annu. Rev. Physiol.* (2017). doi:10.1146/annurev-physiol-022516-034423

309. Reilly, S. The parabrachial nucleus and conditioned taste aversion. *Brain Research Bulletin* (1999). doi:10.1016/S0361-9230(98)00173-7

310. Lin, J. Y., Arthurs, J. & Reilly, S. Conditioned taste aversions: From poisons to pain to drugs of abuse. *Psychon. Bull. Rev.* (2017). doi:10.3758/s13423-016-1092-8

311. Carter, M. E., Han, S. & Palmiter, R. D. Parabrachial calcitonin gene-related peptide neurons mediate conditioned taste aversion. *J. Neurosci.* (2015). doi:10.1523/JNEUROSCI.3729-14.2015

312. Porporato, P. E. Understanding cachexia as a cancer metabolism syndrome. *Oncogenesis* (2016). doi:10.1038/oncsis.2016.3

313. Campos, C. A. *et al.* Cancer-induced anorexia and malaise are mediated by CGRP neurons in the parabrachial nucleus. *Nat. Neurosci.* (2017). doi:10.1038/nn.4574

314. Johansen, J. P., Cain, C. K., Ostroff, L. E. & Ledoux, J. E. Molecular mechanisms of fear learning and memory. *Cell* (2011). doi:10.1016/j.cell.2011.10.009

315. Han, S., Soleiman, M., Soden, M., Zweifel, L. & Palmiter, R. D. Elucidating an Affective Pain Circuit that Creates a Threat Memory. *Cell* (2015). doi:10.1016/j.cell.2015.05.057

316. Campos, C. A., Bowen, A. J., Roman, C. W. & Palmiter, R. D. Encoding of danger by parabrachial CGRP neurons. *Nature* (2018). doi:10.1038/nature25511

317. Han, L. *et al.* A subpopulation of nociceptors specifically linked to itch. *Nat. Neurosci.* (2013). doi:10.1038/nn.3289

318. Mu, D. *et al.* A central neural circuit for itch sensation. *Science (80-.).* (2017). doi:10.1126/science.aaf4918

319. Berquin, P., Bodineau, L., Gros, F. & Larnicol, N. Brainstem and hypothalamic areas involved in respiratory chemoreflexes: A Fos study in adult rats. *Brain Res.* (2000). doi:10.1016/S0006-8993(99)02304-5

320. Guyenet, P. G. & Bayliss, D. A. Neural Control of Breathing and CO2 Homeostasis. *Neuron* (2015). doi:10.1016/j.neuron.2015.08.001

321. Illing, R. B., Michler, S. A., Kraus, K. S. & Laszig, R. Transcription factor modulation and expression in the rat auditory brainstem following electrical intracochlear

stimulation. *Exp. Neurol.* (2002). doi:10.1006/exnr.2002.7895

322. Suzuki, T., Sugiyama, Y. & Yates, B. J. Integrative responses of neurons in parabrachial nuclei to a nauseogenic gastrointestinal stimulus and vestibular stimulation in vertical planes. *Am. J. Physiol. - Regul. Integr. Comp. Physiol.* (2012). doi:10.1152/ajpregu.00680.2011

323. Travers, J. Gustatory Neural Processing In The Hindbrain. *Annu. Rev. Neurosci.* (1987). doi:10.1146/annurev.neuro.10.1.595

324. Ryan, P. J., Ross, S. I., Campos, C. A., Derkach, V. A. & Palmiter, R. D. Oxytocin-receptor-expressing neurons in the parabrachial nucleus regulate fluid intake. *Nat Neurosci* **20**, 1722–1733 (2017).

325. Gimpl, G. & Fahrenholz, F. The oxytocin receptor system: Structure, function, and regulation. *Physiological Reviews* (2001). doi:10.1152/physrev.2001.81.2.629

326. Geerling, J. C. *et al.* Genetic identity of thermosensory relay neurons in the lateral parabrachial nucleus. *Am. J. Physiol. - Regul. Integr. Comp. Physiol.* (2016). doi:10.1152/ajpregu.00094.2015

327. Chavkin, C., Shoemaker, W. J., McGinty, J. F., Bayon, A. & Bloom, F. E. Characterization of the prodynorphin and proenkephalin neuropeptide systems in rat hippocampus. *J. Neurosci.* (1985). doi:10.1523/jneurosci.05-03-00808.1985

328. Morrison, S. F. Central neural control of thermoregulation and brown adipose tissue. *Autonomic Neuroscience: Basic and Clinical* (2016). doi:10.1016/j.autneu.2016.02.010

329. Kim, D. Y. *et al.* A neural circuit mechanism for mechanosensory feedback control of ingestion. *Nature* (2020). doi:10.1038/s41586-020-2167-2

330. Chiang, M. C. *et al.* Divergent Neural Pathways Emanating from the Lateral Parabrachial Nucleus Mediate Distinct Components of the Pain Response. *Neuron* **106**, 927-939.e5 (2020).

331. Fan, W., Boston, B. A., Kesterson, R. A., Hruby, V. J. & Cone, R. D. Role of melanocortlnergic neurons in feeding and the agouti obesity syndrome. *Nature* (1997). doi:10.1038/385165a0

332. Huszar, D. *et al.* Targeted disruption of the melanocortin-4 receptor results in obesity in mice. *Cell* (1997). doi:10.1016/S0092-8674(00)81865-6

333. Van der Ploeg, L. H. T. *et al.* A role for the melanocortin 4 receptor in sexual function. *Proc. Natl. Acad. Sci. U. S. A.* (2002). doi:10.1073/pnas.172378699

334. Rogers, J. H. Calretinin: A gene for a novel calcium-binding protein expressed principally in neurons. *J. Cell Biol.* (1987). doi:10.1083/jcb.105.3.1343

335. Camp, A. J. & Wijesinghe, R. Calretinin: Modulator of neuronal excitability. *International Journal of Biochemistry and Cell Biology* (2009). doi:10.1016/j.biocel.2009.05.007

336. Garfield, A. S. *et al.* A parabrachial-hypothalamic cholecystokinin neurocircuit controls counterregulatory responses to hypoglycemia. *Cell Metab.* (2014). doi:10.1016/j.cmet.2014.11.006

337. Roman, C. W., Derkach, V. A. & Palmiter, R. D. Genetically and functionally defined NTS to PBN brain circuits mediating anorexia. *Nat. Commun.* (2016). doi:10.1038/ncomms11905

338. Chamberlin, N. L. & Saper, C. B. Topographic organization of cardiovascular responses to electrical and glutamate microstimulation of the parabrachial nucleus in the rat. *J. Comp. Neurol.* (1992). doi:10.1002/cne.903260207

339. Madry, C. *et al.* Principal role of NR3 subunits in NR1/NR3 excitatory glycine receptor function. *Biochem. Biophys. Res. Commun.* (2007). doi:10.1016/j.bbrc.2006.12.153

340. Auberson, Y. P. *et al.* N-phosphonoalkyl-5-aminomethylquinoxaline-2,3-diones: In vivo active AMPA and NMDA(glycine) antagonists. *Bioorganic Med. Chem. Lett.* (1999). doi:10.1016/S0960-894X(98)00720-3

341. Schiller, J. *et al.* A Designer AAV Variant Permits Efficient Retrograde Access to Projection Neurons. *Neuron* (2016). doi:10.1016/j.neuron.2016.09.021

342. Campos, C. A. *et al.* Cancer-induced anorexia and malaise are mediated by CGRP neurons in the parabrachial nucleus. *Nat Neurosci* **20**, 934–942 (2017).

343. Ryan, P. J., Ross, S. I., Campos, C. A., Derkach, V. A. & Palmiter, R. D. Oxytocin-receptor-expressing neurons in the parabrachial nucleus regulate fluid intake. *Nat. Neurosci.* (2017). doi:10.1038/s41593-017-0014-z

344. Campos, C. A., Bowen, A. J., Roman, C. W. & Palmiter, R. D. Encoding of danger by parabrachial CGRP neurons. *Nature* **555**, 617–622 (2018).

345. Krashes, M. J. *et al.* An excitatory paraventricular nucleus to AgRP neuron circuit that drives hunger. *Nature* **507**, 238–242 (2014).

346. Cone, R. D. Anatomy and regulation of the central melanocortin system. *Nature Neuroscience* (2005). doi:10.1038/nn1455

347. Wirth, M. M., Olszewski, P. K., Yu, C., Levine, A. S. & Giraudo, S. Q. Paraventricular hypothalamic α-melanocyte-stimulating hormone and MTII reduce feeding without causing aversive effects. *Peptides* (2001). doi:10.1016/S0196-9781(00)00367-3

348. Garfield, A. S. *et al.* A neural basis for melanocortin-4 receptor-regulated appetite. *Nat. Neurosci.* **18**, 863–871 (2015).

349. Barik, A., Thompson, J. H., Seltzer, M., Ghitani, N. & Chesler, A. T. A Brainstem-Spinal Circuit Controlling Nocifensive Behavior. *Neuron* (2018). doi:10.1016/j.neuron.2018.10.037

350. Cherubini, E., Gaiarsa, J. L. & Ben-Ari, Y. GABA: an excitatory transmitter in early postnatal life. *Trends Neurosci.* **14**, 515–519 (1991).

351. Darcq, E. *et al.* RSK2 signaling in brain habenula contributes to place aversion learning. *Learn. Mem.* (2011). doi:10.1101/lm.2221011

352. Hamilton, N. B. & Attwell, D. Do astrocytes really exocytose neurotransmitters? *Nat. Rev. Neurosci.* **11**, 227–238 (2010).

353. Supplisson, S. & Roux, M. J. Why glycine transporters have different stoichiometries. *FEBS Lett.* **529**, 93–101 (2002).

354. Franklin, G. M., Dudzinski, D. S. & Cutler, R. W. Amino acid transport into the cerebrospinal fluid of the rat. *J Neurochem* **24**, 367–372 (1975).

355. Lin, J. Y., Knutsen, P. M., Muller, A., Kleinfeld, D. & Tsien, R. Y. ReaChR: A red-shifted variant of channelrhodopsin enables deep transcranial optogenetic excitation. *Nat. Neurosci.* **16**, 1499–1508 (2013).

356. Melkonian, M. *et al.* Independent optical excitation of distinct neural populations. *Nat. Methods* (2014). doi:10.1038/nmeth.2836

357. Pigeat, R., Chausson, P., Dreyfus, F. M., Leresche, N. & Lambert, R. C. Sleep slow wave-related homo and heterosynaptic ltd of intrathalamic GABAAergic synapses: Involvement of T-type ca2+channels and metabotropic glutamate receptors. *J. Neurosci.* **35**, 64–73 (2015).

358. Krout, K. E., Belzer, R. E. & Loewy, A. D. Brainstem projections to midline and intralaminar thalamic nuclei of the rat. *J Comp Neurol* **448**, 53–101 (2002).

359. Chiang, M. C. *et al.* Parabrachial Complex: A Hub for Pain and Aversion. *J. Neurosci.* **39**, 8225–8230 (2019).

360. Wu, Q., Clark, M. S. & Palmiter, R. D. Deciphering a neuronal circuit that mediates appetite. *Nature* **483**, 594–597 (2012).

361. Fu, O. *et al.* SatB2-Expressing Neurons in the Parabrachial Nucleus Encode Sweet Taste. *Cell Rep.* **27**, 1650-1656.e4 (2019).

362. Deng, J. *et al.* Article The Parabrachial Nucleus Directly Channels Spinal Nociceptive Signals to the Intralaminar Thalamic Nuclei , but Not the Amygdala Article The Parabrachial Nucleus Directly Channels Spinal Nociceptive Signals to the Intralaminar Thalamic Nuclei , bu. 1–15 (2020). doi:10.1016/j.neuron.2020.06.017

363. Krashes, M. J., Lowell, B. B. & Garfield, A. S. Melanocortin-4 receptor-regulated energy homeostasis. *Nat. Neurosci.* **19**, 206–219 (2016).

364. Kühnen, P., Krude, H. & Biebermann, H. Melanocortin-4 Receptor Signalling: Importance for Weight Regulation and Obesity Treatment. *Trends Mol. Med.* **25**, 136–148 (2019).

365. Shah, B. P. *et al.* MC4R-expressing glutamatergic neurons in the paraventricular hypothalamus regulate feeding and are synaptically connected to the parabrachial nucleus. *Proc. Natl. Acad. Sci. U. S. A.* **111**, 13193–13198 (2014).

366. Henson, M. A., Roberts, A. C., Pérez-Otaño, I. & Philpot, B. D. Influence of the NR3A subunit on NMDA receptor functions. *Progress in Neurobiology* (2010). doi:10.1016/j.pneurobio.2010.01.004

367. Tong, G. *et al.* Modulation of NMDA receptor properties and synaptic transmission by the NR3A subunit in mouse hippocampal and cerebrocortical neurons. *J. Neurophysiol.* (2008). doi:10.1152/jn.01044.2006

ABSTRACT

NMDA receptors (NMDARs) are fundamental glutamate-gated ion channels of the central nervous system. The best characterized, and most common, form of NMDARs in the brain is represented by tetrameric complexes composed by two obligatory GluN1 subunits that bind the co-agonists glycine and D-serine, and by two GluN2 subunits binding the agonist glutamate. The biophysical and physiological properties of these conventional NMDARs have been extensively investigated in the last decades, and the mechanisms that allow them to play critical roles in neuronal (patho)physiological events are largely identified.

The NMDAR subunit family, however, comprise a third group, the glycine-binding GluN3 subunits GluN3A and GluN3B. GluN3 subunits contribute to the formation of two distinct NMDAR flavors. First, GluN3A/B receptors can constitute diheteromeric GluN1/GluN3 NMDARs that are activated by glycine and that are totally insensitive to glutamate. On the other hand, GluN3 subunits can generate glutamate-sensitive triheteromeric NMDARs with GluN1 and GluN2 subunits (GluN1/GluN2/GluN3Rs), which possess largely different properties from those of GluN1/GluN2Rs, namely weak block by extracellular Mg^{2+} at hyperpolarized potentials, smaller single channel conductance and reduced permeability to Ca^{2+}.

The physiology of GluN3 subunits has been largely neglected with respect to that of conventional GluN1 and GluN2. GluN3B is present in limited areas of the caudal nervous system. In contrast, the expression of GluN3A is ubiquitous in the brain, but it is assumed to sharply decrease, if not to totally disappear, after the first postnatal weeks. Therefore, its identification in neurons has so far been limited to the juvenile brain, where triheteromeric GluN1/GluN2/GluN3ARs were shown to play an important role in synaptic maturation processes and in the emergence of synaptic plasticity phenomena. On the other hand, before the onset of my thesis GluN1/GluN3ARs had never been identified in native cells probably because of their peculiar activation properties, and had been examined exclusively in recombinant systems. Their functional expression in the adult brain remained debated.

During my thesis, on the basis of novel immunohistological evidence on GluN3A expression in the adult brain, I examined in detail the presence of this unconventional NMDAR subunit in native neurons.

I first identified a unique drug compound, CGP78608, that dramatically potentiates GluN1/GluN3AR currents obtained in response to glycine applications by modifying their activation dynamics. This pharmacological tool allowed me to show that GluN1/GluN3ARs are functional in several brain nuclei, comprising for example the adult Medial and the Lateral Habenula (MHb and LHb), the adult midline and intralaminar nuclei of the thalamus and the juvenile hippocampus, where I demonstrated for the first time the presence of the receptors in native neurons. Importantly, I also contributed to a study illustrating the importance of GluN1/GluN3ARs in the adult MHb for the development of the associations between negatively valued external events and aversive emotional states.

Concerning triheteromeric GluN1/GluN2/GluN3ARs, I could demonstrate that the receptors are functional in the paraventricular nucleus of the adult midline thalamus (PVT). Exploring several brain regions presynaptic to the PVT, I could show that inputs originating from the parabrachial nucleus (PB)

activate the triheteromeric receptors synaptically. A key information relay between the periphery and the anterior brain, the PB mainly hosts glutamatergic cells that show remarkably heterogeneous projections patterns and physiological implications. Among several cell sub-groups examined using viral strategies in transgenic mouse models, I finally identified the projections from neurons expressing the protein calbindin 2 (calb2, or calretinin) and the melanocortin receptors 4 as physiological activators of the receptors. These data demonstrate that not only GluN1/GluN2/GluN3A NMDARs are functional in the adult brain, but also that their expression is tightly regulated, thus suggesting very specific physiological implications.

In conclusion, my experimental work led to a radical shift in our perception of how GluN3A subunits are expressed in the brain and opens new hypotheses on how they can contribute to the activity of neural circuits.

In view of my results, the conventionally assumed notion that this subunit is uniquely expressed at early developmental stages and, thus, that its physiological functions are mainly restricted to control of synaptic maturation processes, must be revisited and expanded. From now on, GluN3A subunit-containing NMDARs will have to be considered as integral components of the molecular machinery that mediates information transfer in the brain, and understanding how the specificity of their properties affects neurons will be an important task for obtaining comprehensive clarification of circuital functions.

RESUME

Les récepteurs NMDA (NMDARs) forment une classe de récepteurs-canaux membranaires activés par le glutamate, le principal neurotransmetteur excitateur du système nerveux central des vertébrés. Ces canaux ioniques perméables au calcium sont nécessaires à l'initiation de diverses formes de plasticité synaptique et sont impliqués dans diverses pathologies dont les attaques cérébrales, les douleurs chroniques et la schizophrénie. Les NMDAR conventionnels, exprimés de manière ubiquitaire dans le cerveau, sont généralement constitués de 4 sous-unités, 2 GluN1 qui lient la glycine et 2 GluN2 qui lient le glutamate. Leurs propriétés biophysiques et physiologiques, ainsi que leur rôles physio(patho)logiques (et les mécanismes mis en jeu) ont été largement étudiés.

En revanche, nous disposons de très peu d'information sur la 3ème famille des NMDARs, la famille GluN, liant la glycine et comprenant deux sous-unités, GluN3A et GluN3B. GluNA/B peuvent former deux types distincts de NMDARs. D'une part, GluN3A/B peuvent s'associer à GluN1 pour former des récepteurs dihétéromériques (GluN1/GluN3Rs) activés par la glycine seule et insensibles au glutamate. D'autre part, les sous-unités GluN3 peuvent s'associer à GluN1 et GluN2 de façon à générer des récepteurs trihétéromériques (GluN1/GluN2/GluN3Rs) qui répondent à la fois à la glycine et au glutamate mais avec des propriétés altérées par rapport aux récepteurs GluN1/GluN2 classiques, à savoir une réduction du bloc par le magnésium extracellulaire à des potentiels hyperpolarisés, une faible conductance et une perméabilité au calcium réduite.

Contrairement aux GluN1 et GluN2 classiques, de nombreux aspects sur la physiologie des sous-unités GluN3 demeurent insaisissables. Les sous-unités GluN3 affichent des profils ontogénétiques différents. L'expression de GluN3B augmente lentement tout au long du développement, mais est limitée à des régions particulières du système nerveux central. A l'inverse, bien que GluN3A s'exprime de façon ubiquitaire dans le cerveau, il est supposé que son expression est limitée uniquement à la vie postnatale précoce ; elle diminue ensuite fortement jusqu'à disparaître à l'âge adulte. Conformément à son profil d'expression, GluN3A a été uniquement identifiée dans des neurones du cerveau juvénile, où l'expression des récepteurs trihétéromeriques semble jouer un rôle important dans la maturation des synapses au cours du développement précoce du cerveau, et la mise en place de phénomènes de plasticité synaptique. Par contre, avant le début de ma thèse, et probablement en raison de leurs propriétés d'activation très particulières, les récepteurs dihétéromériques GluN1/GluN3A n'avaient jamais été observés dans des neurones natifs; leur étude limitée aux systèmes recombinants, les GluN1/GluN3A soulevaient des doutes quant à leur expression fonctionnelle dans le cerveau adulte.

Durant mon doctorat, de nouvelles données immunohistochimiques, montrant une forte expression de GluN3A dans le cerveau **adulte**, ont permis de remettre en cause le dogme de la fenêtre temportelle limitée de l'expression de cette sous-unité. En me basant sur ces données, j'ai donc examiné en détail la présence de GluN3A dans des neurones natifs. J'ai d'abord identifié un antagoniste très puissant de GluN1, la CGP78608, qui potentialise considérablement les courants des GluN1/GluN3ARs, obtenus en réponse à des applications brèves de glycine. Grâce à cet outil pharmacologique, j'ai pu révéler, pour la première fois, la présence de récepteurs dihétéromériques GluN1/GluN3A fonctionnels dans des neurones natifs, plus spécifiquement dans l'hippocampe juvénile. J'ai également pu dévoiler la présence

de GluN1/GluN3ARs fonctionnels dans d'autres structures cérébrales, à noter l'Habenula Médiale (MHb) et Latérale (LHb) de l'épithalamus adulte, ainsi que les noyaux intralaminaires et les noyaux de la ligne médiane du thalamus adulte. Surtout, j'ai contribué à une étude illustrant l'importance des GluN1/GluN3ARs de la MHb adulte dans le développement des associations entre la perception négative d'événements externes et des états émotionnels aversifs.

Par rapport aux récepteurs trihétéromeriques GluN1/GluN2/GluN3A, j'ai pu montré que ces récepteurs sont présents et fonctionnels dans le noyau paraventriculaire du thalamus (PVT) de souris adultes. En explorant plusieurs régions qui projettent vers le PVT, j'ai pu, dans un premier temps, montré que les entrées du noyau parabrachial (PB) du tronc activent les GluN1/GluN2/GluN3AR à la synapse avec le PVT. Point relais critique entre la périphérie et le cerveau antérieure, le PB héberge majoritairement des cellules glutamatergiques qui présentent une hétérogénéité cellulaire remarquable quant à leurs patrons de projections et implications physiologiques.

En utilisant des approches virales et des modèles de souris transgéniques, j'ai pu identifier que les cellules du PB exprimant la proteine calrétinine (Calb2), ainsi que celles exprimant les récepteurs de la mélanocortine 4 (MC4R) activent physiologiquement les GluN1/GluN2/GluN3A à la synapse avec le PVT, contrairement à d'autres sous-populations cellulaires de PB que j'ai examinées. Ces données montrent que les GluN1/GluN2/GluN3ARs sont non seulement fonctionnels dans le cerveau adulte, mais également que leur expression est très fortement régulée, suggérant désormais leurs implications dans des rôles physiologiques spécifiques.

En conclusion, mes données expérimentales, défiant nos anciennes conceptions sur GluN3A, ont mené à un changement radical dans notre perception concernant l'expression de cette sous-unité dans le cerveau, et ont ouvert de nouvelles hypothèses sur leur contribution à l'activité des circuits neuronaux.

Au vu de mes résultats, il est impératif que les notions conventionnelles, qui supposaient que cette sous-unité est uniquement exprimée aux stades précoces du développement, et qui limitaient par conséquent ses fonctions physiologiques à la maturation synaptique durant les stades précoces de développement, soient largement révisées et améliorées. Il faut désormais considérer les récepteurs NMDA incorporant la sous-unité GluN3A comme des composants intégraux de la machinerie moléculaire, servant de médiateur dans le transfert d'informations dans le cerveau; comprendre comment leurs propriétés spécifiques affectent les neurones sera une tâche importante pour arriver finalement à éclaircir et approfondir les fonctions circuits.

nature COMMUNICATIONS

ARTICLE

DOI: 10.1038/s41467-018-07236-4 OPEN

Unmasking GluN1/GluN3A excitatory glycine NMDA receptors

Teddy Grand[1], Sarah Abi Gerges[2], Mélissa David[1], Marco A. Diana[2] & Pierre Paoletti[1]

GluN3A and GluN3B are glycine-binding subunits belonging to the NMDA receptor (NMDAR) family that can assemble with the GluN1 subunit to form unconventional receptors activated by glycine alone. Functional characterization of GluN1/GluN3 NMDARs has been difficult. Here, we uncover two modalities that have transformative properties on GluN1/GluN3A receptors. First, we identify a compound, CGP-78608, which greatly enhances GluN1/GluN3A responses, converting small and rapidly desensitizing currents into large and stable responses. Second, we show that an endogenous GluN3A disulfide bond endows GluN1/GluN3A receptors with distinct redox modulation, profoundly affecting agonist sensitivity and gating kinetics. Under reducing conditions, ambient glycine is sufficient to generate tonic receptor activation. Finally, using CGP-78608 on P8-P12 mouse hippocampal slices, we demonstrate that excitatory glycine GluN1/GluN3A NMDARs are functionally expressed in native neurons, at least in the juvenile brain. Our work opens new perspectives on the exploration of excitatory glycine receptors in brain function and development.

[1] Institut de Biologie de l'Ecole Normale Supérieure (IBENS), Ecole Normale Supérieure, Université PSL, CNRS, INSERM, F-75005 Paris, France. [2] Institut de Biologie Paris-Seine (IBPS) Sorbonne Université, CNRS, INSERM, Neurosciences Paris-Seine (NPS), UPMC Université Paris 06, F-75005 Paris, France. These authors contributed equally: Teddy Grand, Sarah Abi Gerges. These authors jointly supervised this work: Marco A. Diana, Pierre Paoletti. Correspondence and requests for materials should be addressed to M.A.D. (email: marco.diana@upmc.fr) or to P.P. (email: pierre.paoletti@ens.fr)

NMDARs are tetrameric ligand-gated ion channels that serve critical roles in CNS development and function. Normal NMDAR activity is essential for neuronal plasticity and information storage, while NMDAR dysfunction contributes to various CNS disorders including epilepsy, mental retardation, and schizophrenia[1–3]. Conventional NMDARs composed of two GluN1 and two GluN2 subunits require two agonists, glutamate and glycine (or D-serine), for activation[4]. They are highly permeable to Ca^{2+}, exhibit strong voltage-dependency due to Mg^{2+} pore block, and cluster at excitatory synapses where they control synaptic strength by acting as coincidence detectors[5]. The functional diversity and signaling properties of GluN1/GluN2 NMDARs have been extensively characterized during the last 30 years, providing a wealth of information on the molecular basis of excitatory neurotransmission.

Much less is known regarding NMDARs incorporating the two glycine-binding subunits GluN3A and GluN3B, cloned in 1995 and 2001, respectively[6–10]. The general architecture of GluN3 subunits is globally similar to that of GluN1-2 subunits, yet the two families differ by the conspicuous presence of a positive charge in the pore-lining sequence of GluN3, and by the unique structural determinants of the GluN3 glycine-binding site[11,12]. GluN3A and GluN3B subunits also display differential ontogenic profiles. GluN3A is widely expressed in the CNS during early postnatal life and participates in synapse maturation[13–15], before progressively declining in abundance[16]. Conversely, GluN3B expression slowly increases throughout development, albeit remaining restricted to defined CNS regions (e.g. motoneurones[10,17]). GluN3-containing NMDARs are either glutamate/glycine-activated triheteromeric receptors composed of GluN1, GluN2, and GluN3 subunits or glycine-activated diheteromeric receptors composed of GluN1 and GluN3 subunits[18–20]. Both assemblies form cationic channels with strongly reduced Ca^{2+} permeability and Mg^{2+}-block compared to GluN1/GluN2 receptors. Surprisingly, while the GluN3 subunit appears to act as a dominant negative regulator in triheteromeric GluN1/GluN2/GluN3 receptors[21,22], in GluN1/GluN3 diheteromers, the GluN3 subunit has a primary role in receptor activation[10,23,24].

Unconventional glycine-activated GluN1/GluN3 NMDARs have sparked intense curiosity and controversy. First, they constitute a new type of glycine excitatory receptor, since glycine is well established as an inhibitory neurotransmitter in the spinal cord and brainstem[25–27]. Second, they have so far been mostly described in recombinant systems with only sparse evidence for their existence in vivo[28]. Glycine currents produced by unconventional GluN1/GluN3 receptors are small, unstable and difficult to quantify[10,23,24,29–31], complicating the study of these receptors. Third, GluN1/GluN3 receptor pharmacology is meager. Antagonists with good potency and selectivity are missing, while available potentiators do not alter the transient nature of GluN1/GluN3 responses and usually produce complex biphasic effects[23,24,32–34]. In this study, we show that the quinoxalinedione CGP-78608, known to antagonize GluN1/GluN2 receptors[35], acts as an ultra-potent and powerful potentiator of GluN1/GluN3A receptors. The effects produced are unprecedented in their extent with potentiation factors much greater than previously observed with other GluN1-binding molecules. Building on this discovery, we also show that GluN1/GluN3A receptors can alternate between two modes of agonist sensitivity in a redox-dependent manner. In the high-affinity mode, ambient glycine is sufficient to tonically activate the receptors. Lastly, capitalizing on the discovery of the CGP-78608 as a massive enhancer of GluN1/GluN3A receptors, we identify excitatory glycine GluN1/GluN3A receptors as a new type of neuronal receptors, being functionally expressed in the juvenile brain. This work has broad ranging implications for the study of GluN1/GluN3A receptors and of glycine as an excitatory neurotransmitter.

Results

CGP-78608 awakens GluN1/GluN3A receptors. Diheteromeric GluN1/GluN3 receptors display peculiar activation properties with no equivalent in the NMDAR family. In particular, contrasting with GluN1/GluN2 complexes, glutamate is dispensable for their activation[10]. Moreover, while glycine binding to GluN3 subunits triggers channel opening, glycine binding to the neighboring GluN1 subunits has an opposite effect causing autoinhibition by rapid entry into a non-conducting desensitized state. Accordingly, receptors carrying single-point mutations that prevent glycine binding to GluN1 show large and non-desensitizing glycine-activated currents[23,24,30,33]. Taking advantage of these unique gating properties, we sought to find a small molecule compound able to antagonize glycine binding to GluN1 but not to GluN3A. Several GluN1-preferring ligands have already been shown to potentiate GluN1/GluN3 currents[23,24], yet none achieves high level of potentiation together with current stability during prolonged agonist application. Our attention focused on CGP-78608, a NMDAR GluN1 competitive antagonist[35] which, according to radiolabeled binding studies on isolated agonist-binding domains (ABDs), displays a thousand-fold selectivity for GluN1 vs GluN3[11]. We expressed diheteromeric GluN1/GluN3A receptors in HEK293 cells and studied their activity using whole-cell patch-clamp recordings coupled to a fast perfusion system. Application of glycine alone (100 µM) elicited very small (few tens of pA) and rapidly desensitizing currents (Fig. 1a), as previously described[30,31,34]. Pre-application of CGP-78608 (500 nM) dramatically enhanced the glycine-induced currents, which reached several nA in amplitude, and greatly reduced desensitization (Fig. 1a). Overall, peak and steady-state currents were potentiated 128 ± 24 fold (range 50–296; $n = 11$), and 335 ± 266 fold (range 106–876; $n = 11$), respectively (Fig. 1a). Concomitantly, the extent of desensitization was strongly decreased (I_{ss}/I_{peak} increased from 0.30 ± 0.03 [$n = 8$] to 0.80 ± 0.03 [$n = 5$]; $P < 0.001$, Student's t-test) and desensitization kinetics slowed considerably (τ_{des} increased from 81 ± 13 ms [$n = 8$] to 1642 ± 183 ms [$n = 5$]; $P < 0.001$, Student's t-test). A full dose-response curve (Fig. 1b) revealed that CGP-78608 was extremely potent as a potentiator of GluN1/GluN3A-mediated glycine currents, with an estimated EC_{50} in the low nM range (26.3 ± 5.0 nM [$n =$ 4–11]; measured at peak current), closely matching the value found on the isolated GluN1 ABD (6.4 nM; ref. [11]). In line with a classical bimolecular drug-receptor interaction, the effects of CGP-78608 were fully reversible (Supplementary Figure 1a). Furthermore, introduction of the GluN1-F484A mutation to prevent ligand binding to the GluN1 subunit[23,24] almost completely abolished the potentiating effects of CGP-78608 (Fig. 1d and Supplementary Figure 1b), consistent with CGP-78608 binding to GluN1 ABDs of GluN1/GluN3 receptors as it does on conventional GluN1/GluN2 receptors. Unsurprisingly, the amplitudes of glycine-triggered currents carried by GluN1-F484A/GluN3A receptors were much larger than those of wild-type GluN1/GluN3A receptors (Supplementary Figure 1b), confirming the inhibitory role on receptor activation of glycine binding to GluN1.

We obtained further evidence that CGP-78608 produces uniquely large potentiating effects on GluN1/GluN3A receptors by systematic comparison with other GluN1 competitive antagonists previously tested on these receptors[23,24,30]: MDL-29951, the kynurenic acid derivative 7-CKA, and L-689560. Similar to previous experiments, GluN1 competitive antagonists were first pre-incubated before triggering receptor activation by

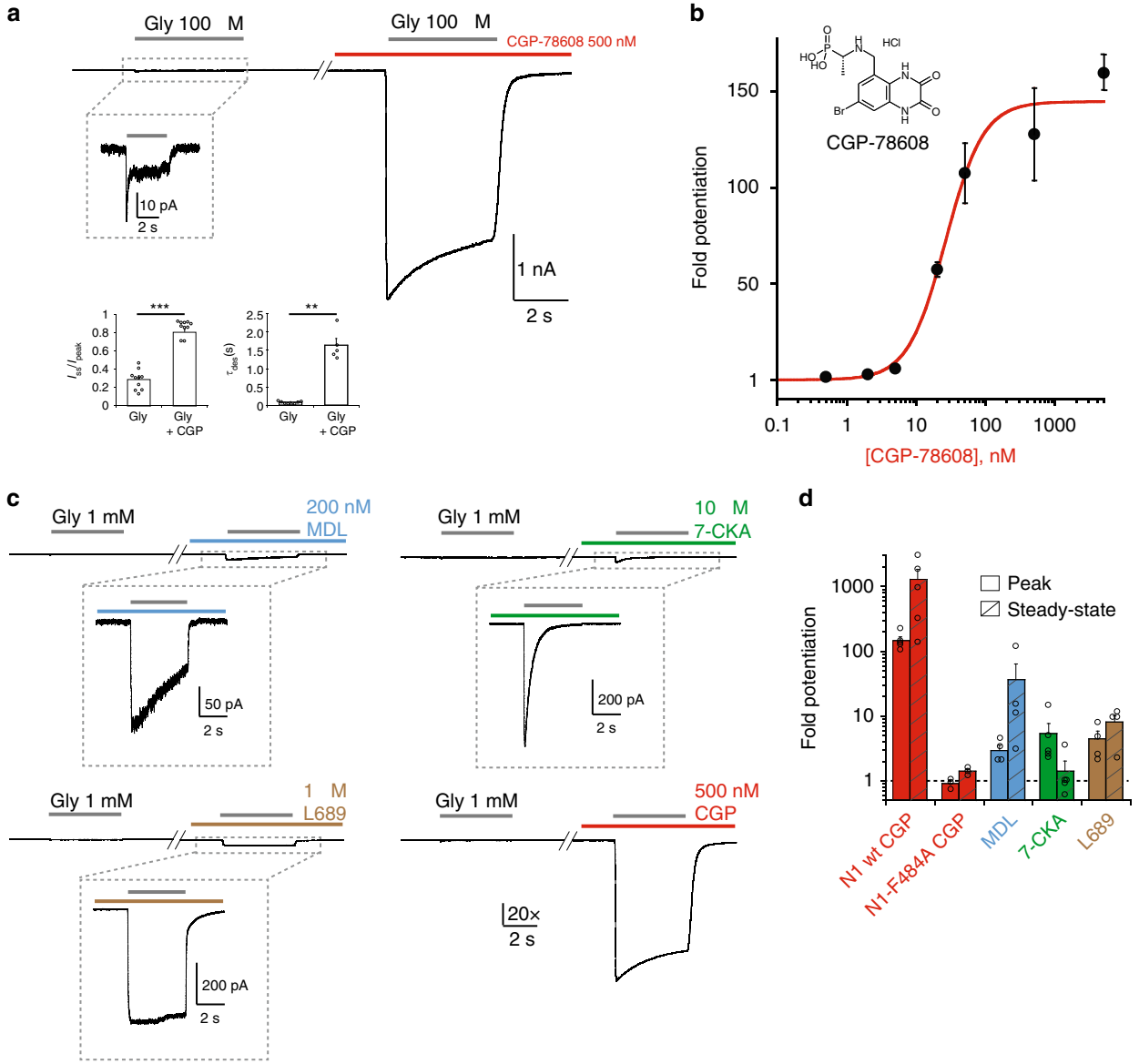

Fig. 1 The GluN1 antagonist CGP-78608 awakes GluN1/GluN3A receptors. **a** Pre-application of CGP-78608 massively potentiates excitatory glycine GluN1/GluN3A receptor responses. Bar graphs indicate effect on extent (I_{ss}/I_{peak}) and kinetics (τ_{des}) of desensitization. $^{***}P < 0.001$, Student's *t*-test, ($n = 10$); $^{**}P = 0.002$, Mann–Whitney test ($n = 10$). **b** CGP-78608 potentiation dose-response curve obtained in presence of 100 μM glycine. Currents were measured at the peak. $EC_{50} = 26.3 \pm 5$ nM, $n_H = 1.45$ ($n = 4$–11). **c** Representative current traces showing the relative potentiation of various GluN1 antagonists compared to CGP-78608. Traces are normalized to the glycine-induced peak currents obtained prior to drug application. **d** Quantification of effects of GluN1 antagonists tested in **c** on peak and steady-state current levels ($n = 4$-6). N1-F484A refers to the GluN1-F484A mutant subunit. All recordings were performed in HEK293 cells. Data are mean ± SEM

applying additional glycine (1 mM). The concentration of each compound was set above its reported GluN1 binding affinity (Ki; see Methods) to insure sufficient binding site occupancy. As illustrated in Fig. 1c, all three compounds potentiated GluN1/GluN3A receptors, yet their effects were singularly less prominent than those produced by CGP-78608. Thus, while CGP-78608 (500 nM) potentiated peak and steady-state currents by >100-fold ($n = 5$) and >1000-fold ($n = 5$), respectively, corresponding values were orders of magnitude lower for MDL-29951, 7-CKA, and L-689560 (Fig. 1d). Strikingly, for these three latter compounds, the magnitude of potentiation and the impact on the shape of the glycine currents differed significantly. 7-CKA produced the largest peak potentiation but desensitization remained profound with little current remaining at steady-state. In contrast, MDL-29951, and to a lesser extent L-689560, greatly enhanced steady-state currents such that glycine responses were measurable during long agonist applications. These different patterns likely relate to the complex interplay between glycine and compound molecules for binding GluN1 and GluN3A subunits (see Discussion). Importantly, though, none of these three drugs produced effects comparable to CGP-78608, considering both the extent of peak and steady-state current potentiation. In agreement with its very high potency (i.e. low EC_{50}), washout experiments revealed slow offset kinetics of CGP-78608 from GluN1/GluN3A receptors, with dissociation time constants in the tens of seconds time scale (both from the active or resting state of the receptor; τ_{off} of 27.6 ± 6.3 s [$n = 6$] and 22.5 ± 4.2 s [$n = 4$], respectively; Fig. 2a). By inverting the order of application between CGP-78608 and glycine, we also found the CGP-78608 potentiation to be strongly state-dependent. Indeed,

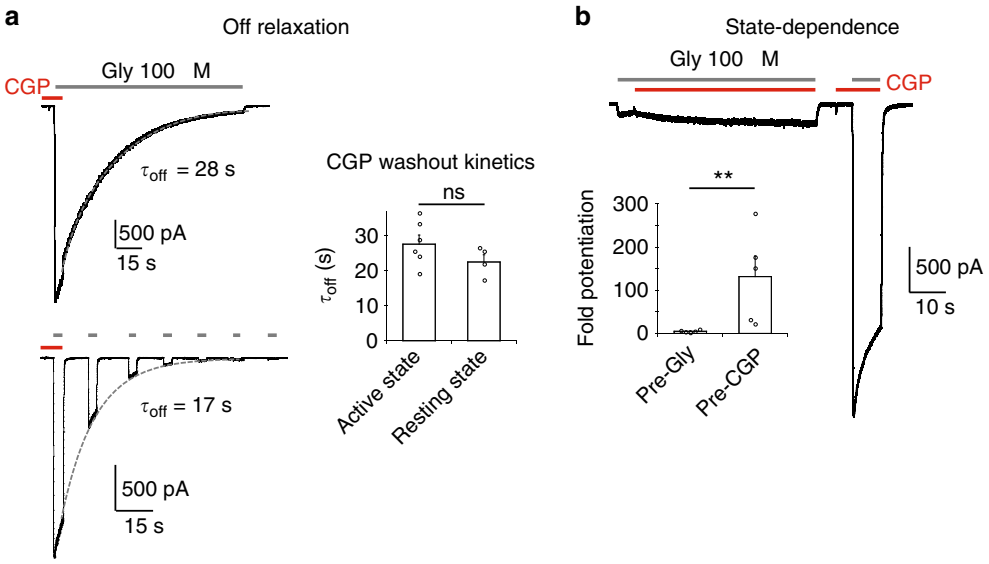

Fig. 2 Kinetics and activity-dependence of CGP-78608 potentiation at GluN1/GluN3A receptors. **a** CGP-78608 washout kinetics in the presence of continuous or pulses of glycine. CGP-78608 was applied at 500 nM. Bar graph: comparison of the CGP-78608 washout kinetics in the active (upper trace) or resting state (lower trace). n.s. $P = 0.198$, Student's *t*-test; ($n = 4$-6). **b** CGP-78608 potentiation is state-dependent. Potentiation by CGP-78608 (500 nM) is greatly reduced when the compound is applied after, rather than before, application of glycine (pre-Gly *vs* post-Gly, respectively). Bar graph: potentiation measured at steady-state. $^{**}P = 0.008$, Mann–Whitney test, ($n = 5$). Data are mean ± SEM

only minimal potentiation was observed on receptors pre-occupied with glycine, while CGP-78608 application before glycine still induced massive effects on the very same receptor population (Fig. 2b). This pre vs post pattern likely finds its origin in the relative affinities of GluN1 and GluN3 ABDs for glycine and CGP-78608 while the receptor transits along the activation pathway (from resting, to active and desensitized states; see Discussion). Using CGP-78608, we also confirmed that D-serine (up to 500 µM) triggered currents of smaller amplitude than those elicited by glycine (100 µM) (Supplementary Figure 1c), in agreement with D-serine having lower efficacy than glycine at GluN1/GluN3A receptors. Finally, we found all salient effects of CGP-78608 (current potentiation, reduction of desensitization, state-dependence) described in HEK293 cells to be conserved in *Xenopus* oocytes, highlighting the robustness of the CGP-78608 effects regardless of the expression system. In many oocytes, application of CGP-78608 unveiled massive glycine-induced currents (several µA), while prior applications of glycine alone on the very same cells virtually produced no detectable currents (Supplementary Figure 1d,e). These results provide additional proof that the compound CGP-78608 is unprecedented in its effects on excitatory glycine GluN1/GluN3A NMDARs. They also reveal that GluN1/GluN3A receptors, despite the small currents recorded when applying glycine only, express at very high levels in heterologous expression systems.

To better assess the activation parameters of GluN1/GluN3A receptors, we next performed glycine concentration-response curves in the presence or absence of CGP-78608. In control conditions, GluN1/GluN3A receptors displayed low µM glycine sensitivity ($EC_{50} = 7.1 \pm 0.4$ µM [$n = 5$–15], peak responses; Supplementary Figure 2a), in agreement with previous estimates[23,24]. In the presence of CGP-78608 (500 nM), in conditions where current responses are several orders of magnitude larger, glycine sensitivity was moderately decreased ($EC_{50} = 39 \pm 0.8$ µM [$n = 6$]; Supplementary Figure 2b). This ~5-fold rightward shift in agonist sensitivity may be due either to a direct competition between glycine and CGP-78608 binding to GluN3A ABD sites, or to an indirect (i.e. allosteric) effect of CGP-78608 binding at GluN1 ABD sites onto GluN3A ABD glycine sites. To distinguish between these two possibilities, we repeated the concentration-response curve experiment with a 10-fold lower CGP-78608 concentration (50 nM). Under such condition, glycine EC_{50} (40 ± 0.8 µM; [$n = 9$]) is almost identical to that measured with 500 nM CGP-78608 (Supplementary Figure 2c). This result strongly suggests that CGP-78608 decreases glycine sensitivity of GluN1/GluN3A receptors through an inter-subunit allosteric effect between GluN1 and GluN3A ABD sites.

Redox treatment transforms GluN1/GluN3A receptor properties. Conventional GluN1/GluN2 NMDARs display a well-characterized redox sensitivity mediated by two critical GluN1 cysteine residues (C744 and C798) forming a disulfide bond, which increases the magnitude of NMDAR-evoked responses when chemically reduced[36–38]. Redox modulation is thought to provide an important regulatory mechanism of NMDAR signaling during normal and diseased brain function[39–43]. Because the redox sensitivity of GluN1/GluN3 receptors remains uncharacterized, we decided to investigate the effects of reducing treatments on glycine responses mediated by GluN1/GluN3A receptors. Recordings from HEK293 cells treated with the reducing agent TCEP (5 mM, 20 min) revealed drastic effects on GluN1/GluN3A glycine-evoked responses (Fig. 3b, c). The most conspicuous effect concerned the shape of the responses. First, when glycine was applied, peak currents from reduced GluN1/GluN3A receptors desensitized to a steady-state current that was more positive than the baseline holding current. Second, upon washout of glycine, very large and slowly decaying tail (or rebound) currents appeared. The size of the peak current induced by glycine application was also greatly increased following TCEP treatment. With the aim of identifying the molecular determinants underlying these effects, we first recorded from GluN1/GluN3A receptors lacking the endogenous GluN1 disulfide bridge responsible for the redox sensitivity of conventional GluN1/GluN2 NMDARs. Despite enhanced current amplitude prior to TCEP treatment, GluN1-C744S-C798S/GluN3A receptor currents remained remarkably sensitive to reduction, displaying the striking shape transformation observed on wild-type GluN1/

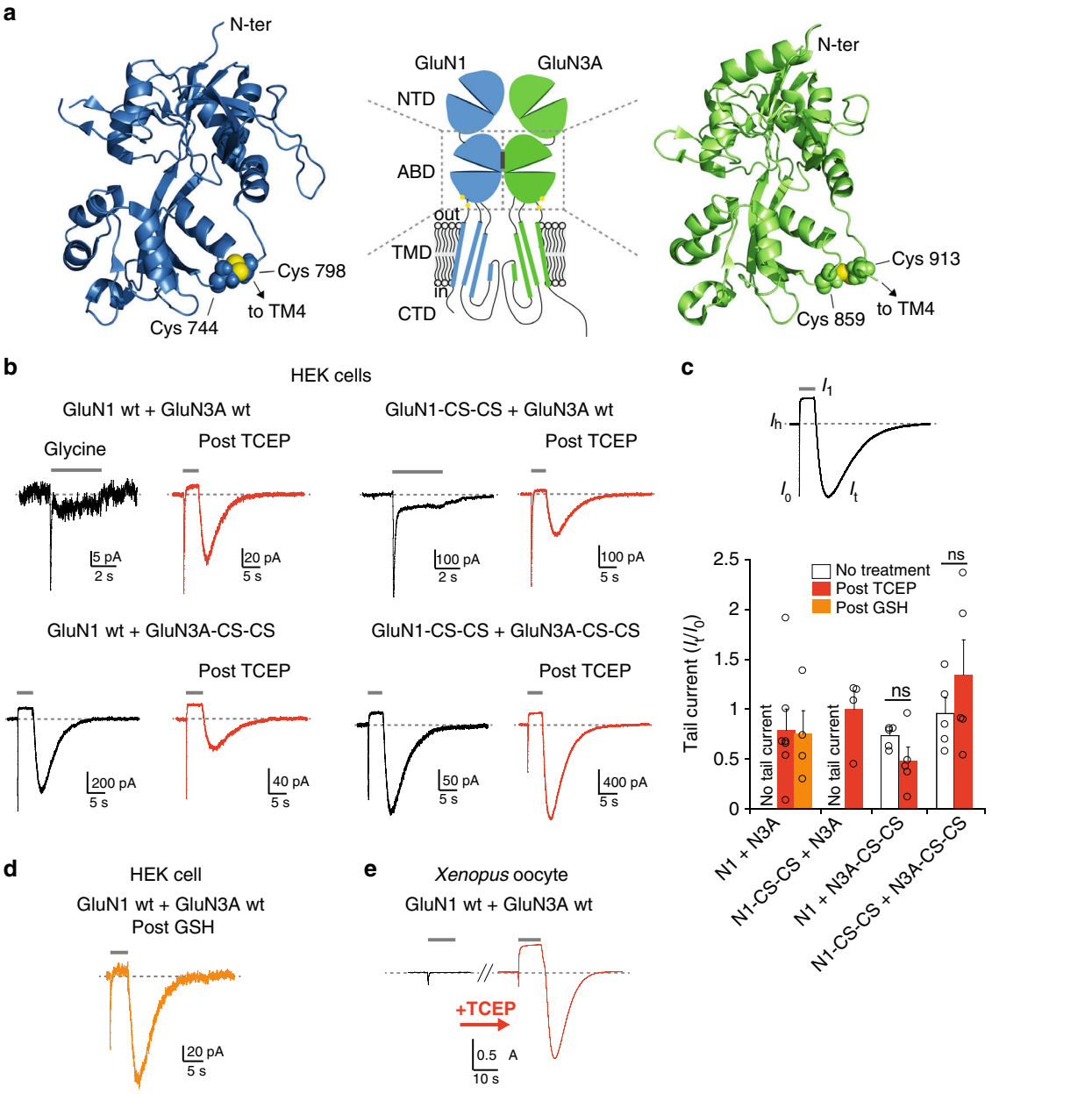

Fig. 3 GluN1/GluN3A receptors display strong redox sensitivity. **a** Structure of the GluN1 and GluN3A ABDs (PDB 4KCC and 4KCD, respectively[55]). Cysteines involved in endogenous redox-sensitive disulfide bridges are highlighted (sulfur atoms shown in yellow). The central cartoon illustrates domain organization in GluN1/GluN3A receptors; NTD, N-terminal domain; ABD, agonist-binding domain; TMD, transmembrane domain; CTD, C-terminal domain. **b** Effect of TCEP treatment (5 mM, 20 min) on wild-type and mutant GluN1/GluN3A receptors expressed in HEK 293 cells. Glycine was applied at 100 µM. Each trace comes from a separate cell. **c** Quantification of tail currents observed upon washout of glycine on wild-type and mutant GluN1/GluN3A receptors. Inset indicates current tags used for quantification. n.s. $P = 0.125$ and 0.337, Student's t-test ($n = 4$–9). Note that non-treated receptors containing wild-type GluN3A subunits do not exhibit tail currents. Data are mean ± SEM. **d** Effect of reduced glutathione (GSH, 50 mM for 20 min) on wild-type GluN1/GluN3A receptors expressed in HEK293 cells. Glycine was applied at 100 µM. **e** Effect of TCEP treatment (5 mM, 20 min) on wild-type GluN1/GluN3A receptors expressed in *Xenopus* oocytes. The pair of current traces corresponds to responses before and after TCEP treatment on the same cell. Glycine was applied at 100 µM

GluN3A receptors (Fig. 3b, c). A critical component of the redox sensitivity of GluN1/GluN3A receptors is therefore independent of the endogenous GluN1-C744-C798 disulfide bridge. Because a homologous disulfide bridge involving C859 and C913 is present in GluN3A[11] (Fig. 3a), we next recorded from mutant GluN1/GluN3A-C859S-C913S receptors. Distinct features emerged (Fig. 3b, c): first, the TCEP sensitivity (on current shape) was lost; second, the current responses in basal conditions (i.e. prior to TCEP treatment) were remarkably similar in shape to those of reduced currents from wild-type receptors. Similar effects - absence of TCEP sensitivity, current shape transformation - were also present on receptors with the disulfide bonds mutated on both subunits (GluN1-C744S-C798S/GluN3A-C859S-C913S; Fig. 3b, c). Finally, we tested the endogenous reducing agent glutathione (GSH) on wild-type GluN1/GluN3A receptors. Similar to TCEP treatment, GSH incubation completely modified the current phenotype, with the appearance of an outward shifted steady-state current and large rebound currents upon removal of

glycine (Fig. 3c, d). Overall, these results show that GluN1/GluN3A receptors are highly redox sensitive, with activation properties that can adopt two strikingly different patterns depending on the redox state. They also identify the endogenous GluN3A ABD C859-C913 disulfide bridge as a key molecular determinant of this redox modulation.

We then turned to *Xenopus* oocytes to better estimate the relative contribution of the GluN1 and GluN3A subunits to the redox sensitivity of GluN1/GluN3A receptors. Indeed, we observed that oocytes better tolerated redox treatment than HEK293 cells, thus allowing robust comparison of currents from the same cell before and after reduction. When applying the reducing agent TCEP to wild-type GluN1/GluN3A receptors, currents radically changed, reproducing faithfully the effects previously observed on HEK293 cells. In particular, reduced receptors exhibited massive rebound currents upon washout of glycine, with much larger peak amplitudes than before TCEP treatment, and slow deactivation kinetics requiring tens of seconds for full recovery (Fig. 3e). Similar effects were observed when using the reducing agent DTE instead of TCEP (Supplementary Figure 3a, b). In addition, following the initial peak current triggered by glycine application, currents stabilized to a steady-state level lower (i.e. reduced inward current) than that measured prior to glycine application (Fig. 3e and see below). Having confirmed the reproducibility of the redox effects in both expression systems, we next aimed at deciphering the specific contribution of each subunit to the redox modulation of GluN1/GluN3A receptors. For that purpose, we assessed the redox sensitivity of receptors expressed in oocytes and lacking either the GluN1-C744-C798 disulfide bridge, or the GluN3A-C859-C913 disulfide bridge, or both. Comparison of mutant receptors revealed a clear dichotomy (Supplementary Figure 3a, b), where the GluN1 disulfide bridge controls current amplitude yet has little effect on the current shape, while the GluN3 disulfide bridge is responsible for the radical change in both current shape and time course.

Tonic activation of reduced GluN1/GluN3A receptors. Given the opposing effects of GluN1 and GluN3A subunits on GluN1/GluN3A receptor activation[23,24], we hypothesized that breaking the GluN3A-C859S-C913S disulfide bond shifts GluN3A glycine sensitivity, but not that of GluN1, to much higher affinity. Rebound currents upon glycine washout would then occur following fast dissociation of glycine from (inhibitory) GluN1 sites while (activating) GluN3 sites are still occupied. We obtained direct evidence that glycine dissociation kinetics are greatly slowed following GluN3A disulfide bond disruption by performing off-relaxation experiments on CGP-78608-bound non-desensitizing receptors. In such conditions, relaxation kinetics following glycine removal were readily observable and quantified (Fig. 4a, b). Comparison of wild-type and mutant receptors revealed that glycine off-relaxations (τ_{off}) were only weakly affected when breaking the GluN1 disulfide bridge (442 ± 208 ms [$n = 5$] for GluN1-C744-C798/GluN3A receptors vs 205 ± 110 ms [$n = 7$] for wt receptors, $P = 0.027$, Student's t-test; Fig. 4b). In contrast, major effects were observed on receptors lacking the GluN3A bridge with glycine deactivation kinetics greatly slowed down (2217 ± 91 ms [$n = 4$] and 2098 ± 196 ms [$n = 5$] for GluN1/GluN3A-C859S-C913S and GluN1-C744S-C798S/GluN3A-C859S-C913S receptors, respectively; $P < 0.001$, Student's t-test comparison with wild-type or GluN1-C744-C798/GluN3A receptors; Fig. 4b). Interestingly, similarly slow time courses were measured for the decay kinetics of rebound currents (Supplementary Figure 3a, b), likely reflecting slow dissociation of glycine from GluN3A (see Discussion). Full glycine concentration-response curves performed in the presence of CGP-78608 confirmed that mutant receptors displayed enhanced agonist sensitivity compared to their wild-type counterparts (13-fold decrease in glycine EC_{50}; Supplementary Figure 2d). Taken together, these results show that the endogenous GluN3A-C859-C913 disulfide bridge plays a major role in controlling glycine sensitivity of GluN1/GluN3A receptors. It does so by governing the residency time of glycine on its GluN3A ABD binding site.

We hypothesized that another consequence of the greatly enhanced glycine sensitivity of reduced GluN1/GluN3A receptors are outward shifted steady-state currents (see Fig. 3 and Supplementary Figure 3). The observation that agonist-induced steady-state currents are smaller than resting currents (measured prior to agonist application) is very unusual and may originate from combined effects of receptor desensitization and tonic activation. Accordingly, prior to glycine application, a fraction of reduced GluN1/GluN3 receptors would be constitutively activated by ambient glycine (estimated at 40–50 nM in recording solutions[44–46]). Following application of high glycine concentrations, more receptors activate, accounting for the fast inward peak current. Subsequently, however, desensitization would take over progressively accumulating all (or the vast majority of) receptors into a long-lasting inactive state, hence accounting for the apparent outward shift in steady-state current level. As illustrated in Fig. 4c, outward current shifts (represented as down bars) were directly and specifically controlled by the redox state of the GluN3A-C859-C913 disulfide bridge, paralleling the effects seen on the rebound currents. To better identify the nature of the constitutive currents recorded in the absence of added glycine, we used CNQX, an antagonist of GluN1/GluN2 NMDARs and AMPA receptors, also known to inhibit GluN1/GluN3A receptors[23,28]. For cells expressing wild-type receptors, CNQX (50 µM) barely changed the holding current (outward current displacement of 0.6 ± 0.06 pA, [$n = 6$]; Fig. 4d), as expected if the receptors were not tonically active. In contrast, for cells expressing GluN1-CS-CS/GluN3A-CS-CS receptors, CNQX strongly affected the holding current, displacing its amplitude by 22.9 ± 8.3 pA, [$n = 7$] ($P = 0.032$ compared to WT, Student's t-test), thus indicating a significant level of constitutive receptor activation (Fig. 4d). As expected, CNQX also inhibited the large tail currents carried by mutant receptors following glycine removal (Fig. 4e). Altogether, these results indicate that according to their redox state, GluN1/GluN3A receptors can switch mode, with differential glycine sensitivity. A single endogenous disulfide bond, residing in the GluN3A ABD lower lobe (GluN3A-C859-C913), controls this functional switch. In receptors with this S–S bond unlocked, glycine concentrations as low as a few tens of nanomolar appear sufficient to permit GluN3A subunit occupation and receptor activation. This ultra-high glycine sensitivity is unprecedented for functional GluN1/GluN3A receptors. However, it echoes surprisingly well the 40.4 nM glycine affinity found by Yao and Mayer[11] using radiolabeled ligand assay on the isolated GluN3A ABD.

Functional GluN1/GluN3A receptors in the juvenile brain. The existence of functional glycine excitatory GluN1/GluN3A NMDARs has not been demonstrated in native neurons until present. In native conditions, similar to heterologous systems, glycine binding to GluN1 subunits may reduce currents to undetectable levels because of receptor desensitization. Given its properties on recombinant GluN1/GluN3A receptors, we foresaw that CGP-78608 would represent a powerful tool for revealing endogenous currents mediated by glycine excitatory GluN1/GluN3A receptors in native tissues. The GluN3A subunit is expressed at high levels and almost ubiquitously at early

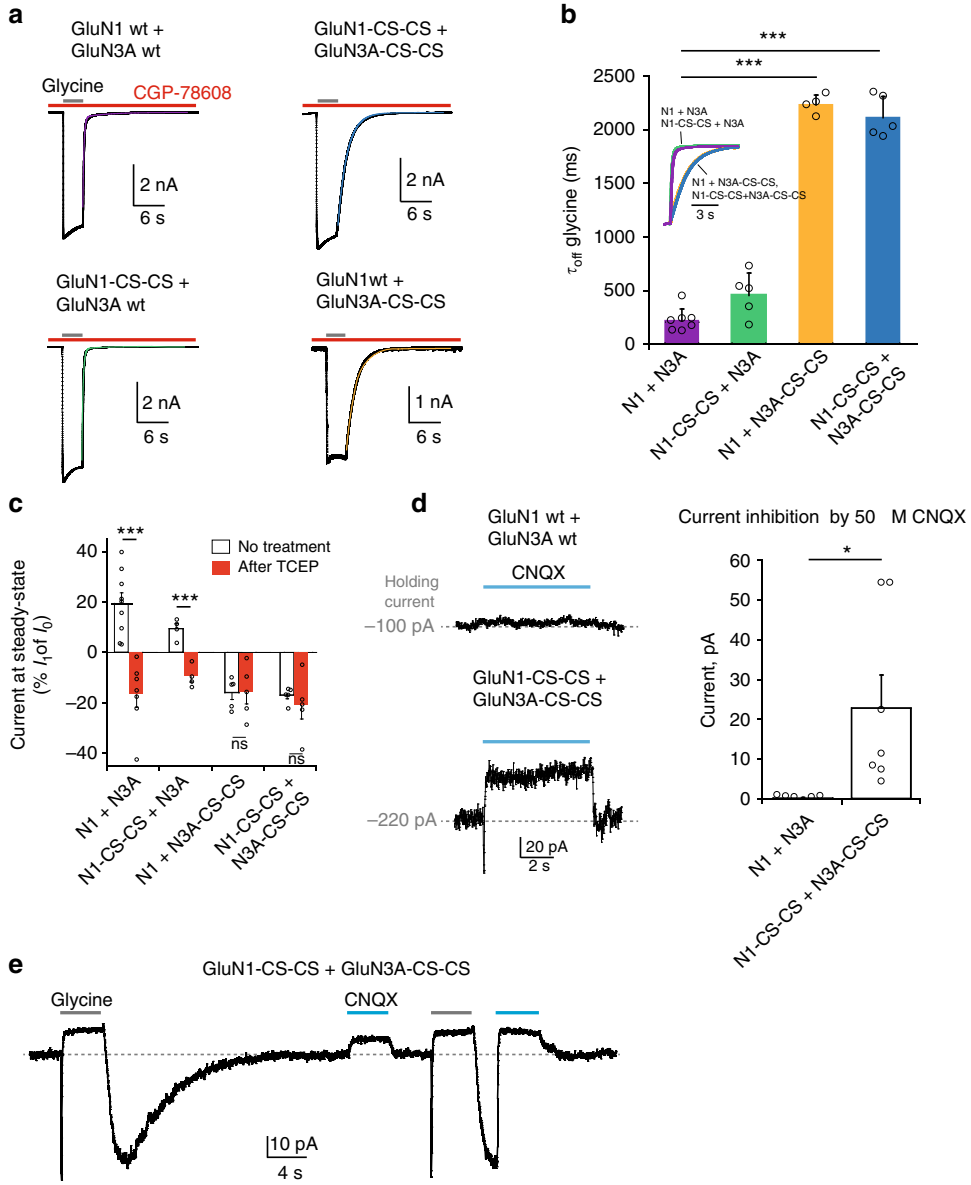

Fig. 4 High-glycine sensitivity and tonic activation of reduced GluN1/GluN3A receptors. **a** Glycine deactivation kinetics of wild-type and mutant receptors in presence of CGP-78608 (500 nM). Glycine was applied at 100 µM. **b** Quantification of glycine deactivation kinetics. *$P = 0.027$, Student's *t*-test; ***$P < 0.001$, Student's *t*-test ($n = 4$–7). Inset: representative current traces and overlaid fits following glycine washout. **c** Quantification of glycine-induced steady-state outward current shifts following TCEP treatment (see Text). Currents at steady-state (I_1) are expressed as percentage of I_0 current (see Fig. 2c). ***$P < 0.001$, Student's *t*-test; n.s. $P = 0.95$ and 0.49, respectively, Student's *t*-test; ($n = 4$–9). **d** Effect of CNQX (50 µM) on the holding current (current measured in the absence of glycine) for both wild-type and mutant GluN1-CS-CS/GluN3A-CS-CS receptors. **e** Effect of CNQX (50 µM) on basal and glycine-induced currents carried by GluN1-CS-CS/GluN3A-CS-CS mutant receptors. Note the strong inhibition by CNQX of the tail current (rebound current following glycine removal). Glycine was applied at 100 µM. All recordings were performed in HEK293 cells. Data are mean ± SEM

developmental stages[16,18,20]. We thus explored the ex vivo presence of functional GluN1/GluN3A heterodimers in the hippocampal CA1 region of juvenile mouse slices (P8-P12). We examined the effects of bath applications of CGP-78608 on currents activated by glycine (10 mM) puffed onto voltage-clamped CA1 pyramidal cells (Fig. 5a). To avoid potential activation of inhibitory glycine receptors, these experiments were performed in a cocktail of neurotransmitter receptor inhibitors including the inhibitory glycine receptor inhibitor strychnine (see Methods). In control conditions, glycine induced very small inward currents in both wild-type and GluN3A-knock-out[13] (GluN3A-KO) mice (mean amplitude: 9.3 ± 1.4 pA [$n = 10$] vs 6.0 ± 0.8 pA [$n = 11$], respectively; Fig. 5b, c). Not significantly different ($P = 0.3$; Mann–Whitney test), these currents are likely due, at least in part, to mechanical artefacts triggered by puffing near the recording electrode.

Bath application of CGP-78608 (1 µM) produced dramatically different effects in WT and GluN3A-KO mice. In wild-type mice, CGP-78608 massively amplified the glycine-induced inward currents to 190.1 ± 58.3 pA ($n = 10$; range: 16.8–640.6 pA; $P = 0.007$ vs control puffs, Wilcoxon signed-rank test), whereas it had no significant effect on currents triggered in GluN3A-lacking animals (mean amplitude of 5.0 ± 0.6 pA [$n = 17$]; $P = 0.9$ vs control puffs in GluN3A-KO animals; $P = 0.00001$ with respect to currents obtained in the presence of CGP-78608 in WT mice; Mann–Whitney test; Fig. 5b, c). Finally, in wild-type mice bath

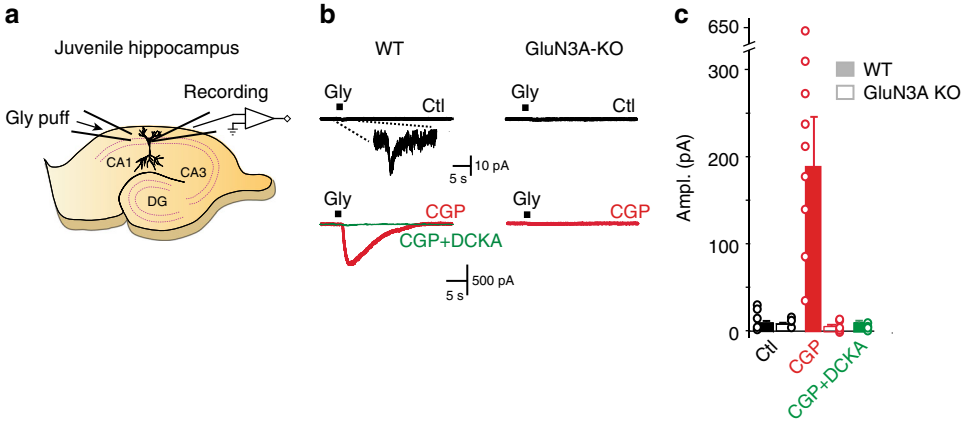

Fig. 5 GluN1/GluN3A receptors are expressed and functional in juvenile hippocampal slices. **a** Schematic representation of the experimental protocol. Glycine (10 mM) is puffed onto voltage-clamped CA1 cells in acute hippocampal slices from young (P8-12) mice. **b** In control conditions, glycine puffs trigger very small inward currents in both wild-type (WT) and GluN3A-KO mice (upper black traces on both left and right). A typical response obtained in WT mice is shown at larger magnification and time scale in the top left inset. Bath application of CGP-78608 (CGP) leads to massive potentiation of glycine-elicited currents in WT mice, but has no effect in GluN3A-KO animals (bottom red traces). In WT mice, addition of DCKA (500 µM), a GluN1 and GluN3A glycine-binding site antagonist, eliminates currents obtained in the presence of CGP-78608 (bottom left green trace), thus further confirming that GluN1/GluN3A receptors mediate the responses to glycine. **c** Quantification of the experimental results obtained in panel **b**. WT mice, full bars; GluN3A-KO mice, empty bars. Data are illustrated as mean ± SEM

application of DCKA (500 µM), a dual GluN1 and GluN3 glycine-binding site antagonist[10,24], almost fully abolished the currents obtained in the presence of CGP-78608 (10.2 ± 2.7 pA [$n = 9$]; $P = 0.001$; Mann–Whitney test). Altogether, these results provide the first demonstration that glycine excitatory GluN1/GluN3A receptors are expressed and functional in juvenile neurons. Moreover, they highlight the power of CGP-78608 as a new tool compound for detecting GluN1/GluN3A receptor conductances in native systems.

Discussion

In many aspects, the functional properties and physiological relevance of excitatory glycine GluN1/GluN3 NMDARs remain a conundrum. Here, we provide novel information on the activation, modulation, and pharmacology of GluN1/GluN3A receptors, as well as on their expression in native neurons. We identify a small molecule compound that massively potentiates and extensively transforms GluN1/GluN3A receptor responses. Moreover, we show that GluN1/GluN3A receptors can switch between two distinct modes of activation with very different agonist responsiveness and kinetics, in a redox-dependent manner. We identify an endogenous GluN3A disulfide bridge, as the main molecular actor responsible for this functional plasticity. Finally, we demonstrate that glycine excitatory GluN1/GluN3A receptors can indeed be expressed and be functional in native systems. Hence, these receptors are not just artefacts of heterologous expression systems. Our work thus transforms our current understanding of these underappreciated receptors, and clarifies the long-standing doubts concerning their presence in brain neurons. By providing new ways to manipulate and interrogate GluN1/GluN3A receptors, our work should also facilitate the search for their physiological function.

Building on the differential contribution of the GluN1 and GluN3A subunits to GluN1/GluN3A receptor activation, we discovered that the GluN1 antagonist CGP-78608 acts as a highly potent and powerful potentiator of GluN1/GluN3A receptors. The extent of current potentiation produced by this compound - several orders of magnitude - greatly exceeds effects previously reported by other GluN1 glycine-binding site antagonists. Moreover, CGP-78608 profoundly transformed the time course of GluN1/GluN3A responses, rendering them much less transient. The enhanced peak amplitude together with the enhanced response stability results in a striking awakening phenotype consisting in a massive overall increase in charge transfer, uncommon in receptor pharmacology. Indeed, many positive allosteric modulators enhance current amplitude without major impact on current time course[47]. Alternatively, drugs can drastically change current shape while having virtually no effect on peak current amplitude, as observed with cyclothiazide on AMPA receptors[48]. The uniqueness of CGP-78608 likely stems from the atypical mechanism of GluN1/GluN3A receptor activation where the same molecule, glycine, serves both as an agonist and a functional antagonist[23,24]. With its high selectivity for GluN1 over GluN3A ABD[11], we suggest that CGP-78608 prevents glycine antagonist effects at GluN1 ABD sites while interfering minimally with the glycine agonist effects at GluN3 ABD sites. In an attempt to formalize this, and other modulatory and gating reactions observed at GluN1/GluN3A receptors, a simple schematic model is proposed (Fig. 6). In this scheme, GluN1/GluN3A receptors can adopt four discrete states along the activation pathway: one resting and one active state, and two desensitized states (Fig. 6a). Upon glycine application, two events resulting in two separate effects occur: receptor activation (i.e. pore opening) by glycine binding to GluN3 sites; receptor inhibition (i.e. entry into desensitized states) following glycine binding to GluN1 sites. These effects can occur either concurrently or sequentially, because GluN3A sites have higher glycine affinity than GluN1 sites[11]. Therefore, exposure to high glycine concentrations leads to small, transient, and rapidly desensitizing responses (Resting- > Active- > Des2; Fig. 6a). Pre-incubation of CGP-78608 prior to glycine application (Pre; Fig. 6b) locks the GluN1 ABD in the open clamshell conformation and prevents glycine binding to GluN1 (Fig. 6b). Little or no CGP-78608 binds to GluN3 given its strong preference for GluN1 (~1000-fold selectivity factor[11]). Following application of saturating glycine, all GluN3 sites are occupied and the receptors fully activate. Meanwhile, little displacement of CGP-78608 from GluN1 sites by glycine occurs, CGP-78608 having much higher affinity as manifested by its long residency time (τ_{off} in the second timescale, see Fig. 2). Hence, the receptors are stabilized in the active state and avoid desensitization, explaining the massive potentiation produced by CGP-

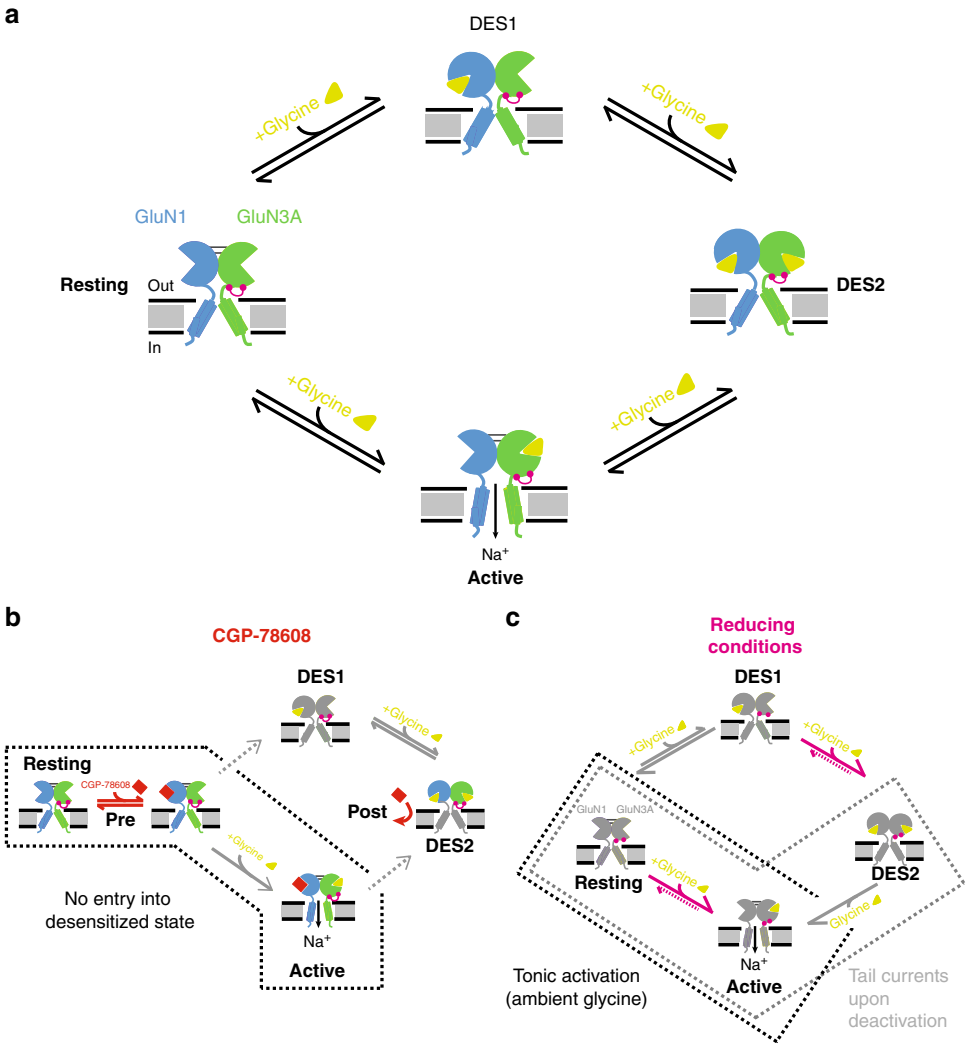

Fig. 6 Schematic model of GluN1/GluN3A activation and modulation. For clarity, a single GluN1/GluN3A dimer is shown and the NTDs omitted. The upper scheme (**a**) shows receptor activation in control conditions. The GluN3A disulfide bridge conferring high redox sensitivity is highlighted in pink. The lower left scheme (**b**) illustrates activation sequence in presence of CGP-78608. Pre indicates application of CGP-78608 before glycine application while Post indicates the opposite. Pre-incubation with CGP-78608 prior to glycine application enhances receptor activity by preventing glycine binding to GluN1 and subsequent entry into desensitized states. The lower right scheme (**c**) illustrates activation sequence of reduced receptors (GluN3A ABD lower lobe disulfide bridge broken). The main modification is a large increase in the affinity of the GluN3A ABD for glycine resulting in tonic receptor activation by ambient glycine

78608. A different scenario occurs when CGP-78608 is applied after glycine (Post; Fig. 6b). Glycine application shifts most of the receptors into a long-lived glycine-bound desensitized state that would adopt a conformation strongly diminishing CGP-78608 binding. Accordingly, little CGP-78608 potentiation is observed. Increased glycine affinity of GluN1 sites of desensitized receptors likely contributes to this strong state-dependence. Several GluN1/GluN2 modulators also show strong state-dependence (e.g. refs. [49,50]), highlighting the importance of receptor conformational landscape in NMDAR pharmacology. The much greater effects of CGP-78608 compared to other GluN1 antagonists (Fig. 1c, d) likely finds its origin from a unique combination of high potency/high selectivity of CGP-78608 for GluN1 ABD sites. The molecular basis of this unique pharmacological profile still remains to be understood. Binding studies on isolated domains indicate that L689650 discriminates between GluN1 and GluN3 ABDs even better than CGP-78608[11], yet functional effects of L689650 on full-length receptors are much smaller than those produced by CGP-78608 (Fig. 1c, d). The phosphonate group of CGP-78608, absent in other tested compounds, could make the difference with its specific chemistry (by stabilizing specific ABD/receptor conformations). Ultimately, structures of GluN3A-antagonist complexes should allow determining how CGP-78608 singles out from other GluN1 antagonists.

The robustness of GluN1/GluN3A receptor expression in heterologous systems has been questioned ever since the cloning of GluN3A. Several attempts failed to detect noticeable current responses following co-expression of GluN1 and GluN3A subunits, be it in *Xenopus* oocytes[7] or HEK cells[29,51]. In studies examining functional GluN1/GluN3 receptors[23,24,31,52], current responses in control conditions are most often small and transient, complicating their analysis. Our results show that glycine-triggered currents barely detectable in control conditions turn into large and sustained responses in the presence of CGP-78608. This demonstrates that excitatory glycine GluN1/GluN3A receptors express very robustly in heterologous systems, at levels comparable to those of GluN1/GluN2 NMDARs. Our redox experiments further establish that GluN1/GluN3A receptor

activability strongly depends on the receptor's microenvironment. We show that depending on the redox state, the receptor can adopt two radically different gating modes, resulting in different current size and shape. The variability in redox state between experimental settings could thus explain, at least in part, the inconsistency and heterogeneity of GluN1/GluN3A receptor responses previously reported in the literature.

Our redox and mutagenesis experiments reveal that a single endogenous disulfide bridge on the GluN3A subunit – GluN3A-C859-C913 - has major influence on the activation properties of GluN1/GluN3A receptors. This bridge acts as a redox-sensitive gating switch that controls the receptor's glycine affinity and gating kinetics. Under oxidizing conditions, when the two cysteines are cross-linked, the receptor displays a glycine sensitivity in the micromolar range, and a typical activation-desensitization-deactivation pattern upon application of high glycine concentrations. Under reducing conditions, when the disulfide bridge is broken, the gating pattern changes completely. The main modification is a large increase in the GluN3A ABD glycine affinity, estimated between one and two orders of magnitude, and manifested by extremely slow glycine dissociation kinetics from activating GluN3A sites. The enhancement in glycine affinity is such that low ambient glycine concentrations (in the nanomolar range) known to contaminate recording solutions[44–46] are sufficient to occupy high-affinity GluN3A sites (but not low-affinity GluN1 sites) and constitutively activate (a fraction of) GluN1/GluN3A receptors. When high glycine concentrations are applied, all receptors activate and then rapidly desensitize, accumulating in the Des2 state (Fig. 6c). This also concerns receptors activated prior to glycine application, which desensitize following glycine binding to unoccupied GluN1 sites, thus explaining the outward current shift observed in the steady-state. Upon its removal, glycine unbinds rapidly from (low-affinity) GluN1 sites but not from (high-affinity) GluN3A sites. Therefore, as they return to the resting state, receptors transit through the GluN3A-only bound state, the sole active state, accounting for the large tail currents. In such a scenario, tail current deactivation kinetics should closely match glycine dissociation kinetics. This is what is observed (Supplementary Figure 3). Unusual current phenotypes strikingly similar to those described here with constitutive activation, outward shifted steady-state currents and large tail currents have been recently described for kainate receptors harboring clinically-relevant mutations in their transmembrane region[53]. These effects are best explained by profoundly altered gating properties - exquisite sensitivity to ambient agonist (i.e. glutamate) and reopening of receptors as they recover from desensitization[53,54]—as we propose here for glycine excitatory GluN1/GluN3A receptors under reducing conditions. The GluN3A-C859-C913 disulfide bridge occupies a strategic location in GluN3A[12,55], connecting the ABD lower lobe to the TMD ion channel[56,57]. We speculate that its removal releases constraints on the GluN3A ABD clamshell, favoring domain closure, agonist (glycine) binding, and opening of the channel gate. A similar mechanism may also be at play at GluN1 subunits[58], although effects on receptor gating appear much more limited.

By disclosing novel gating and modulation properties of GluN1/GluN3A receptors, our work brings out several important points. First, these receptors are highly plastic in their functionality, capable of operating under various regimes (low/high agonist affinity; transient/persistent activity) according to their environment (redox state). Second, from a molecular and cellular perspective, GluN1/GluN3A receptors are not weakly expressing receptors; on the contrary, they express at high levels, although they appear to be strongly inhibited (or apt to be inhibited) in control conditions. This latter finding is particularly important on a physiological point of view. The function and identification of native excitatory glycine GluN1/GluN3A receptors have been pending for years. We now reveal that this is not due to a lack of expression but to problems in their detection. Using the GluN1-antagonist CGP-78608 as a novel tool compound to prevent receptor auto-inhibition by glycine, we now show that GluN1/GluN3A receptors are robustly expressed, and electrically functional, in neurons of the juvenile brain. Without the pharmacological assistance of CGP-78608, the GluN1/GluN3A current responses remain virtually undetectable, thus explaining the lack of information on their functional expression until now. Under normal conditions, the activity of excitatory glycine GluN1/GluN3A receptors may be particularly prone to desensitization, or operate under a low tonic regime, as described for persistent inhibitory GABA-A conductances[59]. Our discovery of the powerful awakening effect of CGP-78608 and of the redox switch of GluN1/GluN3A receptors opens new perspectives on the exploration of excitatory glycine receptors and their role in brain development and function.

Methods

Ethical statement. All procedures involving experimental animals were performed in accordance with the European directive 2010/63/EU on the Protection of Animals used for Scientific Purposes, the guidelines of the French Agriculture and Forestry Ministry for handling animals, and local ethics committee guidelines.

Molecular biology. The pcDNA3-based plasmid encoding the rat GluN1-4a subunit that was used throughout this work was a kind gift from John Woodward (Medical University of South Carolina, USA). The variant GluN1-4a (named GluN1 herein) was preferred to other GluN1 splice variants because of better assembly into functional diheteromeric GluN1/GluN3 receptors[30]. The pcI_NEO plasmid encoding the rat GluN3A subunit was a kind gift from Isabel Perez-Otaño (Universidad de Navarra, Spain). Site-directed mutagenesis and sequencing procedures were performed as previously described[60].

Two-electrode voltage-clamp recordings. Oocytes from *Xenopus lævis* (Xenopus Express, Rennes, France) were used for heterologous expression of recombinant GluN1/GluN3A receptors studied using two-electrode voltage-clamp (TEVC). TEVC recordings were performed 3–4 days following injection. Harvesting and preparation of oocytes was performed as previously described[60] and in the framework of project authorization #05137.02 as delivered by the French Ministry of Education and Research. Each oocyte was co-injected with a mixture of GluN1 and GluN3A cDNA at a concentration of 50 ng/µl and at a 1:1 ratio. The standard external solution contained (in mM): 100 NaCl, 2.5 KCl, 0.3 $BaCl_2$, 5 HEPES, 0.01 DTPA (diethylenetriamine-pentaacetic acid), pH 7.3. Treatments with the reducing agent DTE (dithioerythritol, 5 mM) were performed at room temperature during 15–20 min in a Barth solution. Recordings were performed at −60 mV and at room temperature. Currents were sampled at 100 Hz and low-pass filtered at 20 Hz using an Oocyte Clamp OC-725 amplifier and pClamp 10.5 (Molecular devices). Data analysis was performed using Clampfit 10.5 and Kaleidagraph4 (Synergy Software).

Whole-cell patch-clamp recordings in HEK cells. HEK293 cells were used for heterologous expression of recombinant GluN1/GluN3 receptors studied using whole-cell patch-clamp. Cells were obtained from ECACC (European Collection of Authenticated Cell Culture, catalog number: 96121229) and cultured under standard cell culture conditions (95/5% O_2/CO_2 mixture, 37 °C). Cells were transfected using polyethylenimine with GluN1, GluN3A and GFP plasmids at a 1:3:1 ratio (0.3, 0.9 and 0.3 ng/µl respectively). Recordings were performed 24–48 h following cell transfection. The extracellular solution contained (in mM): 140 NaCl, 2.8 KCl, 1 $CaCl_2$, 10 HEPES and 20 Sucrose (290–300 mOsm), pH adjusted to 7.3 using NaOH. The pipette solution contained (in mM): 115 CsF, 10 CsCl, 10 HEPES and 10 BAPTA (280–290 mOsm), pH adjusted to 7.2 using CsOH. Currents were sampled at 10 kHz and low-pass filtered at 2 kHz using an Axopatch 200B amplifier and Clampex 10.6. Drugs and agonists were applied using a multi-barrel solution exchanger (RSC 200; Bio-logic). Recordings were performed at −60 mV and at room temperature. In experiments with reducing agents, cells were pre-incubated in external solution with Tris(2-carboxyethyl)phosphine (TCEP, 5 mM) or reduced glutathione (GSH, 50 mM) during 20 min.

Whole-cell patch-clamp recordings in CA1 pyramidal cells. Ex-vivo electrophysiological experiments were performed on coronal slices from the brains of juvenile wild-type (WT) and GluN3A-KO mice originating from the same litters (8–12 days old). Slices were prepared as described previously[61]. Briefly, mice were anesthetized with isofluorane before decapitation. After isolation, the portion of the

brain containing the hippocampus was placed in bicarbonate-buffered saline (BBS) at 2–5 °C for a few minutes. Slices (300 µm) were then cut using a 7000 smz-2 vibratome (Campden). The slicing procedure was performed in an ice-cold solution containing (in mM): 130 K^+- gluconate, 15 KCl, 0.05 EGTA, 20 Hepes, 25 glucose, 1 $CaCl_2$, and 6 $MgCl_2$ supplemented with DL-APV (50 µM). Slices were then transferred for a few minutes to a solution containing (in mM): 225 D-mannitol, 2.5 KCl, 1.25 NaH_2PO_4, 25 $NaHCO_3$, 25 glucose, 1 $CaCl_2$, and 6 $MgCl_2$, and finally stored for the rest of the experimental day at 32–34 °C in oxygenated BBS, containing (in mM): 115 NaCl, 2.5 KCl, 1.6 $CaCl_2$, 1.5 $MgCl_2$, 1.25 NaH_2PO_4, 26 $NaHCO_3$, and 30 glucose (pH 7.4 after equilibration with 95% O_2 and 5% CO_2). For all recordings, slices were continuously superfused at 32–34 °C with oxygenated BBS supplemented with NBQX (10 µM; Tocris), SR95-531 (5 µM; Tocris), strychnine (50 µM; Sigma), and TTX (500 nM; Latoxan).

CA1 neurons were recorded from both the ventral and the dorsal hippocampus. Cells were visualized with a combination of Dodt contrast, and an on-line video contrast enhancement. CA1 cells could be easily identified in the red light with which slices were visualized using a CoolSnap HQ2 CCD camera (Photometrics) run by MetaMorph (Universal Imaging). Whole-cell recordings were performed with an EPC-10 double amplifier (Heka Elektronik) run by PatchMaster (Heka). Patch pipettes (resistance 2–3 MΩ) were filled with an intracellular solution containing (in mM): 120 $CsMeSO_3$, 4.6 $MgCl_2$, 10 HEPES, 10 K_2-creatine phosphate, 15 BAPTA, 4 Na_2-ATP, 0.4 Na_2-GTP, 1 QX-314, pH 7.35 with CsOH (~300 mOsm). Series resistance was partially compensated (max 65%), whereas liquid junction potentials were not corrected. Recordings were performed at a holding potential of −60 mV. Puffing pipettes filled with BBS supplemented with glycine (10 mM), NBQX (2 µM), SR95-531 (2 µM), strychnine (50 µM), and D-APV (100 µM), were placed above the slice surface, close to the recording pipettes. Brief (0.5–1 s) puffs were then delivered every 60–120 s via a Picospritzer II (General Valve Corporation).

Pharmacology and data analysis. CGP-78608 dose-response curve (DRC) experiments were performed using 100 µM glycine. In these, and most other, experiments, CGP-78608 was systematically applied before agonist perfusion. CGP-78608 DRC was fitted using the following equation: $I_{rel} = 1 + ((a\text{-}1)/(1 + ([C]/EC_{50})^{nH})$ were $[C]$ is the compound concentration, a is the maximal potentiation and n_H the Hill coefficient. EC_{50}, a and n_H were set as free parameters. Agonist DRCs were fitted with the following Hill equation: $I_{rel} = 1/(1 + (EC_{50}/[A])^{nH})$, were $[A]$ is the agonist concentration, and EC_{50} and n_H set as free parameters. Desensitization and glycine or CGP-78608 washout kinetics were fitted using single exponentials with Clampfit 10.5 analysis software. When comparing the effects of various GluN1 competitive antagonists on GluN1/GluN3A current responses, glycine was used at 1 mM. To insure sufficient GluN1 binding site occupancy, the concentrations of CGP-78608 (500 nM), MDL-29951 (200 nM), 7-CKA (10 µM), and L689560 (1 µM) were set above their Ki values for GluN1 ABD (6.4 nM, 140 nM, 2.6 µM, 29.3 nM; radiolabeled glycine displacement assays on isolated domains[11] or native receptors for MDL-29951[62]). For MDL-29951, in order to insure that larger effects may have not been missed, a higher concentration was also tested (2 µM), yet potentiating factors were found to be smaller than those observed at 200 nM. This is likely due to MDL-29951 binding at GluN3A ABD and inhibiting GluN1/GluN3A receptors.

The compound [(1 *S*)-1-[[(7-Bromo-1,2,3,4-tetrahydro-2,3-dioxo-5-quinoxalinyl)methyl]amino]ethyl]phosphonic acid hydrochloride (CGP-78608, Tocris) was prepared as a stock solution of 25 mM in 2.2 eq NaOH solution. 2-carboxy-4,6-dichloro-1H-indole-3-propanoic acid (MDL-29951, Cayman Chemical), 7-Chlorokynureic acid (7-CKA, Tocris), *trans*-2-Carboxy-5, 7-dichloro-4-phenylaminocarbonylamino-1,2,3,4-tetrahydroquinoline (L689560, Tocris) and 6-Cyano-7-nitroquinoxaline-2,3-dione (CNQX, Alomone) were prepared in DMSO at stock concentrations of 2 mM, 10 mM, 2 mM, and 50 mM, respectively. 5-7-Dichlorokynurenic acid (DCKA, Tocris) stocks (50 mM) were prepared in a 1 eq NaOH solution. Glycine (1 mM; Sigma), strychnine (10 mM; Sigma), 6-Imino-3-(4-methoxyphenyl)-1(6 H)-pyridazinebutanoic acid hydrobromide (SR95-531; 10 mM; Tocris), 2,3-Dioxo-6-nitro-1,2,3,4-tetrahydrobenzo[f]quinoxaline-7-sulfonamide disodium salt (NBQX; 10 mM; Tocris), D-(-)-2-Amino-5-phosphonopentanoic acid (D-APV; 50 mM; Tocris) stocks were all prepared in water. Finally, Tetrodotoxin (TTX; 500 µM; Latoxan) was aliquoted in an acetic acid (2%) water solution.

Statistical analysis. Data are presented as mean ± standard error of the mean (SEM). Sample number (n) refers either to the number of recorded oocytes or HEK293 cells (Figs. 1–4), or to the number of recorded CA1 cells (Fig. 5). Unless otherwise stated, two-sided statistical analysis of the data shown in Figs. 1–4 was conducted using either two sample Student's t-test or the Mann–Whitney test when Equal Variance test failed. Data obtained from different conditions in Fig. 5 were compared statistically either with Mann–Whitney or Wilcoxon signed-rank test, as indicated in the text. Tests were performed using either SigmaPlot (Systat Software) or house-built routines in Igor (Wavemetrics). Statistical significance is reported in the figures according to the following symbols *, ** and ***, which indicate P values below 0.05, 0.01, and 0.001, respectively. n.s. = not significant.

Data availability

The datasets generated and analysed during the current study are available from the corresponding authors on reasonable request.

Received: 15 May 2018 Accepted: 12 October 2018
Published online: 13 November 2018

References

1. Traynelis, S. F. et al. Glutamate receptor ion channels: structure, regulation, and function. *Pharmacol. Rev.* **62**, 405–496 (2010).
2. Paoletti, P., Bellone, C. & Zhou, Q. NMDA receptor subunit diversity: impact on receptor properties, synaptic plasticity and disease. *Nat. Rev. Neurosci.* **14**, 383–400 (2013).
3. Sanz-Clemente, A., Nicoll, R. A. & Roche, K. W. Diversity in NMDA receptor composition: many regulators, many consequences. *Neuroscientist* **19**, 62–75 (2013).
4. Paoletti, P. Molecular basis of NMDA receptor functional diversity. *Eur. J. Neurosci.* **33**, 1351–1365 (2011).
5. Bliss, T. V. & Collingridge, G. L. A synaptic model of memory: long-term potentiation in the hippocampus. *Nature* **361**, 31–39 (1993).
6. Ciabarra, A. M. et al. Cloning and characterization of chi-1: a developmentally regulated member of a novel class of the ionotropic glutamate receptor family. *J. Neurosci.* **15**, 6498–6508 (1995).
7. Sucher, N. J. et al. Developmental and regional expression pattern of a novel NMDA receptor-like subunit (NMDAR-L) in the rodent brain. *J. Neurosci.* **15**, 6509–6520 (1995).
8. Andersson, O., Stenqvist, A., Attersand, A. & von Euler, G. Nucleotide sequence, genomic organization, and chromosomal localization of genes encoding the human NMDA receptor subunits NR3A and NR3B. *Genomics* **78**, 178–184 (2001).
9. Nishi, M., Hinds, H., Lu, H. P., Kawata, M. & Hayashi, Y. Motoneuron-specific expression of NR3B, a novel NMDA-type glutamate receptor subunit that works in a dominant-negative manner. *J. Neurosci.* **21**, RC185 (2001).
10. Chatterton, J. E. et al. Excitatory glycine receptors containing the NR3 family of NMDA receptor subunits. *Nature* **415**, 793–798 (2002).
11. Yao, Y. & Mayer, M. L. Characterization of a soluble ligand binding domain of the NMDA receptor regulatory subunit NR3A. *J. Neurosci.* **26**, 4559–4566 (2006).
12. Yao, Y., Harrison, C. B., Freddolino, P. L., Schulten, K. & Mayer, M. L. Molecular mechanism of ligand recognition by NR3 subtype glutamate receptors. *EMBO J.* **27**, 2158–2170 (2008).
13. Das, S. et al. Increased NMDA current and spine density in mice lacking the NMDA receptor subunit NR3A. *Nature* **393**, 377–381 (1998).
14. Roberts, A. C. et al. Downregulation of NR3A-containing NMDARs is required for synapse maturation and memory consolidation. *Neuron* **63**, 342–356 (2009).
15. Larsen, R. S. et al. NR3A-containing NMDARs promote neurotransmitter release and spike timing-dependent plasticity. *Nat. Neurosci.* **14**, 338–344 (2011).
16. Wong, H. K. et al. Temporal and regional expression of NMDA receptor subunit NR3A in the mammalian brain. *J. Comp. Neurol.* **450**, 303–317 (2002).
17. Wee, K. S., Zhang, Y., Khanna, S. & Low, C. M. Immunolocalization of NMDA receptor subuhnit NR3B in selected structures in the rat forebrain, cerebellum, and lumbar spinal cord. *J. Comp. Neurol.* **509**, 118–135 (2008).
18. Henson, M. A., Roberts, A. C., Perez-Otano, I. & Philpot, B. D. Influence of the NR3A subunit on NMDA receptor functions. *Prog. Neurobiol.* **91**, 23–37 (2010).
19. Pachernegg, S., Strutz-Seebohm, N. & Hollmann, M. GluN3 subunit-containing NMDA receptors: not just one-trick ponies. *Trends Neurosci.* **35**, 240–249 (2012).
20. Perez-Otano, I., Larsen, R. S. & Wesseling, J. F. Emerging roles of GluN3-containing NMDA receptors in the CNS. *Nat. Rev. Neurosci.* **17**, 623–635 (2016).
21. Perez-Otano, I. et al. Assembly with the NR1 subunit is required for surface expression of NR3A-containing NMDA receptors. *J. Neurosci.* **21**, 1228–1237 (2001).
22. Sasaki, Y. F. et al. Characterization and comparison of the NR3A subunit of the NMDA receptor in recombinant systems and primary cortical neurons. *J. Neurophysiol.* **87**, 2052–2063 (2002).
23. Madry, C. et al. Principal role of NR3 subunits in NR1/NR3 excitatory glycine receptor function. *Biochem. Biophys. Res. Commun.* **354**, 102–108 (2007).
24. Awobuluyi, M. et al. Subunit-specific roles of glycine-binding domains in activation of NR1/NR3 N-methyl-D-aspartate receptors. *Mol. Pharmacol.* **71**, 112–122 (2007).

25. Curtis, D. R. et al. Inhibition of spinal neurons by glycine. *Nature* **215**, 1502–1503 (1967).
26. Legendre, P. The glycinergic inhibitory synapse. *Cell. Mol. Life Sci.* **58**, 760–793 (2001).
27. Bowery, N. G. & Smart, T. G. GABA and glycine as neurotransmitters: a brief history. *Br. J. Pharmacol.* **147**, S109–S119 (2006).
28. Pina-Crespo, J. C. et al. Excitatory glycine responses of CNS myelin mediated by NR1/NR3 "NMDA" receptor subunits. *J. Neurosci.* **30**, 11501–11505 (2010).
29. Smothers, C. T. & Woodward, J. J. Pharmacological characterization of glycine-activated currents in HEK 293 cells expressing N-methyl-D-aspartate NR1 and NR3 subunits. *J. Pharmacol. Exp. Ther.* **322**, 739–748 (2007).
30. Smothers, C. T. & Woodward, J. J. Expression of glycine-activated diheteromeric NR1/NR3 receptors in human embryonic kidney 293 cells Is NR1 splice variant-dependent. *J. Pharmacol. Exp. Ther.* **331**, 975–984 (2009).
31. Cummings, K. A., Belin, S. & Popescu, G. K. Residues in the GluN1 C-terminal domain control kinetics and pharmacology of GluN1/GluN3A N-methyl-d-aspartate receptors. *Neuropharmacology* **119**, 40–47 (2017).
32. Madry, C., Betz, H., Geiger, J. R. & Laube, B. Supralinear potentiation of NR1/NR3A excitatory glycine receptors by Zn^{2+} and NR1 antagonist. *Proc. Natl Acad. Sci. USA* **105**, 12563–12568 (2008).
33. Kvist, T., Greenwood, J. R., Hansen, K. B., Traynelis, S. F. & Brauner-Osborne, H. Structure-based discovery of antagonists for GluN3-containing N-methyl-D-aspartate receptors. *Neuropharmacology* **75**, 324–336 (2013).
34. Cummings, K. A. & Popescu, G. K. Protons potentiate GluN1/GluN3A currents by attenuating their desensitisation. *Sci. Rep.* **6**, 23344 (2016).
35. Auberson, Y. P. et al. N-phosphonoalkyl-5-aminomethylquinoxaline-2,3-diones: in vivo active AMPA and NMDA(glycine) antagonists. *Bioorg. Med. Chem. Lett.* **9**, 249–254 (1999).
36. Aizenman, E., Lipton, S. A. & Loring, R. H. Selective modulation of NMDA responses by reduction and oxidation. *Neuron* **2**, 1257–1263 (1989).
37. Kohr, G., Eckardt, S., Luddens, H., Monyer, H. & Seeburg, P. H. NMDA receptor channels: subunit-specific potentiation by reducing agents. *Neuron* **12**, 1031–1040 (1994).
38. Sullivan, J. M. et al. Identification of two cysteine residues that are required for redox modulation of the NMDA subtype of glutamate receptor. *Neuron* **13**, 929–936 (1994).
39. Choi, Y. B. & Lipton, S. A. Redox modulation of the NMDA receptor. *Cell. Mol. Life Sci.* **57**, 1535–1541 (2000).
40. Sanchez, R. M. et al. Novel role for the NMDA receptor redox modulatory site in the pathophysiology of seizures. *J. Neurosci.* **20**, 2409–2417 (2000).
41. Yang, Y. J. et al. Reversal of aging-associated hippocampal synaptic plasticity deficits by reductants via regulation of thiol redox and NMDA receptor function. *Aging Cell.* **9**, 709–721 (2010).
42. Kumar, A. & Foster, T. C. Linking redox regulation of NMDAR synaptic function to cognitive decline during aging. *J. Neurosci.* **33**, 15710–15715 (2013).
43. Kim, J. Y., Ko, A. R., Hyun, H. W., Min, S. J. & Kim, J. E. PDI regulates seizure activity via NMDA receptor redox in rats. *Sci. Rep.* **7**, 42491 (2017).
44. Kleckner, N. W. & Dingledine, R. Requirement for glycine in activation of NMDA-receptors expressed in *Xenopus*oocytes. *Science* **241**, 835–837 (1988).
45. Lerma, J., Zukin, R. S. & Bennett, M. V. Glycine decreases desensitization of N-methyl-D-aspartate (NMDA) receptors expressed in *Xenopus*oocytes and is required for NMDA responses. *Proc. Natl Acad. Sci. USA* **87**, 2354–2358 (1990).
46. Johnson, J. W. & Ascher, P. Equilibrium and kinetic study of glycine action on the N-methyl-D-aspartate receptor in cultured mouse brain neurons. *J. Physiol.* **455**, 339–365 (1992).
47. Hackos, D. H. & Hanson, J. E. Diverse modes of NMDA receptor positive allosteric modulation: mechanisms and consequences. *Neuropharmacology* **112**, 34–45 (2017).
48. Sun, Y. et al. Mechanism of glutamate receptor desensitization. *Nature* **417**, 245–253 (2002).
49. Horak, M., Vlcek, K., Petrovic, M., Chodounska, H. & Vyklicky, L. Jr. Molecular mechanism of pregnenolone sulfate action at NR1/NR2B receptors. *J. Neurosci.* **24**, 10318–10325 (2004).
50. Yi, F. et al. Structural basis for negative allosteric modulation of GluN2A-containing NMDA receptors. *Neuron* **91**, 1316–1329 (2016).
51. Matsuda, K., Fletcher, M., Kamiya, Y. & Yuzaki, M. Specific assembly with the NMDA receptor 3B subunit controls surface expression and calcium permeability of NMDA receptors. *J. Neurosci.* **23**, 10064–10073 (2003).
52. Mesic, I. et al. The N-terminal domain of the GluN3A subunit determines the efficacy of glycine-activated NMDA receptors. *Neuropharmacology* **105**, 133–141 (2016).
53. Guzman, Y. F. et al. A gain-of-function mutation in the GRIK2 gene causes neurodevelopmental deficits. *Neurology* **3**, 129 (2017).
54. Lu, H. W., Balmer, T. S., Romero, G. E. & Trussell, L. O. Slow AMPAR synaptic transmission is determined by stargazin and glutamate transporters. *Neuron* **96**, 73–80 (2017).
55. Yao, Y., Belcher, J., Berger, A. J., Mayer, M. L. & Lau, A. Y. Conformational analysis of NMDA receptor GluN1, GluN2, and GluN3 ligand-binding domains reveals subtype-specific characteristics. *Structure* **21**, 1788–1799 (2013).
56. Karakas, E. & Furukawa, H. Crystal structure of a heterotetrameric NMDA receptor ion channel. *Science* **344**, 992–997 (2014).
57. Lee, C. H. et al. NMDA receptor structures reveal subunit arrangement and pore architecture. *Nature* **511**, 191–197 (2014).
58. Furukawa, H. & Gouaux, E. Mechanisms of activation, inhibition and specificity: crystal structures of the NMDA receptor NR1 ligand-binding core. *EMBO J.* **22**, 2873–2885 (2003).
59. Semyanov, A., Walker, M. C., Kullmann, D. M. & Silver, R. A. Tonically active GABA A receptors: modulating gain and maintaining the tone. *Trends Neurosci.* **27**, 262–269 (2004).
60. Mony, L., Zhu, S., Carvalho, S. & Paoletti, P. Molecular basis of positive allosteric modulation of GluN2B NMDA receptors by polyamines. *EMBO J.* **30**, 3134–3146 (2011).
61. Otsu, Y. et al. Functional principles of posterior septal inputs to the medial habenula. *Cell Rep.* **22**, 693–705 (2018).
62. Baron, B. M. et al. Potent indole- and quinoline-containing N-methyl-D-aspartate antagonists acting at the strychnine-insensitive glycine binding site. *J. Pharmacol. Exp. Ther.* **262**, 947–956 (1992).

Acknowledgements

This work was supported by the French government (Investissements d'Avenir ANR-10-LABX-54 MEMO LIFE and ANR-11-IDEX-0001-02 PSL* Research University), Agence Nationale de la Recherche (ANR grant GluBrain3A to M.A.D. and P.P.), and the European Research Council (ERC Advanced Grant #693021 to P.P.). We thank Nobuki Nakanishi and Stuart Lipton (Scintillon Institute, San Diego, CA, USA) for providing the GluN3A-KO mouse line. We also thank Boris Barbour and Mariano Casado for critical reading of the manuscript.

Author contributions

T.G., M.A.D., and P.P. designed the project. T.G. performed all the experiments on recombinant receptors and S.A.G. performed the experiments on hippocampal slices. M. D. provided technical support in molecular biology and cell culture. T.G., S.A.G., and P. P. analyzed the data, and T.G., M.A.D., and P.P. wrote the manuscript. M.A.D. and P.P. supervised the project.

Additional information

Supplementary Information accompanies this paper at https://doi.org/10.1038/s41467-018-07236-4.

Competing interests: The authors declare no competing interests.

Reprints and permission information is available online at http://npg.nature.com/reprintsandpermissions/

Publisher's note: Springer Nature remains neutral with regard to jurisdictional claims in published maps and institutional affiliations.

NEUROSCIENCE

Control of aversion by glycine-gated GluN1/GluN3A NMDA receptors in the adult medial habenula

Y. Otsu[1]*†, E. Darcq[2]†, K. Pietrajtis[3]†, F. Mátyás[4,5,6], E. Schwartz[3], T. Bessaih[3], S. Abi Gerges[3], C. V. Rousseau[1]‡, T. Grand[1], S. Dieudonné[1], P. Paoletti[1], L. Acsády[4], C. Agulhon[7], B. L. Kieffer[2], M. A. Diana[3]§

The unconventional *N*-methyl-D-aspartate (NMDA) receptor subunits GluN3A and GluN3B can, when associated with the other glycine-binding subunit GluN1, generate excitatory conductances purely activated by glycine. However, functional GluN1/GluN3 receptors have not been identified in native adult tissues. We discovered that GluN1/GluN3A receptors are operational in neurons of the mouse adult medial habenula (MHb), an epithalamic area controlling aversive physiological states. In the absence of glycinergic neuronal specializations in the MHb, glial cells tuned neuronal activity via GluN1/GluN3A receptors. Reducing GluN1/GluN3A receptor levels in the MHb prevented place-aversion conditioning. Our study extends the physiological and behavioral implications of glycine by demonstrating its control of negatively valued emotional associations via excitatory glycinergic NMDA receptors.

Glycine is a major inhibitory neurotransmitter of the central nervous system, which acts via anion-permeable receptors. It is also a well-characterized coagonist of excitatory *N*-methyl-D-aspartate receptors (NMDARs) via GluN1 subunits (*1*). In addition, glycine binds the unconventional NMDAR subunits GluN3A and GluN3B, which generate atypical glutamate-activated triheteromeric NMDARs with GluN1 and GluN2 subunits (*2*), as well as glycine-gated diheteromeric excitatory complexes with GluN1 (*3*). GluN3B is appreciably expressed only in caudal areas (*4*). GluN3A expression is broader but assumed to be limited to early development (*2*). Mainly examined in recombinant systems (*5*), native GluN1/GluN3A receptors (GluN1/GluN3ARs) have been identified in the juvenile hippocampus (*6*) but never in adult neurons.

We found strong immunohistochemical expression of GluN3A subunits in the ventral subdivision of the medial habenula (MHb) of adult mice (Fig. 1A) (*7*), an area that mediates aversive behaviors (*8*–*12*). We investigated GluN3A-immunostained sections with electron microscopy (EM) to identify the ultrastructural localization of the subunit. Frequently in juxtaposition with glial structures, all the 3,3-diaminobenzidine (DAB)–labeled profiles were identified as postsynaptic dendrites and somata (n = 92) (Fig. 1B). Supported by further confocal microscopy results (fig. S1), these data demonstrated that GluN3A subunits were abundantly expressed in adult MHb neurons.

We next examined whether GluN3A subunits formed operational GluN1/GluN2/GluN3ARs. These receptors show reduced rectification compared with GluN1/GluN2 NMDARs (*2*). We thus examined the current-voltage (*I*-*V*) curves of synaptic (*13*) and puff-evoked NMDAR currents in MHb neurons from wild-type (WT)

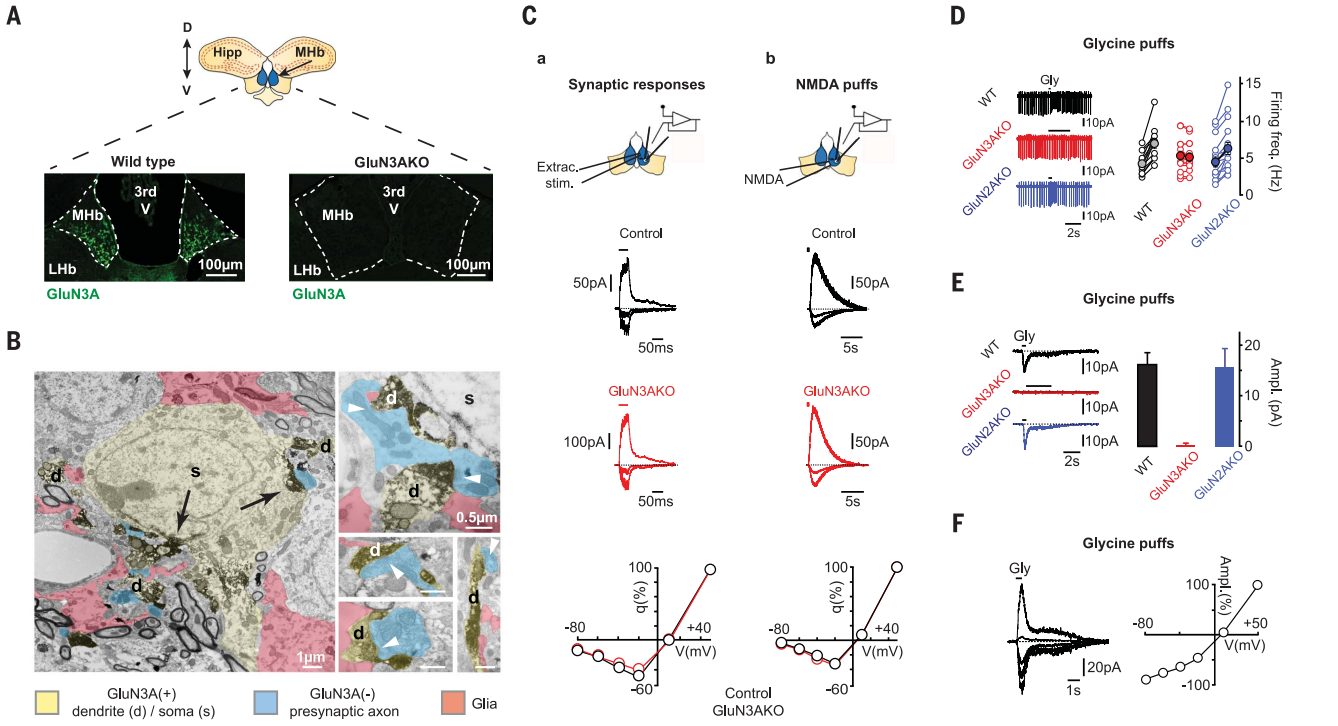

Fig. 1. Functional GluN1/GluN3ARs in the adult MHb. Both (**A**) confocal and (**B**) electron microscopy demonstrated that GluN3A subunits are expressed in the ventral MHb. DAB EM staining [black deposits in (B)] was detected in dendrites (yellow), close to glial extensions (red), rarely in somas (black arrows), but never in axons (blue; white arrowheads highlight presynaptic specializations). Hipp, hippocampus; LHb, lateral habenula; 3rd V, third ventricule. (**C**) GluN1/GluN2/GluN3ARs are not functional in the MHb. No difference was found in the rectification of NMDAR currents in WT (black) and GluN3AKO (red) mice, elicited by extracellular stimulation (a) or pressure-ejected NMDA (b). (**D**) Glycine puffs increased firing rates in MHb cells from control and GluN2AKO mice, but not from GluN3AKO animals. (**E** and **F**) Similarly to heterologous GluN1/GluN3R currents, glycine induced outwardly rectifying, rapidly rising and inactivating currents in control and GluN2AKO, but not GluN3AKO, neurons. Data are illustrated as averages ± SEM.

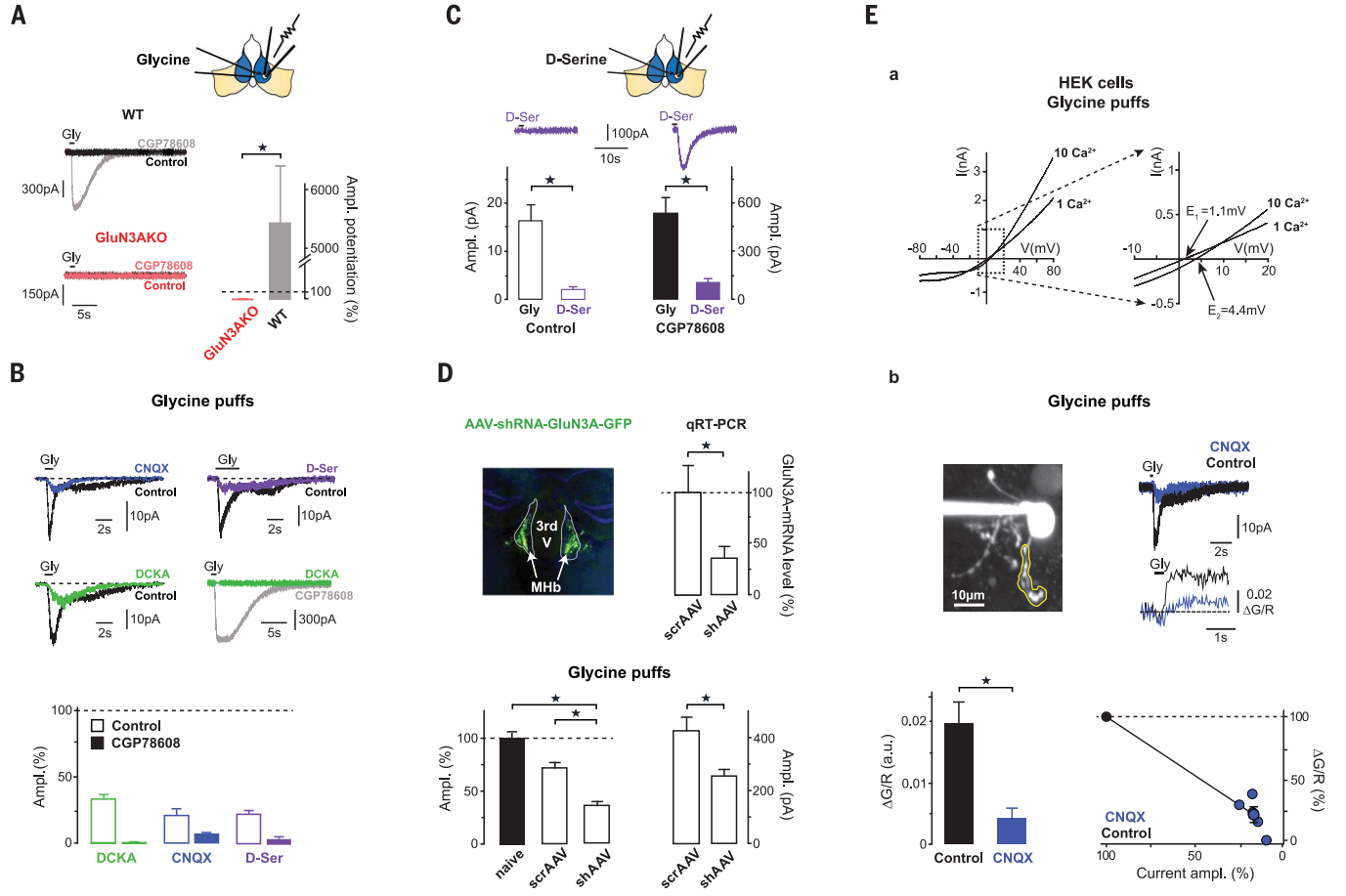

Fig. 2. Properties of GluN1/GluN3Rs in the MHb. (**A**) GluN1 subunit block with CGP78608 potentiated glycine-elicited currents. (**B**) Bath applications of CNQX (blue), 5,7-DCKA (green), and D-serine (purple) antagonized control and potentiated GluN1/GluN3AR currents. (**C**) Pressure-ejected D-serine had only partial agonist effects on GluN1/GluN3ARs. (**D**) Viral expression in the MHb of a GluN3A-targeting shRNA (AAV-shRNA-GluN3A-GFP and shRNA) led to reduction of GluN3A mRNA levels, and of glycine-induced currents with respect to scrambled RNA–expressing mice (scrAAV). Percentage values and absolute amplitudes are illustrated in the lower graphs. (**E**) GluN1/GluN3ARs are Ca^{2+} permeable. Changing extracellular Ca^{2+} concentrations led to a significant reversal potential shift [(a), highlighted on the right] in heterologous systems expressing GluN3A and point-mutated, glycine-insensitive GluN1 subunits. In the presence of synaptic receptor antagonists and Ca^{2+} channel blockers, two-photon imaging revealed glycine-elicited Ca^{2+} transients in ex vivo MHb neurons (b). ΔG/R, ratio between green fluorescence increases and basal red fluorescence. Stars represent statistically significant differences. Data are illustrated as averages ± SEM.

and GluN3A knock-out (GluN3AKO) (*14*) mice, in which excitatory transmission to the MHb is not modified (fig. S2). No significant differences were found (Fig. 1C, a and b), suggesting the absence of functional receptors.

To investigate whether glycine-activated GluN1/GluN3ARs were operational, glycine (1 or 10 mM) was pressure-ejected while recording spontaneous firing activity (*13*) in the loose cell-attached configuration (LCA). In all tested WT neurons, glycine puffs (300 to 500 ms) potently increased firing in the presence of D-2-amino-5-phosphonovalerate (D-APV) and strychnine (Fig. 1D). This excitatory effect was not attributable to conventional NMDARs, because it was present in GluN2AKO mice (Fig. 1D), where GluN1/GluN2 NMDARs are nearly undetectable (*13*). The effect on firing activity was absent in GluN3AKO mice (Fig. 1D), supporting the presence of GluN1/GluN3ARs in the MHb.

Glycine puffs induced rapidly rising and inactivating inward currents in voltage clamp recordings of both WT and GluN2AKO ex vivo MHb neurons performed in the presence of D-APV and strychnine. The currents could not be elicited in GluN3AKO mice (Fig. 1E). As in recombinant systems, the glycine-evoked currents showed slight outward rectification (Fig. 1F).

We investigated the pharmacology of the glycine-induced currents. In recombinant systems, occupation of the higher-affinity GluN3A site activates the receptor, whereas glycine binding to GluN1 entrains rapid desensitization (*5*, *15*). We recently discovered that the GluN1 antagonist [(1*S*)-1-[[(7-Bromo-1,2,3,4-tetrahydro-2,3-dioxo-5-quinoxalinyl)methyl]amino]ethyl] phosphonic acid (CGP78608) enhanced receptor

[1]Institut de Biologie de l'École Normale Supérieure (IBENS), INSERM U1024, CNRS UMR8197, École Normale Supérieure, Université PSL, 75005 Paris, France. [2]Department of Psychiatry, School of Medicine, Douglas Hospital Research Center, McGill University, Montreal, QC H4H 1R3, Canada. [3]Sorbonne Université, CNRS, INSERM, Neurosciences Paris Seine – Institut de Biologie Paris Seine (NPS-IBPS), 75005 Paris, France. [4]Laboratory of Thalamus Research, Institute of Experimental Medicine, Hungarian Academy of Sciences, 1083 Budapest, Hungary. [5]Research Centre for Natural Sciences Institute of Cognitive Neuroscience and Psychology, 1117 Budapest, Hungary. [6]Department of Anatomy and Histology, University of Veterinary Medicine, 1078 Budapest, Hungary. [7]Integrative Neuroscience and Cognition Center, CNRS UMR8002, Glia-Glia and Glia-Neuron Interactions Group, Paris Descartes University, 75006 Paris, France.
*Present address: Pain Management Research Institute, Kolling Institute of Medical Research, Northern Clinical School, The University of Sydney and Royal North Shore Hospital, St. Leonards, NSW 2065, Australia. †These authors contributed equally to this work. ‡Present address: Neural Circuit Dynamics and Decision Making, Pasteur Institute, 75015 Paris, France.
§Corresponding author. Email: marco.diana@upmc.fr

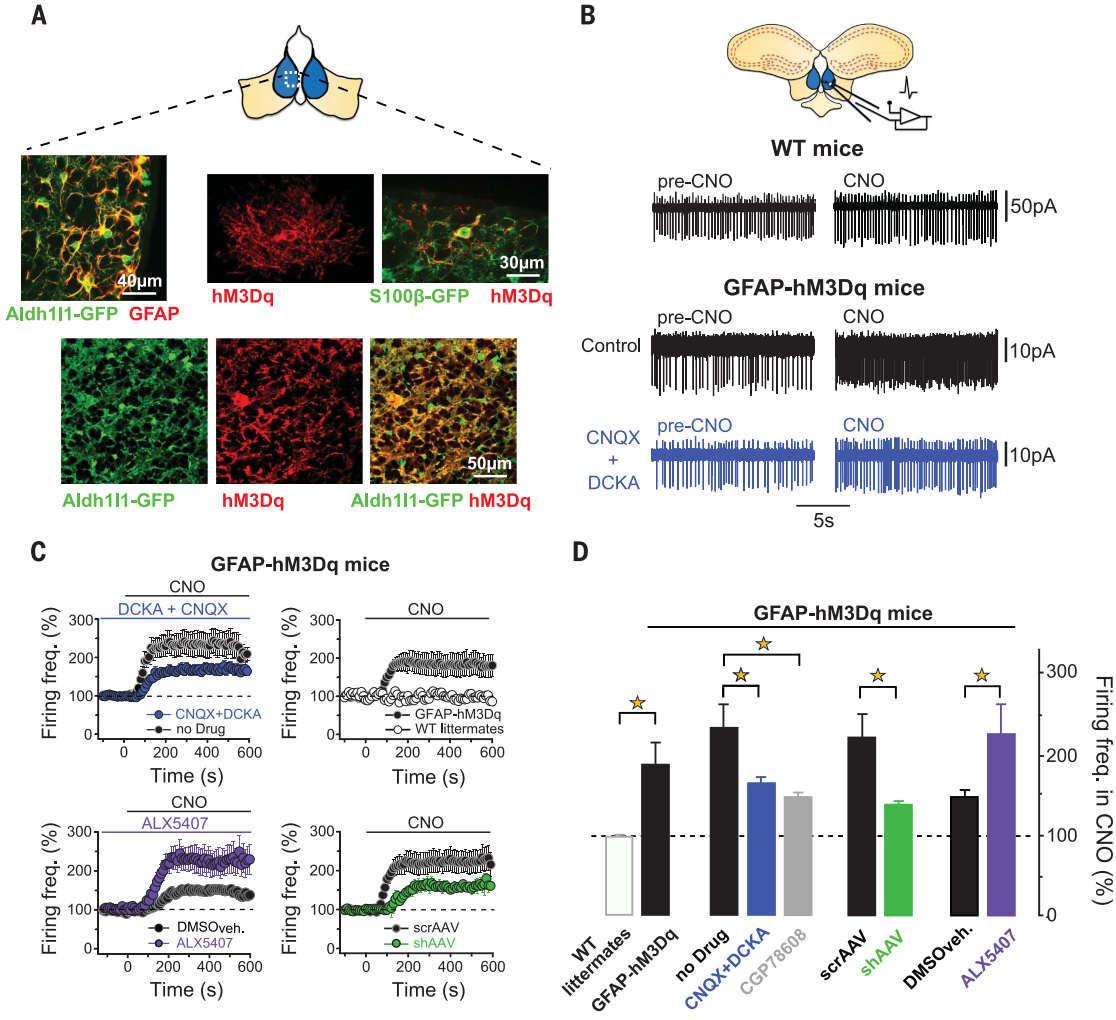

Fig. 3. Glial activation in GFAP-hM3Dq mice increases neuronal excitability via GluN1/GluN3ARs. (**A**) The specific expression of hM3Dq receptors in MHb glia was demonstrated by the colocalization of GFAP and GFP in aldehyde dehydrogenase-1 family member l1-green fluorescent protein (Aldh1l1-GFP) mice, and of hM3DqRs and GFP in GFAP-hM3Dq::Aldh1l1-GFP and GFAP-hM3Dq::S100β-GFP mice. (**B**) CNO applications increased spontaneous firing rates of MHb neurons. Representative traces preceding and following CNO are shown for specified experiments. The average time courses (**C**) and quantifications (**D**) of the CNO effects are depicted for all the experiments. The smaller increase of the firing rate in CGP78608 than in control likely derived from reduced affinity for glycine in the presence of the drug (*6*). DMSO veh., dimethyl sulfoxide vehicle. Stars represent statistically significant differences. Data are illustrated as averages ± SEM.

responses by reducing desensitization (*6*). We found that CGP78608 (1 μM) potentiated and prolonged the responses in WT but not GluN3AKO mice (Fig. 2A). 6-Cyano-7-nitroquinoxaline-2,3-dione (CNQX), 5,7-Dichlorokinurenic acid (5,7-DCKA), and D-serine inhibit the currents produced by GluN1/GluN3Rs (*3*, *5*, *6*, *15*). These drugs also potently inhibited the responses to glycine in MHb neurons (Fig. 2B). Direct applications of D-serine increased neuronal excitability (fig. S4) and elicited currents (Fig. 2C) to a lesser extent than glycine (*3*, *15*). With the exception of zinc, which had no effects (*16*) (fig. S5), the pharmacological profile of the native currents thus mirrored that of recombinant GluN1/GluN3Rs.

We injected the MHb with a short hairpin ribonucleic acid (shRNA)–expressing adeno-associated virus (AAV) targeting the GluN3A subunit (AAV5-shRNA-GluN3A) (*17*). The virus efficiently reduced both the messenger RNA levels of GluN3A in the MHb (Fig. 2D) and the amplitude of the glycine-induced currents compared with scrambled RNA (AAV5-scrRNA-GluN3A)–expressing mice (Fig. 2D).

The permeability of GluN1/GluN3ARs to calcium (Ca^{2+}) remains uncertain (*3*, *18*). We examined this question by first analyzing in human embryonic kidney (HEK) cells a GluN1/GluN3AR variant with potentiated glycine responses (GluN1-F484A/GluN3A) (*5*, *6*). Increasing the extracellular Ca^{2+} concentration led to a shift of the reversal potential of the responses to glycine (Fig. 2E, a), which demonstrated significant Ca^{2+} permeability, although smaller than for WT GluN1/GluN2A receptors (fig. S6).

Using two-photon microscopy in the presence of synaptic and Ca^{2+} channel blockers, we could detect glycine-evoked Ca^{2+} transients originating from GluN1/GluN3ARs in ex vivo MHb cells (Fig. 2E, b). We concluded that native GluN1/GluN3A receptors were also permeable to Ca^{2+}.

We then searched for physiological sources of glycine. We had previously found that the MHb was completely devoid of glycinergic neuronal specializations (fig.S1) (*19*). Thus, we tested whether glial cells could control extracellular glycine levels in mice expressing the excitatory DREADD (designer receptor exclusively activated by designer drugs) hM3Dq under the control of the promoter of the glial fibrillary protein (GFAP). In these mice, hM3Dq receptor (hM3DqR) activation triggers Ca^{2+} elevations specifically in glial cells (*20*). We confirmed that hM3DqR expression was exclusively glial (Fig. 3A and fig. S7).

To determine whether GluN1/GluN3ARs mediated glia-neuron interactions in the MHb, we recorded ex vivo spontaneous firing activity in GFAP-hM3Dq mice (Fig. 3). Application of the hM3DqR agonist clozapine-*N*-oxide (CNO; 10 μM), produced rapid firing rate increases. Preincubation with 5,7-DCKA and CNQX strongly reduced the effect of CNO, suggesting a substantial contribution from GluN1/GluN3ARs (Fig. 3). CGP78608 application significantly augmented basal firing rates (fig. S3), indicating that ambient glycine may suffice to bind GluN3A. The potentiation of the firing rate triggered by CNO was instead reduced by CGP78608 preincubations.

Furthermore, the effect of CNO was significantly smaller in GFAP-hM3Dq mice injected with the AAV5-shRNA-GluN3A-GFP than with AAV5-scrRNA-GluN3A-GFP virus (GFP, green

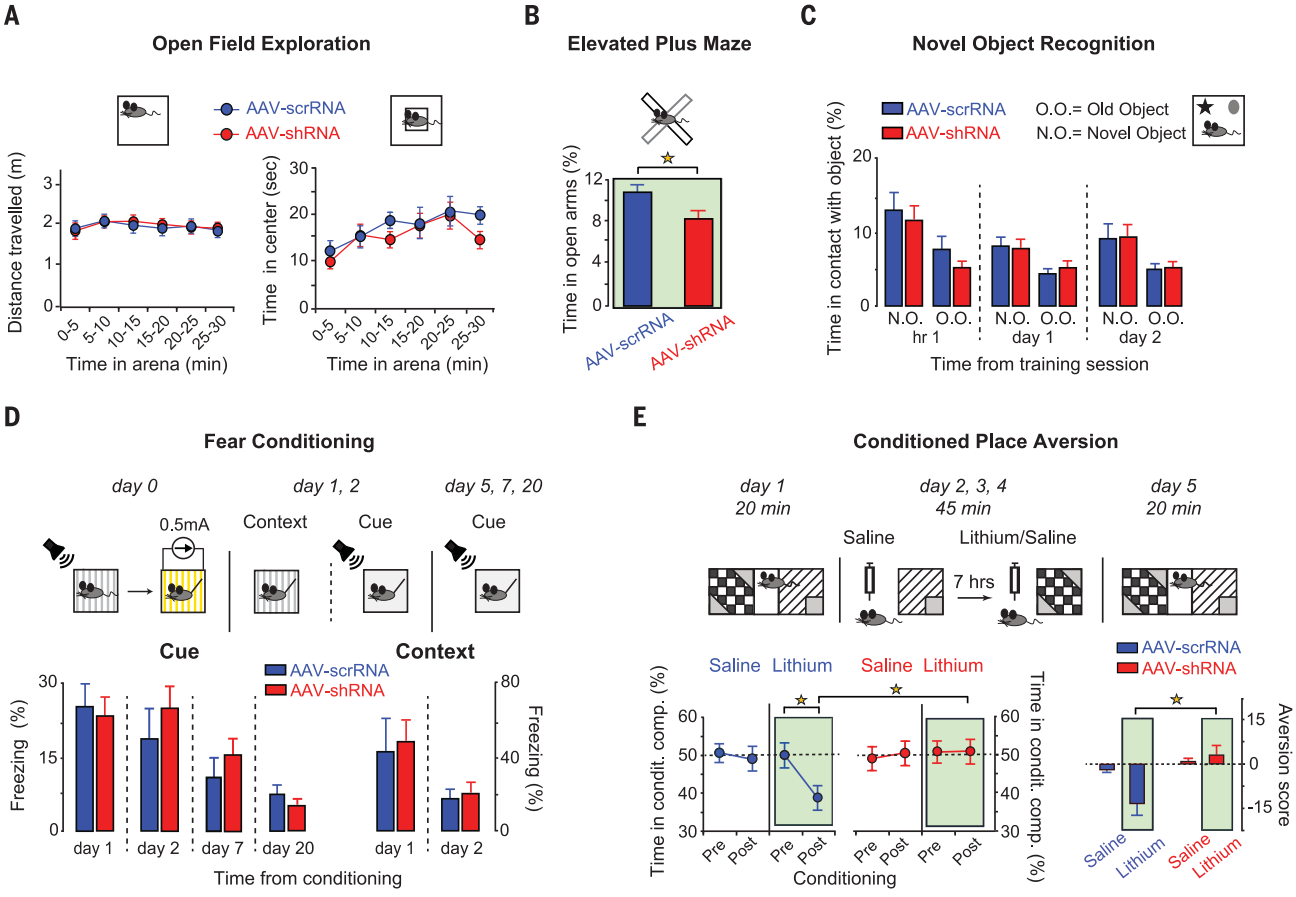

Fig. 4. MHb GluN1/GluN3ARs control place-aversion conditioning. (**A**) No difference was detected between AAV-shRNA-GluN3A– and AAV-scrRNA-GluN3A–injected mice in the distance traveled in an open field and in the time spent in its center. (**B**) Knocking down MHb GluN3A expression was mildly anxiogenic as indicated by the shorter time spent by GluN3A-deficient mice in the open arms of an elevated plus maze. Object exploration times and cue- and context-induced freezing were similar in (**C**) novel object recognition and (**D**) fear conditioning tests, respectively. (**E**) After lithium conditioning, AAV-shRNA-GluN3A–injected mice developed no aversion for the malaise-associated compartment in contrast to scrRNA-expressing animals. Data are illustrated as averages ± SEM.

fluorescent protein) (Fig. 3). In contrast to GlyT2 (fig. S1), we found expression in MHb glia of the membrane glycine transporter GlyT1 (fig. S8), which can contribute to glial glycine accumulation (*21*). In the presence of the GlyT1-specific blocker *N*-[(3*R*)-3-([1,1'-Biphenyl]-4-yloxy)-3-(4-fluorophenyl)propyl]-*N*-methylglycine (ALX5407), CNO applications increased firing rates to greater values than in control (Fig. 3, C and D), likely because of greater buildup of extracellular glycine levels. Together, these experiments suggested that glial cells potentiated neuronal activity via activation of GluN1/GluN3ARs.

Finally, we examined whether GluN1/GluN3ARs in the adult MHb were behaviorally relevant in mice injected with either the AAV5-shRNA-GluN3A-GFP or the AAV5-scrRNA-GluN3A-GFP virus (fig. S9). No differences were detected in locomotor and exploratory activity in an open field arena (Fig. 4A). In contrast, the test mice spent significantly less time in the open arms of an elevated place maze, suggesting that reduced GluN1/GluN3AR levels in the MHb were mildly anxiogenic (Fig. 4, A and B). GluN1/GluN3ARs in the MHb did not modulate learning and memory capabilities, because test and control mice scored similarly in a novel object recognition test (Fig. 4C).

The MHb can contribute to the development of negatively valued emotional states. We thus examined the behavioral outcomes of a fear conditioning protocol (Fig. 4D). We found no difference between AAV5-shRNA– and AAV5-scrRNA–injected mice in the freezing time elicited either by the cued or the contextual stimulus (Fig. 4D).

Finally, we examined lithium-induced conditioned place aversion, a paradigm that relies on intact MHb function (*22, 23*). In contrast to AAV5-scrRNA animals, lithium-treated AAV5-shRNA mice did not develop aversion for the conditioned compartment (Fig. 4E). Overall, these results indicate that impaired GluN3A signaling in the MHb alters the capability of associating negatively valued external conditions with internal aversive states.

In addition to its ubiquitous role as an inhibitory neurotransmitter, glycine can exert excitatory actions via unconventional GluN1/GluN3A NMDARs. Our study unveils a functional role of this aspect of glycine physiology by demonstrating that full expression of GluN1/GluN3ARs in the MHb is mandatory for modifying the internal emotional landscape in response to specific environmental challenges.

REFERENCES AND NOTES

1. P. Paoletti, *Eur. J. Neurosci.* **33**, 1351–1365 (2011).
2. I. Pérez-Otaño, R. S. Larsen, J. F. Wesseling, *Nat. Rev. Neurosci.* **17**, 623–635 (2016).
3. J. E. Chatterton *et al.*, *Nature* **415**, 793–798 (2002).
4. K. Matsuda, Y. Kamiya, S. Matsuda, M. Yuzaki, *Brain Res. Mol. Brain Res.* **100**, 43–52 (2002).
5. C. Madry *et al.*, *Biochem. Biophys. Res. Commun.* **354**, 102–108 (2007).
6. T. Grand, S. Abi Gerges, M. David, M. A. Diana, P. Paoletti, *Nat. Commun.* **9**, 4769 (2018).
7. R. S. Larsen *et al.*, *Nat. Neurosci.* **14**, 338–344 (2011).
8. M. Agetsuma *et al.*, *Nat. Neurosci.* **13**, 1354–1356 (2010).
9. C. D. Fowler, Q. Lu, P. M. Johnson, M. J. Marks, P. J. Kenny, *Nature* **471**, 597–601 (2011).
10. A. Görlich *et al.*, *Proc. Natl. Acad. Sci. U.S.A.* **110**, 17077–17082 (2013).

11. J. Zhang *et al*., *Cell* **166**, 716–728 (2016).
12. S. Molas, S. R. DeGroot, R. Zhao-Shea, A. R. Tapper, *Trends Pharmacol. Sci.* **38**, 169–180 (2017).
13. Y. Otsu *et al*., *Cell Rep.* **22**, 693–705 (2018).
14. S. Das *et al*., *Nature* **393**, 377–381 (1998).
15. M. Awobuluyi *et al*., *Mol. Pharmacol.* **71**, 112–122 (2007).
16. C. Madry, H. Betz, J. R. Geiger, B. Laube, *Proc. Natl. Acad. Sci. U.S.A.* **105**, 12563–12568 (2008).
17. T. Yuan *et al*., *Neuron* **80**, 1025–1038 (2013).
18. J. C. Piña-Crespo *et al*., *J. Neurosci.* **30**, 11501–11505 (2010).
19. K. Giber *et al*., *Nat. Neurosci.* **18**, 562–568 (2015).
20. C. Agulhon *et al*., *J. Physiol.* **591**, 5599–5609 (2013).
21. F. Zafra *et al*., *J. Neurosci.* **15**, 3952–3969 (1995).
22. E. Darcq *et al*., *Learn. Mem.* **18**, 574–578 (2011).
23. L. J. Boulos *et al*., *Neuropsychopharmacology* 10.1038/s41386-019-0395-7 (2019).

ACKNOWLEDGMENTS

We thank M. Galante, R. Lambert, and N. Leresche for critically reading the manuscript; M. McNicholas and S. Kirchherr for assistance during behavioral experiments; and B. Mathieu at the IBENS Imaging Facility. N. Nakanishi and S. Lipton (Scintillon Institute) provided the GluN3AKO mice and M. Mishina (Tokyo University) provided the GluN2AKO line. The anti-GluN3A antibody was a gift from M. Watanabe (Hokkaido University). We thank C. Bellone (Geneva University) for the scr/shRNA-expressing viruses. **Funding:** This study was supported by fellowships (NKTH-)ANR-09-BLAN-0401 to S.D., M.A.D., and L.A., and ANR-17-CE16-0014 to P.P., S.D., B.L.K., and M.A.D.; by Emergence Sorbonne (S17JRSU003) and CNRS (PICS 7415) to M.A.D.; by the European Research Council (693021) to P.P.; by ERC-FRONTHAL (742595) to L.A.; by grants FK124434 and 2017-1.2.1-NKP-2017-00002 to F.M.; and by the National Institute of Drug Abuse (05010) and the National Institute on Alcohol Abuse and Alcoholism (16658) to B.L.K. C.V.R. was supported by FRM grant FDT20100919977. C.A. was supported by a Paris School of Neuroscience "Chair of Excellence" award and by a NARSAD Y.I. Award. **Author contributions:** M.A.D. designed and developed the project. Y.O. and M.A.D. performed the electrophysiology with K.P., S.A.G., T.B., and E.S. K.P., C.V.R., and C.A. performed confocal immunohistochemistry. F.M. performed electron microscopy under supervision of L.A. E.D. performed the behavioral tests under the supervision of B.L.K., with M.A.D. and K.P. T.G. performed the HEK experiments under supervision of P.P. S.D. contributed equipment. C.A. provided transgenic mice. M.A.D. wrote the manuscript, which was edited by all authors. **Competing interests:** The authors declare no competing interests. **Data and materials availability:** Data values and statistics are included as supplementary materials.

SUPPLEMENTARY MATERIALS

science.sciencemag.org/content/366/6462/250/suppl/DC1
Materials and Methods
Figs. S1 to S9
Table S1
References (*24*–*39*)

View/request a protocol for this paper from *Bio-protocol*.

7 May 2019; accepted 17 September 2019
10.1126/science.aax1522